PROCEEDINGS OF THE 3rd JOINT SYMPOSIUM ON THE NATURAL HISTORY AND GEOLOGY OF THE BAHAMAS

June 2019

Edited by David Griffing, Mark Kuhlmann and Troy Dexter

Gerace Research Centre
San Salvador, The Bahamas
2023

PROCEEDINGS

OF THE

THIRD JOINT SYMPOSIUM

ON THE

NATURAL HISTORY AND GEOLOGY OF THE BAHAMAS

Edited by

David Griffing, Mark Kuhlmann and Troy Dexter

ORGANIZER:

Troy A. Dexter

Executive Director
Gerace Research Centre
University of The Bahamas
San Salvador, The Bahamas

2023

ISBN: 978-0-935909-71-5

TABLE OF CONTENTS

FOREWARD

The 3rd Joint Symposium on the Natural History and Geology of The Bahamas was held at the Gerace Research Centre (GRC) on the island of San Salvador during June 8-12, 2019. Few would have guessed at the challenges that faced the field station and its staff, in the following years. The spread of the COVID-19 virus led to the closure of The Bahamas borders on March 17, 2020. This was followed by months of restrictions on domestic travel and curfews (as well as occasional complete lockdowns) within the country. Although the country re-opened its borders and removed mandatory quarantine for visitors on November 1, 2020, the challenges of pre-travel testing for large student groups and institutional concerns over international travel during the ongoing pandemic meant that utilization of the GRC facilities was impractical for many additional months. For example, Hartwick College cancelled all off-campus, travel-based courses slated for January 2021, and only one international course out of seven proposed for January 2022 actually ran.

The COVID pandemic also created unprecedented challenges for both the educator-researchers and the students that normally populate GRC facilities and benefit from interaction with the island's peoples and natural resources. These challenges included (but were not limited to) pivoting from in-person to fully online education with little to no time for preparation, an extended period of hybrid online and in-person college courses with frequent subsequent rolling absences in classes, and ongoing anxiety related to daily changes in COVID infection numbers on campuses. As a consequence, student enrollments decreased on many college campuses and faculty retrenchment began. This left remaining instructors struggling to maintain programs with fewer faculty.

The good news is that widespread vaccination and increasing COVID immunity within communities around the globe has meant that educational travel and placed-based learning is back, alive and well at the GRC once again! The scheduled 4th Symposium to be held at the GRC in June will shine a spotlight on the value of field education in The Bahamas. Many of us also look forward to a time when governmental policies revolving around research permitting make student-faculty collaborative research a practicality for us once again.

Papers in the following conference proceedings were developed from the work presented at the 3rd Joint Symposium and cover a wide array of topics typical of the diverse, important research conducted in The Bahamas and in similar sub-tropical to tropical areas with implications for The Bahamas. As in the past, they are divided up into peer-reviewed full-length research articles, editor-reviewed notes and short articles, and contributed abstracts.

Faculty Conference Chairs/Editors: David Griffing (Geology) and Mark Kuhlmann (Natural History), Hartwick College

Keynote Address

NOTES FROM THE EDGE OF THE ARCHIPELAGO: CARBONATE GEOLOGY AND SAN SALVADOR

Joan R. Mylroie and John E. Mylroie

Department of Geosciences
Mississippi State University
Mississippi State, MS 39762USA

ABSTRACT

San Salvador Island, the Bahamas, has been a leading location for the study of carbonate geology for more than four decades. Initially established as the College Center of the Finger Lakes Bahamian Field Station, geology research began in the early 1970s and by the 1980s the "CCFL" was hosting field trips for national and international organizations, and established the Geology Symposium series that attracted carbonate researchers from across America and overseas. The proceedings volumes from those symposia published significant original research, and the field trip guides for the off-island field trips associated with those symposia expanded the carbonate geology models for San Salvador across the Bahamian Archipelago. Current research by the authors has focused on the depositional and dissolutional cycles that resulted from glacioeustasy over the last million years).

.

Chairs' Note: We wish to thank Joan and John Mylroie for going "above-and-beyond" by agreeing to be our conference keynote presenters. Our original keynote had to unexpectedly cancel due to a family emergency, and the Mylroies agreed to fill in at short notice. Already slated to co-present five abstracts before taking on the keynote, we joked that we might need to rename the conference the 1st Mylroie Symposium! All kidding aside, we can think of very few individuals so key to the development and success of the GRC as a vehicle for promoting field education, scientific exploration and conservation in the Bahamas.

UNUSUAL KARST PHENOMENA FROM CAT ISLAND, BAHAMAS

Nancy Albury[1], Michael Lace[2], Joan Mylroie[3], John Mylroie[3*]

[1]National Museum of The Bahamas, Antiquities, Monuments and Museum Corporation, Marsh Harbour, Abaco, Bahamas

[2]Coastal Cave Survey, West Branch, IA, 52358 USA

[3]Dept. of Geosciences, Mississippi State University, Mississippi State, MS, 39762 USA *(corresponding author)
mylroie@geosci.msstate.edu

ABSTRACT

Cat Island, Bahamas, contains some unusual island karst features. Cat's Cradle, a blue hole in the east-central Cat Island, is a progradational collapse structure that breached a large eolian calcarenite dune. The subaerial walls of the collapse are stepped at 3 m elevation, with the upper wall set back farther than the lower wall. This upper wall contains a complete ring of flank margin caves that open onto the bench above the blue hole. If the mixing model for flank margin speleogenesis is correct, then the blue hole was marine during the 6 m high MIS 5e sea-level highstand.

A 2 km long section of the east coast of Cat Island is a late Pleistocene back-beach breccia facies, indicating strand plain progradation, followed by wave erosion of that plain to create back-beach breccia, and subsequent continuing progradation of the strand plain. The fresh-water lens followed that progradation and created flank margin caves within the breccia facies, indicating the rapidity with which flank margin cave speleogenesis operates, as the entire sequence of rock deposition and dissolution had to be accomplished within the ~ 9 ka long MIS 5e event.

Big Cave, in central Cat Island, is located at 55 m elevation on a shoulder of Mount Alvernia, the highest point in The Bahamas at 62 m elevation. The cave has all the small- and large-scale bedrock morphologies found in flank margin caves, but cannot be a flank margin cave in the traditional sense given its elevation above any possible Quaternary sea-level highstand. Cave genesis within freshwater lens perched on a terra rossa paleosol has been previously offered as a possible explanation.

INTRODUCTION

A karst reconnaissance trip was made by the authors to Cat Island, Bahamas, from February 3 to February 18, 2016. The purpose of this expedition was to locate, survey, and catalogue cave and karst features as part of a project of the Coastal Cave Survey, an informal cave research group that specializes in coastal and island caves. This work built on reconnaissance done in February 2006 for the Cat Island field trip (Figure 1) to be run in June of that year by the Gerace Research Centre as part of the 13th Symposium of the Geology of The Bahamas and Other Carbonate Regions (Mylroie *et al.* 2006). The 2016 expedition also built on much earlier work by Rob Palmer and colleagues that had specialized on the caves of Cat Island (McHale 1986; Palmer 1986; Palmer *et al.* 1986). The geology of Cat Island has not been well studied, the manuscript by Lind (1969) on coastal landforms being one of the few pieces of geologic literature available before 2006. The 2006 field guide reconnaissance trip led to a return to Cat Island by several participants to study specific

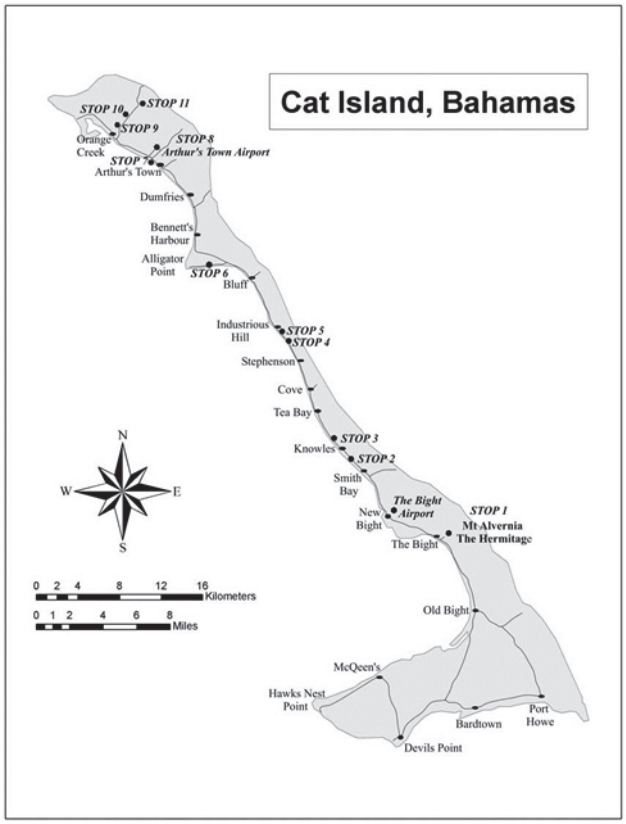

Figure 1. Map of Cat Island, showing the three areas reported in this paper. The map, adapted from Mylroie, et al., 2006, also shows the field trip stops for the June 2006 GRC field trip.

features of the island's geology (e.g. Curran *et al.* 2008; Glumac *et al.* 2011, 2012). The caves documented during the 2016 field season formed a critical component of a paper that has re-interpreted Quaternary sea-level in the Bahamian Archipelago (Mylroie *et al.* 2020). The 2006 field guide remains the most comprehensive assessment of the geology of Cat Island (Mylroie *et al.* 2006). The cave and karst results from both the 2006 and 2016 expeditions were presented at the National Speleological Society annual meeting in July of 2016 (Albury, et al. 2016) as well as at the Third Joint Symposium on the Natural History and Geology of the Bahamas (Albury *et al.* 2019). The purpose of this paper is to highlight three specific aspects of that work that have broad impact on our understanding of Bahamian geology, karst processes, and Quaternary sea-level.

METHODS

The initial effort was to locate and map all currently subaerial caves on Cat Island. Submerged caves, such as those associated with blue holes, were not part of the study, although blue holes were noted when found. A few cave locations were already printed on the Bahamian government's Lands and Surveys topographic maps. Many were known to the local island residents, but this knowledge has deteriorated over the four decades the corresponding author has worked in the Bahamas, as the younger generation knows little about the interior of their own islands, and the older generation, who often did slash and burn agriculture in the interior of their islands, is dying off. Still, the local population remains the best source of information about cave locations. Commonly it is basic field reconnaissance of the islands by this research team that actually located the caves. Colleagues who work in the interior of islands for other research projects, such as animal or plant studies, share information on the caves that they find. Prior work was extremely useful (McHale 1986; Palmer 1986; Palmer et al. 1986). The interior of the Bahamian islands is commonly difficult to traverse; the expression used is that "the bush is too high to walk over and too low to walk under". Trail cutting is critical in these situations. High canopy forest is present in some island interiors, and fieldwork there is relatively easy, but for most areas on Cat Island, it is hard work. Aerial reconnaissance was useful, mostly for locating larger cave entrances, especially ceiling collapses and blue holes.

Caves located in the field were initially georeferenced in the field with Garmin Etrex series units, utilizing the WGS84 datum and with an average horizontal EPE (estimated projected error) of 2 to 3 meters. As elevation data from this method is of limited accuracy, cave elevation data were supplemented with orthographic surface surveys to apparent sea-level (where feasible) and cave surveys correlated to subterranean tidal pools to the nearest 0.1 meter and within modern microtidal environments (i.e., a tidal range of <1 meter). The data set was then correlated to

satellite imagery, available DEM models and topographic maps.

Each flank margin cave was mapped by use of compass, inclinometer and tape (or laser range finder), with passage detail sketched to scale and annotated. The resulting cave map data are reduced and drafted using computer software Compass (www.fountainware.com) and Adobe Illustrator, respectively. The maps were then analyzed to provide additional morphometric parameters (NIH Image J software – www.NIH.gov) including the total aerial footprint of the cave. The maximum height of each phreatic dissolutional surface represents a minimum fresh-water lens position, and by extension, sea-level position at the time of cave origin. Cave length, the traditional measurement of cave size, is not an appropriate value for flank margin caves, which are connections of globular chambers and passages. The aerial footprint is a better measure of the cave size in this circumstance (Mylroie 2007; Waterstrat, *et al*. 2010). Flank margin caves form in the distal margin of the fresh-water lens where the lens is thin (Mylroie and Mylroie 2007; Mylroie 2013), therefore aerial footprint is a suitable proxy of cave volume as the vertical range of the cave is restricted.

The cave data were collected under permit from the Bahamian government, through the Bahamas Environment, Science and Technology Commission (BEST), who control release of such information. Cave location information is especially sensitive, given the vulnerability of caves and cave deposits to vandalism, desecration, and looting.

RESULTS

Breccia block facies

The first feature of interest was found while hiking northward along the east coast of Cat Island to cut a trail into a blue hole seen by a private airplane while flying into Cat Island with one of the authors aboard (Figure 1). The coast in this area is a bench about 3 to 8 m above sea-level. The bench is a mixture of beach, lagoonal, and breccia block facies (Figure 2). Because the breccia block facies is covered in part by terra rossa paleosol (Figure 2B), the initial interpretation was a solution collapse breccia similar to what is seen on the south coast of San Salvador Island at French Bay (Florea *et al.* 2001). Closer examination revealed that the blocks were covered by the terra rossa paleosol, but that the terra rossa material was not providing a matrix for supporting the blocks, the blocks instead rested in a clean, white sand (Figure 2C). Such breccia block facies are found all across the Bahamas, as first described in detail by Carew and Mylroie (1985; 1995) at Grotto Beach on San Salvador Island, where a Pleistocene example in the rock record is adjacent to a Holocene example currently in the process of formation. The terra rossa covering the breccia block facies, and the lagoonal facies adjacent to the blocks at 6 m elevation, demonstrate that the breccia block facies is Pleistocene in age, most likely from the last interglacial, MIS substage 5e. The MIS 5e highstand is believed to have lasted in The Bahamas from 124 to 115 ka (Thompson *et al.* 2011).

At numerous locations along this bench, flank margin caves of modest size are developed in the breccia block facies, the largest being Dragon Cave (Figures 3 and 4). This cave is entered from a roof collapse and contains numerous phreatic dissolutional features, indicating development within the MIS 5e fresh-water lens. The configuration of the cave does not favor a sea cave pseudokarst interpretation. Secondary calcite speleothems are present (Figure 4D). The cave meets all the requirements of a flank margin cave (Mylroie and Mylroie 2007, 2013; Waterstrat *et al.* 2010). A few other caves on the bench, of a similar nature, were also mapped.

Cat's Cradle blue hole

The second feature of interest is the blue hole located inland of the bench with the breccia block facies (Figure 1). This blue hole, Cat's Cradle, is a progradational collapse feature that has penetrated the side of an eolian calcarenite ridge, producing high walls that lead down to water (Figures 5 and 6). The high wall has a bench, or step in it 3 m above water level, and which contains numerous small caves of phreatic origin,

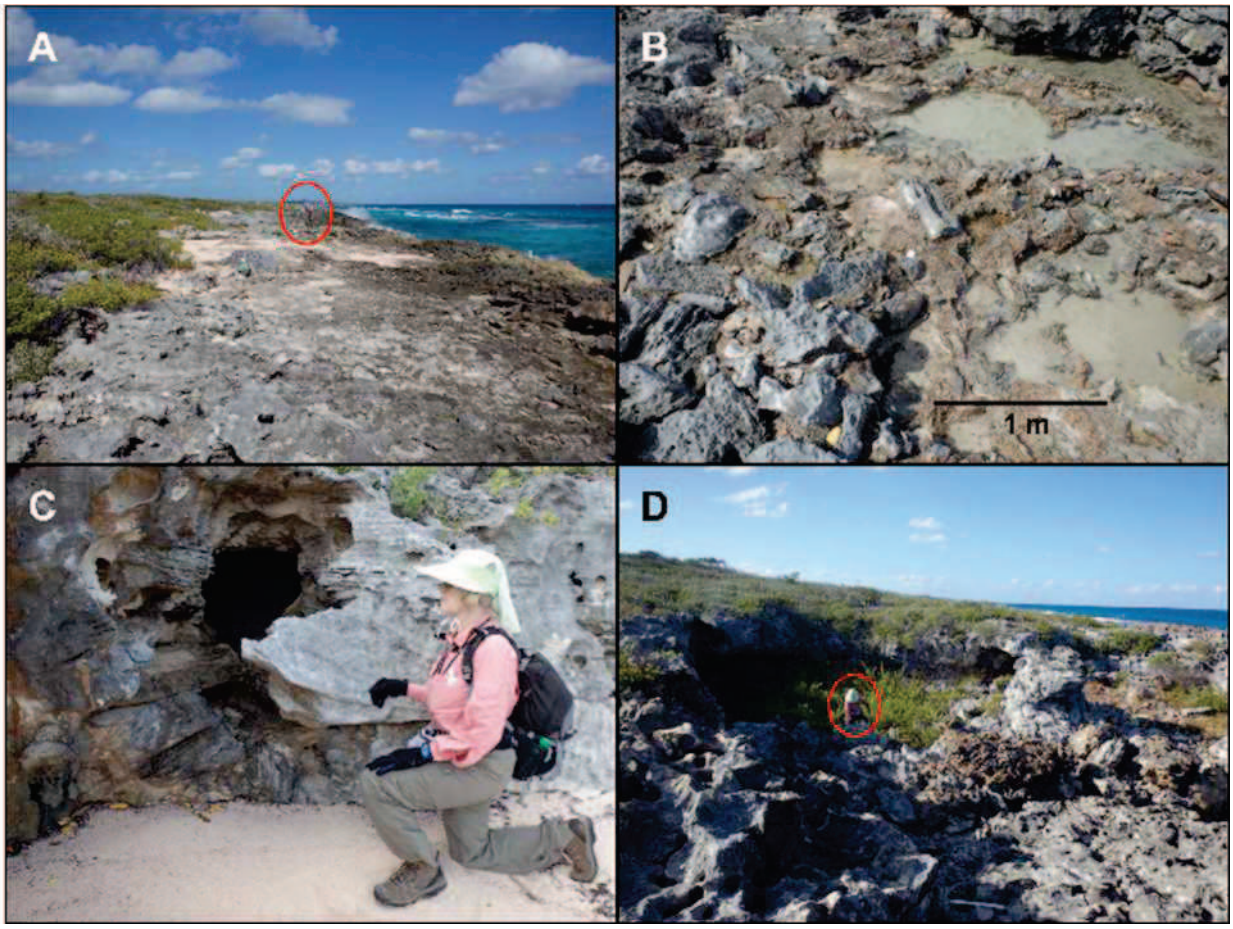

Figure 2. The coastal area from eastern Cat Island where the breccia block facies outcrops were found. A. General view of the bench, looking north, person in oval for scale. B. Surface outcrop of the breccia block facies, with overlying terra rossa paleosol that gives the appearance that the outcrop is a solution collapse breccia. C. Back beach cliff, showing the breccia block facies in vertical section, with a small dissolution cave. The terra rossa paleosol material is not present: a sand matrix partially supports the blocks. D. The collapse entrance to Dragon Cave, the largest of many flank margin caves found on the coastal bench, person in oval for scale.

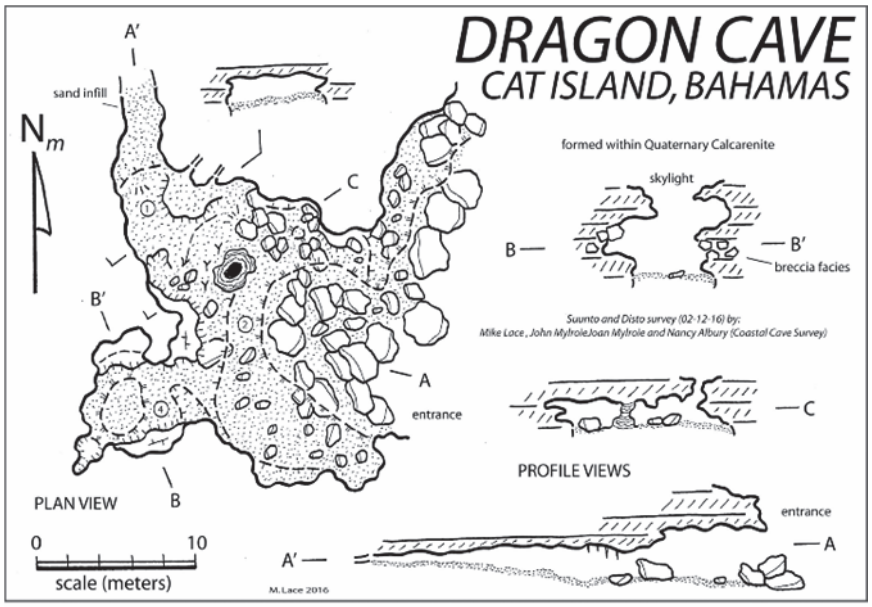

Figure 3. Map of Dragon Cave.

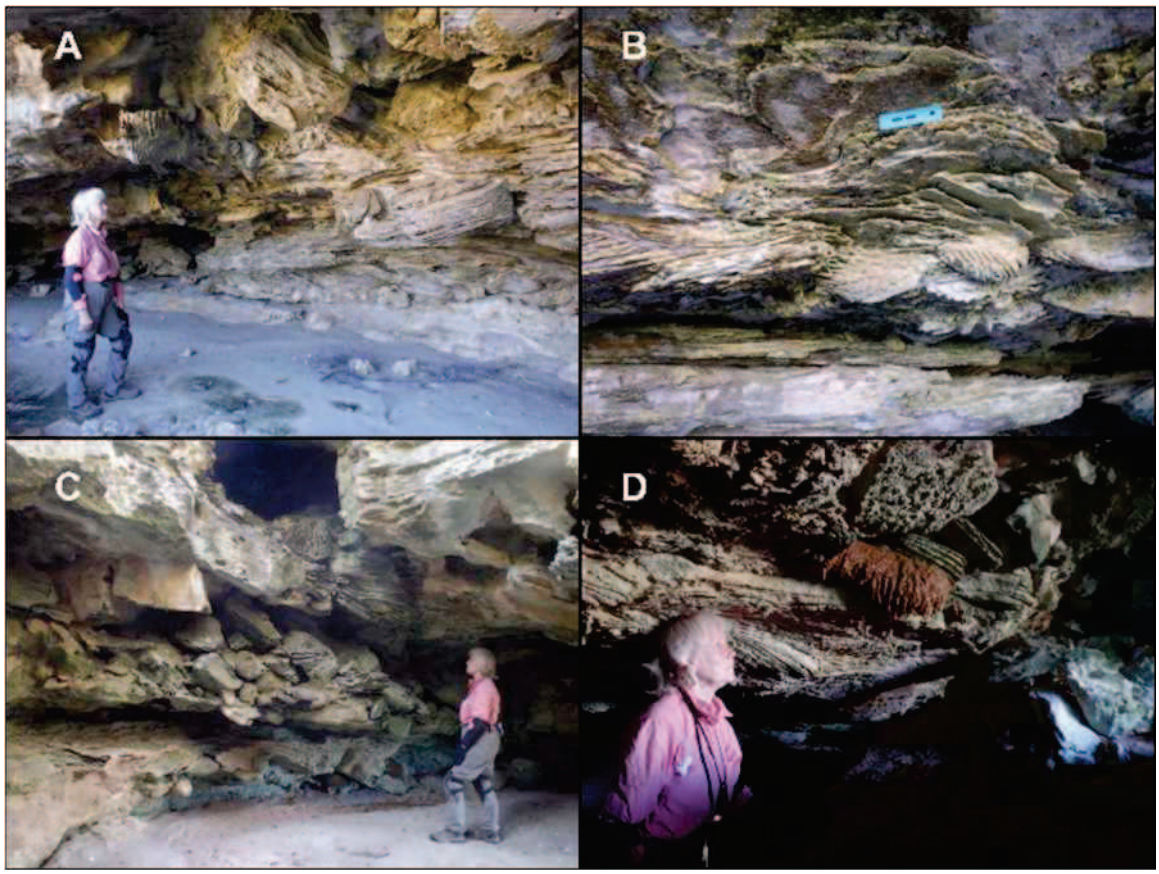

Figure 4. Inside Dragon Cave. A. Entrance room, showing chaotic breccia blocks in a sand matrix. B. Close up of the breccia block facies, showing cross-bedded lagoonal sands between the blocks; small ruler 4 cm long for scale. C. Phreatic dissolutional features cutting through the breccia block facies. D. Calcite flowstone in cave wall of breccia blocks.

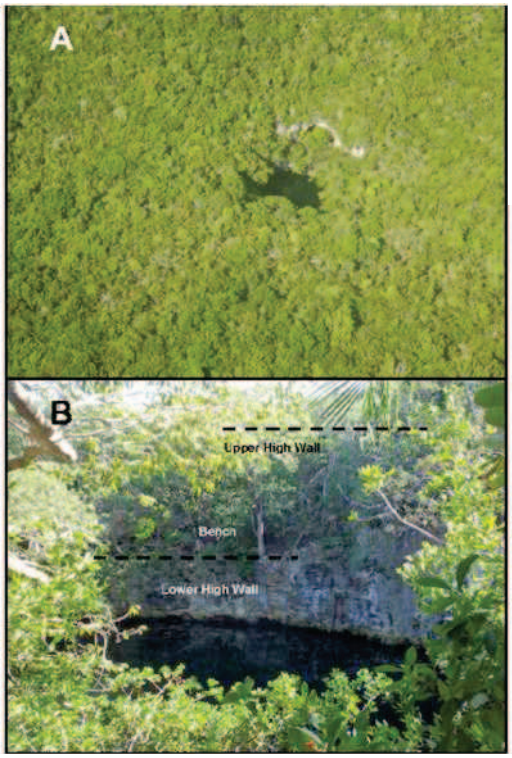

Figure 5. Cat's Cradle blue hole. A. As seen from the air. The high wall is visible to the upper right of the actual water body of the blue hole. B. The blue hole, showing the upper and lower high wall condition, with the bench in between.

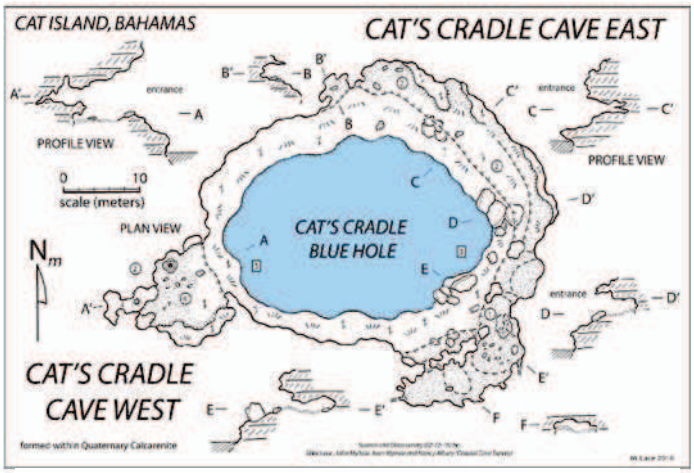

Figure 6. Map of Cat's Cradle blue hole and associated flank margin caves.

which ring the blue hole and all open inward toward the blue hole (Figure 7). The blue hole currently contains water of marine salinity (~35 ppt).

Big Cave

The third feature is located on a hilltop immediately adjacent to the Hermitage monastery at Mount Alvernia (Figure 1), the highest location in The Bahamas at 206 feet (62 m). A small cave, incongruously named Big Cave, is located here (Evans 1984; Taylor 2000). It has an entrance leading inward from the side of the hill, as well as some breached bell holes that open to the surface above the cave (Figure 8). The cave has dissolutional surfaces of apparent phreatic origin, a few calcite speleothems, and chambers large enough to stand upright in. The cave was used as a church to hold mass by a Father Jerome while the monastery was being built (Evans 1984; Mylroie *et al.* 2006; Taylor 2000). The cave is at an elevation of 180 feet (55 m), well above the position of any past Quaternary sea-level. On the west side of Mt Alvernia, just below the hill crest and in front to the monastery is a feature called Burial Cave (Taylor 2000). Taylor (2000) refers to this feature as a "natural arch" but site investigation in 2006 could not determine if the feature is natural or artificial. A slatted gate allows one to peer inside, and a stone wall divides the chamber, with Father Jerome's body allegedly behind the wall (Taylor 2000).

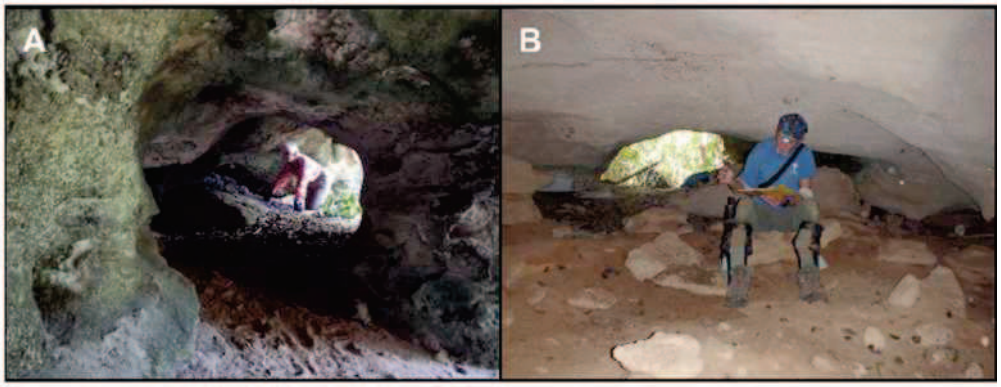

Figure 7. Flank margin cave passages associated with the southeastern side of Cat's Cradle blue hole. A. Oval tube leading inward from the blue hole bench. B. Interior room with smooth phreatic surfaces.

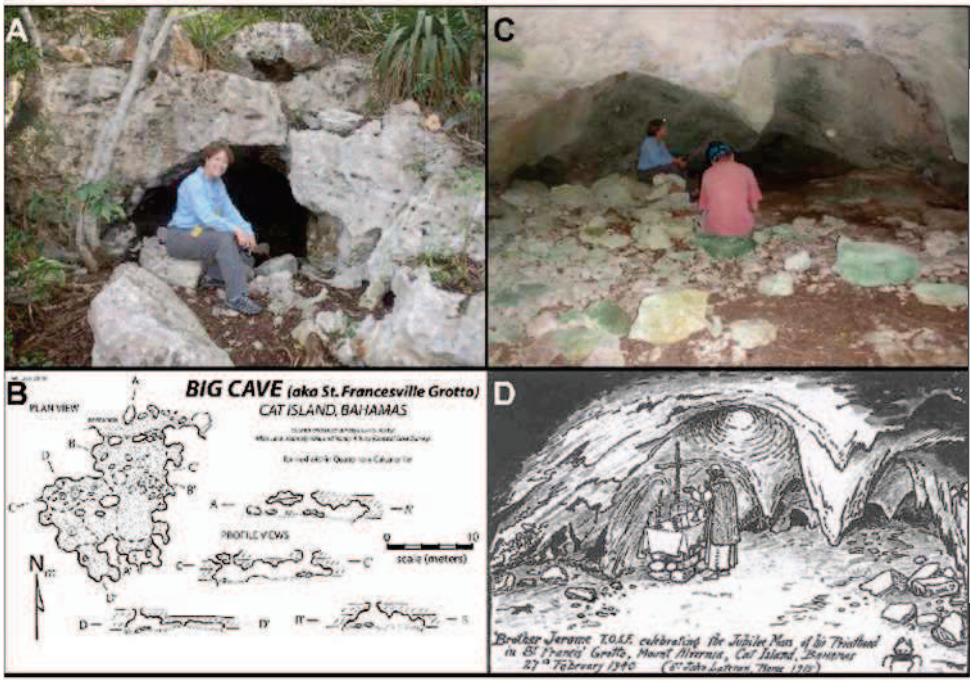

Figure 8. Big Cave, adjacent to Mount Alvernia. A. The entrance to the cave; the hilltop can be seen above the seated individual. B. Map of Big Cave. C. Interior main chamber of the cave. Person to the left is sitting on rocks that once were the altar in part D. D. A drawing of Father Jerome holding mass in Big Cave, from Taylor (2004) (Note: the name used for the cave in the figure is "St Francis Grotto").

DISCUSSION

Breccia block facies

The breccia block facies provide two important contributions. First, this is the most extensive outcrop of such facies as has been observed by the authors on the 15 Bahamian islands (and four similar islands in the Turks and Caicos) where we have conducted field work. The breccia block facies indicates how rapidly deposition and lithification events occur in young carbonates. The production of carbonate allochems for this facies, their emplacement as beach rock, and the subsequent disarticulation of that beach rock by wave energy, with entombment in lagoonal sands and prograding beach sands, all occurred during the first part of MIS 5e, which was only 9,000 years long in the Bahamas (Thompson *et al.* 2011). Syngenetically, the fresh-water lens invaded the prograding beach that began to infill parts of the lagoon, and flank margin caves developed within that breccia block facies before the end of MIS 5e ~115 ka, as outlined by Figure 9. Such syngenetic cave development in young carbonates has been part of a recent description and classification of how fast dissolutional caves can form in young carbonates (White *et al.* 2018).

Second, the development of flank margin caves in the breccia block facies is also an indication of how ground water dissolution occurs in eogenetic carbonates when water and solute transport is by diffuse flow. The essential outcome is that the facies characteristics have little impact on cave development, and the morphology of the cave thus produced, regardless of whether the facies are lagoonal sands, framework reefs, eolianites, or as in this case, breccia block facies. Because most cave and karst studies, until recently, have been done in carbonate telogenetic rocks in continental settings, where turbulent flow in fractures, bedding planes, joints and faults governs ground water flow and the subsequent cave morphology, the differences contrast with cave development in locations such as The Bahamas was long unrecognized (Mylroie and Mylroie 2007, 2017, 2019). The breccia block facies on Cat Island is an outstanding example of the rapidity of flank margin cave development, and the unique morphologies produced in eogenetic carbonates by diffuse flow regardless of facies type.

Cat's Cradle blue hole

Cat's Cradle blue hole is a classic blue hole that appears to be the result of progradational collapse of a large dissolution void at depth. The models for blue hole origin are reviewed by Mylroie, et al., 1995; the most common type of blue hole, and the ones that produce large, circular pipes leading deeply downwards, are thought to be formed by progradational collapse. Larson and Mylroie (2018) demonstrated that the large voids at depth that cause the collapse, and accommodate the collapse material, develop from large conduit systems that form on the Bahama Banks when sea-level is below the bank top and as a result these banks become very large islands. Such conditions support production of turbulent flow conduits, which are senescent at today's high sea-level but can still be explored by cave divers.

Cat's Cradle is somewhat unusual in that the collapse has prograded up through the side of an eolianite ridge, to produce there 8 to 10 meters of vertical wall between the land surface and the water in the blue hole, which is at current sea-level (Figure 5). Most blue holes of the progradational type open onto lowland plains in The Bahamas, and the amount of relief between the land surface and the blue hole water is only one or two meters. This aspect makes Cat's Cradle look a bit like a cenote from the Yucatan of Mexico (e.g. Mylroie *et al.* 1995) as opposed to a typical Bahamian blue hole.

The location of the eolianite ridge in the pathway of the progradational collapse means that during MIS 5e, when sea-level was 6 m higher than at present, there would have been mixing between the waters of the blue hole (likely to be sea water) and the fresh-water lens in the surrounding ridge. This mixing, and other associated chemical reactions involving organics and their decay, formed flank margin caves in a ring around the blue hole (Figures 6 and 7). These caves promoted instability in the high wall surrounding the blue hole, and after the end of MIS 5e; their partial collapse resulted in a bench being developed in the high wall at the elevation

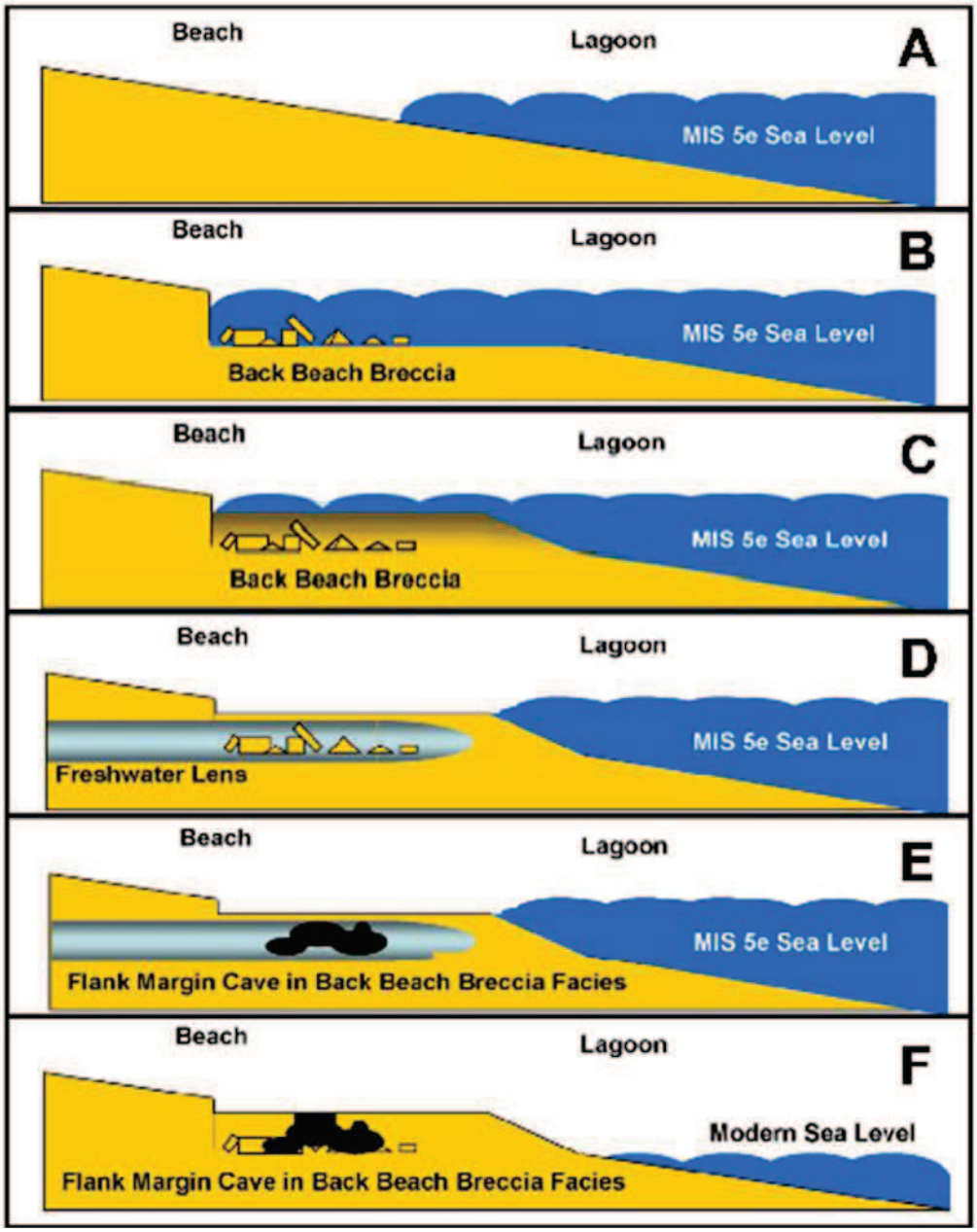

Figure 9. Development of the breccia block facies and subsequent flank margin caves. A. During the MIS 5e sea-level highstand, with sea-level 6 m higher than present, a prograding beach is formed. B. Beachrock formation, and wave attack create breccia blocks. C. Continued sand deposition entombs the breccia blocks to create the breccia block facies. D. Because new land has been created by sand progradation, the fresh-water lens advances into the breccia block facies. E. Flank margin caves form in the lens margin. F. Modern sea-level conditions; a terra rossa paleosol has developed on the breccia block facies, and many of the flank margin caves have breached to the surface.

of the caves; Figure 10 details a diagrammatic model of the evolution of Cat's Cradle blue hole. The presence of the flank margin caves also means the blue hole formed during or prior to the MIS 5e sea-level highstand, so as to bring two different water bodies in contact with each other during that highstand.

Big Cave

Big Cave is very problematic, as has been noted since its modern documentation (Mylroie *et al.* 2006; Mylroie 2013; Mylroie *et al.* 2020). The cave contains all the dissolutional signatures found in flank margin caves, but cannot have been produced by mixing of fresh water and sea water

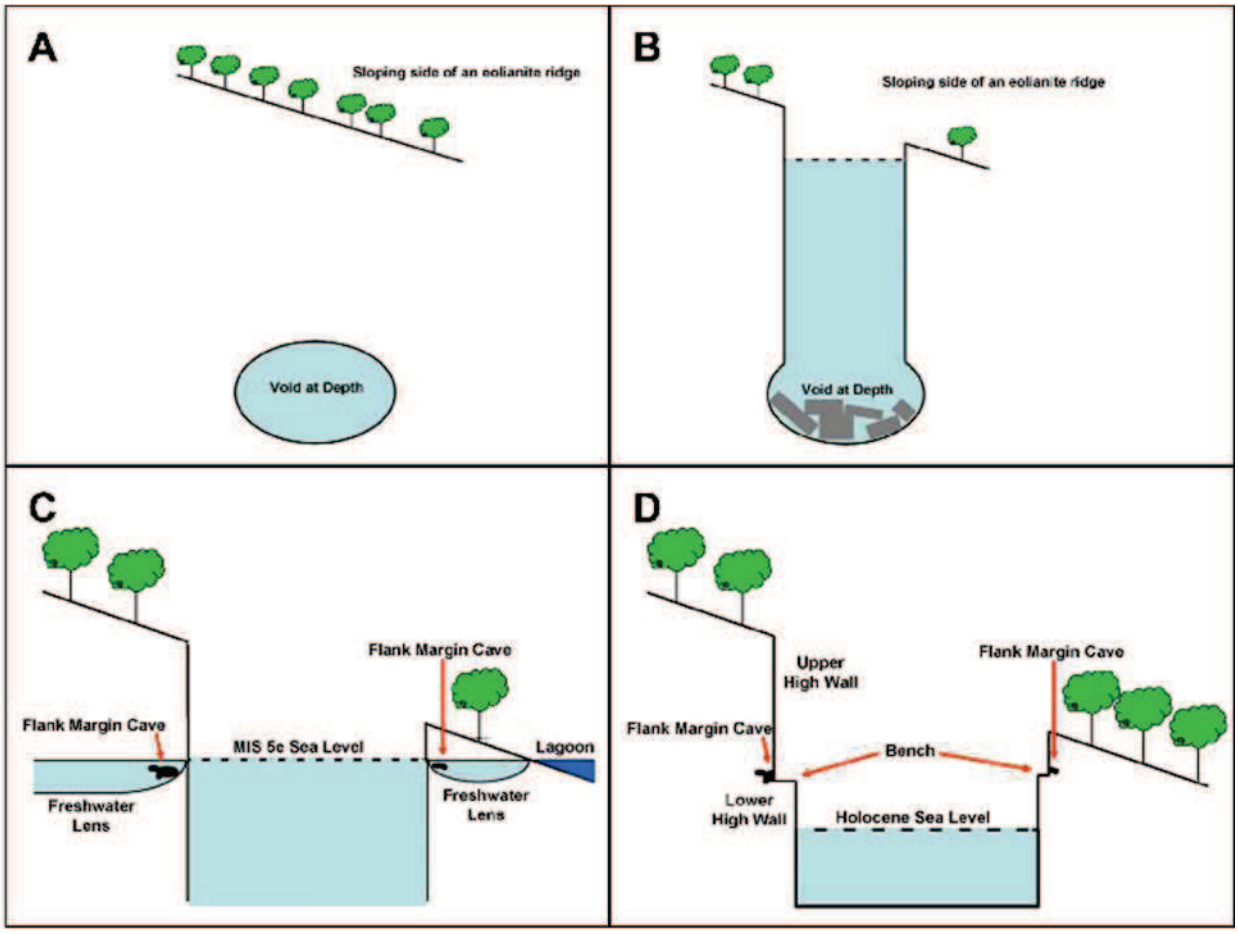

Figure 10. Evolution of the Cat's Cradle blue hole. A. During a glacioeustatic sea-level lowstand, the Great Bahama Bank is completely subaerially exposed and a large conduit is formed. B. Progradational collapse of a portion of that conduit before or during MIS 5e breaches the surface. During MIS 5e, the water level in the blue hole is 6 m above present. C. The freshwater lens surrounding the blue hole is different in chemistry than the water in the blue hole, and flank margin caves develop on the blue hole perimeter by mixing dissolution. D. After sea-level fall, partial collapse of the caves creates the bench seen today.

as it is located tens of meters higher than any known Quaternary sea-level in The Bahamas, or globally for other similar non-tectonic stable carbonate platforms. Because of the very uniform nature of flank margin caves around the world (*e.g.* Mylroie 2013), this cave type has become associated with any cave development by diffuse flow in an eogenetic carbonate rock. In other words, all flank margin caves have diffuse flow regimes during speleogenesis, but not all caves formed by diffuse flow are flank margin caves.

So how did Big Cave form? As noted earlier, organics have been implicated as one of the possible driving mechanisms for the speleogenesis of flank margin caves (e.g. Mylroie and Mylroie 2007), and was used to explain the development

of banana holes in The Bahamas (Harris *et al.* 1995), although additional mechanisms now seem applicable (Mylroie 2013). Recently, organics have again been promoted as a major driver of dissolution in eogenetic carbonates (*e.g.* Gully *et al.* 2016). As noted in Harris *et al.* (1995), mixing dissolution can occur between descending vadose water and the phreatic fresh water of the fresh-water lens as well as by classic sea water/fresh water mixing. Coupled with the oxidation of organics, vadose mixing may be enough to form dissolutional caves in a perched freshwater body totally separated from any direct marine water influence. Eolian calcarenites, or simply eolianites, are about as homogenous and isotropic as any sand-sized sedimentary rock. In The Bahamas, the eogenetic nature of the eolianites means that they have very high primary porosity, and that porosity has not yet been lost to burial and diagenesis (the mesogenetic realm), so the accompanying permeability is also high. These characteristics allow fluids to move through the rock and to interact with it in three dimensions. Mixing, combined with oxidation of organics in such porous and permeable material, even in fresh water, can produce voids large enough for human exploration.

The key to explaining Big Cave is to identify a mechanism for perching of fresh water other than by its density contrast with sea water. A possible candidate is a terra rossa paleosol, which can be very cemented and micritic, capable of retarding downward vadose flow and allowing it to accumulate as a perched water body. The influence of terra rossa paleosols in the development of caves in Quaternary eolianites has been described (Mylroie *et al.* 2020) as a way to perch a water table (Figure 11).

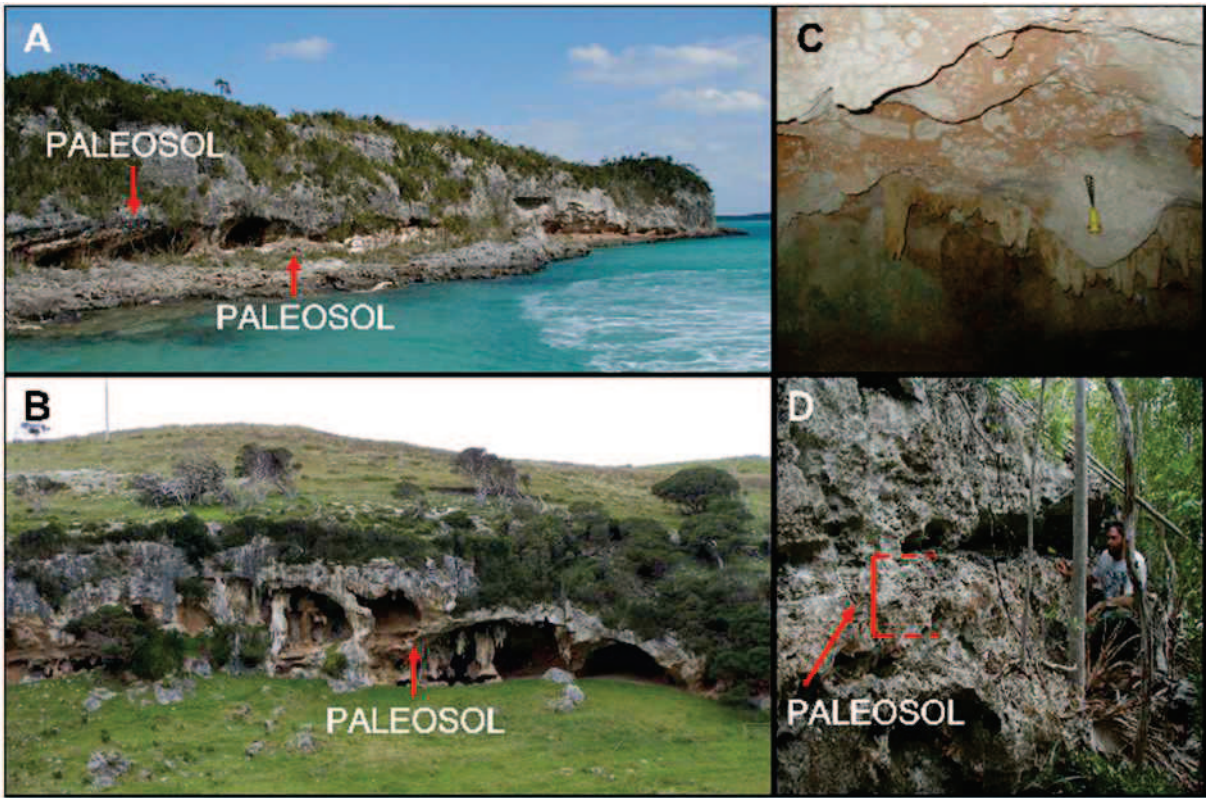

Figure 11. Role of terra rossa paleosol on speleogenesis in eolian calcarenites. A. Indian Point, Long Island, Bahamas, cave development is vertically constrained by two paleosols. B. Tarragal Caves, South Australia, similar situation as in A, with a single paleosol separating caves. C. Red Roof Cave, Indian Point, Long Island Bahamas, the ceiling is a paleosol. D. Immediately outside Red Roof Cave, the weathered paleosol is almost impossible to see, evident only by the small voids perched on it. From Mylroie et al., in press.

Field work in the Big Cave area has been minimal. The effort so far has been to map the cave (Figure 8), but the supposed terra rossa paleosol has not yet been detected. In weathered outcrops, such paleosols are notoriously hard to document (*e.g.* Figure 11C versus 11D). If Burial Cave were truly natural, a similar speleogenesis mechanism would need to be proposed for its development.

If the paleosol argument cannot be proven, then there is a conundrum as to how to form a feature like Big Cave. As Mylroie (2013) and Mylroie *et al.* (2018) have discussed, Big Cave represents a challenge to the flank margin cave model. It is not so much a challenge to that model, which works very well in sea-level environments, as it is a question about how caves form in eogenetic eolian calcarenites that are not flank margin caves but show clear evidence of development in a diffuse flow hydrologic setting.

CONCLUSIONS

The three features from Cat Island discussed in this paper: breccia block facies, Cat's Cradle blue hole, and Big Cave, all present interesting phenomena that relate both to cave formation in eogenetic carbonate rocks, and also implications for sea-level magnitude and position in the Quaternary in The Bahamas. Both the breccia block facies and Cat's Cradle blue hole demonstrate the rapidity with which flank margin caves can form, and their subsequent influence on the landscape immediately around them. Big Cave is a clear anomaly: is that its true status or does it represent something that is more common than we have previously recognized? In any case, field work is planned to examine the Big Cave area thoroughly to see if a terra rossa paleosol or some other factor can explain its unusual position in the topography of Cat Island.

ACKNOWLEDGMENTS

The authors thank the Gerace Research Centre for assistance with obtaining research permits from the Bahamas Environment, Science and Technology (BEST) Commission for continuing research projects G-102 and G-180. Thanks also to the many land owners, both public and private, who allowed access to their land, and often provided useful cave location information.

LITERATURE CITED

Albury, N. A., Lace, M. J., Mylroie, J. E., and Mylroie, J. R. (2016) Island Karst Update: New Phenomena from Cat Island, Bahamas. 2016 National Speleological Society Convention Program, 86.

Albury, N. A., Lace, M. J., Mylroie, J. R., and Mylroie, J. E. (2019) Unusual karst phenomena from Cat Island, Bahamas. In Dexter, T., ed., Abstracts and Program, The 3rd Joint Symposium on the Natural History and Geology of The Bahamas, 2.

Curran, H.A., Wilson, M.A., and Mylroie, J.E. (2008), Fossil palm frond and tree trunk molds: occurrence and implications for interpretation of Bahamian Quaternary carbonate eolianites. eds. Freile, D., and Park, L.E.., Proceedings of the Thirteenth Symposium on the Geology of the Bahamas and Other Carbonate Regions (San Salvador, Bahamas, Gerace Research Centre), 183-195.

Evans, A.G. (1984), The Conscious Stone, A Biography of John C. Hawes. Polding Press, Melbourne, 300 p.

Florea, L., Mylroie, J. and Carew, J. (2001) Karst genetic model for the French Bay Breccia deposits, San Salvador, Bahamas: Theoretical and Applied Karstology, 13-14, 57-65.

Glumac, B., Curran, H.A., Motti, S.A., Weigner, M.M., and Pruss, S.B. (2011), Polygonal sandcracks: Unique sedimentary desiccation structures in Bahamian ooid grainstone. Geology, 39, 615-618.

Glumac, B., Curran, H.A., Weigner, M.M., Motti, S.A., and Pruss, S.B. (2012) Distribution of oolitic sediment along a beach-to-offshore transect, Pigeon Cay, Cat Island, Bahamas: New insights into modern ooid formation, ed. Gamble, D.W., and Kindler, P., Proceedings of the 15th Symposium on the Geology of the Bahamas and other Carbonate Regions (San Salvador, Gerace Research Centre), 71-81.

Gulley JD, Martin JB, Brown A. (2016). Organic carbon inputs, common ions and degassing; rethinking mixing dissolution in coastal eogenetic carbonate aquifers. Earth Surface Processes and Landforms, 41, 2098-2110.

Harris, J. G., Mylroie, J. E., and Carew, J. L. (1995) Banana holes: Unique karst features of the Bahamas: Carbonates and Evaporites, 10, 215-224.

Larson, E.B, and Mylroie, J.E., 2018, Diffuse Versus Conduit Flow in Coastal Karst Aquifers: The Consequences of Island Area and Perimeter Relationships: Geosciences. 8, 268., doi:10.3390/geosciences8070268.

Lind, A.O. (1969). Coastal Landforms of Cat Island, Bahamas. Research Paper 122, Department of Geography, University of Chicago, 156 p.

McHale, M. (1986) Preliminary biological investigations in the terrestrial caves of Cat Island, Bahamas. Cave Science 13, 83-86.

Mylroie, J. E., Carew, J. L., and Moore, A. I. (1995) Blue holes: Definition and genesis: Carbonates and Evaporites, 10, 225-233.

Mylroie, J. E. (2007) Cave surveys, cave size, and flank margin caves: Compass and Tape, 17, 8-16.

Mylroie, J. E. and Mylroie J. R. (2007) Development of the Carbonate Island Karst Model: Journal of Cave and Karst Studies, 69, 59-75.

Mylroie, J. E. (2013) Coastal Karst Development in Carbonate Rocks. eds. Lace, M. J., and Mylroie, J. E., Coastal Karst Landforms. Coastal Research Library 5, Springer, Dordrecht, p. 77-109.

Mylroie, J. E., Carew, J. L., Curran, H. A., Freile, D., Sealey, N. E., and Voegeli, V. J. (2006) Geology of Cat Island, Bahamas: A Field Trip Guide. San Salvador Island, Gerace Research Centre.

Mylroie, J. E. and Mylroie, J. R., Bahamian Flank Margin Caves as Hypogene Caves, 2017, *In:* Klimchouk, A. B., Palmer, A. N., De Waele, J,. Auler, A. S., and Audra, P., eds., Hypogene Karst Regions and Caves of the World, Springer, Dordrecht, p. 757-768. DOI 10.1007/978-3-319-53348-3_51

Mylroie, J.E., Lace, M.J., Albury, N., and Mylroie, J.R. (2018) Mid-Quaternary sea-level highstands in the Bahamian Archipelago: Evidence from karst denudation and flank margin cave position: Geological Society of America Abstracts with Program, 50, doi: 10.1130/abs/2018AM-315535.

Mylroie, J. E., and Mylroie, J. R., 2019 (abstract), The effect of facies variations of eogenetic carbonates in the development of flank margin caves. Geological Society of America Abstracts with Program. 51, ISSN 0016-7592 doi: 10.1130/abs/2019AM-331208.

Mylroie, J. E., Lace, M. J., Albury, N.A. and Mylroie, J.R. (2019) Flank margin caves and the position of Mid to Late Pleistocene sea level in the Bahamas: Journal of Coastal Research, 36, 249-260..

Palmer, R.J. (1986), Preliminary studies of speleogenesis on Cat Island, Bahamas. Cave Science 13, 79-82.

Palmer, R.J., McHale, M., and Hartlebury, R. (1986) The caves and blue holes of Cat Island. Cave Science 13, 71-78.

Taylor, J. J. (2000) Between Devotion and Design, The Architecture of John Cyril Hawes, 1876-1956. University of Western Australia Press, 428 p

Thompson W.G., Curran H.A., Wilson M.A. and White B. (2011) Sea-level oscillations during the last interglacial highstand recorded by Bahamian corals: Nature Geoscience 4: 684-687

Waterstrat, W. J., Mylroie, J. E., Owen, A. M., and Mylroie, J. R. (2010) Coastal caves in Bahamian eolian calcarenites: Differentiating between sea caves and flank margin caves using quantitative morphology: Journal of Cave and Karst Studies. 72, 61-74.

White, S. Q., Grimes, K. G., Mylroie, J. E., and Mylroie J. R. (2018) The earliest time of karst cave formation: Cave and Karst Science, 45, 15-18.

ADHESION-RIPPLE STRUCTURES IN QUATERNARY CARBONATE EOLIANITES, SAN SALVADOR ISLAND, THE BAHAMAS

Mario V. Caputo

6326 La Reina Drive
Tujunga, California 91042 USA
(909) 214-7742
mvcaputo@earthlink.net

ABSTRACT

Newly discovered eolian adhesion ripples and related pseudo-crosslaminations occur in calcarenites of the Pleistocene Cockburn Town Member, Grotto Beach Formation and in the Holocene North Point Member, Rice Bay Formation, San Salvador Island, the Bahamas. Typified by heights and spacings of < 1 cm (0.4 in), the ripple marks are asymmetrical with wavy to lobate crests. Although associated pseudo-crosslaminations resemble true cross-stratification, they reflect only the direction from which the ripples had migrated and climbed and not true paleowind direction. Adhesion ripples and pseudo-crosslaminations described herein compare directly with those formed in siliciclastic (non-carbonate) sand. In modern sedimentary environments, dry sand, driven by wind, is captured by wet sand through surface tension and capillary action. Small bulbous ripples build up, migrate and climb into the wind, and deposit pseudo-crosslaminations that dip downwind. Preservation of adhesion structures in carbonate sedimentary rocks of San Salvador Island records episodes of windy rainstorms in the Northeast Trade Wind region during Quaternary time.

INTRODUCTION

An eolian or wind-blown origin for Pleistocene and Holocene bedrock of San Salvador Island, the Bahamas has been known since the initial observations by Adams (1980). Sedimentary structures created unequivocally by eolian ripple, grainfall, and grainflow processes, as explained by Hunter (1977a, b), have been recognized in the French Bay and Cockburn Town Members of the Grotto Beach Formation (Caputo, 1989, 1993, 1995) and in the Holocene North Point Member of the Rice Bay Formation (White and Curran, 1985, 1988; Caputo, 1993, 1995).

Adhesion ripples are created by relatively dry wind-driven sand adhering to wet sand by surface tension and capillary action, and have been known since van Straaten (1953). Kocurek and Fielder (1982) summarized the history of study on adhesion structures mainly in siliciclastic sand and sandstone. They further classified adhesion structures as adhesion ripple, adhesion wart, and adhesion plane bed according to their physical appearance and strata they deposit (Figure 1). Modern adhesion ripples are known to build-up and migrate into wind currents and can be likened to larger, ripple-like bedforms called antidunes that migrate upcurrent in subaqueous channelized flows (Gilbert, 1914), and volcanic antidunes that migrate upcurrent in fluidized pyroclastic flows (Wohletz and Sheridan, 1979).

The purpose of this study is to describe and document the first-time discovery and identification of new sedimentary structures exposed locally in Pleistocene and Holocene carbonate sedimentary rocks on San Salvador Island, and provide evidence for their origin by eolian adhesion ripples. The first-ever discovery of adhesion ripple structures in

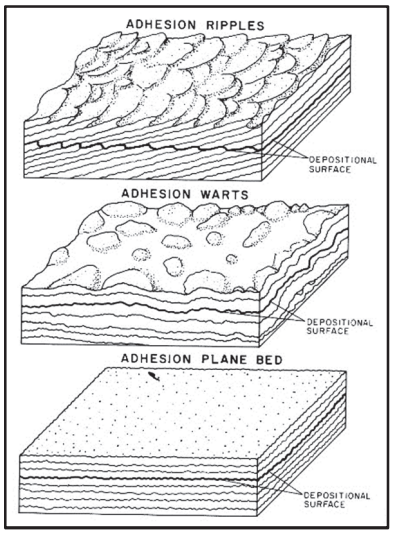

Figure 1. The family of adhesion structures: adhesion ripples, adhesion warts, and adhesion plane bed classified in Kocurek and Fielder (1982, p. 1,230). Used with permission from the Society of Economic Paleontologists and Mineralogists (SEPM).

carbonate eolianites of Quaternary age on any Bahamian island was by Hunter (late 1980s) at Bannerman Point near the southern limit of Eleuthera Island (Hunter, 2011, written communication).

STUDY SITES

In early summer, 2010, eolian adhesion structures were discovered in the Pleistocene Cockburn Town Member of the Grotto Beach Formation on southern San Salvador Island, and in the Holocene North Point Member of the Rice Bay Formation at North Point (Figure 2). Along the southern margin of the island, Pleistocene sites, S1 and S2, are on a topographic bench along sea cliffs between the easternmost pocket of French Bay called Blackwood Bay and an area of sea cliffs referred to as the Gulf (i.e. Snow Bay of other maps) further east (Figure 3). Site S1 is located at 23° 56' 50" N latitude and 74° 30' 30" W longitude, and is approximately 55 meters (180 ft) by foot-pace east of an erosional embayment called "the Cut." Site S2 is located at 23° 56' 50" N latitude and 74° 31' 11" W longitude.

Both sites are approached by traveling south to Sandy Point from the Gerace Research Centre on Queen's Highway along the western side of the island (Figure 3). At its southernmost limit, Queen's Highway turns sharply east at the junction with a segment of paved road, 200 m (~0.125 mi) long, that leads to a human-made structure labeled "jetty" on the map of southern San Salvador Island, Bahamas (Sheet 2, Bahamas Government, 1972) and labeled "government dock" (Index map, Mylroie, 1988). From this junction, Queen's Highway continues eastward and parallel to northern French Bay. At about the longitude of Blackwood Bay, a segment of the unmaintained road -an artifact of an abandoned housing project- branches southeastward from Queen's Highway and proceeds eastward to the Gulf area and beyond to Sandy Hook (Figure 4).

Adhesion structures are also found in the North Point Member of the Rice Bay Formation (Figure 2) on the east side of the North Point peninsula (Figure 3). The structures are exposed in the seaward-sloping headwall of a rocky cove at study site E3 (see Figure 8 in Caputo, this volume).

ADHESION STRUCTURES IN QUATERNARY EOLIANITES

Description

Pleistocene Cockburn Town Member, Grotto Beach Formation at site S1. In the Pleistocene Cockburn Town Member at site S1, two sets of calcarenite microridges, a term used by Hunter (1969), are exposed on eroded, weathered bedding surfaces (Figures 5A, B). In plan or bedding-plane view, microridge crests are <1-2 cm high (0.4-0.8 in), and are wavy, lobate, and bifurcated (Figure 5A. In profile view, crests are rounded to pointed. Slopes facing northeast (42°-53° and 67°-75° azimuth are narrower and steeper than the wider less steep slopes that face southwest.

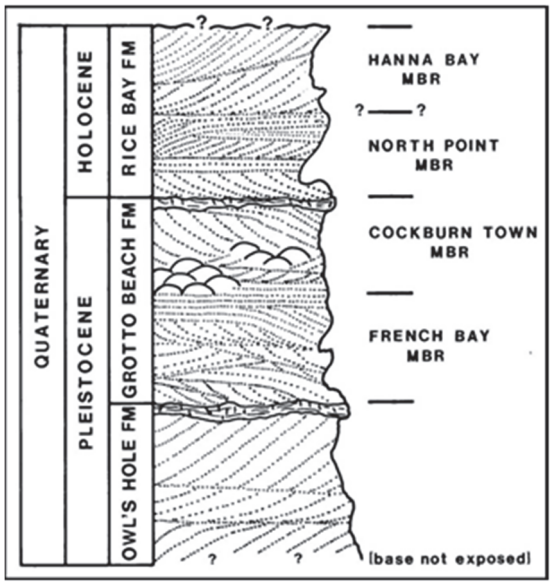

Figure 2. Lithostratigraphic subdivisions of carbonate bedrock on San Salvador Island. The Cockburn Town Member of the Grotto Beach Formation and North Point Member of the Rice Bay Formation are stratigraphic units in which adhesion structures are found. Redrawn and modified from Carew and Mylroie (1995).

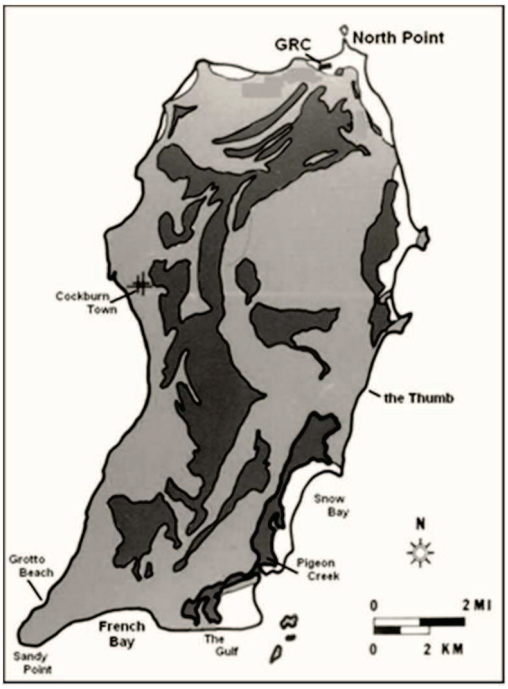

Figure 3. A simplified geologic map of San Salvador Island shows the general distribution of Quaternary bedrock and principal locations (labeled) mentioned in this report. Much of the island is underlain by Pleistocene limestone (medium gray). Holocene limestone (white) crops out discontinuously along the northern and eastern margins of the island. Interior and coastal lakes are shown by irregular dark gray areas. Redrawn and modified from Carew and Mylroie (1995). GRC = Gerace Research Centre.

Figure 4. Aerial image of part of the southern coast of San Salvador Island, and sites S1 and S2 where adhesion structures were discovered in the Cockburn Town Member, Pleistocene Grotto Beach Formation. Image courtesy of Google Earth.

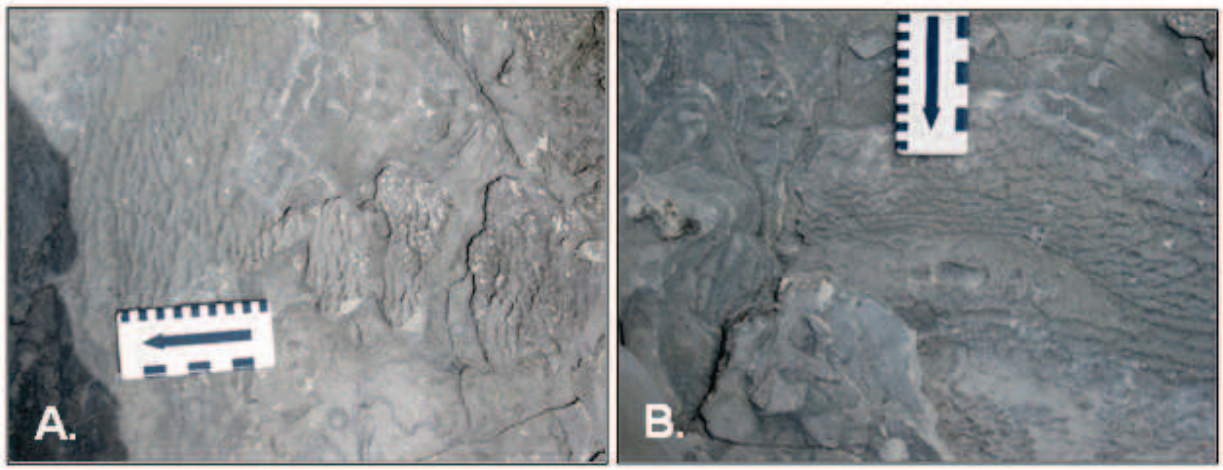

Figure 5. Ripple-form microridges in the Cockburn Town Member at site S1. A. First set: subparallel, wavy crests with steeper slopes that face northeast (arrow on scale). Scale is marked in centimeters and in inches. B. Second set of adhesion ripples: parallel wavy to lobate crests near lower right corner of scale, which is marked in centimeters and in inches. Arrow on scale points northeastward, in direction toward which steep ripple-slopes face.

Pleistocene Cockburn Town Member, Grotto Beach Formation at site S2. Microridges on a bedding-plane exposure of the Cockburn Town Member at site S2 are similar to those at site S1 (Figures 6A, B). Pointed, wavy crests, spaced 1 cm (0.4 in) apart, trend north-northeast to south-southwest (4° azimuth), and display wide gentle slopes facing westward and narrow steep slopes facing eastward (96° azimuth). Lenticular beds, up to 10 cm (4.0 in) thick), display internal structures that resemble normal foreset laminations but are actually pseudo-crosslaminations described by Hunter (1973). Their nature will be explained in a later section, Interpretation and Discussion. These foresets are straight to slightly convex upward, dip 30°-44° west, and are interbedded with strata deposited by non-adhesion, ordinary wind ripples (Figure 6C). Compare with Figure 6D (courtesy of Ralph Hunter), which shows a stratum, 3-8 cm (2-3 in) thick, composed of pseudo-crosslaminations deposited by eolain adhesion ripples in strata equivalent to the North Point Member on Eleuthera Island, Bahamas.

North Point Member, Rice Bay Formation at site E3, North Point Peninsula. At least four lenticular beds, up to 6 cm (2.4 in) thick, are found locally interbedded with normal wind-ripple laminations in bedrock swales at site E3 in the North Point Member, Rice Bay Formation on the east side of the North Point peninsula (Figures 7A, B, C). See Figure 8 in Caputo (this volume) for location of site E3. The beds are traceable laterally over a distance 4.6 to 7.1 meters (15 to 23 ft) to where they wedge-out into enclosing normal wind-ripple laminations (Figure 7A). Coastal erosion and weathering have stripped back layers of rock to expose bedding surfaces characterized by dimples less than 0.5 cm (0.2 in) deep and by wavy microridges (Figure 7B) with shape and dimensions similar to those exposed in the Pleistocene Cockburn Town Member in sea cliffs on southern San Salvador. The microridges are asymmetrical with steepest slopes that face east-northeast (76° average azimuth). Nearly vertical outcrop surfaces reveal pseudo-crosslaminations with apparent dips to the southwest. Dip angles are 16° to 19° near the base of one particular pseudo-crosslaminated bed and increase to 53° toward the upper bounding surface of the bed (Figure 7C).

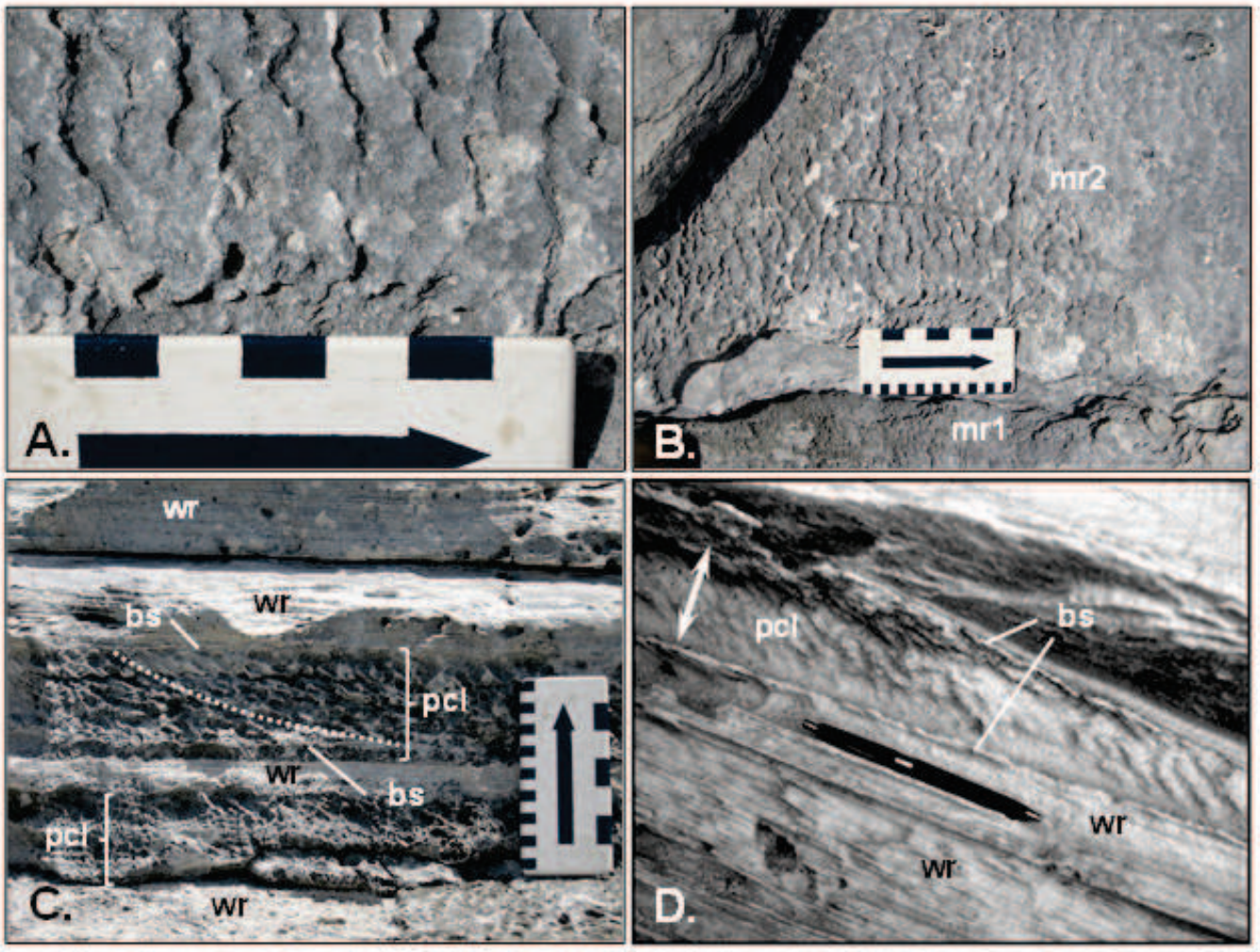

Figure 6. Surface and internal bedding structures in Cockburn Town Member, Grotto Beach Formation at site S2 on south San Salvador Island (photographs A-C). A. Local bedding-plane view of wavy microridges. Steep slopes (highlighted by shadows) face northeastward, in direction of arrow on scale, which is marked in inches. B. Zoom-out view of wavy microridges (mr1) in 6A, and underlying set of microridges (mr2). Scale is marked in inches and centimeters. Arrow points northeast. C. Vertical outcrop face parallel to current direction for 2 beds of pseudo-crosslaminations (pcl) interbedded with sets of parallel wind-ripple laminations (wr). Upper and lower bounding surfaces (bs) define contacts with wind-ripple (wr) strata. Single white dotted curve highlights shape of pseudo-crosslaminations for upper bed. Scale is marked in centimeters and inches. D. Localized bed of pseudo-crosslaminations (pcl) (white double arrow) defined by upper and lower bounding surfaces (bs) and underlain by wind-ripple laminations (wr). Pseudo-crossaminations dip 35°-37° to the right. Holocene North Point Member (?), Light House Point (also known as East End Point or Eleuthera Point (John Mylroie, 2020, written communication), southernmost Eleuthera Island, Bahamas. Photograph taken by Ralph Hunter in the 1980s and used with permission. Pen is 14 cm (5.5 in) long.

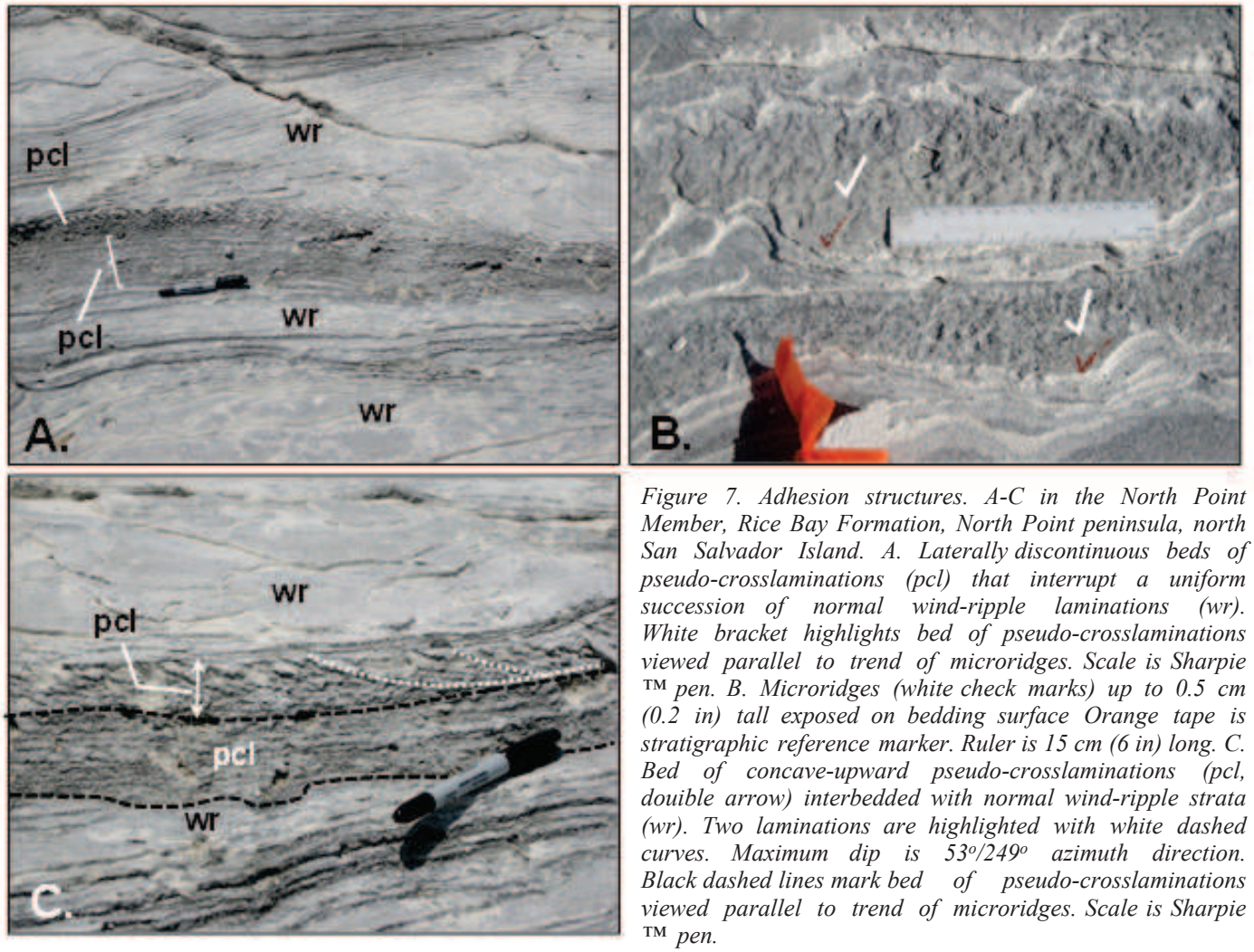

Figure 7. Adhesion structures. A-C in the North Point Member, Rice Bay Formation, North Point peninsula, north San Salvador Island. A. Laterally discontinuous beds of pseudo-crosslaminations (pcl) that interrupt a uniform succession of normal wind-ripple laminations (wr). White bracket highlights bed of pseudo-crosslaminations viewed parallel to trend of microridges. Scale is Sharpie ™ pen. B. Microridges (white check marks) up to 0.5 cm (0.2 in) tall exposed on bedding surface Orange tape is stratigraphic reference marker. Ruler is 15 cm (6 in) long. C. Bed of concave-upward pseudo-crosslaminations (pcl, douible arrow) interbedded with normal wind-ripple strata (wr). Two laminations are highlighted with white dashed curves. Maximum dip is 53°/249° azimuth direction. Black dashed lines mark bed of pseudo-crosslaminations viewed parallel to trend of microridges. Scale is Sharpie ™ pen.

Interpretation and Discussion

Eolian adhesion ripples. Ripple-like microridges exposed on bedding surfaces of the Pleistocene Cockburn Town Member, Grotto Beach Formation and Holocene North Point Member, Rice Bay Formation are eolian adhesion ripples. They are nearly identical in morphology and physical dimensions to modern siliciclastic (i.e. non-carbonate) adhesion ripples described and illustrated in Hunter (1973), Reineck and Singh (1980), and Kocurek and Fielder (1982), and especially to those on Plum Island, Massachusetts (Figures 8A, B).

The adhesion ripple marks in the Cockburn Town and North Point Members could be considered similar to wrinkle marks or runzelmarken described and pictured in Reineck and Singh (1980). However, wrinkle marks are only surface structures, and do not transport sediment and deposit stratification as ripples do. Instead, they develop by wind distorting the surface of a mass of water-saturated fine sand and silt to create the small ridges and furrows of wrinkle marks. The overall shape, larger size, and associated pseudo-crosslaminations all support an adhesion-ripple origin for the calcarenite microridges described herein.

In another example, the ripple-like microridges studied herein are comparable in shape and size to rain-impact ripples described in Clifton (1977). However, a rain-impact interpretation cannot be supported for the following three reasons (Clifton, 2011, oral communication). Reason 1: Rain-impact ripples develop steep lee slopes that face downwind

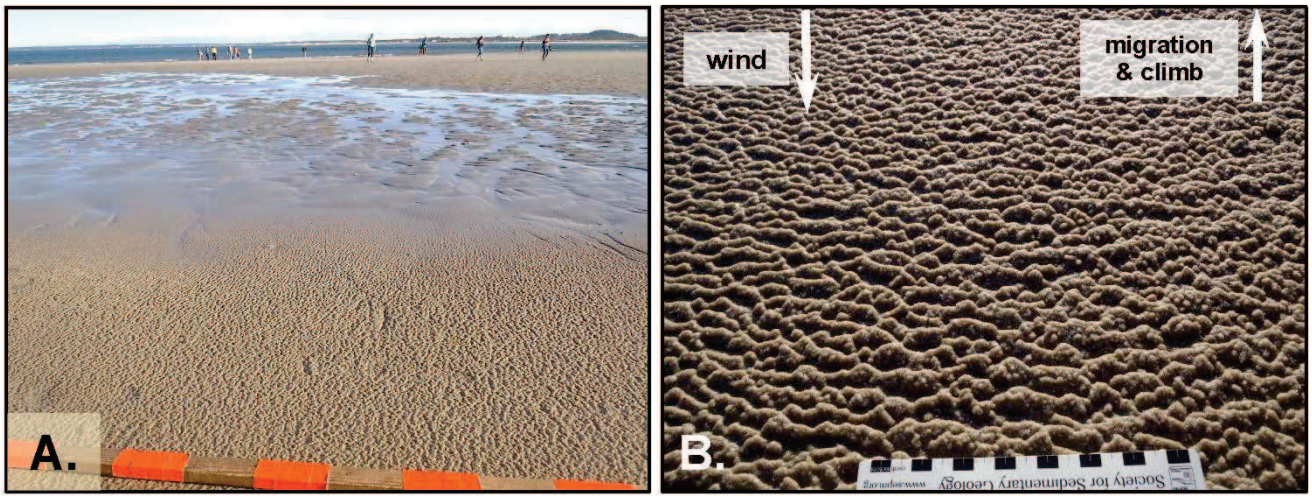

Figure 8. Modern eolian adhesion ripples in siliciclastic sand. A. Adhesion ripples forming on wet, low-tide beach, Plum Island, Massachusetts. Staff is marked in decimeters. B. Bumpy, bulbous adhesion ripples on wet low-tide beach, Plum Island, Massachusetts. Steep "stoss" slopes face upwind (toward photo top). Less steep "lee" slopes (in shadow) face downwind (toward photo bottom). Ruler is marked in centimeters. Photographs by Bosiljka Glumac and used with permission.

However, known eolian adhesion ripples migrate with their steep "stoss" slopes facing upwind. The steep "stoss" slopes for the adhesion ripples (microridges) interpreted in this study face northeast and upwind relative to the Northeast Trade Winds active during Quaternary time for San Salvador Island.

Reason 2: Bedform climbing is absent and stratification is not deposited. As will be explained in a later section, ripples and dunes climb by necessity in order to deposit stratification. In the sedimentary rocks studied here, the occurrence of eolian adhesion ripples and associated pseudo-crosslaminations, which are inclined at an angle with respect to overlying and underlying strata, is evidence that adhesion ripples, as bedforms, climbed in order to deposit pseudo-crosslaminations.

Reason 3: Rain-impact ripples are seen, so far, only as surface features in modern sediment and have low preservation potential in rocks. The physical presence of eolian adhesion ripples in the Quaternary sedimentary rocks on San Salvador is evidence for preservation and further nullifies a case for a rain-impact origin for the ripple-like microridges identified in this study.

Cross-stratification. Subaqueous (i.e. underwater) ripples and dunes and eolian dunes deposit dipping or inclined strata called cross-stratification (also called cross-strata or cross-bedding) as they move in a water or wind current. Sediment is eroded simply from the stoss or upcurrent slope and is transferred to the lee or downcurrent slope where it is deposited as cross-stratification mainly by grainflow (i.e avalanching) and grainfall (Figure 9). Cross-strata are so named because they "cross" or are inclined with respect to the general horizontal layering of sedimentary deposits (Figure 10).

By comparison with subaqueous ripples, wind ripples are not as tall; only about 1-2 cm (0.4-0.8 in) high and grain avalanching on lee slopes is absent. Eolian ripples migrate with the wind and build-up and deposit sand in the following simplified manner. Coarser grains are impelled by saltation (i.e. grain hopping or jumping) impacts and advance by rolling and sliding to the ripple crest where they settle. The result is an upward-coarsening wind-ripple stratum (Figure 11).

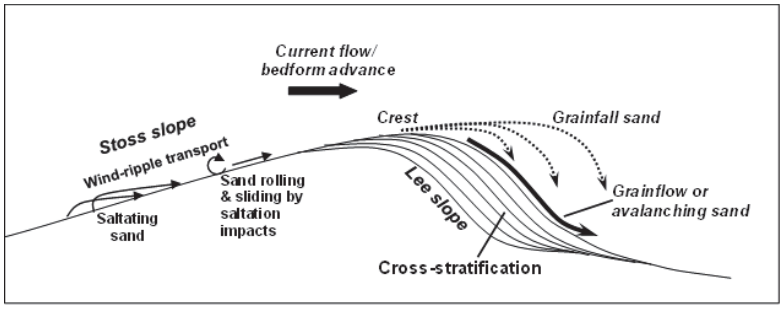

Figure 9. Simple profile of an ordinary subaqueous dune or ripple or eolian dune to show a conventional stoss slope that faces upcurrent, and lee slope that faces downcurrent. Sand is mobilized by wind ripples, grainfall, and grainflow to deposit cross-stratification on the lee slope that downcurrent.

Figure 10. Sets of cross-straification (inclined grayish strata) in between nearly horizontal pinkish bounding surfaces. Trees are several meters tall. Jurassic eolian Navajo Sandstone at Zion National Park, southwest Utah.

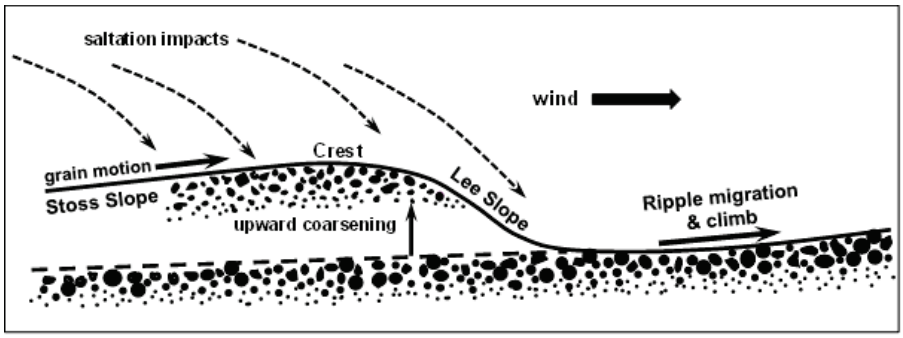

Figure 11. Simple profile of a non-adhesion eolian ripple to show essential morphological parts: stoss slope (upwind facing), crest (ripple summit), and lee slope (downwind facing). Propelled by kinetic energy imparted by saltation impacts, coarsest grains roll and slide along stoss slope and settle at the crest or tumble down lee slope to form an upward-coarsening stratum. Redrawn and modified from Collinson and others (2006, p. 90).

Eolian pseudo-crosslaminations. The thin dipping or inclined sedimentary layering in localized beds of the Cockburn Town and North Point Members (Figures 6C and 7C), including that in Figure 6D from Eleuthera Island, Bahamas, appear as cross-stratification. A viewer is given the impression that these cross-stratified beds were deposited either by tall ripples or by small dunes. See previous section, *Cross-stratification.* The resemblance to true cross-stratification is made apparent by the traces of bounding surfaces (wrinkled bounding surfaces in Figure 12), which, although dip in the direction of wind flow, they do not indicate the direction of movement in wind of the adhesion ripples themselves. In this sense, the dipping strata are pseudo-crosslaminations (Hunter, 1973) or pseudobeds (McKee, 1965).

For a normal wind ripple, the crests and lee slopes face downwind and are the sites of sediment accumulation. The gentle stoss slopes face upwind. However, this relationship between ripple shape and wind direction is reversed in eolian adhesion ripples. The "stoss" slopes of eolian adhesion ripples are steep slopes, face upwind, and are the

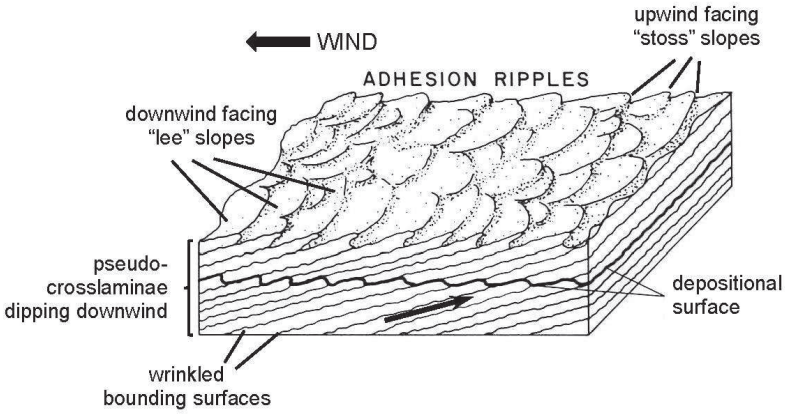

Figure 12. The sedimentary nature of eolian adhesion ripples in a wet, sandy environment. Steep "stoss" slopes face upwind and are sites of capture of wind-transported sand by surface tension and capillary action. Adhesion ripples migrate and climb upwind (black arrow on front panel) and leave traces of their upwind climb as wrinkled bounding surfaces. Modified from Kocurek and Fielder (1982, p. 1230); used with permission from Society of Economic Paleontologists and Mineralogists (SEPM).

sites of sand accumulation (Figure 12).

How adhesion ripples form. In a coastal eolian dune field, low-relief interdune swales may be wetted temporarily either by rain, storm overwash, spring-tide flooding, or by streams (i.e. wadis) that flow among the dunes. Rain will also moisten dunes but low-lying interdunes are likely places where water can pool and remain wet longer. Loose dry sand is reworked by wind from the beach or adjacent dunes, and saltates across the wet, sandy surfaces. Adhesion ripples are born when the loose, dry sand is captured by wet sand through surface tension and capillary action of water. Multiple ripples develop as sand, saltating in the wind stream, adheres to the steep upwind "stoss" slope through water capillarity. Consequently, the ripples build out by "stoss" slope accretion and migrate and climb into the wind to form the bumpy, bulbous ripple surface (Figure 8B). As long as areas of wet sand and sand capture persist, adhesion ripples will continue to form.

Bedform climbing. The nature of sediment transport in normal subaqueous or eolian ripples and dunes compels them to climb over the next downcurrent bedform in order to leave behind a stratified deposit. Otherwise, in the absence of bedform climb, that deposit will be removed by erosion. The angle of bedform climb is controlled by the amount of sediment available and the strength of the current to move it laterally (Harms et al., 1982; Hunter, 1977b).

Because adhesion ripples migrate and climb into the wind, the pseudo-crosslaminations formed dip downwind. Each downwind-dipping lamination is the depositional product of one climbing adhesion ripple and is delineated by upper and lower bounding surfaces (wrinkled bounding surfaces in Figure 12), which mark the passage of adhesion ripples above and below as they climb into the wind.

The angle of climb for eolian adhesion ripples is controlled by wind speed, angle of descent of saltation impacts (see Figure 11), the amount of dry sand available, and the water content of the sand mass over which the dry sand saltates. The wetter the sand, the capillary attraction between dry and wet sand increases and the angle of climb for adhesion ripples increases (Kocurek and Fielder, 1982). The gently increasing angle of climb of concave-upward pseudo-crosslaminations in beds of the Cockburn Town and North Point Members (see previous sections and Figures 6C and 7C) suggests that the water content of the wet mass of sand over which dry sand saltated increased slightly upward over time.

CONCLUDING REMARKS

Adhesion ripples and the pseudo-crosslaminations they deposit are newly discovered sedimentary structures in the Cockburn Town Member of the Pleistocene Grotto Beach Formation and in the North Point Member of the Holocene Rice Bay Formation on San Salvador Island, the Bahamas. They reinforce the interpretation of a coastal eolian dune system for these lithostratigraphic units.

Adhesion ripple marks cropout on bedding surfaces as low-amplitude, wavy and lobate microridges oriented roughly northwest-southeast, perpendicular to the Northeast Trade Wind direction during Quaternary time for the Bahamas. Steep "stoss" slopes face easterly and upwind, in the direction of ripple migration. When adhesion ripples were mobile, they climbed one over the other into the wind. In so doing, they deposited pseudo-crosslaminations that dip downwind and westerly. Although these laminations deceptively resemble foresets of cross-stratification, they record only the easterly direction of upwind climb of the adhesion ripples, and not the lee slope build-out and migration of the ripples that is typical for normal current ripples and dunes.

By comparison with modern adhesion ripples observed in siliciclastic, non-carbonate sediment, the Quaternary adhesion ripples on San Salvador evolved from loose, dry carbonate sand, re reworked by wind from backshore beaches and eolian dunes. The wind-driven dry sand eventually saltates across areas of wet sand. Here, surface tension and capillary action of the water in the wet sand capture the dry sand grains. The results are steep "stoss" slopes of bumpy, bulbous adhesion ripples that accrete or build out into the wind. As the ripples climb into the wind, they deposit pseudo-crosslaminations that dip downwind.

In modern coastal eolian environments, wetting of an area of sand can be achieved either by rain, storm-washover, or spring tidal flooding enhanced by wind, especially of low-lying interdunes. It is unlikely that the coastal dune fields preserved in the Cockburn Town and North Point Members were washed by tidal or storm floods. There is outcrop evidence for reef, nearshore tidal, and shoreline deposits that underlie the eolian rocks in the Cockburn Town Member (Carew and Mylroie, 1995). However, no outcrop evidence has been uncovered, so far, to suggest episodes of tidal or storm currents invading the Pleistocene eolian environment. For the Holocene North Point Member, it is also unlikely that the coastal dune field was affected by any marine incursion, given that global sea level was 2 meters (6.6 ft) lower than present sea level (John Mylroie, 2020, written communication).

Conclusively, episodic rain was responsible for wetting parts of the coastal dune fields preserved in the Cockburn Town and North Point Members. Intervals of laterally discontinuous adhesion ripples and their pseudo-crosslaminated deposits are interbedded locally with cross-bedded dune strata in the Pleistocene Grotto Beach Formation (Caputo, 1989, 1995) and with dominantly wind-ripple strata in the North Point Member (Caputo, this volume). This sedimentary relationship suggests that conditions of dry, loose, wind-blown carbonate sand in dunes and in wind ripples were interrupted briefly by rain-wetting and adhesion-ripple sedimentation. The gentle upward-concave shape of pseudo-crosslaminations indicates a slight increase in the water content of the wet sand and a slight increase in the angle of climb of the adhesion ripples. When rainfall stopped and storm clouds moved on, the wet sand dried, adhesion-ripple sedimentation terminated, and dry dune and wind-ripple sedimentation resumed until the next rainfall. Consequently, a record of localized, short-lived dry-wet-dry cycles is preserved in these Quaternary sedimentary rocks on San Salvador Island.

ACKNOWLEDGMENTS

Sincere appreciation for their helpful, insightful reviews goes to Tom Anderson (emeritus professor, Sonoma State University, CA), Ed Clifton (emeritus geologist, USGS, Menlo Park, CA), Ralph Hunter (emeritus geologist, USGS, Menlo Park, CA), Pascal Kindler (emeritus professor, University of Geneva, Switzerland), and John Mylroie (emeritus professor, Mississippi State University).

The following institutions are recognized gratefully for granting research and collecting permits in the study of Quaternary eolianites on San Salvador Island: Commission for Bahamas Environment, Science, and Technology (BEST), the Gerace Research Center, and the Bahamas Department of Agriculture.

I dedicate my work to Ralph Hunter and Ed Clifton, profound mentors in helping me understand eolian signatures in sediment and sedimentary rocks.

REFERENCES SITED

Adams, R. W. (1980). "General guide to the geological features of San Salvador (first edition), ed. D. T. Gerace (San Salvador: College Center of the Finger Lakes, Bahamian Field Station), 1-66.

Bahamas Government (1972). Bahamas, San Salvador, 1:25,000 scale topographic map, contour interval: 20 feet, Sheet 1, Nassau, New Providence, Bahama Islands, southern San Salvador Island.

Caputo, M. V. (1989). "Selective cementation of eolian stratification in Pleistocene calcarenites, San Salvador Island, Bahamas," in Proceedings of the 4th Symposium on the Geology of the Bahamas, ed. J. E. Mylroie (San Salvador Island, Bahamian Field Station, 61-72.

Caputo, M. V. (1993). "Eolian structures and textures in oolitic-skeletel calcarenites from the Quaternary of San Salvador Island, Bahamas: New perspectives on eolian limestones, Ch. 17," in Mississippian Oolites and Modern Analogs, Studies in Geology, #35, eds. B. D. Keith and C. W. Zuppann (Tulsa, OK: American Association of Petroleum Geologists), 243-259.

Caputo, M. V. (1995). "Sedimentary architecture of Pleistocene eolian calcarenites, San Salvador Island, Bahamas," in Terrestrial and Shallow Marine Geology of the Bahamas and Bermuda, Special Paper 300, eds. H. A. Curran and B. White (Boulder, CO: Geological Society of America), 63-76.

Carew, J. L., and Mylroie, J. E. (1995). "Depositional model and stratigraphy for the Quaternary geology of the Bahama Islands," in Terrestial and Shallow Marine Geology of the Bahamas and Bermuda, Special Paper 300, eds. H. A. Curran and B. White (Boulder, CO: Geological Society of America), 5-32

Clifton, H. E. (1977). Rain-impact ripples. Journal of Sedimentary Petrology, 47, 678-779.

Collinson, J. Mountjoy, N., and Thompson, D. (2006). "Chapter 6: Depositional structures of sands and sandstones," in Sedimentary Structures, (Harpenden, Hertfordshire, England: Terra Publishing), 74-137.

Gilbert, G. K. (1914). The transportation of debris by running water: U. S. Geological Survey Professional Paper 86, 263 p.

Hunter, R. E. (1969). Eolian microridges on modern beaches and a possible ancient example. Journal of Sedimentary Petrology, 39, 1573-1578

Hunter, R. E. (1973). Pseudo-crosslamination formed by climbing adhesion ripples. Journal of Sedimentary Petrology, 43, 1125-1127.

Hunter, R. E. (1977a). Basic types of stratification in small eolian dunes. Sedimentology, 24, 361-387.

Hunter, R. E. (1977b). Terminology of cross-stratified layers of climbing ripple structures. Journal of Sedimentary Petrology, 47, 697-706.

Kocurek, G., and Fielder, G. (1982). Adhesion structures. Journal of Sedimentary Petrology, 52, 1229-1241.

McKee, E. D. (1965). "Experiments on ripple lamination," in Sedimentary Structures and Their Hydrodynamic Interpretation, Special Publication 12, ed. G. V. Middleton (Tulsa, OK: Society of Economic Paleontologists and Mineralogists), 66-83.

Mylroie, J. E., editor (1988). Proceedings of the 4th Symposium on the Geology of the Bahamas, San Salvador Island, Bahamas: Bahamian Field Station, ix.

Reineck, H. -E., and Singh, I. B. (1980). Depositional Sedimentary Environments. Berlin: Springer-Verlag.

van Straaten, L. M. J. U. (1953). Rhythmic pattern on Dutch North Sea Beaches. Geologie en Mijnbouw, 15, 31-43.

White, B., and Curran, H. A. (1985). "The Holocene carbonate eolianites of North Point and the modern marine environments between North Point and Cut Cay," in Pleistocene and Holocene Carbonate Environments on San Salvador Island, Bahamas, Guidebook for Field Trip Number 2, ed. H. A. Curran (Fort Lauderdale, FL: College Center of the Finger Lakes, Bahamian Field Station), 73-94.

White, B., and Curran, H. A. (1988). Mesoscale sedimentary structures and trace fossils in Holocene carbonate eolianites from San Salvador Island, Bahamas. Sedimentary Geology, 163-184.

Wohletz, K. H., and Sheridan, M. F. (1979). "A model of pyroclastic surge," in Ash Flow Tuffs, Special Paper 180, eds. C. E. Chapin and W. E. Elston (Boulder, CO: Geological Society of America, 177-194.

DOME AND COPPICE DUNES: A REINTERPRETATION OF HOLOCENE CARBONATE EOLIANITES, NORTH POINT, SAN SALVADOR ISLAND, THE BAHAMAS

Mario V. Caputo

6326 La Reina Drive
Tujunga, California 91042 USA
(909) 214-7742 mvcaputo@earthlink.net

ABSTRACT

Earlier studies of the North Point Member, Rice Bay Formation on San Salvador Island, Bahamas clearly indicated sedimentation by wind during Holocene time. New views presented in this report of the internal structure of bedrock mounds and inter-mound swales, which characterize the physical appearance of the North Point Member, compelled a revisit to North Point and suggest dome dunes as the parent eolian dune for the North Point Member. Parallel, laterally continuous, and inversely graded *cyclic laminae* are the primary architectural elements that dominate internal structure in both bedrock mounds and swales. In bedrock mounds, these laminae preserve entire dune-forms in windward-set, topset, brinkset, foreset, and toeset strata. In bedrock swales, they record near horizontal sedimentation. Sets of *slipface crossbeds*, deposited by short-lived grainflows on dune slopes, are localized, secondary architectural elements. The cryptic nature of eolian *grainfall strata* renders them challenging to discern in outcrop. They are generally identifiable in association with slipface crossbeds and are subordinate architectural elements in eolian dome dunes.

Rainfall and coastal moisture rendered the dome-dune sand cohesive. Consequently, slipface grainflows depositing foreset sandflow strata were infrequent. Elliptical outlines exposed on a wave-cut bench on the east side of the North Point peninsula are erosional remnants of small-scale, elongate coppice dunes that accreted vertically by sand-trapping plants at the coastal margin of the main dune field. Axes of elongation of these coppice dunes are northeast-southwest, a trend consistent with inferred flow of Northeasterly Trade Wind at the time. Abundant wind-ripple laminations, scarcity of sandflows, mound-swale landscape of the present-day North Point peninsula, and the near 360^{o} span of dip azimuths of foreset cyclic laminae, bedset bounding and reactivation surfaces, and bedrock-mound-slopes argue for dome dunes that deposited the main dune ridge of the North Point eolianites. In the path of unobstructed Northeast Trade Wind, calcareous crusts and coastal plants enhanced vertical accretion and lateral expansion of eolian dome dunes to create the North Point peninsula during Holocene time on San Salvador.

INTRODUCTION

Overview

Quaternary geologic history of San Salvador Island, the Bahamas, is preserved in carbonate sedimentary rocks that were deposited in coeval reef, nearshore shelf, beach, and wind-blown environments. Sand-sized skeletal parts of once-living organisms: shell, coral, and algal fragments, and sand-sized nonskeletal grains: ooids, fecal pellets,

and peloids constitute the framework grains (allochems) that have been biomineralized mainly by invertebrate organisms on the nearshore marine shelf. Rocks composed of such framework grains are classified as carbonate sandstones or *calcarenites* (Grabau 1904; Pettijohn 1957), "sparites" (Folk 1962), and grainstones (Dunham 1962). Sayles (1931) introduced the term, *eolianites* (aeolianites, British spelling), for sedimentary rocks deposited in wind-blown or *eolian* environments. The paradox for general carbonate eolianites is that the framework grains are typically created in either a marine or subaqueous environment. For modern and ancient Bahamian carbonate eolianites, constituent sand-sized grains were formed by mainly biogenic processes on the nearshore marine shelf. Later, grains were transported by wave-, tidal-, and storm-currents, deposited on beaches, and ultimately reworked and deposited by eolian processes to form what is considered a nonmarine or terrestrial deposit of dunes, interdunes, and dune-field margins.

Geologic and Geographic Setting

The Great Bahama bank or platform of the North Atlantic Ocean is a structural feature built mostly of carbonate sedimentary rocks as old as Jurassic and some older evaporite and siliciclastic sedimentary rocks underlain by deformed continental lithosphere of the North American tectonic plate (Kindler *et al.* 2010; Mullins and Lynts 1977). The Bahamas are a chain of islands emerging from carbonate platforms and extend southeastward from Grand Bahama Island to Great Inagua Island; weather and climate are influenced by the Northeast Trade Winds (Figure 1). San Salvador Island emerges from a small, isolated carbonate platform east of the Great Bahama Bank, and has served for decades as a center for geologic, archeologic, anthropologic, oceanographic, and biologic research supported by housing, conference, and laboratory facilities at the Gerace Research Centre (GRC) located on northern San Salvador (Figure 2A).

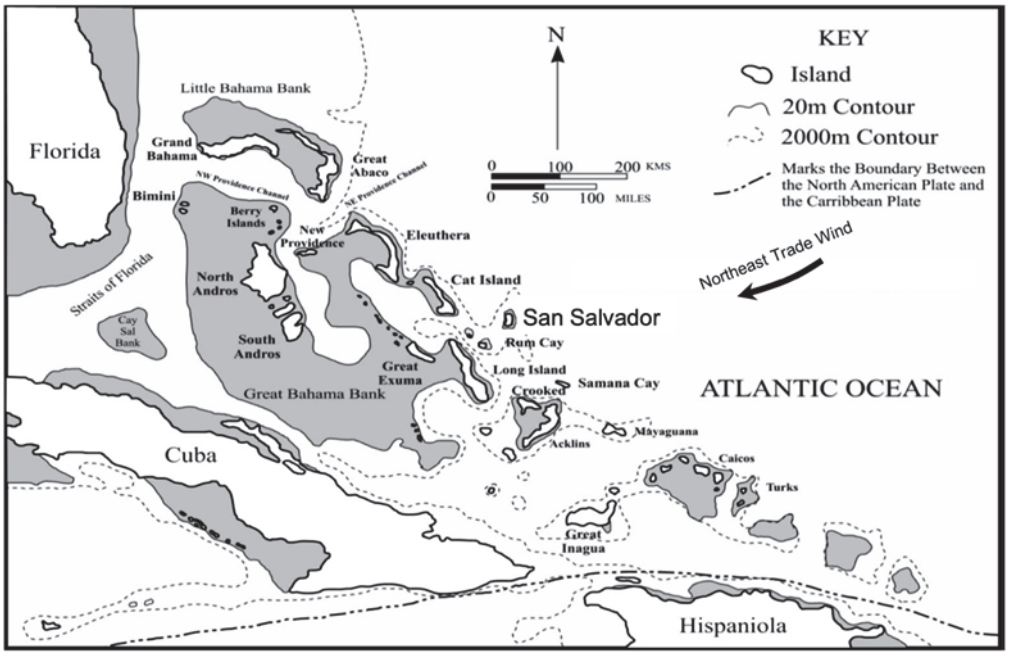

Figure 1. The Bahama Islands, including San Salvador, and the carbonate platforms (gray) from which they emerge in the North Atlantic Ocean. Gray areas at the margins of Florida, Cuba, and Hispaniola show extent of continental shelves. Adapted from Walker (2006) in Kindler et al. (2010) and used with permission from Gerace Research Centre.

Stratigraphic Setting

Orange- and yellow-colored areas on a simple geologic map of San Salvador Island (Figure 2A) show the generalized areal distribution of respective Pleistocene and Holocene sedimentary bedrock and correspond with the orange- and yellow-colored lithostratigraphic intervals of Figure 2B. The pioneering work of Carew and Mylroie (1995) refined the stratigraphic work of earlier geologists and built the original stratigraphic framework for San Salvador that proved useful for the greater Bahamas. Type localities were designated on San Salvador for the enduring lithostratigraphic units: the Pleistocene Owl's Hole and Grotto Beach Formations, and Holocene Rice Bay Formation, and respective member subdivisions. Kindler *et al.* (2010) supplemented this lithostratigraphic framework by recognizing units correlative with the Owl's Hole and Grotto Beach Formations on Great Inagua and Eleuthera Islands. They further recognized a lower Pleistocene Misery Point Formation on Mayaguana Island (southeast of San Salvador, Figure 1), an uppermost Pleistocene Whale Point Formation on Eleuthera Island (northwest of San Salvador, Figure 1), and Miocene and Pliocene deposits on Mayaguana Island.

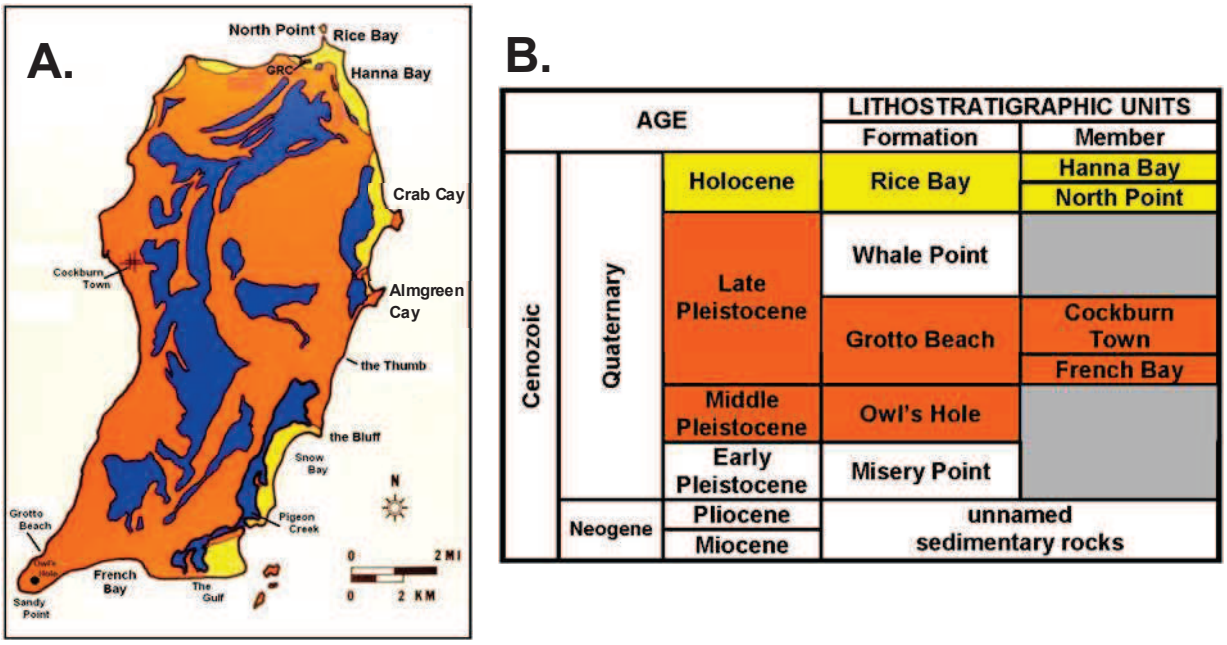

Figure 2. Bedrock lithostratigraphy and geography of San Salvador Island, the Bahamas. A. A generalized geologic map of San Salvador Island shows the areal distribution of middle and late Pleistocene (orange) and Holocene (yellow) lithostratigraphic units and their type locations. Pleistocene: Owl's Hole Fm (Owl's Hole), Grotto Beach Fm (Grotto Beach), French Bay Mbr (French Bay), Cockburn Town Mbr (Cockburn Town). Holocene: Rice Bay Fm (Rice Bay), North Point Mbr (North Point), and Hanna Bay Mbr (Hanna Bay). Colors correspond with those in Figure 2B. Other map features: interior bodies of water (blue), and Gerace Research Centre (GRC). Modified from Carew and Mylroie (1995). B. Quaternary and older lithostratigraphic units defined for the greater Bahamas. Only the Pleistocene Owl's Hole and Grotto Beach Formations and Holocene Rice Bay Formation are recognized on San Salvador Island. Redrawn from Carew and Mylroie (1995) and Kindler et al. (2010).

Purpose and Goals

This paper summarizes the results of a field study of Holocene eolianites exposed along the North Point peninsula, San Salvador Island, the Bahamas, conducted during summers, 2010 and 2013. The goals are to document sedimentary details that characterize the internal structure of the North Point Member, Rice Bay Formation, and to present an alternative interpretation on the type of eolian dune that deposited this eolianite.

Years before undertaking this study, I noticed bimodal foreset dip-directions in crossbed sets in the North Point Member, westward on the west side of the peninsula and eastward on the east side of the peninsula. I proposed testable hypotheses and field work to explain the bimodal dip pattern of foresets. One hypothesis is that westward-dipping foresets reflect normal northeasterly Trade Wind directions while eastward-dipping foresets reflect times of reversals in the Northeasterly Trade Wind, possibly related to El Niño conditions in the Pacific Ocean. A second hypothesis is that westward-dipping foresets reflect times of normal fair-weather flow of the Northeast Trade Winds, while eastward-dipping foresets reflect occasional storm winds blowing from the west, temporarily supplanting the Northeasterly Trade Wind. However, these hypotheses are refuted in this paper by evidence for eolian dome dunes and inter-dome swales.

Study Site and Methods

Within a 1.6 km (1.0 mile) walk eastward from the Gerace Research Centre lies North Point of San Salvador Island. It is a narrow ridge of rock, extends due north from the island proper, and is the northernmost point of land for the island (Figures 3A, B). In this report, the entire narrow ridge of rock is referred informally as the North Point peninsula. The peninsula once extended further north to where the island of Cut Cay is today. Sometime within the last 500 years, continued wave erosion broke through a low-lying narrow strip of land and detached the present-day North Point peninsula from Cut Cay (White and Curran, 1985). Fully accessible ground surface and moderately accessible rocky and sandy shore lend themselves to an investigation of the morphology and internal structure of Holocene carbonate eolianites preserved in the North Point Member, Rice Bay Formation.

Eleven accessible study sites on North Point peninsula were selected where photographs were taken, sketches were drawn, eolian strata were identified, and partial stratigraphic sections were measured and described. Angles and azimuth of dip of internal strata and of slopes of bedrock mounds were measured with a Brunton™ pocket transit. Sites are labeled according to their location on the east side of the peninsula as sites E1 through E10, and on the west side as site W1 (Figure 4). Stratigraphic sections were constructed by hand-leveling up from the shoreline to the highest level of exposure of a bedrock mound. Some photographic views are from the footpath that runs along the length of the peninsula northward from the Queen's Highway.

PREVIOUS WORK ON CARBONATE EOLIANITES

Historical

Since the central work on siliciclastic sediment by Henry Clifton Sorby in the 1800s, much experimentation and field work have advanced an understanding of how unconsolidated sediment is transported at the sediment-fluid interface by flowing water (subaqueous) and wind (eolian) to create bedforms such as ripples and dunes and internal architecture of cross-stratification. Eolian cross-strata have been

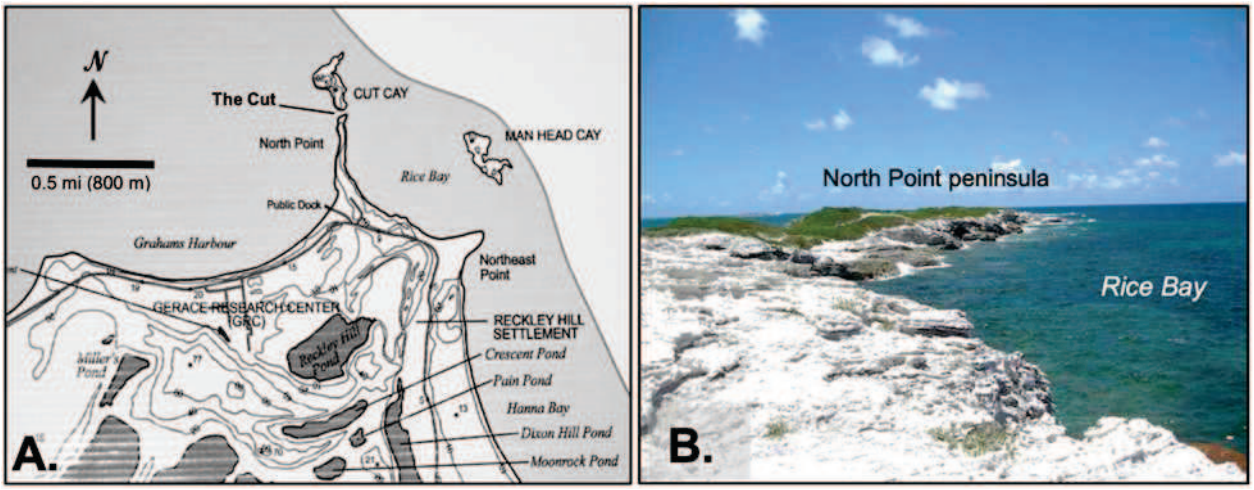

Figure 3. The North Point peninsula, northern San Salvador Island. A. Map perspective of the North Point peninsula relative to the Gerace Research Centre (spelled "Center" on map) and neighboring locations: Man Head Cay, Rice Bay, Grahams Harbour, Cut Cay, and the Cut. Courtesy of Gerace Research Centre, © 2003, and Department of Geological Sciences, Indiana University, Bloomington. B. Peninsula surface of bedrock mounds and plant-overgrown eolian sand hills. Eastern shoreline of formidable bedrock mounds modified by waves into headlands and rocky coves.

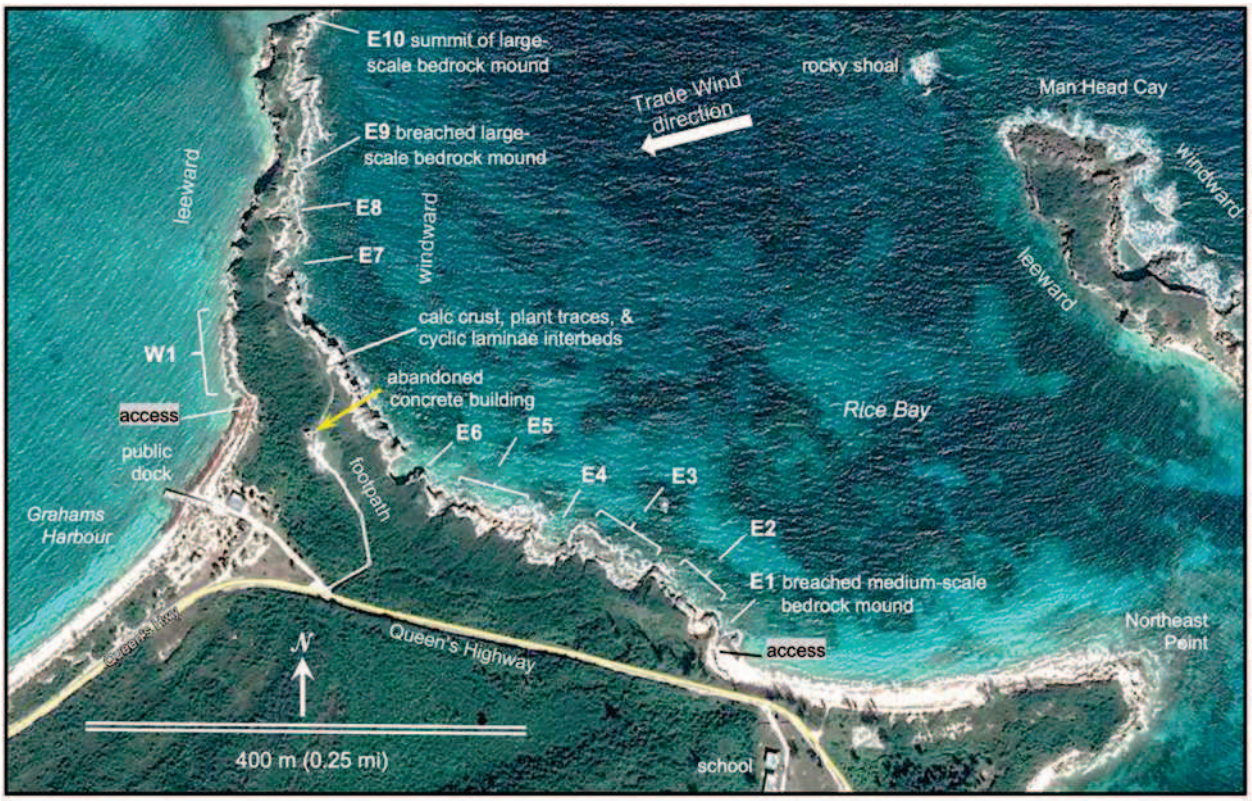

Figure 4. Aerial view of the North Point peninsula, San Salvador Island. Marked are locations of study sites where observations of surface and internal architecture of bedrock mounds and swales were recorded, measured, and photographed for this study. Study sites on east side are E1-E10. Study site on west side is W1. Image extends only to the northern tip of North Point peninsula. The "Cut" and Cut Cay are not shown. Image courtesy of Google Earth.

recognized in modern and ancient carbonate sand and sandstones (i.e. calcarenites) since the time of Charles Darwin during his voyages on the *HMS Beagle* in the early 1850s (Fairbridge 1995). Nelson (1837) is probably the first to make note of cross-stratified carbonate eolianites as a significant component of the bedrock of Bermuda, and Nelson (1853) drew some of the earliest sketches of carbonate "aeolian rock" from the Bahamas. Evans (1900) is acknowledged for his detailed study of the internal structure of carbonate eolianites in India. McKee and Ward (1983) assembled an encyclopedic reference on carbonate eolianites known in areas of the world where wind, climate, and marine conditions combine to build and preserve cross-stratified carbonate eolian dunes. Abegg *et al.* (2001) provided a much needed overview of carbonate eolianites and assembled a line-up of papers by authors who recognized ancient carbonate eolianites ranging in age from Paleozoic to Quaternary. Noteworthy in that book is the paper by Blay and Longman (2001), who identified cross-stratified carbonate eolianites on the volcanic island of Kauai, Hawaii.

On San Salvador Island

Previous work on the Quaternary calcarenites on San Salvador offered early interpretations on morphology and internal structure of formative eolian dunes. Adams (1980) and geoscientists after him have recognized the striking cross-stratified internal structure of Quaternary carbonate eolianites on San Salvador Island, and complementary terrestrial features: root and stem casts of plants, insect burrows, subaerial crusts, paleosols, and invertebrate fossils. Adams (1980) further alluded to mound- or dome-like Holocene dunes on the North Point peninsula when he described large-scale cross-strata on leeward, windward, and flanking dune slopes but considered the dune morphology as lobate, as did White and Curran (1985, 1988). Caputo (1995) applied azimuth measurements of crossbed foresets and linear trends in remnant paleo-topography and concluded that the French Bay and Cockburn Town Members of the Pleistocene Grotto Beach Formation were deposited by lobate, sinuous-crested dune ridges in northeasterly wind along the southern and eastern margin of San Salvador.

For an eolian dune, a set of cross-strata or foresets is usually comprised of sandflow beds deposited by grainflow or sand avalanches on dune slopes. Typically associated with eolian sandflows are inversely graded laminations deposited by migrating wind ripples, and fine-grained grainfall strata deposited by sand settling from suspension in wind (Hunter 1977a, 1981) (Figure 5). White and Curran (1985, 1988) recognized signature eolian ripple-, grainfall-, and sandflow-strata in the Holocene North Point Member, Rice Bay Formation on the North Point peninsula on San Salvador Island. In their 1988 paper, they were first to notice the association between grain texture, diagenesis, and weathering patterns of the different eolian strata in the Holocene North Point Member. This association was further demonstrated not only in eolian strata of the North Point Member but in recognizable eolian strata in Pleistocene calcarenites cropping out at the eastern, southern, and southwestern margins of San Salvador by Caputo (1989, 1993, 2015). In those studies, thin sections revealed that textural and diagenetic traits of wind-ripple-, grainfall-, and sandflow-strata can be correlated directly to weathering patterns seen in outcrops. Finer grained, tightly packed, and well cemented strata as in grainfall laminations and in basal parts of inversely graded wind-ripple laminations, weather into protruding micro-ledges. In contrast, coarser grained, loosely packed,

and poorly cemented strata, as in sandflow beds and in upper parts of inversely graded wind-ripple laminations, weather as micro-recesses.

Wind-ripple strata in modern and ancient carbonate and siliciclastic deposits differ from water-ripple strata by their thin, upward coarsening laminations and faintly developed foreset laminations (Figure 6). Comparative features of eolian and subaqueous ripple strata summarized in Table 1 are derived from studies of siliciclastic sediments and rocks but apply also to carbonate eolian deposits. The presence of inversely graded wind-ripple laminations are positive indicators of an eolian origin for modern and ancient deposits that preserve them (Hunter 1981; Kocurek and Dott 1981.

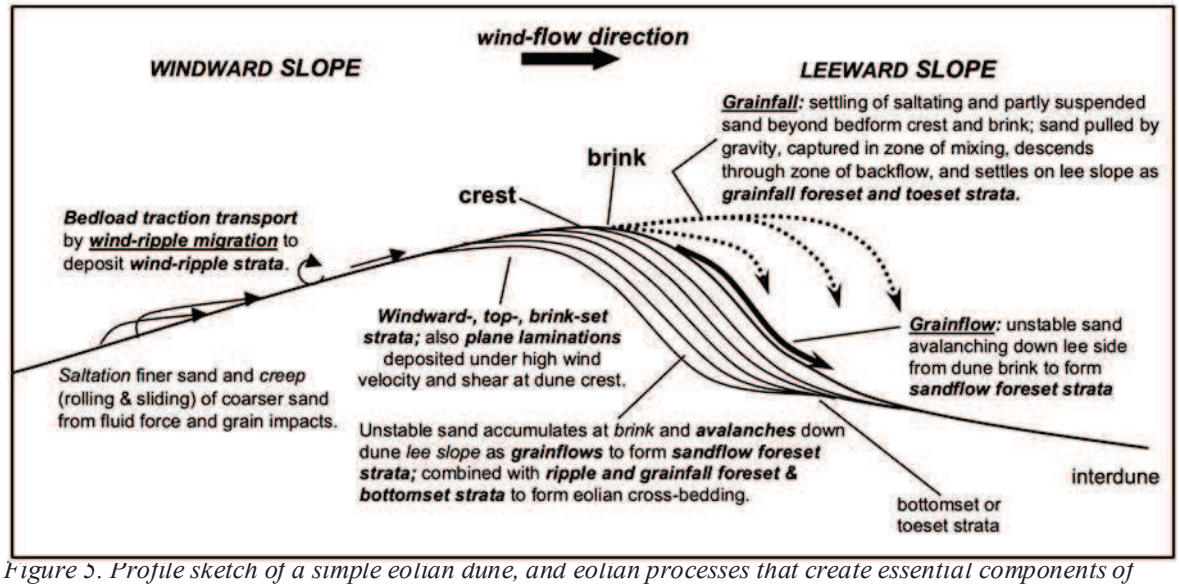

Figure 5. Profile sketch of a simple eolian dune, and eolian processes that create essential components of internal structure: 1) wind-ripple migration by traction transport (saltation and creep) to form wind-ripple strata, 2) grainfall of partly saltating and suspended sand settling on leeward slope of dune to form grainfall strata, and 3) grainflow of unstable sand avalanching down leeward slope to form sandflow foreset strata (from Caputo 2017; used with permission from Pacific Section SEPM, Society for Sedimentary Geology).

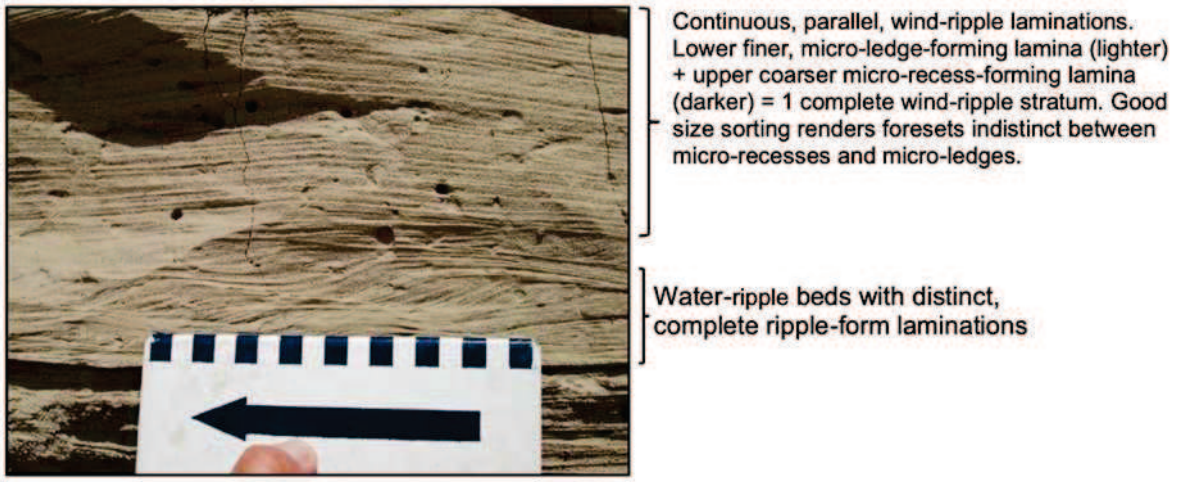

Figure 6. Contrasting wind- and water-ripple strata in siliciclastic sand. Exposure is in valley wall in alluvial Carrizo Wash, Anza-Borrego Desert, California. Water-current flow was to the left. Paleo-wind direction is indeterminable in the absence of distinct ripple foreset-laminae. Scale is in centimeters (modified from Caputo, 2017). See Table 1.

Table 1. Comparison of sedimentary characteristics between wind-ripples and water-ripples and their deposits (from Caputo, 2017; used with permission from Pacific Section SEPM, Society for Sedimentary Geology). See Figure 6.

Sedimentary Characteristics		Wind-Ripples	Water-Ripples
Bedform	Amplitude	**2-10 mm (0.08-0.40 in)** (Collinson et al., 2006; Hunter, 1977a)	**up to 6-8 cm (2.4-3.2 in)** (Ashley, 1990)
	Spacing	**5-20 cm (2-8 in)** (Lancaster, 1995)	**10-20 cm (4.0-8.0 in)** (Harms et al., 1982)
Grain Texture	Size	**Very fine- to medium-grained sand** (Lancaster, 1995)	**Silt to coarse-grained sand** (Middleton and Southard, 1984)
	Sorting	**Good** (based on above grain-size range)	**Poor** (based on above grain-size range)
	Grading	**Inverse/Upward-coarsening** (Collinson et al., 2006; Schenk, 1983)	**Normal/Upward-fining** (Simons et al., 1965)
Internal Stratification	Strata Thickness	**typically 1-10mm (0.04-0.4 in); average 2.0 mm** (Hunter, 1977b)	**Up to 6-8 cm (2.4-3.2 in)** (based on ripple amplitude)
	Cross-lamination	**Faintly developed cross-laminae** (Hunter, 1977a; Kocurek and Dott, 1981)	**Well-developed cross-laminae** (Kocurek and Dott, 1981)

KEY PHYSICAL FEATURES OF THE HOLOCENE NORTH POINT MEMBER ON NORTH POINT

Present-day Mound-Swale Topography

One key feature that lends support to the eolian-dune origin for the Holocene North Point Member is the present-day topography of the North Point peninsula. High-relief *bedrock mounds* and low-relief inter-mound *bedrock swales* are the characteristic physiographic features expressed by the North Point Member (Figures 7A-D). Ideal exposures are on the windward side of the North Point peninsula; from the nearest approach of the Queen's Highway near Rice Bay beach to the end of the peninsula (Figure 4). Bedrock mounds are exactly that; dome or hemispherical, positive-relief surface features. They are semi-circular to semi-oval in map view and vary in height from south to north, from the island mainland to Cut Cay, along the axis of the peninsula. From the eastern limit of the sandy beach at Rice Bay, bedrock mounds are only a few meters high. Continuing northward, bedrock mounds peak at more than 10 m (33 ft) in height about midway along the peninsula then decrease to less than 10 m (33 ft) in height approaching the tip of the peninsula and beyond to Cut Cay (Figure 8).

Internal stratification of Bedrock Mounds and Inter-mound Swales

Internal sedimentary architecture or structure of bedrock mounds and swales of the North Point peninsula further supports a re-interpretation of the eolian-dune origin for the Holocene North Point Member on San Salvador as follows: 1) internal stratification mimics and is parallel to the hemispherical shape of bedrock mounds, 2) internal strata and mound slopes dip in nearly all compass directions (see Table 2), and 3) the internal strata of bedrock mounds are laterally continuous with strata of inter-mound swales (Figures 7A-D).

Depositional and erosional processes operating in a sedimentary environment impart an internal arrangement of sedimentary components - architectural elements or internal structure- to a body of sediment or sedimentary rock. They yield clues as to how the deposit was constructed. Architectural elements are the building-blocks of a sedimentary deposit and range in scale from framework grains and intergranular pores (Caputo 1995) to the sediment fill of basins (Walker 1992).

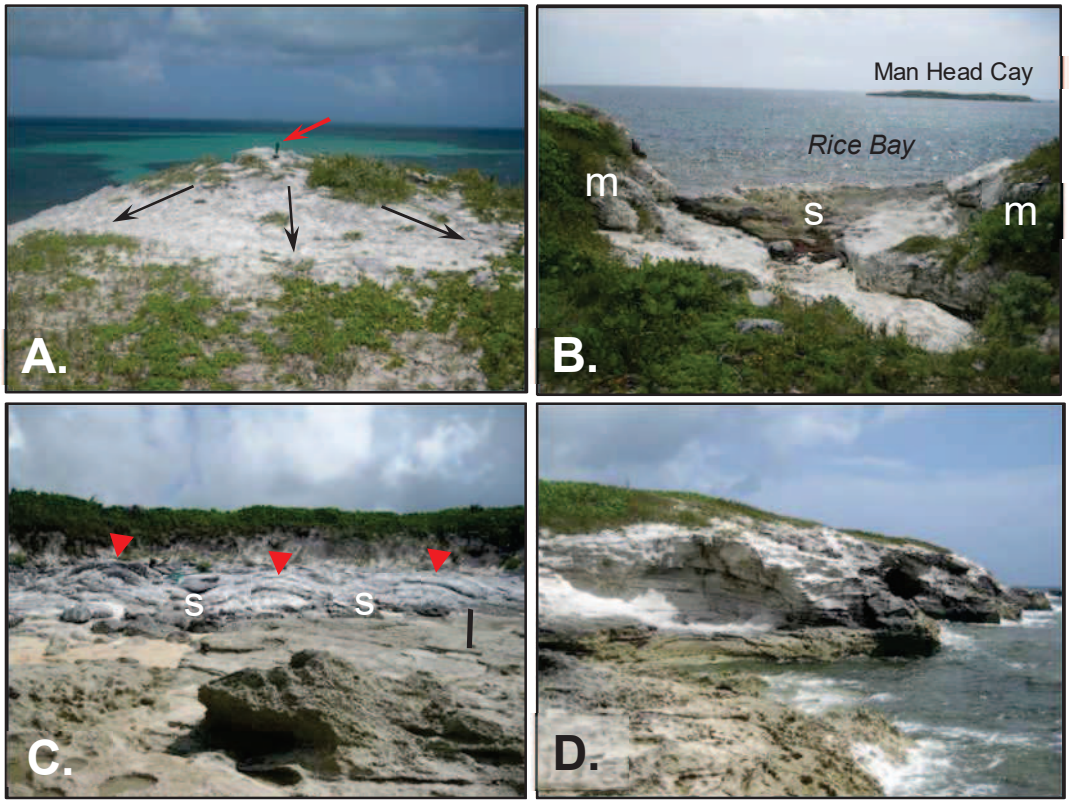

Figure 7. Outcrop features of the Holocene North Point Member, North Point peninsula, San Salvador Island. A. Large-scale bedrock mound exposed at study site E10 near the northern limit of the peninsula. Black arrows indicate slope directions of mound surface and dip of internal stratification. Red arrow points to short sledgehammer for scale. B. Bedrock swale (s) wetted by high tides and storm waves between headland-forming bedrock mounds (m). View from eastern North Point peninsula toward Rice Bay and Man Head Cay. C. Small-scale bedrock mounds (red triangles) with surfaces and internal bedding laterally continuous with that of inter-mound swales (s) overlain by modern eolian sand and maritime plants. Black scale bar is 1 m (3.3 ft) long. Rocky cove at study site E2. D. Large-scale breached bedrock mound with characteristic convex-upward, arching roof and internal strata. Dip directions of visible surface and internal strata span clockwise from north-northeast to southwest. Study site E9.

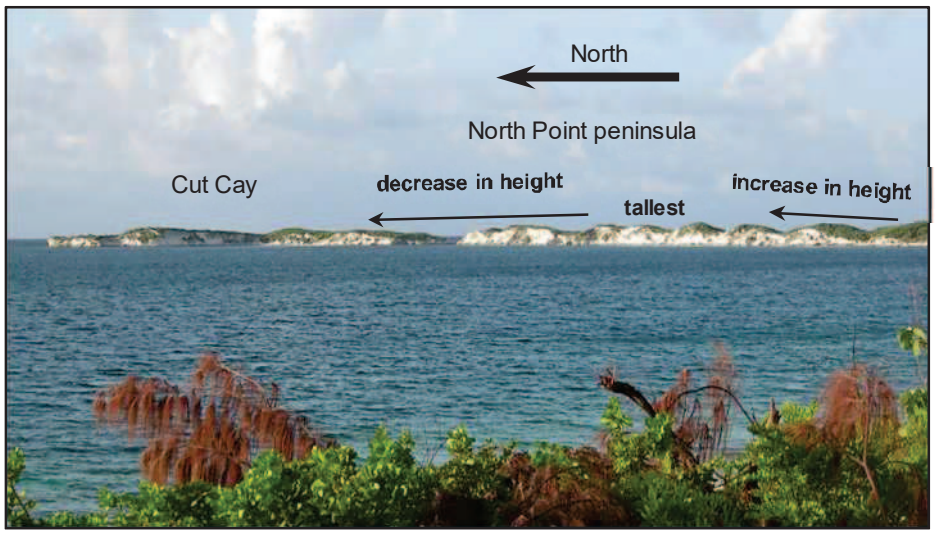

Figure 8. Bedrock mound and swale landscape of present-day North Point peninsula and Cut Cay. Mound height increases, reaches a maximum, then decreases northward along the peninsula to Cut Cay. Photograph is approximately the northern two-thirds of the peninsula; photograph taken from the Queen's Highway near front entrance of the Gerace Research Centre.

Eolian architectural elements at the stratification scale are wind-ripple-, grainfall-, and sandflow-strata. They result from wind-ripple, grainfall, and grainflow processes
the carbonate eolianites on San Salvador Island. Grain-scale architectural elements for Quaternary carbonate eolianites on San Salvador are described in Caputo (1989, 1993). *Cyclic laminae* and *slipface crossbeds* are the stratification-scale architectural elements that are essential to a discussion of an eolian-dune origin for the North Point Member.

Cyclic laminae. Fine sandy laminations notably constitute the greatest proportion of internal stratification comprising both mound and swale bedrock. They are designated herein as the primary architectural elements in the North Point Member. The descriptive name, cyclic laminae, refers to a persistent recurrence of alternating white and gray laminations (2-5 mm; 0.1-0.2 in thick) of fine and medium calcareous sand grains, the textural, packing, and cementing attributes of which control a weathering pattern of regularly alternating micro-ledges and recesses (Caputo 1989, 1993) (Figure 9A). Cyclic laminae: 1) fill bedrock swales with nearly horizontal, alternating light and dark "pin-stripe laminations" (Fryberger and Schenk 1988) (Figure 9A); 2) weather locally along stratification contacts to form pseudoripples (Kocurek and Dott 1981) (Figure 9B); 3) occur in sets of concave-upward, low-angle foreset laminations, and convex-upward, arching beds that conform to the morphology of bedrock mounds (Figures 9C-F); 4) are punctuated by semi-uniform intervals of calcareous crusts with plant-stem trace fossils (Figure 9G), 5) comprise convex-upward windward-set, topset, and brinkset strata; 6) comprise foreset strata locally interrupted by reactivation surfaces; and 7) completely preserve entire dune-forms (Figure 10).

Slipface crossbeds. Secondary architectural elements in the North Point Member are herein named *slipface crossbeds.* They are what constitute conventional foreset bedding of cross-stratification. However in the North Point Member, their occurrence is markedly lesser in abundance relative to cyclic laminae. They are distinguished by the following characteristics: 1) upward-coarsening, medium-grained texture, 2) beds up to 3.0 cm (1.2 in) thick that taper down-dip into toesets of cyclic laminae, and 3) in transverse view, their lens-shaped cross-sections encased in grainfall strata (Figures 11A, B, C). Erratic northward and southwestward dip azimuths of sandflow crossbeds are inconsistent with those of mound-slopes, cyclic laminae and their bounding surfaces, all of which span nearly 360^{o} (Table 2).

Grainfall strata. The grainfall sedimentary process and resulting grainfall strata (Figure 5) are found typically interstratified with sandflow beds (i.e. slipface crossbeds of this report) (Figures 11B, C), are addressed in Caputo (1989, 1993, 1995), and are not essential to the reconstruction of the Holocene eolian dunes in this report.

Figure 9 on facing page. Details of interior structure of bedrock mounds and swales, North Point Member. A. Bed of cyclic laminae or "pin-stripe laminations" (Fryberger and Schenk, 1988) cropping out as white finer-grained micro-ledges alternating with gray, coarser-grained micro-recesses. Near vertical exposure of inter-mound swale-fill. Scale is marked in centimeters. B. Cyclic laminae (cl) and associated pseudoripples (pr) on weathered and eroded bedrock surface. Scale is 18 cm (7 in) long. Arrow points in direction of ripple migration and climb. C. Intricate concave-upward sets of cyclic laminae (cl) within bounding surfaces (solid black curves), and interbedded slipface crossbeds (red arrows). Cyclic laminae above yellow dashed line conform to hemispherical shape of bedrock mound. Study site E5. Scale is 18 cm (7 in) long. D. Partial profile of medium-scale bedrock mound composed of cyclic laminae excavated by wave erosion. Study site E1. Black vertical bar is 1 m (3.3 ft) long. E. Intersecting, large-scale bedrock mounds (outlined by white dashed curves) constructed of cyclic laminae (cl). West side, midway along North Point peninsula, north of study site W1. Red arrow points to cylindrical boat-bumper (flotsam) for scale. F. View of interior of upper bedrock mound composed of cyclic laminae (cl) and localized sets of slipface crossbeds (sf) (doubly pointed yellow arrows. Bed outlined by red dashed lines (bounding surfaces) displays down-dip transition from cyclic laminae (cl) to slipface crossbeds (sf) then back to cyclic laminae (cl). Study site E5. Rectangular scale is 18 cm (7 in) long (white arrow). G. Ledge- and bench-forming beds composed of plant-stem trace fossils and calcareous crusts (ptf) alternating with cyclic laminae (cl). Cliff top east of abandoned concrete building (see Figure 8). Scale is 18 cm (7 in) long (red arrow).

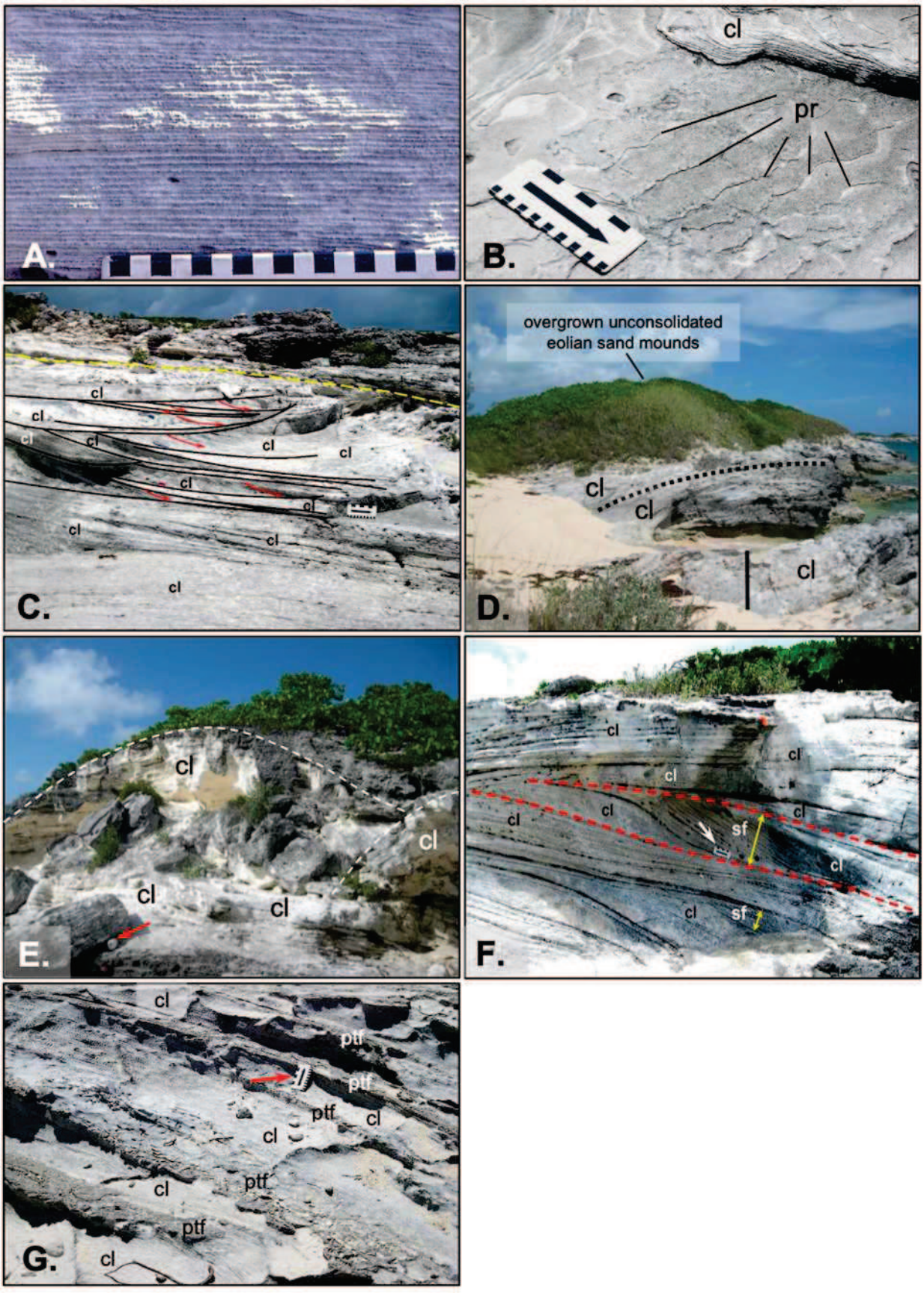
A.
B.
cl
pr
C.
cl
D.
overgrown unconsolidated
eolian sand mounds
E.
F.
sf
G.
ptf

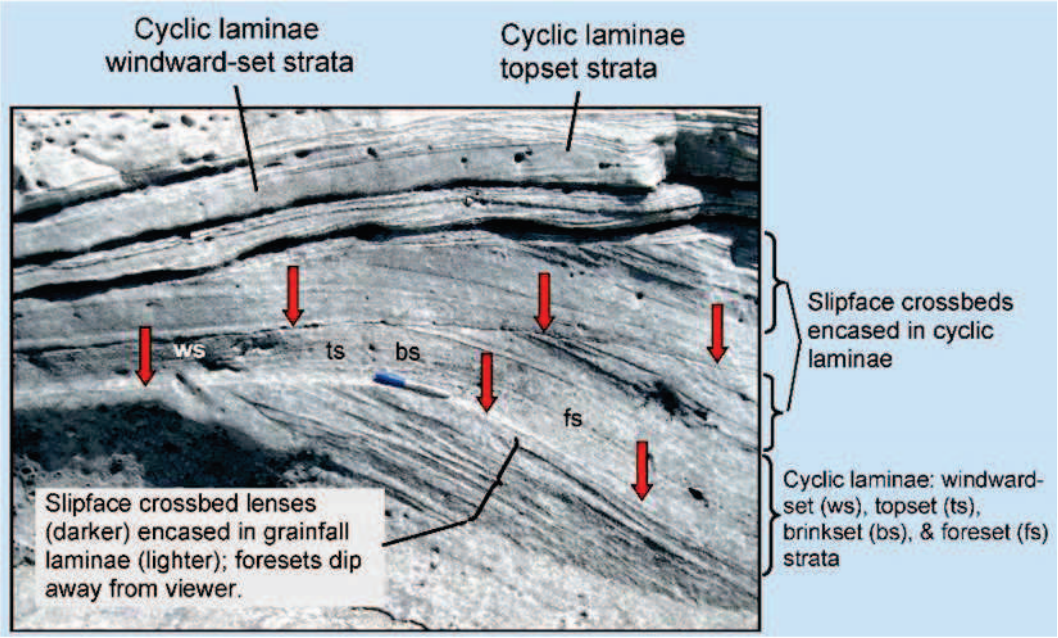

Figure 10. Complete dune-form strata constructed of cyclic laminae preserved as windward set (ws), topset (ts), brinkset (bs), and foreset (fs) strata. Note arching of uppermost windward and topset strata. Localized slipface crossbeds are marked by brackets along middle right edge of photograph. Reactivation surfaces are marked by red arrows. Blue Sharpie™ pen for scale. Modified from Caputo (2019).

Figure 11. Slipface crossbeds. A. Longitudinal view of sets of tangential to angular slipface crossbeds (sf) wedging downdip into toesets of cyclic laminae and separated by microledge-forming grainfall laminae. Interior of weathered, eroded bedrock mound. West side North Point peninsula. Red Sharpie™ pen for scale (black arrow). B. Longitudinal view of wedge-shaped bed of slipface crossbeds (two beds are marked with red arrows) overlain by sets of cyclic laminae (cl). Slipface crossbeds taper down-dip into toesets of cyclic laminae and are outlined by light-colored, micro-ledge-forming grainfall strata. Scale is 18 cm (7 in) long. C. Transverse, down-dip view of lenses of slipface crossbeds, encased by white, lenticular outlines of grainfall strata underlain by cyclic laminae (cl). Blue Sharpie™ pen for scale.

Table 2. Span of dip directions (in degrees azimuth) for foreset cyclic laminae, bounding surfaces, and slopes of bedrock mounds. n = number of measurements at each study site. See Figure 4 for location of study sites.

Site	Azimuth Span of Dip: Internal Stratification & Mound Slopes	n
E1	82°-310°	14
E2	29°-338°	10
E3	8°-355°	30
E8	4°-350°	18
W1	3°-336°	25

Erosional remnants of strata crop out 4 to 6 cm (1.6 to 2.4 in) above a wave-washed bench as concentric, elliptical ridges that vary in length from 2-4 m (6.6-13.2 ft) along their long axes. Truncated strata along the elliptical outlines dip away from the core of each ellipse in all compass directions. The elliptical shape and bedding attitude resemble a view on a geologic map of an anticline, and suggest that, perhaps, some volume of bedrock mass in the vertical dimension had been stripped away over time by wave erosion, leaving the remains of strata curving around in elliptical configurations, the axes of which trend generally northeast-southwest (Figure 12A, B).

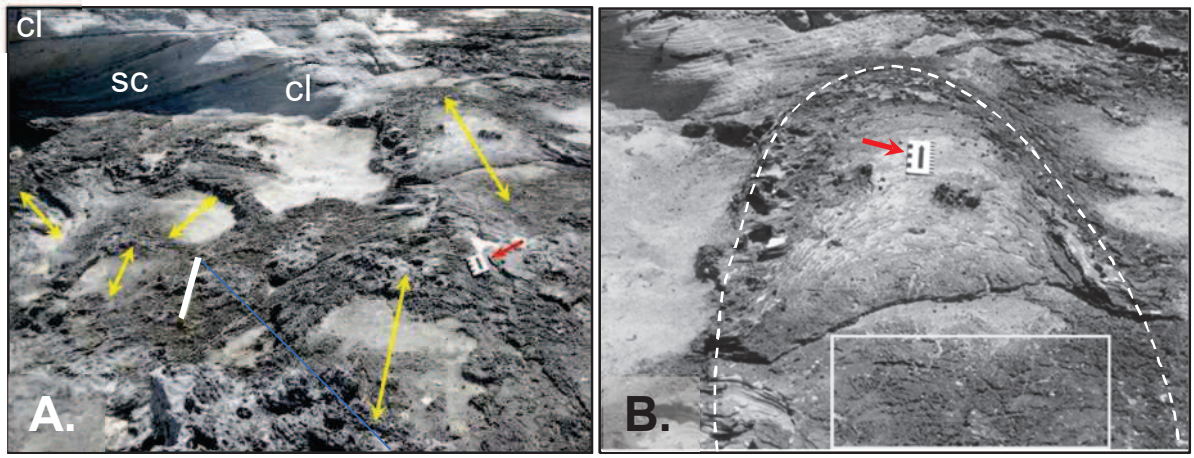

Figure 12. Concentric elliptical configurations made by ridges of erosional remnants of strata protruding up on a wave-washed bench cut into bedrock of the North Point Member at study site E5. A. Concentric erosional remnants of bedding in elliptical outlines; long-axes (yellow arrows) trend NE-SW. Headwall of cove is composed of cyclic laminae (cl) and slipface crossbeds (sc). White bar scale at center left is 0.6 m (2.0 ft) long; scale at center right (red arrow) is 18 cm (7 in) long. B. Close-up of part of the longest elliptical bedding trace (upper right in A) outlined by white dashed curve. Azimuth trend is 236°. Fossil impressions of unidentifiable plant material are preserved in area enclosed in white rectangle. Scale (red arrow) is 18 cm (7 in) long.

EOLIAN DUNE INTERPRETATIONS FOR QUATERNARY EOLIANITES

Earlier Lobate Dune Interpretation for the North Point Member on San Salvador Island

Structure and origin of Bahamian and Bermudan carbonate eolianites of Quaternary age have been attributed to coast-parallel eolian dune ridges that evolved from coalesced, elongate lobate dunes (e.g. Mackenzie 1964a, b; McKee and Ward 1983), or what Ball (1967) referred to as "eolian spillover lobes." White and Curran (1985, 1988) published the first interpretations of eolian dunes for the North Point Member on San Salvador and proposed a lobate-dune origin for Holocene eolian dunes that deposited the North Point Member on San Salvador Island. Amplifying the lobate-dune interpretation, they described the Holocene North Point dunes as a series of downwind-extending lobes that advanced principally westward, and concluded that over time, individual lobate dunes coalesced laterally to form the north-south trending dune ridge of the North Point peninsula. The protruding lobes yielded a wavy ridge-crest perpendicular to the prevailing Northeast Trade Wind, and the "…hummocky dune ridge…with undulating topography…" of the North Point peninsula today.

Relative to eolian dunes that are normal to wind flow, such as transverse, barchan, and parabolic dunes, a lobate eolian dune is an elongated, finger-like eolian bedform, characterized by a convex downwind-facing leeside in longitudinal view, and lateral slopes in transverse view where grainflows can potentially mobilize and deposit sandflow cross-strata. As an example, Pleistocene lobate dunes interpreted by Mackenzie (1964a, b) on the Bermuda islands are up to 20 m (66 ft) high, with axial lengths of up to 100 m (330 ft). Crossbed sets are up to 23 m (~75 ft) thick and are composed of convex-upward sandflow foresets that conform to the leeside profile of the lobate dune. He described how lobate dunes merged laterally to form a continuous shore-parallel dune ridge perpendicular to onshore wind.

Lobate dunes have not yet been recognized in any morphological classifications of eolian dunes (e.g. Lancaster 1995; McKee 1979a; Pye and Tsoar 1990). They can be considered as terrestrial counterparts to submarine spillover lobes, which have been observed in oolitic sand belts in the Bahamas (Ball 1967). Although Quaternary eolianites on Bahamian islands and other worldwide locations where carbonate sand is generated are composed of marine allochemical grains, they differ in internal structure from those deposited by submarine spillover lobes in the following ways as described by Ball (1967): 1) complete dune-form preservation enhanced by early subaerial cementation and plant stabilization, 2) thicker cross-bed sets, 3) root casts interbedded with thin laminations, which are similar to the interbeds of cyclic laminae the $CaCO_3$ crusts, and the plant-stem fossils described herein. Blay and Longman (2001) conceptualized ideal, elongated lobate dunes in Quaternary carbonate eolianites on Kauai, Hawaii (Figure 13).

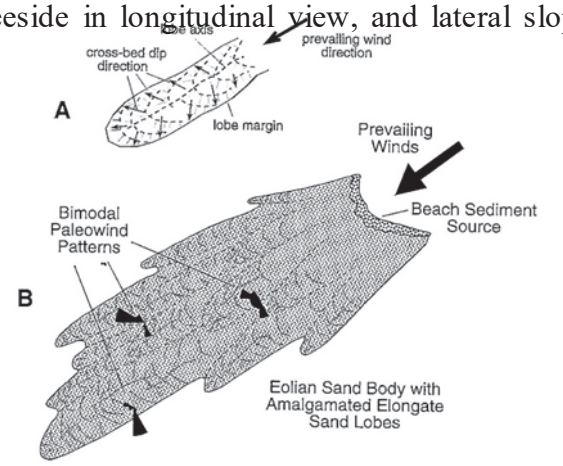

Figure 13. Lobate eolian dunes as interpreted by Blay and Longman (2001) for the carbonate eolianites exposed on southwestern Kauai, Hawaii. A. Basic intrinsic features of a single, elongated lobate dune inferred from eolianite outcrops. B. Depositional model for Quaternary carbonate eolianites resulting from the coalescing of individual eolian lobate dunes to form the amalgamated eolian calcarenite body. Used with permission from SEPM (Society for Sedimentary Geology).

Dome Dune Re-interpretation for the North Member on San Salvador Island

While earlier ideas proposed for Holocene sedimentation in the North Point Member by eolian lobate dunes or eolian counterparts to marine spillover lobes ideas are compelling, the outcrop features preserved in the North Point Member and described in this report support a case for eolian sedimentation in a complex of dome dunes during Holocene time. See also Caputo and Glumac (2013) and Caputo (2019). The outcrop features are: 1) dome- or hemispherical-shapes of bedrock mounds with internal stratification that conforms to the external dome shape, 2) cyclic laminae, which are the products of wind-ripple sedimentation, dominate the internal structure of bedrock mounds (i.e. dome dunes) and continue laterally into inter-mound swales (interdune areas between domes), 3) rare mobilization of carbonate sand by grainflows on dune slopes is evidenced by the low abundance of slipface crossbeds in the North Point Member and further suggests little lee slope accretion, 4) consistent dip azimuths in nearly all compass directions of dome-dune slopes and internal dome stratification, and 5) the present-day mound and swale landscape of the North Point peninsula is a relic of the mound and swale eolian landscape created by the vertical upbuilding of dome dunes on the North Point peninsula during Holocene time **(**see Figure 8).

Another name that may be applied to the carbonate eolian dome dunes preserved in the North Point Member is *medaño*, which is a Spanish name used for coastal sand hills built of siliciclastic sand. It is a unique, unvegetated coastal dune that is similar to a dome dune because it forms in bidirectional or poly-directional winds that transport sand upslope (probably by wind ripples) toward the crest from several directions and is relatively stable despite the lack of plants (Goldsmith 1985).

Wiggs (2019) classified dome dunes as a type of free or mobile dune, which can later be stabilized or anchored. He did not specifically describe a stabilizing or anchoring process. However, in the case of the North Point dome dunes, calcareous crusts and plants and plant-roots were the stabilizing and anchoring agents. Bristow and Lancaster (2004) documented the migration of a 1-meter-high, slipfaceless dome dune with poor sand retention in the siliciclastic Namib sand sea of Namibia, southwest Africa. Sand had been removed by deflation, then transferred by wind from a pre-existing dome dune to a new location downwind to the north-northeast. The Holocene North Point dome dunes did not advance downwind through lateral slipface accretion like eolian transverse, barchan, parabolic, and lobate dunes do. Unlike the small dome dune in the Namib desert of Bristow and Lancaster (2004), the Holocene North Point dome dunes were extremely efficient in retaining sand because dune build-up proceeded through vertical upbuilding or accretion of strata deposited by wind-ripples, aided by sea spray, early subaerial cementing, $CaCO_3$ encrusting, and plant stabilizing.

Wind-ripple sedimentation preserved as cyclic laminae in the North Point Member was responsible also for lateral expansion of dome flanks and overlapping adjacent dome dunes (Figure 14). Lateral expansion and dune overlap suggest that the North Point dome dunes would be classified as *compound dunes*, composed of two or more of the same dune type that overlap or are superimposed on one another according to McKee (1979a; Wiggs 2019), and *accumulating dunes,* characterized by little or no net advance or elongation, according to Tsoar (2008).

The increase then decrease in height of the Holocene dome dunes northward along North Point peninsula (see Figure 8)

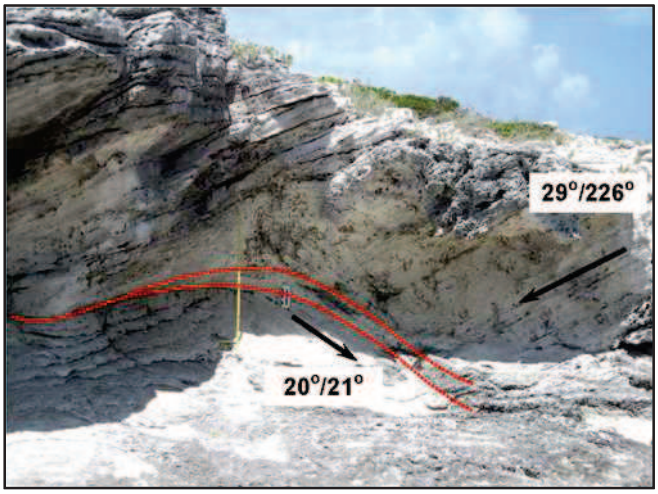

Figure 14. View of a shallow notch formed by cavernous weathering and wave erosion of the North Point Member at study site E5. During its growth, a larger mature eolian dome dune had expanded over a younger dome dune, the crest of which is outlined with red dotted curves. Stratification measurements: Mature dome dune: 29° dip in a 226° azimuth direction (southwest). Younger dome dune: 20° dip in a 21° azimuth direction (north-northeast).

suggests that eolian dunes may have grown initially on an isolated rocky cay a few tens of meters north of mainland San Salvador. Present-day North Point peninsula was not yet a landform. This location was the depocenter, where the thickest and tallest dome dunes developed. With continued sand accumulation and vertical accretion, enhanced by $CaCO_3$ crusts and plant growth, the dome-dune ridge expanded northward to the location of present-day Cut Cay and southward over a shallow bedrock shelf to ultimately attach itself to the mainland of San Salvador Island and become the modern North Point peninsula.

McKee (1966) and Qian *et al.* (2020) postulated that dome dunes may be transitional forms between incipient sand patches and more advanced barchan and transverse dunes, which migrate laterally by slipface accretion in wind. Incipient sand patches may have evolved into smaller coppice dunes and ultimately into larger dome dunes. However, the transition from dome dunes to laterally migrating transverse or barchan dunes did not happen at the site of the North Point peninsula for the following reasons: 1) no evidence of features characteristic of transverse and barchan dunes, 2) dome-dune growth was interrupted periodically by precipitation of calcareous crusts and growth of coastal plants, then halted early by subaerial cementation, and 3) sparse sandflow foresets indicating only brief slope failures and sand avalanches and not extensive lateral migration.

Internal Dome-dune Structure

Using Hunter (1977a, b) as foremost references, White and Curran (1985, 1988) and Caputo (1993, 1995) positively identified the three fundamental types of eolian stratification preserved in the Holocene North Point Member: wind-ripple-, sandflow-, and grainfall-strata. The inversely graded, fine sandy cyclic laminae described herein are the products of sand transported and deposited by wind-ripples on dome dunes preserved in the North Point Member. Pseudoripples (Kocurek and Dott, 1981) in Figure 10B are remnants of thin wind-ripple laminations, eroded and weathered back along lamination planes. Spacing of the headwardly-eroded edges is nearly equivalent to the distance between successive ripple crests when ripple migration was active, and further attests to the wind-ripple origin of the cyclic laminae.

In their interpretations on the eolian origin of the North Point Member, White and Curran (1988) were first to observe vertical successions of wind-ripple strata interbedded with calcareous crusts and associated trace fossils of plant stems. Analysis by Glumac *et al.* (2013) and observations herein confirmed their interpretation. During the growth of Holocene dunes at North Point, eolian sedimentation proceeded by wind ripples in increments of several centimeters (inches) in a given interval of time. Dune growth was paused seasonally or more frequently during a year by rain, which rendered the carbonate sand wet and cohesive,

retarded sediment transport, and fostered plant growth and the precipitation of calcareous crusts on dune surfaces. At the onset of the next dry period, available loose sand was remobilized in wind ripples, dune sedimentation and growth resumed until the next wet period, and the dry-wet cycles repeated vertically through time.

The following factors suppressed grainflows and therefore are responsible for the low abundance of slipface crossbeds in the dome-dune bedding of the North Point Member: 1) dune-slope stabilization by grain cohesion from wetting in rain and salt spray from waves; 2) cyclical precipitation of $CaCO_3$ crusts; 3) growth of maritime plants; and 4) unobstructed strong wind that kept fine sand suspended beyond dune slopes; preventing grainfall sand from settling near dune brinks, where sand collects, becomes unstable, and remobilizes as grainflows (McKee 1966).

Coppice Dune Re-interpretation for the North Point Member on San Salvador Island

The elliptical configurations of low, concentric ridges of truncated strata, dipping away from a central core and cropping out at the bedrock surface on the east side of the North Point peninsula, are interpreted as erosional remnants of eolian coppice dunes, a name for small, oval or elliptical, vegetated dunes coined by Melton (1940). Modern eolian coppice dunes, also called nebkha dunes (Nickling and Wolfe 1994) or anchored vegetated dunes (Hesp and Smyth 2019; Pye and Tsoar 1990), build-up vertically without lateral migration and are common to both coastal and inland dune fields. A trace fossil of plant material associated with one of the elliptical patterns (Figure 12B) supports the idea of smaller plant-anchored, eolian coppice dunes co-existing with larger dome dunes. A corollary to this interpretation is that the larger dome dunes may have begun their growth as smaller coppice dunes or proto-dome dunes (a term modified from Warren 2013), a meter (3.3 ft) high or less, and later grew vertically at the center of the main dome-dune field into mature dome dunes. (i.e. the taller bedrock mounds on the North Point peninsula today). The northeast-southwest trends of long axes of the interpreted coppice dunes in the North Point Member are consistent with a southwesterly flow for the Northeast Trade Winds during Holocene time on San Salvador. Figure 15 captures a "snapshot" of the sedimentary scenario when coppice and dome dunes developed during Holocene time at the location of the North Point peninsula.

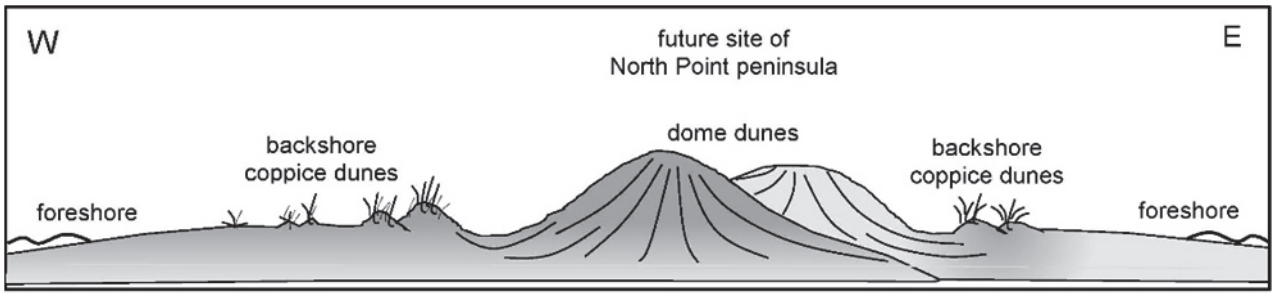

Figure 15. Hypothetical morpho-sedimentary setting of the North Point peninsula during Holocene sedimentation of the North Point Member. View is northward.

Coppice dunes growing today along the eastern shore of San Salvador may serve as possible modern analogues for the coppice dunes interpreted herein for the North Point Member (Figure 16A and B). On beaches there, heaps of dead seaweed have been washed onto the upper foreshore as a wrackline by wave swash at high tide or during storms. Eventually, plant seeds and wind-blown carbonate sand becomes trapped in the network of stems and fronds of the dead seaweed. Grasses and other plants, fostered by moisture from wave spray and rainfall, sprout from the trapped seeds. Eolian sand, saltating from the foreshore and lower backshore, is trapped by the swash debris and by shore plants sprouting at the swash line. Eventually sand accumulates into a plant-anchored mound as roots take hold and radiate to secure the mound of sand. A mature, mound-like coppice dune can grow vertically 1-2 m (3.3 to 6.6 ft) high as the base expands laterally and if plant growth can keep pace with the piling up of sand (Hesp and Smyth 2019) (Figure 17). Slipfaces are absent, wind ripples likely dominate traction transport of sand, and primary internal stratification is probably disturbed or destroyed by plant roots.

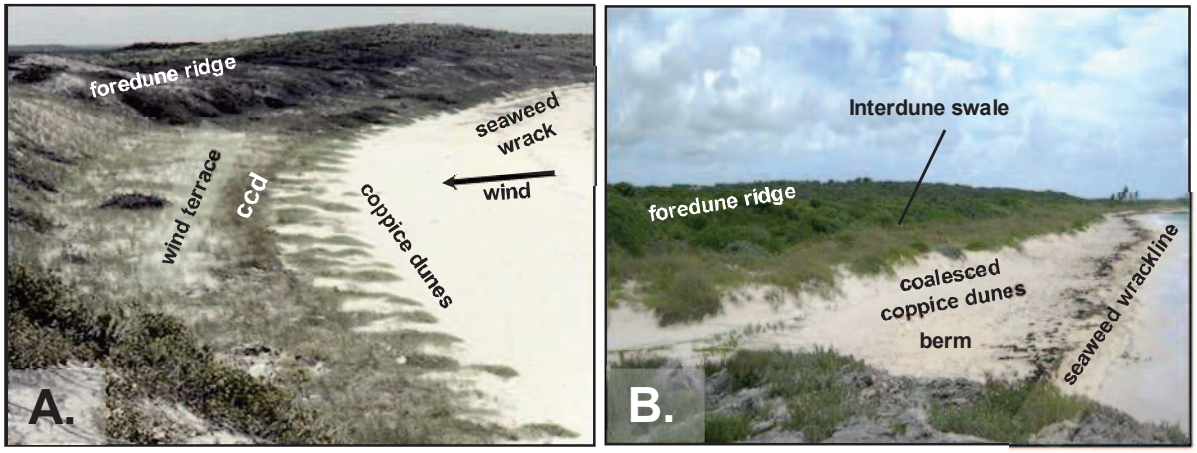

Figure 16. Recent eolian coppice dunes and coastal geomorphology of eastern San Salvador. A. At Snow Bay, eastern San Salvador (see Figure 2A for location), clumps of seaweed washed in by waves, trap plant-seeds and carbonate sand. Plant-growth keeps pace with vertical build-up of trapped sand to form elongate and elliptical coppice dunes, 1-2 m (3.3-6.6 ft) high, oriented parallel and subparallel to onshore wind. Morpho-sedimentary components shoreward of coppice dunes: older foredune ridge of coalesced coppice dunes (ccd), wind terrace, and oldest, tallest foredune ridge. B. Stages in the evolution of a coastal dune system from the shore landward: seaweed wrackline, berm, coalesced coppice dunes to form the youngest dune ridge separated by interdune swale from the older, higher, overgrown foredune ridge. Beach at the Thumb (see Figure 2A for location).

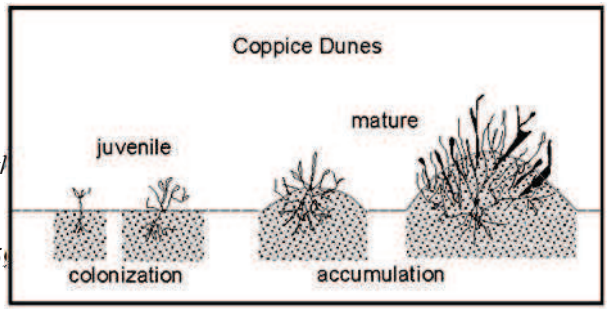

Figure 17. Possible model to explain the general development of coppice dunes, from juvenile to mature, at coastal and inland eolian environments. Wind-blown sand is trapped and stabilized by colonizing shore plants and their roots. Coppice dune growth progresses from juvenile to mature as plant growth keeps pace with sand buildup. Adapted and redrawn from Figure 7.3, p. 15[illegible] in Hesp and Smyth (2019).

CONCLUDING REMARKS

Much of the work on general eolian processes operating in coastal and inland dune fields and sand seas (i.e. ergs, an Anglicized Arabic word for eolian sand seas) has offered insight into the morphology, morphometry, sand texture, and origin of eolian dunes. Numerous studies have been published on modern barchan, transverse, parabolic, and large, complex linear and star dunes, and their depositional record in sedimentary rocks. This report may be the first to interpret a dome dune origin for carbonate sedimentary rocks on a tropical island. To date, I uncovered one publication (Thompson 1969) that interpreted an eolian dome-dune origin for a Triassic quartzose sandstone in England.

During Holocene time, an eolian dome- and coppice-dune complex evolved at the present-day site of the North Point peninsula and is preserved in the North Point Member of the Rice Bay Formation on San Salvador Island. Component allochemical sand was generated on the adjacent nearshore shelf during high stands of sea level by biomineralizing corals, molluscs, and algae and biochemical precipitating of ooids, fecal pellets, and peloids. Later, storm and normal marine currents mixed skeletal and nonskeletal grains and deposited the carbonate sediment on foreshore beaches where it was redistributed by wind and piled into dunes on backshore beaches. Juvenile, precursor coppice dunes were initiated by sand-trapping grasses and other plants, and, over time, matured, coalesced, and possibly provided a base for growth of eolian dome dunes. The eolian system continued to evolve as stationary, larger dome dunes accreted vertically, aided by $CaCO_3$ encrusting and plant stabilizing under the influence of the Northeast Trade Winds.

Sand-sized carbonate sediment was transported by wind ripples and deposited as cyclic laminae, which are preserved as windward-set, topset, brinkset, and foreset strata in dome dunes and horizontal to concave laminae in inter-dome swales. They are volumetrically dominant over other eolian strata and are the primary architectural elements in the North Point Member. Because the abundance of grainfall strata was negligible and not essential to the interpretation of eolian dome dunes, they were not assigned a rank in the scheme of architectural elements. Slipface crossbeds were essential to interpreting eolian dome dunes, but their low abundance relative to cyclic wind-ripple laminae rendered them secondary architectural elements. They were the depositional product of short-lived grainflows on temporary slipfaces of larger, mature dome dunes. Their paucity is directly related to the low amount of deposited grainfall sand and the incremental stabilizing of dome-dune surfaces by salt spray, calcareous crusts, and coastal plants. The eolian dome- and coppice-dune interpretation proposed herein for the North Point Member is based on evidence from outcrops and is made with little recourse to the few published sources, which contain sparse sedimentary details on eolian dome dunes (Table 3).

Figure 18 is an interpretive reconstruction of the eolian coppice- and dome-dune setting thought to exist during Holocene time at the future site of the North Point peninsula. Positions of lettered images show spatial locations where architectural elements described and shown earlier in the referenced figures would likely occur.

Table 3. Outcrop characteristics that suggest a dome- and coppice-dune origin for eolianites of the North Point Member, Rice Bay Formation on San Salvador Island.

Features Similar to Those Described in Modern Siliciclastic Eolian Dome Dunes	**References**
Oval to circular mound morphology, rounded summit; composed of sand-sized grains	Bigarella *et al.* (1969); Bristow and Lancaster (2004); Halsey and Catto (1994); Hesp and Smyth (2019); Lancaster (1995); McKee (1966, 1979, 1982), Pye and Tsoar (1990); Qian *et al.* (2020) and references cited therein
Few if any slipfaces, low proportion of sandflow cross-bedding and associated grainfall strata	
Distinguishing Features of Dome Dunes in the North Point Member Not Described in Modern Siliciclastic Eolian Dome Dunes	
Taller dune height, up to 10 m (33 ft)	
Greater dune height fostered by sand cohesion from coastal salt spray, and $CaCO_3$ encrustation and plant growth	
arching internal stratification that conforms to external dome shape	
Dominant wind-ripple processes depositing windward, crest, brink, and foreset strata	
Eolian dunes characterized only by vertical accretion and lateral expansion and no lateral foreset accretion	
No evidence for transitioning to downwind migrating transverse and barchan eolian dunes	
Nearly 360° azimuth slope directions of bedrock mounds and dip directions of internal stratification	
Small eolian coppice dunes that are peripheral to the dome dune field and may be precursor dunes on which larger dome dunes evolved	

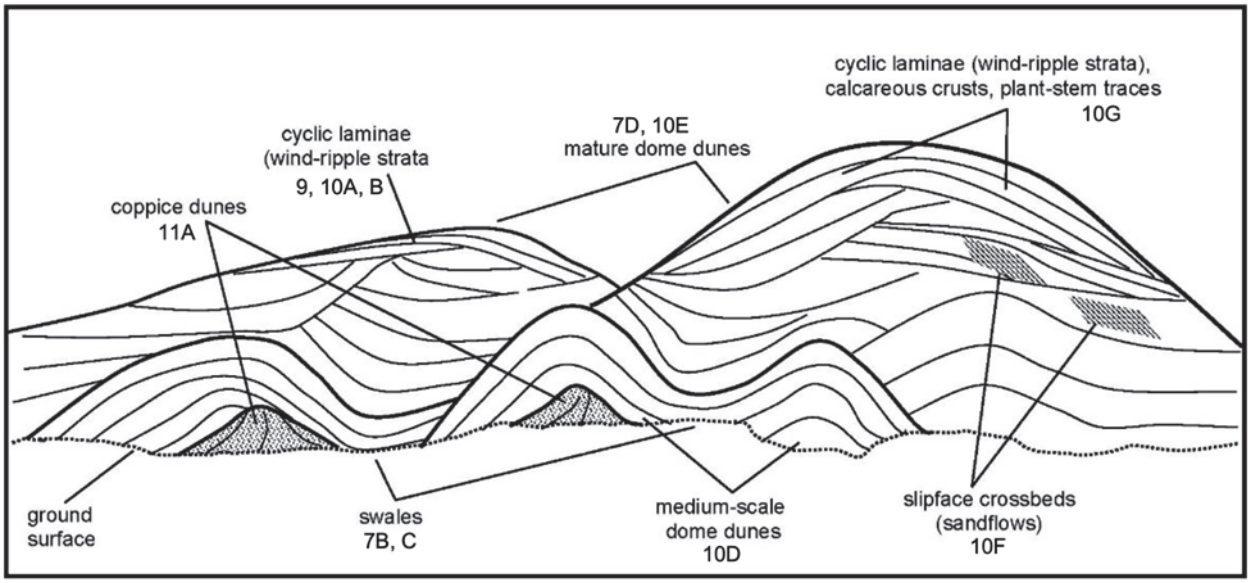

Figure 18. Interpretive diagram of the Holocene dome- and coppice-dune and swale complex in the North Point Member. Dune surfaces are outlined with bold curved lines; concordant and discordant bounding surfaces of wind-ripple bedsets are drawn as thin curved lines. Numbers and letters of figures in this report are placed in the diagram to show where outcrop features would occur hypothetically in this eolian system. Modified from Caputo (2019).

SUGGESTIONS FOR FUTURE WORK

Field methods that led to the interpretation of dome- and coppice-type dunes in the North Point Member at North Point, San Salvador Island, may serve useful for identifying eolian dune types, in the Holocene Hanna Bay Member of the Rice Bay Formation at the northern margin of San Salvador, and in the Pleistocene French Bay and Cockburn Town Members of the Grotto Beach Formation at the southern margin. Little information on dune type, internal structure, and paleogeographic conditions for the Hanna Bay Member has been published.

Caputo (1995) had suggested tentatively that the dune forms preserved in the Grotto Beach Formation resemble sinuous-crested, coastal foredune ridges with lunate recesses and linguoid lobes along the dune leeside. He further described the Pleistocene eolianite preserved in the Grotto Beach Formation may prove to be composed of lobate dunes that had merged to form a dune ridge transverse to wind similar to those described by Mackenzie (1964a, b), Ball (1967), and White and Curran (1988). Further careful, systematic distinguishing of wind-ripple, sandflow, and grainfall strata, and measuring azimuth directions of inclined foreset strata are needed.

Future field projects:

1. Document eolian calcarenite bodies in the Hanna Bay, French Bay, and Cockburn Town Members, including geometry, internal structure, and azimuths of dipping strata, reactivation surfaces, and windward and leeward dune slopes.
2. Systematically measure and record dip directions for slipface crossbeds (i.e. sandflow strata) in the North Point Member.
3. Gather and record GPS coordinates for precise locations of sites where observations were recorded for the North Point Member on the North Point peninsula.
4. Register a field project with the Gerace Research Centre and obtain permission from the Bahamian government to trench interiors of representative coppice dunes at sandy beaches on eastern San Salvador. Document plant-root burrows and internal physical structures of carbonate coppice dunes.
5. Re-examine an unusual structure, resembling stacked chevron- or teepee-like sedimentary structures up to a meter thick in the vertical dimension exposed on the east side of the North Point peninsula. Component wind-ripple laminae intersect at a sharp-pointed crest and dip in opposite directions from this crest. The structure may be evidence for eolian shadow dunes, another type of anchored, vegetated dune.

ACKNOWLEDGMENTS

Meals and housing were kindly and carefully provided by the kitchen and housekeeping staff during my stays at the Gerace Research Centre (GRC). Tom and Erin Rothfus were co-directors of GRC at the time field work was conducted for this project. Tom accommodated my requests for a vehicle to transport field equipment and rock samples to and from North Point, French Bay, and the Gulf. Among her other responsibilities, Erin was most adept at maintaining the history and log of research activity on San Salvador and the greater Bahamas. Like the founding directors of the Centre, Don and Kathy Gerace, Troy Dexter, whom I met during the 2019 Natural History and Geology conference on San Salvador, is most approachable and likeable as the new Executive Director for the Centre. Rochelle Hanna, chief secretary who anchored administrative responsibilities at the Centre, deserves sincerest, heartfelt thanks for her helpfulness and her warm, generous spirit. She has retired from GRC and I wish her well. I'll always be grateful to John Mylroie (emeritus professor of geology, Mississippi State University) for introducing me to the Quaternary eolianites on Salvador in the 1980s.

I am deeply grateful to my following colleagues, who are also friends and mentors: Tom Anderson (emeritus professor of geology, Sonoma State University), Ed Clifton (retired, U. S. Geological Survey, Menlo Park. He left planet Earth and the geologic community before

this report was published), Ralph Hunter (retired, U. S. Geological Survey, Menlo Park), and Pascal Kindler (emeritus professor of geology, University of Geneva, Switzerland). These folks offered invaluable, insightful reviews of earlier versions of this paper. The final version of this paper benefited exceedingly from additional comments by Tom Anderson, Ed Clifton, and John Mylroie, and from discussions with Bosiljka Glumac and H. Allen Curran (emeritus professor of geology) both of Smith College, Northampton, Massachusetts.

Appreciation goes to the Commission for Bahamas Environment, Science, and Technology (BEST) for granting permission through GRC research code G251 to investigate Quaternary eolianites on San Salvador, and to the Bahamas Department of Agriculture for allowing the transport of rock samples from the Island to the States.

LITERATURE CITED

Abegg, F.E., Harris, P.M., and Loope, D.B. (2001). Modern and Ancient Carbonate Eolianites: Sedimentology, Sequence Stratigraphy, and Diagenesis, Special Publication No. 71. Tulsa: SEPM (Society for Sedimentary Geology), 207 p.

Adams, R.W. (1980). "General guide to the geological features of San Salvador," in Field Guide to the Geology of San Salvador (first edition), ed. D.T. Gerace (San Salvador: College Center of the Finger Lakes, Bahamian Field Station), 1-66.

Ashley, G.M., (1990). Classification of large-scale subaqueous bedforms: A new look at an old problem. Journal of Sedimentary Petrology, 60, 160-172.

Ball, M.M. (1967). Carbonate sand bodies of Florida and the Bahamas. Journal of Sedimentary Petrology, v. 37, 556-591.

Bigarella, J.J., Becker, R.D., and Duarte, G.M. (1969). Coastal dune structures from Paraná (Brazil). Marine Geology, 7, 5-55.

Blay, C.T., and Longman, M.W. (2001). "Stratigraphy and sedimentology of Pleistocene/Holocene carbonate eolianites, Kauai, Hawaii," in Modern and Ancient Carbonate Eolianites: Sedimentology, Sequence Stratigraphy, and Diagenesis, Special Publication No. 71, eds. F.E. Abegg, P.M. Harris, and D.B. Loope, D.B. (Tulsa, OK: Society for Sedimentary Geology), 93-116.

Bristow, C.S., and Lancaster, N. (2004). Movement of a small slipfaceless dome dune in the
Namib Sand Sea, Namibia. Geomorphology, 59, 189-196.

Caputo, M.V. (1989). "Selective cementation of eolian stratification in Pleistocene calcarenites, San Salvador Island, Bahamas," in Proceedings of the 4th Symposium on Geology of the Bahamas, ed. J.E. Mylroie (San Salvador Island, the Bahamas, Bahamian Field Station), 61□72.

Caputo, M. V. (1993). "Eolian structures and textures in oolitic□skeletal calcarenites from the Quaternary of San Salvador Island, Bahamas: new perspectives on eolian limestones, Ch. 17," in Mississippian Oolites and Modern Analogs, Studies in Geology, #35, eds. B.D. Keith and C.W. Zuppann (Tulsa, OK: American Association of Petroleum Geologists), 243-259.

Caputo, M.V. (1995). "Sedimentary architecture of Pleistocene eolian calcarenites, San Salvador Island, Bahamas," in Terrestrial and Shallow Marine Geology of the Bahamas and Bermuda, Special Paper 300, eds. H.A. Curran and B. White (Boulder, CO: Geological Society of America) 63-76.

Caputo, M.V. (2017). "The nature of eolian sedimentation-a primer," in Jurassic World: Architecture of Eolian Dunes, Ephemeral Streams, and Marine Shoreline-Page Sandstone, Carmel Formation, Navajo Sandstone, Southwest Utah, Field Trip Guidebook 120, authors Caputo, M.V., and Anderson, T.B. (Pacific Section, Society for Sedimentary Geology), 33-57.

Caputo, M.V. (2019). North Point San Salvador Island reinterpreted: Evolution and internal architecture of eolian dome dunes. Abstracts and Program, The 3rd Joint Symposium on the Natural History and Geology of the Bahamas. Gerace Research Centre, University of the Bahamas, San Salvador, Bahamas, 5.

Caputo, M.V., and Glumac, B. (2013). Sedimentary architecture and morphology of a dome dune complex in Holocene eolian calcarenites, San Salvador Island, Bahamas. Denver, CO: Abstracts with Programs, Geological Society of America Meeting and Exposition, 344.

Carew, J.L., and Mylroie, J.E. (1995). "Depositional model and stratigraphy for the Quaternary geology of the Bahama Islands," in Terrestrial and Shallow Marine Geology of the Bahamas and Bermuda, Special Paper 300, eds. H.A. Curran and B. White (Boulder, CO: Geological Society of America), 5-32.

Collinson, J., Mountjoy, N., and Thompson, D. (2006). "Chapter 6: Depositional structures of sands and sandstones," in Sedimentary Structures, authors Collinson, J., Mountjoy, N., and Thompson, D. (Harpenden, Hertfordshire, UK: Terra Publishing), 74-137.

Dunham, R.J. (1962). "Classification of carbonate rocks according to depositional texture," in Classification of Carbonate Rocks-A Symposium, Memoir 1, ed. W.E. Ham (Tulsa, OK: American Association of Petroleum Geologists), 108-121.

Evans, J.W. (1900). Mechanically-formed limestones from Junagarh (Kathiawar) and other localities. Geological Society of London Quarterly Journal, 56, 559-583.

Fairbridge, R.W. (1995). Eolianites and eustasy: Early concepts on Darwin's voyage on *HMS Beagle.* Carbonates and Evaporites, 10, 92-101.

Folk. R.L. (1962). "Spectral subdivision of limestone types," in Classification of Carbonate Rocks-A Symposium, Memoir 1, ed. W.E. Ham (Tulsa, OK: American Association of Petroleum Geologists), 62-84.

Fryberger, S.G., and Schenk, C.J. (1988). Pin-stripe lamination-a distinctive feature of modern and ancient eolian sediments. Sedimentary Geology, 55, 1-15.

Glumac, B., Caputo, M.V., and Brisson, S. (2013). Relation between stratification and surficial vs. penetrative origin of caliche crusts in carbonate eolianites on San Salvador Island, Bahamas. Denver, CO: Abstracts with Programs, Geological Society of America Meeting and Exposition, p. 244.

Goldsmith, V. (1985). "Coastal dunes" in Coastal Sedimentary Environments, ed. R.A. Davis (New York, Springer-Verlag), 303-378.

Grabau, A.W. (1904). On the classification of sedimentary rocks. American Geologist, 33, 228-247.

Halsey, L.A., and Catto, N.R. (1994). Geomorphology, sedimentary structures, and genesis of dome dunes in western Canada. Géographie Physique et Quaternaire, 48, 97-105.

Harms, J.C., Southard, J.B., and Walker, R.G. (1982). Structures and Sequences in Clastic Rocks, Short Course No. 9. Tulsa: Society of Economic Paleontologists and Mineralogists (SEPM), 249 p.

Hesp, P.A., and Smyth, T.A.G. (2019). "Anchored dunes," in Aeolian Geomorphology-A New Introduction, eds. I. Livingston and A. Warren (Hoboken, NJ: John Wiley & Sons), 157-178.

Hunter, R.E. (1977a). Basic types of stratification in small eolian dunes. Sedimentology, 24, 361-387.

Hunter, R.E. (1977b). Terminology of cross-stratified sedimentary layers and climbing ripple structures. Journal of Sedimentary Petrology, 47, 697-706.

Hunter, R.E. (1981). "Stratification styles in eolian sandstones: Some Pennsylvanian to Jurassic examples from the Western Interior U.S.A.," in Recent and Ancient Nonmarine Depositional Environments: Models for Exploration, eds. F.G. Ethridge and R.M. Flores (Tulsa, OK: Society of Economic Paleontologists and Mineralogists Special Publication No. 3, 315-330.

Kindler, P., Mylroie, J.E., Curran, H.A., Carew, J.L., Gamble, D.W., Rothfus, T.A., Savarese, M., and Sealey, N.E. (2010). Geology of Central Eleuthera, Bahamas: A Field Trip Guide: San Salvador Island, Bahamas, Gerace Research Centre, 74 p.

Kocurek, G., and Dott, R.H., Jr., (1981). Distinctions and uses of stratification types in the interpretation of eolian sand. Journal of Sedimentary Petrology, 51, 579-595,

Lancaster, N. (1995). Geomorphology of Desert Dunes. London and New York: Routledge, 290 p.

Mackenzie, F.T. (1964a). Geometry of Bermuda calcareous dune cross bedding. Science, 144, 1449-1450.

Mackenzie, F.T. (1964b). Bermuda Pleistocene eolianites and paleowinds. Sedimentology, 3, 52-64.

McKee, E.D. (1966). Structures of dunes at White Sands National Monument, New Mexico (and a comparison of structures of dunes from other selected areas). Sedimentology, 7, 3-69.

McKee, E.D. (1979a). "Introduction to a study of global sand seas, Chapter A," in A Study of Global Sand Seas, ed. E.D. McKee (Washington, D. C.: U. S. Government Printing Office), 1-19.

McKee, E.D. (1979b). "Sedimentary structures in dunes, Chapter E," in A Study of Global Sand Seas, ed. E.D. McKee (Washington, D. C.: U. S. Government Printing Office), 83-113.

McKee, E.D. (1982). Sedimentary Structures in Dunes of the Namib Desert, South West Africa, Special Paper 188. Boulder, CO, Geological Society of America, 64 p.

McKee, E.D., and Ward, W.C. (1983). "Eolian environment," in Carbonate Depositional Environments, Memoir 3 (Tulsa, OK: American Association of Petroleum Geologists), 131-170.

Melton, F.A. (1940). A tentative classification of sand dunes-its application to dune history in the southern high plains. Journal of Geology, 48, 113-174.

Middleton, G.V., and Southard, J.B. (1984). Mechanics of Sediment Movement, Short Course No. 3. Tulsa: Society of Economic Paleontologists and Mineralogists (SEPM), 401 p.

Mullins, H.T., and Lynts, G.W. (1977). Origin of the northwestern Bahama Platform: Review and reinterpretation. Geological Society of America Bulletin, 88, 1447-1461.

Nelson, R.J. (1837). On the geology of the Bermudas. Geological Society of London Transactions, 5, 103-123.

Nelson, R.J. (1853). On the geology of the Bahamas, and on coral formations generally (as read by Sir Charles Lyell, vice president of the Geological Society, 1852). Geological Society of London Quarterly Journal, 9, 200-215.

Nickling, W.G., and Wolfe, S.A. (1994). The morphology and origin of nebkhas, region of Mopti, Mali, West Africa. Journal of Arid Environments, 28, 13-30.

Pettijohn, F.J. (1957). Sedimentary Rocks. New York, Harper and Rowe Publishers.

Pye, K., and Tsoar, H. (1990). Aeolian Sand and Sand Dunes. London: Unwin Hyman, 396 p.

Qian, G., Yang, Z., Luo, W., Dong, Z., and Lu, J. (2020). Morphological and sedimentary characteristics of dome dunes in the northeastern Qaidam Basin, China. Geomorphology, 350, 1-13.

Sayles, R.W. (1931). Bermuda during the Ice Age. American Academy of Arts and Sciences, 66, 381-467.

Schenk, C.J. (1983). "Textural and structural characteristics of some experimentally formed eolian strata," in Eolian Sediments and Processes, eds. M.E. Brookfield, and T.S. Ahlbrandt (Amsterdam: Elsevier Scientific Publishers), 41-49.

Simons, D.B., Richardson, E.V., and Nordin, C.F. (1965). "Sedimentary structures generated by flow in alluvial channels," in Primary Sedimentary Structures and Their Hydrodynamic Interpretation, Special Publication 12. ed. G.V. Middleton (Tulsa, OK: Society of Economic Paleontologists and Mineralogists), 34-52.

Thompson, D. (1969). Dome-shaped aeolian dunes in the Frodsham Member of the so-called "Keuper" Sandstone Formation (Scythian-Anisian: Triassic) at Frodsham, Cheshire (England). Sedimentary Geology, 3, 263-289.

Tsoar, H. (2008). Types of aeolian sand dunes and their formation. Lecture Notes in Physics, 582, 403-429.

Walker, L.N. (2006). The caves, karst and geology of Abaco Island, Bahamas. [master's thesis]. [Starkville (MS)]: Mississippi State University.

Walker, R.G. (1992). "Facies, facies models, and modern stratigraphic concepts," in Facies Models, Response to Sea Level Change, eds. R.G. Walker and N.P. James (Geological Association of Canada), 1-14.

Warren, A. (2013). Dunes-Dynamics, Morphology, History. Chichester, West Sussex, UK: Wiley-Blackwell, 219 p.

White, B., and Curran, H.A. (1985). The Holocene carbonate eolianites of North Point and the modern marine environments between North Point and Cut Cay, Pleistocene and Holocene Carbonate Environments on San Salvador Island, Bahamas, Field Trip Guidebook for Geological Society of America, ed. H.A. Curran (Fort Lauderdale, FL: CCFL Bahamian Field Station), 73-94.

White, B., and Curran, H.A. (1988). Mesoscale sedimentary structures and trace fossils in Holocene carbonate eolianites from San Salvador Island, Bahamas. Sedimentary Geology, 163-184.

Wiggs, G. (2019). "Desert dunes: form and process," in Aeolian Geomorphology-A New Introduction, eds. I. Livingston and A. Warren (Hoboken, NJ: John Wiley & Sons), 133-155.

LIFE & DEATH IN AN ANCHIALINE ARCHIPELAGO

Eric S. Cole

Biology Department, St. Olaf College, 1520 St. Olaf Ave., Northfield, MN 55057

ABSTRACT

This report summarizes 20 years of natural history observation regarding animal diversity from 24 anchialine ponds on San Salvador Island and 16 ponds on the island of Eleuthera in the Bahamas, with special attention to the invertebrates. These ponds exhibit a wide range of species richness that appears correlated with their subterranean connectivity to the ocean. Greater species richness occurs in ponds with an intermediate degree of connectivity. Ponds with low connectivity become hypersaline or exhibit wildly fluctuating temperatures and salinity associated with storm events and periods of drought. Predictably, such ponds exhibit low invertebrate diversity. Ponds with high-volume subterranean conduits frequently support larger predators from the coastal environment access, and again, invertebrate diversity suffers. There appears to be a sweet spot with sufficient connectivity to permit the tidal fluxes that can buffer a pond against dramatic changes in temperature and salinity, while restricting access to larger predatory species. Anchialine ponds support species jackpots, where organisms, often rare on the open coast, undergo dramatic population expansions. Curiously, many species that successfully colonize the inland ponds exhibit various modes of clonal reproduction. The ponds themselves appear sensitive to dramatic environmental changes, both natural and manmade. The combination of restricted colonization followed by explosive population expansion within habitats that exhibit extreme physical and biotic characteristics makes the anchialine ponds a uniquely active evolutionary theater. After many visits, and stimulated by recent events in the world, I find myself compelled to close with reflections on our shared natural history ethos.

INTRODUCTION

Anchialine ponds (Gr. γχίαλος = "**near the sea**"; AN-key-ah-lin), (Stock *et al.*, 1986), include a wide range of inland salt-water habitats. In the Pacific, saltwater ponds have been well studied on the islands of Palau (Dawson and Hamner 2005; Dawson *et al.* 2009) and Hawaii (Seidel *et al.* 2016), but they have also been studied in the Mediterranean (Novosel *et al.* 2007), Bermuda (Stock *et al.* 1986; Thomas *et al.* 1992), and famously in the cenotes and underground water-ways of the Yucatan (Calderón-Gutiérrez et al. 2018). They are often associated with exotic life-assemblages, rapid evolutionary adaptation of their inhabitants, and almost inevitably they are faced with threats to their biotic integrity. Far less attention has been paid to the rich anchialine assemblage of the Bahamian archipelago.

Originally, anchialine ponds were defined as "*pools with no surface connection with the sea, containing salt or brackish water, which fluctuates with the tides*" (Holthuis 1973). This definition excludes salt ponds on the one hand, with no measurable connection to the sea, and lagoons with conspicuous coastal water connections. Other anchialine explorers have focused on the subterranean dimension of these habitats to the exclusion of their associated surface waters. Stock *et al.* (1986) defines them as "*bodies of haline waters usually with a restricted exposure to open air always with more or less extensive subterranean connections to the sea and showing noticeable marine as well as terrestrial influences*." Other authors even refer to them as "*underground estuaries*" (Bishop *et al.* 2015). The fact is, salt-water inland water bodies occur along a gradient of connectivity with the

sea: extreme isolation at one end of the spectrum and open lagoons on the other.

The Bahamian archipelago is rich in anchialine habitats that capture the full spectrum of ocean connectivity. San Salvador Island alone boasts 40 or more such ponds while Eleuthera has over 200. In the Bahamas, anchialine ponds have a variety of geologic origins effecting both their physical characteristics and their biotic diversity. Their origins are intimately associated with historic cycles of glaciation coupled with fluctuating sea levels (van Hengstum *et al.* 2019) and have been usefully characterized by Park *et al.* (2014). As sea levels rise, carbonate sand deposition leads to the creation and growth of wind-blown dunes and valleys (or "inter-dune swales"). Further sea-level elevation raises ground-water within the island's interior, ultimately breaching the bottoms of inter-dune swales and filling curvilinear lakes and ponds that hug the contours of the flanking, lithified dunes. These can be quite isolated from the ocean coast. Closer to the coast, lakes also form from lagoons that have been cut off from the ocean by sand deposition ("high-stand depressions", Park *et al.* 2014). Flooded inter-dune swales and cut-off lagoons are constructional lakes and ponds, forming as a consequence of sand deposition and rising sea level. Without a well-developed cavern connecting such lakes to the sea, and under regimens of low-rainfall and high evaporation, these ponds typically form hypersaline habitats, hostile to most forms of animal life. Destructional ponds form when processes of carbonate dissolution create voids in the subterranean island limestone that collapse, creating the famous blue holes. Dissolution processes can intersect constructional processes to create flooded inter-dune swales or cut-off lagoons with subterranean conduits permitting exchange with coastal waters. These processes have been vividly described by Carew & Mylroie (1994), Mylroie and Carew (1995), Mylroie and Mylroie (2007), and Mylroie (2019).

This gradient of connectivity determines both abiotic characteristics of a pond (salinity and temperature) and their biodiversity or community richness. Of particular interest to this study is the invertebrate diversity. Satellite imagery can help identify ponds with a high likelihood of biotic richness. Ponds with marine salinities (frequently possessing subterranean conduits connecting them to the sea) appear blue in satellite imagery. Pea-green profiles indicate hypersaline lakes or ponds lacking zoetic diversity. Brown-black profiles typically imply brackish ponds with tannins from the surrounding mangrove or bush darkening the often-fresh surface-waters that can be layered over the denser saltwater forming a halocline. From field reconnaissance (24 lakes and ponds on San Salvador Island and 16 on the island of Eleuthera) it is evident that "blue" ponds have the greatest likelihood of complex invertebrate communities, but even among these, there are a few exceptionally rich ponds that deserve special attention, biodiversity sweet spots.

I offer a simple, straightforward model suggesting that invertebrate diversity within anchialine ponds is highest in ponds with an "intermediate" level of connectivity to the ocean. Too little connectivity and evaporation exceeds precipitation leading to hypersaline conditions that suppress invertebrate colonization and survival. Too much connectivity, either through conduits or overland during storm surge events, and large grazers and predators gain access to a pond where they contribute to predation pressures (much like on the open coast). Moderate connectivity supports colonization from coastal marine populations while suppressing predation. Organisms that are uncommon or even rare along the open coast often exhibit explosive population expansions in these inland refuges (population "jackpots"). Rising sea levels and increasingly severe storms have added to the dynamism of anchialine habitats, connecting or breaching formerly isolated ponds or subsequently severing connections with the sea through sand deposition. In this paper, I provide an overview of a brief (and very superficial) natural history survey of a variety of anchialine ponds on the islands of San Salvador and Eleuthera. It should be noted that many of the organisms found in these ponds are being studied in rich detail by other researchers with more tightly focused research aims. This paper addresses patterns of invertebrate diversity

within anchialine habitats in broad strokes, in particular drawing attention to five propositions:

1) Anchialine ponds serve as refugees, with "jackpots" of rare or uncommon species released from the predatory pressures encountered on the open coast.

2) Many organisms that have been successful anchialine colonists reproduce asexually or through some form of hermaphroditism or even parthenogenesis, life-history traits well-suited to colonization of these remote habitats.

3) There is a biodiversity "sweet spot" on the spectrum of connectivity that creates the richest invertebrate assemblage: too much connectivity and large grazers and predators are let in and ponds begin to resemble a heavily grazed lagoon; too little connectivity and colonization and species-diversity become restricted. In such cases, the abiotic system becomes sensitive to catastrophic weather-driven habitat change as there are no tides to mitigate a sudden influx of fresh, cold rainwater during a hurricane or buffer the system from excess evaporation during dry spells.

4) Anchialine habitats are dynamic, undergoing catastrophic change as well as slow motion editing and revision of community structure.

5) The same restrictions on migration that create a refuge for select marine organisms also promote their rapid evolutionary change.

METHODS AND MATERIALS

Ponds were identified using satellite imagery made available through Google Earth Pro. Underwater surveys were performed using mask, fins and snorkel in 24 ponds on San Salvador Island, and 16 ponds on the island of Eleuthera, (See Figures 1, 2, and Tables 1, 2). Surveys included multiple hours in each pond, often by several observers over multiple visits spanning two decades of research (less in the less populous or less biodiverse habitats), snorkeling with camera and specimen bags. Occasionally specimens were collected for close-up photography and identification back on land. Specimens were returned when practical, though not when they appeared to have deteriorated. Temperature and salinity measurements were made using a hand-held Quanta probe. Images were captured using an Olympus TG5 underwater camera with housing and a Bluewater Photo 1000 lumen Focus light. Sun protection was achieved using neck-gaiter, booties, and full body skins (to avoid introduction of potentially toxic sun lotion or insect repellents).

RESULTS AND NATURAL HISTORY OBSERVATIONS

Anchialine ponds serve as refuges for marine invertebrates forming population "jackpots"

Release from coastal predation and interspecific competition ("ecological release", Kohn 1972) can result in dramatic population expansion of select species within the Bahamian ponds. Six Pack Pond on San Salvador Island (Figure 3) is non-tidal, lacks a conspicuous cave or conduit, and is over 3 km from the nearest coastline, yet Six Pack has a highly productive though species-poor marine community. It is nearly a perfect monoculture of *Batophora oerstedii* (a fuzzy finger algae). Unusually rich populations of *Batophora* and other Dasyclad algae have been noted in many anchialine habitats in the Bahamas (Woolbright *et al.* 2019). Molluscs present in Six Pack Pond include just three snails: *Battilaria minima*, *Cerithium lutosum* and *Cerithidea costata*, and five bivalves: *Polymesoda maritima*, *Anomalocardia auberiana*, *Isognomon alatus** (flat tree oyster), *Pinctada longisquamosa** (scaly pearl oyster) and *Brachidontes exustus** (the burnt mussel). This represents a classic euryhaline (salt-tolerant) molluscan assemblage (Teeter 1995), supplemented with a few mangrove prop-root species (marked with an asterisk) (Edwards *et al.* 1990). The dominance of this species assemblage in anchialine ponds is so iconic that it has been recognized as a marker for geologic habitat identification (the "*Anomalocardia auberiana* assemblage", Hagey & Mylroie 1995). Six Pack Pond also supports large populations of just two fish species, *Cyprinodon variegatus* (a pupfish) and *Gambusia spp*. (a mosquitofish).

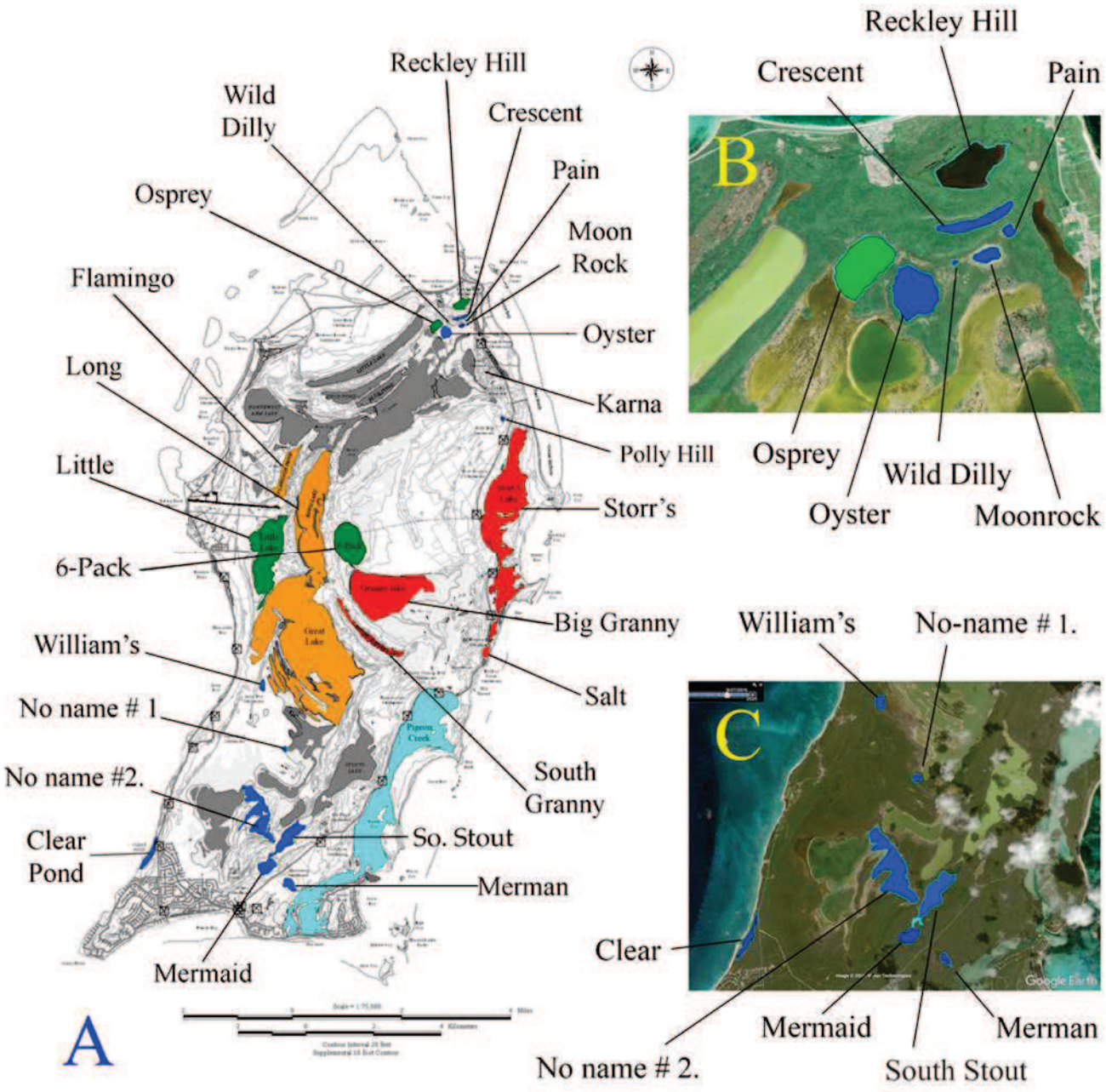

Figure 1. Twenty four lakes surveyed for animal diversity on San Salvador Island. Turquoise indicates lagoon with surface connection to the sea. Red indicates hypersaline (at times ≥ 80 TDS), orange: modestly hypersaline (TDS= 50-80 g/L), green saltier than ocean but habitable (40-50 g/L TDS), dark blue: fully marine (TDS 34-39 g/L). Asterisks indicate ponds of special interest. (A) Map is modified from one published by Robinson and Davis (1999), San Salvador Island GIS Database, University of New Haven and Gerace Research Centre. (B & C) Modified satellite images downloaded from Google Earth 7-11-2020, (images from 9/6/2019, 9/27/2015), Maxar Technologies. Preliminary physical characteristics and GPS coordinates appear in Table 1.

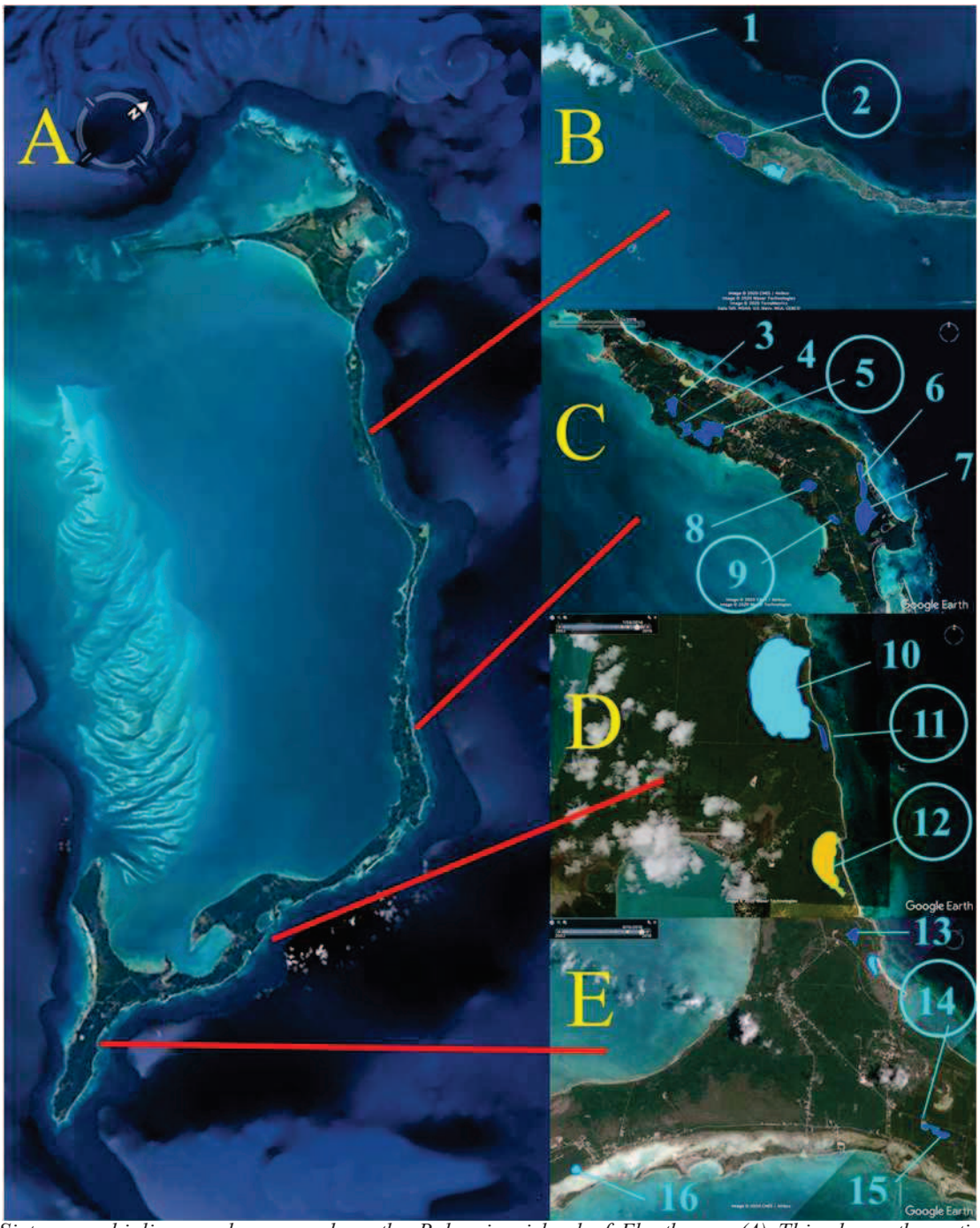

Figure 2. Sixteen anchialine ponds surveyed on the Bahamian island of Eleuthera. (A) This shows the entire island of Eleuthera. (B) This shows the northernmost ponds surveyed during our visits (note, there are more ponds further north!) (C) This indicates a rich collection of ponds just south of Governor's Harbor, (D) This map indicates ponds just north of Rock Sound, and (E) displays ponds on the far south end of the island. Circles specify ponds of special interest: (2) Sweeting's Pond, (5) Big Oyster Pond, (9) Un-named ("Synaptula") Pond, (11) Un-named ("Nurse-shark") Pond, (12) Red Pond and (14) Un-named ("Hawksbill") Pond. Ponds have been colored dark blue to indicate marine or near marine conditions (TDS ~ 35 g/L). Turquoise are fully marine lagoons with surface connections to the sea. Orange indicates ponds that were hypersaline at least sometime in recent history. Satellite images were modified from Google Earth images downloaded 7-11-2020, (9/6/2019, 9/27/2015), Landsat/ Copernicus, Maxar Technologies. Preliminary physical characteristics and GPS coordinates appear in Table 2.

Despite being species-poor, the organisms that have established themselves in Six Pack Pond (Figure 3) are remarkably dense. Virtually every frond of *Batophora* algae is decorated with a tiny sea grass anemone (*Bunodeopsis* sp.), a budding, nonsexual species that is well-adapted for clonal colonization. In 2006, a year and a half after Hurricanes Frances & Jean, juvenile scaly pearl oysters (*P. longisquamosa*) were found decorating the *Batophora* beds to a density of 250 individuals per square meter (Cole *et al.* 2006). This is in dramatic contrast to San Salvador's coastal sea grass habitat where, after 25 years, I have found only a single adult specimen of this *Pinctada*. It is probably no coincidence that this single specimen was located next to the outflow pipe of the GRC field station marine tanks where my research teams often held spawning adults collected from the inland ponds for study. We also found dense adult *Pinctada* populations in three of the larger (conduit-fed) ponds on Eleuthera (Great Oyster Pond, Little Oyster Pond, and Sweetings Pond). Six Pack Pond also provides refuge for a small, locally abundant hydromedusan jellyfish *Aquorea floridana* (Erdmann *et al.* 2009).

Figure 3. Six Pack Pond, San Salvador Island. From 12/2014. Google Earth, Landsat/ Copernicus, Maxar Technologies. Accessed 9-29-2019). Top left: image of shoreline from East trail entrance. Bottom left: characteristic Batophora monoculture during "peak" season with pupfish (Cyprinodon variegatus).

South of Edwin's Turtle Lake on Eleuthera (a popular tourist attraction), there is a less popular pond surrounded by a mature red mangrove forest. The bottom is covered in flocculent sediment with few conspicuous metazoans. *Rhizophora* prop-roots surrounding the pond support a calcareous green-algal garden that is the preferred real estate for two invertebrates: an opisthobranch gastropod (bubble snail, *Bulla sp*.) and a naked sea cucumber (*Synaptula hydriformis)* (Figures 4 A,B). This is the healthiest population of synaptids we have encountered from the Florida Keys, San Salvador, Eleuthera, and even Guadeloupe in the lesser Antilles where the species was first described by LeSueur (1824). *Synaptula* has a known affinity for calcareous algal outcrops (Jennifer Fricke and Richard Turner, personal communications), and the *Rhizophora* (mangrove) prop-roots of this pond

are uniquely rich in this particular habitat. It forms a *Synaptula* "Garden of Eden".

In another small pond on Eleuthera fed by a subterranean conduit, the cave shrimp, *Barbouria cubensis*, appear to have found a uniquely supportive refuge (Figure 4C). Without predation, this population also appears to have exploded.

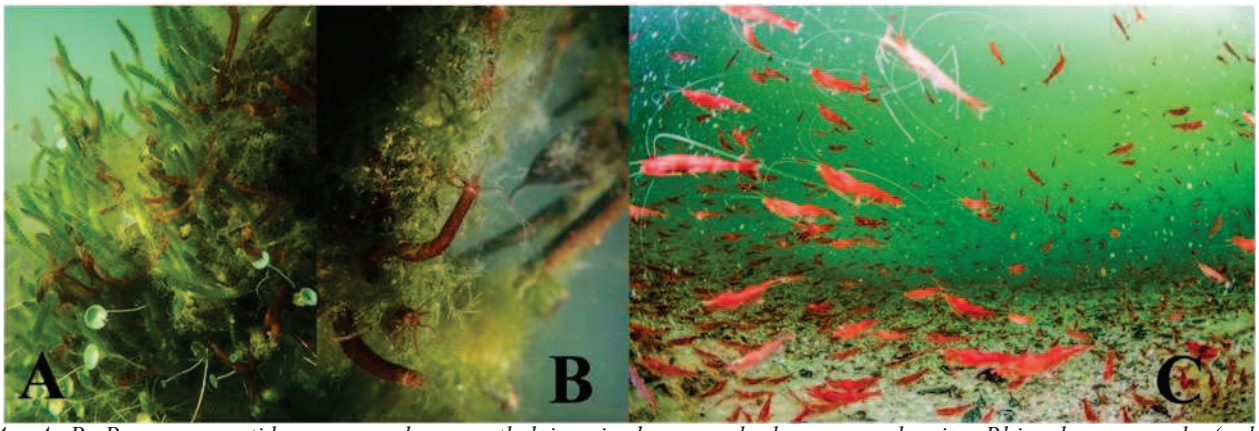

Figure 4. A, B, Brown synaptid sea cucumbers nestled in mixed green-algal masses adorning Rhizophora mangle (red mangrove) prop-roots. C. An impressive population of Barbouria cubensis in a small, conduit-fed pond on Eleuthera. Photo by Shane Gross. https://www.shanegross.com/index.

An anchialine pond boasting extraordinary species jackpots is Sweetings Pond on Eleuthera. In 1985, Aronson and Harms (1985) counted 434 brittle stars, *Ophiothrix oerstedii*, per square meter on the pond floor compared with 3.2 individuals/m^2 from a nearby coastal site. Even a casual observer is impressed by the abundance of white nudibranchs grazing the algal gardens of Sweetings Pond (the fringe-back dondice, *Dondice occidentalis)* and brilliant red file clams (*Ctenoides scabra*) that are normally confined to under-sea ledges and rock crypts on the outer coast (Figures 5, A,B). In Sweetings Pond, file clams decorate carbonate outcrops in a way that seems highly exposed and conspicuous. There is also an impressive population of lined sea horses (*Hippocampus erectus*) that are extremely uncommon on the open coast (Figure 5C).

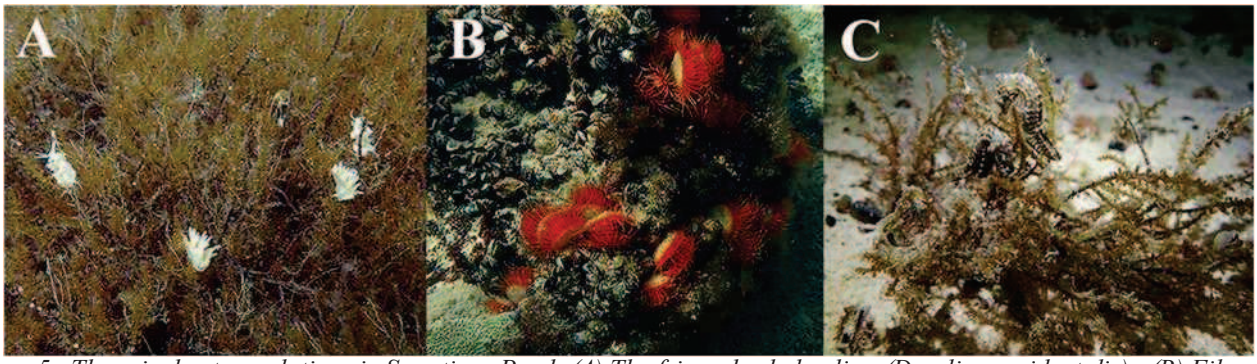

Figure 5. Three jackpot populations in Sweetings Pond: (A) The fringe-back dondice, (Dondice occidentalis); (B) File clams (Ctenoides scabra); (C) Lined sea horses (Hippocampus erectus).

Asexual, hermaphroditic, or parthenogenetic life histories favor successful colonization

For a species to become established in the more isolated anchialine habitats, it must overcome many of the same obstacles associated with island colonization. A single specimen of a sexually-reproducing species is unlikely to co-colonize with a partner permitting them to establish a breeding population. With regard to this point, it may be no accident that many organisms that have successfully colonized anchialine habitats are well-adapted for clonal colonization, reproducing as sequential hermaphrodites (*Pinctada longisquamosa,* the scaly pearl oyster), simultaneous hermaphrodites

(*Bulla sp*., the bubble snail), or even self-fertilizing, simultaneous hermaphrodites (*Synaptula hydriformis,* the naked sea cucumber and *Rivulus marmoratus*, the mangrove killifish). A single virgin individual from one of the latter species has the potential to establish an entire population within even the most isolated locations. The sea grass anemone (*Bunodeopsis* sp.) abundant in Six Pack Pond can reproduce by asexual budding. Closely related species have been shown to reproduce by shedding tentacles, even swallowing shed tentacles that regenerate and develop into entire polyps (Cutress 1979; Panikkar, 1937). *Aiptasia*, a rapidly reproducing anemone common to both Oyster Pond and Mermaid Pond on San Salvador Island (Mitchell 2017) as well as numerous ponds on Eleuthera, is capable of both sexual and asexual reproduction. A related species can bud off clones, each of which can subsequently develop into either male or female forms (Schlesinger *et al.* 2010). *Barbouria cubensis*, the red cave shrimp, may also be a protandric simultaneous hermaphrodite, though this has not yet been confirmed (Baeza *et al.* 2018). All these species exhibit reproductive strategies that make them especially adept as colonizing machines.

A gradient of connectivity with a "sweet spot" for invertebrate biodiversity

Ponds with low-connectivity. These include a great number of the flooded inter-dune swales and cut-off lagoons including South Granny and Storr's Lake on San Salvador Island and Red Pond on Eleuthera. Most ponds with little or no connectivity exhibit hypersaline environments inimical to all but the hardiest metazoan life (we have observed brine shrimp, *Artemia*, in Salt Pond on San Salvador Island). Storr's Lake is well known for the cyanobacterial mats and stromatolites that accrete in the hypersaline shallows. Six Pack Pond (described above for San Salvador Island) represents an enigma in that, while isolated from the ocean and exhibiting no measurable tidal displacement (two students camped along its shores monitored a tide-gauge for 16 consecutive hours… no tidal change), it maintains tolerable salinity (~40-45 PPT) and supports a species-poor yet highly productive community of marine organisms (see above). In brief, ponds with low connectivity typically exhibit species-poor invertebrate communities.

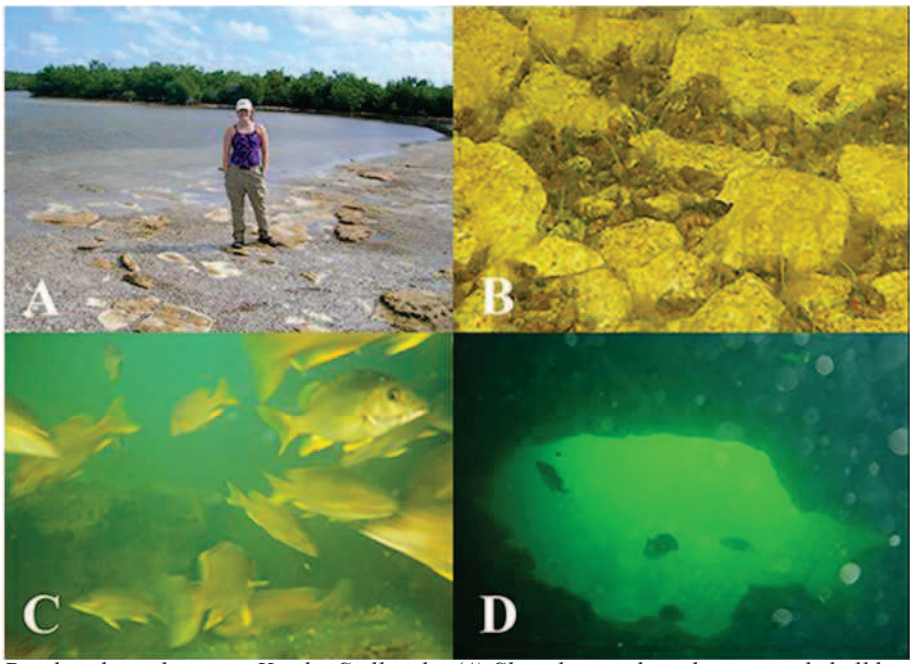

Figure 6. Merman Pond with co-discover, Keisha Sedlacek. (A) Shoreline with carbonate and shell hash. (B) Impoverished invertebrate community on carbonate bottom. (C) Schoolmasters at entrance to sinkhole. (D) Entrance to conduit from inside the cavern looking out.

Ponds with high-connectivity. Subterranean caverns linking inland ponds to the sea can serve as conduits for large predators and grazers. The consequence of increased connectivity can be observed in Merman Pond just east of Mermaid Pond on San Salvador Island (Figure 6). The shallow perimeter exhibits plenty of hard-carbonate substrate as well as flocculent sediments and, to the east, an abundance of *Rhizophora* prop-root habitat. The richness of habitat would lead one to anticipate a highly diverse invertebrate community. Infrared satellite imagery indicates that the pond remains cool. That said, the abundance of invertebrates is conspicuously low, including mostly members of the limited *Anomalocardia* assemblage described above. In the center of the pond is a substantial collapse feature with an impressive underwater cave entrance (2 m tall, 3 m wide). This sink-hole supports a rich population of large coastal reef fish including schoolmaster snappers (*Lutjanus cyanopterus)*, yellow mojarra (*Gerres cinereus)*, and crested gobies (*Lophogobius cyprinoides*) as well as American eels and, on one visit, a modest sized barracuda (White *et al*. 2007). The pond's margins support half-beaks (*Hemiramphus* spp.) and a tiny pipefish (*Syngnathu*s spp.).

American eels (*Anguilla rostrata*) are catadromous freshwater fish, migrating out to sea in order to breed and returning to freshwater between breeding seasons or to mature. Merman is a marine pond, occasionally and temporarily becoming brackish in response to large rainfall events, but returning to marine conditions as the conduit flushes its waters with daily tides. It is curious that adult eels appear content to accept Merman Pond (and 3 Roses Cave) as a freshwater habitat. (Juvenile eels have been collected from a freshwater marsh just south of the Gerace Research Centre on San Salvador Island). It seems likely that, despite Merman Pond affording excellent habitat, access to predators through its substantial conduit has significantly reduced its invertebrate diversity and abundance especially when compared with the rich invertebrate community only 600 meters away in neighboring Mermaid Pond. It may be significant that Merman Pond also exhibits a dramatic (>20 cm) tidal flux with very little time lag, whereas Mermaid Pond exhibits a similar tidal flux that is substantially delayed (>90 minutes) from the coastal tide.

Ponds with moderate-connectivity (the sweet spot). Of more than 40 ponds on San Salvador Island, two exhibit unusually rich invertebrate communities (though others play a close second in terms of species richness). These are Oyster Pond and Mermaid Pond. What seems to characterize these sweet spots of invertebrate diversity is that both offer solid substrate for colonization (mangrove prop-roots and carbonate outcroppings rising out of the soft-sediments) and subterranean conduits with sufficient connectivity with the ocean to drive tidal changes (20 cm or more). Perhaps significantly, the tidal changes for both high-diversity ponds are substantially delayed with respect to coastal tides (1 hr 54 minutes for Oyster Pond, measured on Jan. 15, 2001, > 2 hr for Mermaid Pond), suggesting that, while exhibiting substantial tidal flux, they are none-the-less remote and/or restricted. In neither pond have we observed large predators or grazers from the coastal communities. In both ponds, the ubiquitous anchialine pupfish and mosquitofish are supplemented by schools of Atlantic silversides, *Menidia menidia*, observed during night snorkels around the conduits of Oyster Pond and even during the day in Mermaid Pond. Silversides might serve as an indicator species for moderate connectivity.

Nothing prepared us for the pond diversity on Eleuthera Island. After visiting only 16 ponds, my team encountered four sweet spots. Two of these have already received a lot of attention: Edwin's Turtle Lake (a popular tourist attraction) and Sweetings Pond (increasingly known for its striped sea horse population). The water body that attracted my attention was Great Oyster Pond, a relatively unvisited site south of Governor's Harbor and Edwin's Turtle Pond. This pond is tidal and possesses a rich variety of habitats from algal beds, sea grass flats, and soft-sediment (floc) bottoms to vertical carbonate outcrops. *Casseiopea* jellyfish are abundant, as are small fish (*Gambusia* and *Cyprinodon*) and a truly remarkable assemblage of marine invertebrates

Figure 7. Great Oyster Pond (A) Male Cyprinodons cruising algal beds. (B) Casseiopea jellyfish. (C) A biotic outcrop including urchins (Lytechinus) and an unidentified pink sponge. (D) A predatory tulip snail (Fasciolaria tulipa) prowling the Pinctada-laden Thalassia sea grass beds. (E) An anemone (Aiptasia) on red algal bed. (F) A species-rich assemblage of colorful marine sponges under a calcareous ledge. (G) High-density bed of scaly pearl oysters (Pinctada longisquamosa) on Thalassia.

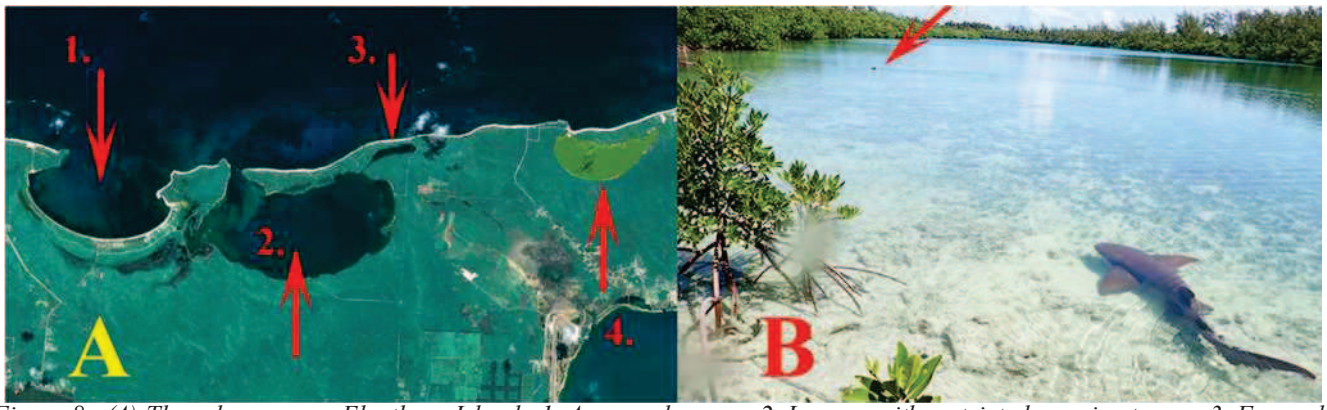

Figure 8. (A) Three lagoons on Eleuthera Island. 1. An open lagoon; 2. Lagoon with restricted opening to sea; 3. Formerly cut-off pond with man-made channel connecting it to pond 2; 4. Cut-off lagoon with pea green profile (Red Pond). (B) A pair of breeding nurse sharks from tiny pond 3. (Dorsal fin of male "courter" can be seen at top left). Image from Google Earth, 2/27/02. Accessed 7/18/2020, Maxar Technologies. Couple mated minutes after this photograph was taken.

Figure 9. Red Pond on Eleuthera. Arrows indicate site of 2014 storm Damon wash-over. Note, change from pea green (hypersaline conditions) to marine blue. By 2019 image, beach was restored, and Red Pond is isolated. Images from Google Earth, Maxar Technologies.

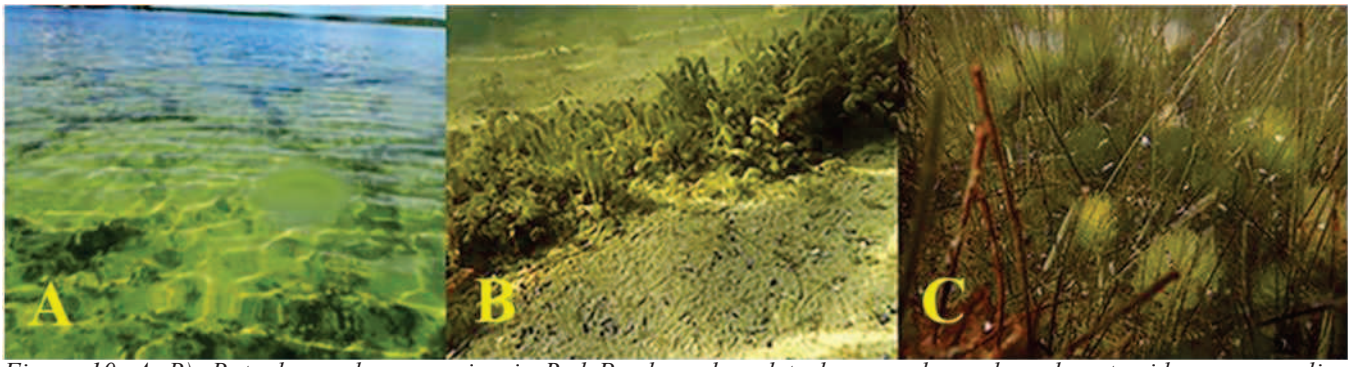

Figure 10. A, B), Batophora algae growing in Red Pond, anchored to large, polygonal, carbonate ridges surrounding patches of loose sediment. C) Halodule (sea grass) and Penicillus (algae) colonizing loose sediments, with small gastropod grazers.

including sponges, anemones, molluscs, and echinoderms (Figure 7).

Anchialine habitats are dynamic

We encountered several examples of anchialine ponds whose connectivity to the sea (or to other ponds) had been altered in recent history with dramatic consequences. Just north of Red Pond on Eleuthera (pond 4 in Figure 8), there is a coastal lagoon nearly cut off from the sea (pond 2). South of it (right) is a narrow pond that has been artificially connected to the larger lagoon via a 230-meter long channel cut by man into the karst (pond 3). It is almost certain that this narrow pond was originally isolated from the ocean by a substantial lithified dune and was likely hypersaline in character. A snorkel survey revealed that this pond has become a rich sanctuary for all kinds of reef fish and even green sea turtles. It had also been discovered by local nurse sharks, who have adopted it as a breeding site. Three adult sharks were observed over 2 short visits; two were mating along the shallow shore (Figure 8 B).

In this same cluster of lagoons, Google Earth images taken before December 2014 reveal that Red Pond (pond 4 in Figure 8A) is cut off from the sea, separated by a small dune with evidence of past wash-overs (Figure 9). The Google Earth image in Figure 8 matches that of a classic hypersaline pond. The pond's name (Red Pond) is consistent with the observation that, from shore, hypersaline ponds appear red due to the halophilic algae and microbes that populate the water column. Halophilic (salt-loving) algae and cyanobacteria change their pigment abundance from chlorophyll to carotene (green to red) in response to rising salt concentrations (Al-Hasan *et al.* 1987; Marshall 1982; Teeter 1995). Satellite images after this date reveal the waters of Red Pond to be blue and transparent, even revealing features of the pond bottom (Figure 9). It appears that the dune has been breached, re-connecting Red Pond to the sea. The catastrophic transformation of this hypersaline pond into an open lagoon has a precise date: Dec. 10, 2014. This was when tropical storm Damon struck Eleuthera, nearly washing out the famous "glass bridge" on the north end of the island. It seems clear that this storm also breached the dune separating Red Pond from the sea, initiating a colonization event of a previously unpopulated pond.

In June, 2019 (five years after the hypersaline pond became a marine lagoon), we surveyed Red Pond by snorkel. Two things were remarkable. First, the pond had been colonized by coastal marine organisms. We encountered *Batophora* as well as *Halodule* seagrass and *Penicillus* (the latter two species NOT typical of a hypersaline environment). *Batophora*, which requires hard substrate to attach to, had formed polygonal tracks crisscrossing the soft sediment bottom (Figure 10A). Upon closer examination, the algae appeared to be anchored to raised, polygonal carbonate ridges. We suspect these polygonal tracks are relics of Red Pond's hypersaline past. Carbonate "megapolygons" have been associated with microbial mats in hypersaline, evaporation flats (Aref *et al.* 2014). They have also been described as arising from shallow intertidal or supratidal environments, as sediments follow cycles of desiccation, (creating polygonal cracks), wetting (causing expansion), and crystallization causing enlargement of the central platform and uplifting at the margins (Assereto and Kendall 1971, 1977).

Whatever their origin, these polygonal carbonate ridges form a solid substrate in Red Pond and have been colonized by the anchorage-dependent marine algae following the Damon inundation. The carbonate ridges are undercut and occupied by gobies (possibly *Lophogobius*). These small fish have excavated floc dens under the polygonal crusts. We observed larger schooling fish as well, though we were unable to identify them. Significantly, at the time of my visit, the surface connection between Red Pond and the sea had once again been blocked with sand. What had briefly been a lagoon was once again a pond (Figure 9). With evaporation exceeding precipitation, Red Pond is almost certainly on a return trajectory from marine to hypersaline conditions, with a concomitant extinction of its newly established residents. On a

larger time-scale, and with sea level rising, we are likely to see more of these cut-off lagoons breached and colonized in a similar fashion.

Evidence of a different slow-motion catastrophe can be found along the shores of Granny Pond on San Salvador Island (Figure 11). Most years, this large body of water is hypersaline (TDS = 80 g/L, Jan. 2006), and casual sampling has revealed little or no animal life. Paradoxically, the shoreline has a beach that is a half-meter deep in shell hash revealing that, at some time in its recent past, the pond was habitable. In January of 2009 following Hurricane Noel (Oct. 2008: little storm damage but 24 inches of rain), the salinity in Granny dropped from 80 to 49 g/L, well within tolerable limits for many anchialine organisms. The familiar red foamy waters had become clear, allowing us to snorkel and observe for the first time a rich stromatolite environment, a magnificent microbial crust, and a still sparse population of live gastropods.

Figure 11. A) "Granny Pond". B) Granny Pond's "shell hash" beach. C) Close-up of shell hash including gastropods and bivalves, machete blade for scale. (Google Earth, Maxar Technologies, GPS Coordinates: 24° 02' 38.61" N, 74° 29' 18.92" W, accessed 9/29/2019).

The deluge not only dropped the salinity of this big pond but connected it to its more productive and more stable neighbor 6-Pack Pond, allowing organisms to re-colonize and launching, no-doubt, another tragic cycle of colonization, isolation, and extinction.

These examples highlight the dynamic nature of anchialine ponds and their rapidly changing biota. Historic changes in pond connectivity are recorded in the fossil record as well (Hagey and Mylroie 1995; Teeter 1995; Park *et al.* 2009; Park 2012). As storms pass, connectivities change and newcomers are swift to colonize and exploit freshly available habitat. One can imagine a steady flow of organisms into anchialine habitats, with greater or lesser restriction to their immigration and, in some cases, almost seismic waves of death and extinction, grooming the community for the hardiest and best-adapted colonists. It is difficult to imagine a more forceful landscape for rapid evolutionary change.

Gradual change in organism assemblages within the Anchialine Ponds

I have described catastrophic changes that can occur in species composition in response to sudden changes in marine connectivity, both natural and man-made, but more subtle changes are taking place in species composition and community structure as well. When first published, the Field Guide to the Inland Ponds (Godfrey *et al.* 1993), described tunicates in both Crescent Pond and Oyster Pond on San Salvador Island. When I visited these ponds from 1995-2001 and surveyed organisms both along the shore and around the conduits, tunicates were not in evidence. I first believed that sponges had been mis-identified as tunicates, but having observed species turnovers throughout the years, it seems

possible that tunicates were present during these early surveys and were subsequently lost.

In Oyster Pond (San Salvador Island), I first observed beautiful serpulids (Christmas tree worms) decorating the red mangrove prop-roots in 1994. That was following an unusually long interval without hurricane activity. It has been 20 years since serpulids vanished from Oyster Pond. Some years, a species of sponge will become prominent, only to vanish or diminish again. In 2008, I noticed that the prop-roots in Mermaid Pond, where I had formerly collected oysters, were supporting a species of red algae from the *Laurencia* complex (possibly *Palisada poiteaui*). What began as a modest incursion exploded over the next two years, until I could no longer find my oysters. They had disappeared under bushels of the red algal over-growth. I rediscovered them only by burrowing through armfuls of the stuff to expose the *Rhizophora* prop-root where they remained stubbornly anchored. In later years, though the *Laurencia* persisted, oysters appeared to migrate to the periphery of the red-algal shrouds, where they once again could filter planktonic algae from the water column unobstructed. It is a cautionary tale that visitors to the ponds may not be observing a definitive stable community of organisms, but a snapshot of a community that is almost certainly in flux.

Rapid evolutionary change

The conditions that have created anchialine sweet spots, excellent habitat and limited connectivity to the sea, also create conditions that favor rapid evolutionary change: limited gene flow and founder-effect genetic bottlenecks. Individual ponds exhibit profoundly different physical characteristics while providing widely divergent selection pressures on subpopulations of the same species.

In one example, scaly pearl oysters (*Pinctada longisquamosa*) are relatively uncommon in most of the inland ponds. I have observed live populations in only six ponds on San Salvador Island and two ponds on Eleuthera. By contrast, they are richly abundant in sea grass beds on the Gulf side of the Florida Keys. On San Salvador Island, the *Pinctada* from Oyster Pond and Six Pack Pond are markedly different despite being separated by only 6 kilometers. Oysters from both Oyster and Mermaid Ponds have elaborate scales (Figure 12 A). Oysters from Six Pack Pond are smooth-shelled, with greatly reduced scales (Figure 12B). There also appear to be differences in frequency of pigment stripes on the shell and soft-tissue pigments (Cole *et al.* 2016). The most impressive difference between these populations is in their reproductive life histories. Oyster Pond *Pinctada* populations (as with most wild populations) exhibit protandrous hermaphroditism. They begin their reproductive lives male and switch unidirectionally to female (Cole *et al.* 2010, Halvorson *et al.* 2012). Oysters from Six Pack Pond, on the other hand, exhibit bidirectional sex determination. Large adults from Oyster Pond are almost exclusively female, while those from Six Pack Pond are 50:50 male and female.

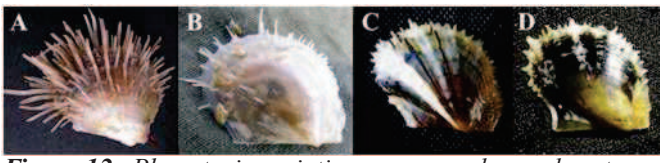

***Figure 12**. Phenotypic variation among scaly pearl oysters (Pinctada longisquamosa) photographed from different islands, and from different ponds on the same island. A) Mermaid and B) Six Pack Ponds (San Salvador Island), C) Great Oyster Pond and D) Sweetings Pond (Eleuthera).*

Evolutionary changes in *Pinctada* characteristics appear between island populations as well as between isolated ponds on a given island. The oysters from Great Oyster Pond on Eleuthera have developed a rich suite of shell pigments never seen in the San Salvador populations. Sweetings Pond oysters, while also richly pigmented, are distinct from Great Oyster Pond oysters in that their pigments show greater shell coverage, while Great Oyster Pond oyster pigments are more restricted to delicate bands and stripes (compare Figures 12 C & D).

There are a great many examples of rapid evolutionary changes in populations from different ponds and different islands in the Bahamas. The fact that these ponds have only become ponds since the last Ice Age reminds us

that the habitats themselves are less than 10,000 years old. Consequently, changes in the phenotypic characters within neighboring pond populations have almost certainly emerged on a similar, rapid timeline.

Anchialine Commuters?

During a snorkel survey of a small, *Batophora*-rich pond on the south side of Eleuthera, my team and I discovered a juvenile hawksbill turtle (*Eretmochelys imbricate)* perched 15-20 feet down on the ledge of a massive underwater cavern (Figure 13). This pond clearly had a destructional origin through karst dissolution and collapse. The hawksbill may have been captive for some time in that the trailing edge of its carapace had mature *Batophora* algae growing along its margin.

Figure 13. A) Hawksbill turtle perched near sink-hole/conduit feature in a small pond on south Eleuthera. (Batophora is growing off posterior margin of shell). B) Turtle after capture and before release. C) First encounter between our camera-mounted juvenile hawksbill and an aggressive green sea turtle off of Powell Point, Cape Eleuthera. (See video: https://youtu.be/xkEZ_pA7580). Photo credits to Nathan J. Robinson, Cape Eleuthera Institute.

Dr. Nathan Robinson of the Cape Eleuthera Institute assisted us in capturing the turtle, and tissue samples were taken. We then transported the hawksbill to the Cape Eleuthera Institute, where we secured a video camera with a time-release fastening onto the carapace, and released the turtle into a nearby harbor. The camera was recovered hours later, and we were able to witness the hawksbill's encounter with a native green turtle out on the reef. Finding a hawksbill in a tiny, inland pond over a kilometer from the ocean was somewhat mystifying. Islanders have introduced sea turtles to some of the inland ponds as tourist attractions (see Edwin's Turtle Lake) and historically as a source of food (Carew and Mylroie 1994). That said, this particular pond seemed an odd choice as it holds no tourist appeal and appears to be a difficult place to retrieve a turtle from. (The conduit was easily 10 m deep before tapering). The other possibility is that this turtle actually navigated the large submarine conduit from open coastal waters (over a kilometer away). This unlikely possibility is given credibility by a second hawksbill encounter in Clear Pond on San Salvador Island.

Clear Pond is a classic cut-off lagoon. The pond is only a few hundred meters from the ocean and cut off from the sea by a narrow dune. The landward shoreline abuts the Queen's Highway and a gently rising hillside. Despite being a classic constructional, high-stand depression or cut-off lagoon, there is a conduit on the landward side of the pond (Dalman 2009). Possession of a conduit reflects destructional processes at work as well (carbonate dissolution). This highlights the complex intersection of geologic and hydrologic processes at work on the islands. The water issuing from this opening, which paradoxically abuts the inland shore not the seaward side, seemed brackish, suggesting that the cavern may open onto the freshwater lens beneath the inland hillside. Milling about in the scour created by the rather forceful current from this conduit were snappers and other lagoon fish. Previous researchers even reported a barracuda (Dalman 2009). Perched under an overhanging rock was yet another, this time full-grown, hawksbill turtle

(6/11/2019). This pond, which is shallow (maximum depth < 1M) and actually "hot" to the touch (35°C), seems an unlikely place for an islander to cache a purloined sea turtle. Furthermore, upon my return, the turtle had vanished. We were convinced it had re-entered the cave system. Snorkeling into the cavern's entrance, we found the walls thickly covered with marine sponges, nearly 20 cm deep in places, preferred food for hawksbill sea turtles. We must at least entertain the notion that sea turtles are capable of traversing some of the larger submarine conduits emerging inside an anchialine pond, and may actually do so at will.

DISCUSSION

A Goldilocks scenario drives invertebrate community richness

Surveys of 40 ponds on the islands of San Salvador and Eleuthera in the Bahamas reveal that Google Earth imagery can be used to identify habitats potentially rich in invertebrate bio-diversity. Ponds with weak or nonexistent connectivity to the sea tend to be predictably low in zoological diversity. Ponds with strong ocean connections exhibit only modest biodiversity reflecting, we suspect, higher predation and grazing from typical lagoon or reef denizens. Ponds with only moderate connectivity exhibit the sweet spot for biodiversity, a "Goldilocks" scenario.

Anchialine ponds are refuges for marine diversity, a call for conservation

Ecological release (absence of predators or competitors) allows the rare colonist to undergo a population explosion creating jackpots of often uncommon coastal species. This raises two issues. First, these population jackpots represent a natural refuge for select coastal organisms, making them high-profile targets for vigorous conservation efforts. Second, given the general decline of coastal marine communities, these pockets of organismal diversity may actually be capable of supporting a kind of reverse colonization (Bellemain and Ricklefs 2008). Attention is typically paid towards how an island habitat becomes colonized. Less attention is paid to the possible emigration of organisms from an "island" to the "mainland" (in this case the "island" is the anchialine pond, and the "mainland" is the open coast). This provides a spotlight on why these habitats should receive urgent protection.

Engines of evolutionary change (islands within islands)

Islands have long been celebrated for their role in accelerating evolutionary change, and for bringing about conspicuous, rapid species radiation (MacArthur & Wilson 1963, 1967). The Bahamas have served up numerous case-histories of rapid species diversification and endemism among their terrestrial inhabitants: *Anolis* (Losos 1990; Mahler *et al.* 2013), *Cerion* (Goodfriend & Gould 1996; Harasewych & Tenorio 2018), and *Cyclura* (Schwartz *et al.* 1977; Richardson *et al.* 2019) as well as among the island's anchialine inhabitants: *Cyprinodons* (Martin & Wainwright,2013; Turner *et al.* 2008), *Gambusia* (Martin *et al.* 2013; Fowler *et al.* 2018), and *Hippocampus* (Masonjones 2019; Rose *et al.* 2016). To this growing list we can now add *Pinctada longisquamosa*, the scaly pearl oyster, whose soft-tissue pigment, shell anatomy and coloration, as well as life-history characteristics have seemingly adapted to variations in individual pond environments (Cole *et al.* 2010, Halvorson *et al.* 2012).

A NATURAL HISTORY ETHOS.

Ethos: the characteristic spirit of a culture, era, or community as manifested in its beliefs and aspirations. During these investigations, I've grown increasingly aware of my own impact on these extraordinary natural habitats. In penance, I'd like to draw attention to an *Ethos* that the many good naturalists who have come before have tried to transmit, and which I have imperfectly emulated in my own work. We don't often think about or discuss these issues with one another or with our students who are

acutely tuned to the tenor of our relationship with nature. For future generations:

Leave behind the sun lotion. We can cover ourselves head to foot with long-sleeved clothing (or a light-weight snorkel skin), and purchase a light-weight flexible neck gaiter that can be pulled up over one's head for sun coverage ($12 at Amazon). This does not impede use of a face mask as it is very thin and flexible material, and offers excellent sun protection for ears and neck. This also minimizes the introduction of the potentially toxic compounds present in many sun-screens, to the often-sensitive small pond environments.

Leave behind the dive-fins. Pond environments are smaller than the open coast, and fins are not really necessary. They also do a lot to disturb sediments, and local benthic communities, especially around the more public access points. This will slow you down, and that is also a good thing. It encourages observation of more natural behaviors among the pond's denizens as they are less alarmed by one's approach.

Become horizontal. Walk-ins massacre soft-bodied organisms that have had no opportunity to adapt to foot traffic. This is true of both the inland ponds and the coastal intertidal community. A good rule of thumb is that every step is a killing step, and the sooner one gets horizontal in the water, the less damage one inflicts.

Limit multi-lake visits. Every pond is a natural experiment in colonization and adaptive species radiation. It could be argued that wading and diving birds bring about a constant dispersal of organisms between neighboring ponds. That said, sequential snorkels almost certainly elevate the transmission of larval organisms in the residual pond waters trapped in one's gear, and introduces an un-natural source of cross contamination. (Consider the example of our lonely *Pincatada* appearing at the outflow pipe at the Gerace Research Centre).

Be mindful and prudent when collecting. Whenever possible or practical, gently return living specimens to the location from which they were captured. Do this both to lessen the impact of your visit, and to make a statement to your students and colleagues. (This may not always be advisable if the specimen has suffered severe deterioration while in captivity.)

When studying in the Bahamas, include the Bahamians. One cannot help reflect during a year when statues of Columbus are toppling and we are forced to confront the many unearned privileges we enjoy, that we who have been so enriched by our visits to the islands have found so few ways to share our academic and research privileges with the islanders themselves (see https://www.scientificamerican.com/article/the-problem-of-colonial-science/). This isn't for lack of wanting to give back. The faculty and students I have met are eager to share in every way that they can. Good and sincere efforts have been made to partner activities at the Gerace Research Institute with the College of the Bahamas. In the spirit of broadening our support, I'd like to draw attention to a wonderful, if tiny, institute that I recently learned about on the island of Eleuthera. C.O.R.E. (Center for Ocean Research and Education), run by Dr. Owen O'Shea, is something special. These folks are "*committed to providing free marine science education to students and schools on the island of Eleuthera, to run parallel with, and complement existing government science programs. In partnership with these schools, we aim to share our vision for the sustainable use of this most valuable resource, and to educate young Bahamians with a view to cultivating the next generation of science leaders and environmental thinkers for this country.*" Dr. O'Shea is doing a lot to bring the world of marine science to the islanders themselves. We can support them at https://www.coresciences.org .

ACKNOWLEDGMENTS

Thanks to: Nathan J. Robinson, Cape Eleuthera Institute, and NOAA "Our Way Together Program", for the funds that purchased CEI's underwater "turtle" cameras. Thanks to extraordinary Conservation Photographer: Shane Gross, for sharing his *Barbouria* photograph from Eleuthera and for his deep appreciation of marine conservation. Thanks to fellow explorers: Liam Edgar, Ken Hobson, John and Karna Campion

and a host of intrepid St. Olaf College undergraduates over the years. Thanks to Heidi Johnson & Ethan Freid, (Leon Levy Native Plant Preserve and Bahamian National Trust) for hosting our January 2019 research visit, and for modeling best practices as we visited the inland ponds. Thanks to Troy A. Dexter, Executive Director, Gerace Research Institute, University of the Bahamas for providing support during our San Salvador visits; and Owen Shea, (executive director of C.O.R.E., the Center for Ocean Research and Conservation), who provided guidance and a warm welcome during our visits; John Rucker and Tina Niemi, (University of Missouri at Kansas City) led me to the conduit at Clear Pond on San Salvador Island, the site of our second hawksbill turtle encounter. This work was conducted under a 2017 BEST research permit, B-229, as well as previous research permits.

Table 1. San Salvador

Pond name	GPS	Physical characteristics			Habitats					
"casual"		Tidal	Conduit identified?	Salinity (TDS g/L)	FLOC	Sand	Carbonate	Sea Grass	Calcareous algae (biotic outcrops)	Prop-roots
Reckley Hill	24-06-53 N, 74-27-37 W	YES	YES	marine	YES	no	YES	N/O	N/O	YES
Crescent	24-06-47 N, 74-27-21 W	YES	YES	marine	YES	no	YES	YES	N/O	YES
Pain	24-06-44 N, 74-27-22 W	YES	YES	marine	YES	no	YES	N/O	N/O	no
Moon Rock	24-06-39 N, 74-27-28 W	YES	YES	marine	YES	no	YES	N/O	N/O	no
Oyster	24-06-35 N, 74-27-44 W	YES	YES	marine	YES	no	YES	no	YES	YES
"Karna"	24-05-42 N, 74-26-58 W	no	no	brackish	N/O	no	N/O	no	N/O	YES
Poly Hill	24-05-05 N, 74-26-47 W	YES	YES	marine	YES	no	YES	N/O	N/O	YES
Storr's Lk.	24-03-22 N, 74-27-10 W	no	no	hypersaline	YES	no	cyanobacteria	no	N/O	YES
Big Granny	24-02-40 N, 74-29-24 W	no	no	hypersaline	YES	no	cyanobacteria	no	N/O	no
Salt	24-01-23 N, 74-27-02 W	no	no	hypersaline	YES	no	YES	no	N/O	no
South Granny	24-02-14 N, 74-29-40 W	no	no	hypersaline	YES	no	no	no	N/O	no
South Stout	23-58-11 N, 74-30-44 W	?	no	marine	YES	no	N/O	N/O	N/O	YES
"Merman"	23-57-44 N, 74-30-29 W	YES	YES	marine	YES	no	YES	N/O	N/O	YES
(Airmail) *"Mermaid"*	23-57-54 N, 74-30-53 W	YES	YES	marine	YES	no	YES	N/O	YES	YES
Clear Pond	23-58-24 N, 74-32-49 W	YES	YES	brackish	YES	no	N/O	N/O	N/O	N/O
No-name 1	23-59-52 N, 74-30-30 W	?	no	marine	YES	no	N/O	N/O	N/O	YES
No-name 2	23-58-24 N, 74-30-45 W	?	YES	marine	YES	no	YES	N/O	N/O	YES
William's Pond	24-00-47 N, 74-30-59 W	YES	YES	marine	YES	no	N/O	N/O	N/O	YES
6-Pack	24-03-25 N, 74-29-21 W	no	no	> marine	YES	no	YES	YES	N/O	no
Little Lk	24-03-01 N, 74-31-09 W	no	YES	marine	YES	no	YES	N/O	N/O	YES
Long Lk	24-03-46 N, 74-30-22 W	no	no	> marine	YES	no	N/O	N/O	N/O	N/O
Flamingo	24-03-57 N, 74-30-47 W	no	no	marine	YES	no	YES	N/O	N/O	N/O
Osprey	24-06-43 N, 74-27-52 W	YES	YES	> marine	YES	no	N/O	N/O	N/O	YES
Wild Dilly	24-06-36 N, 74-27-36 W	YES	YES	marine	YES	no	YES	no	N/O	YES

Table 2. Eleuthera

Pond name	GPS	Physcial characteristics			Habitats					
"casual"		Tidal	Conduit identified?	Salinity (TDS g/L)	FLOC	Sand	Carbonate	Sea Grass	Calcareous algae (biotic outcrop)	Prop-roots
1. (?)	25-23-56 N, 76-33-40 W	N/O	N/O	marine (?)	N/O	N/O	N/O	N/O	N/O	N/O
2. Sweetings Pond	25-21-52 N, 76-31-06 W	YES	YES	marine (?)	firm	N/O	YES	YES	red algae	YES
3. Turtle Lake	25-10-23 N, 76-12-43 W	N/O	N/O	marine (?)	YES	N/O	N/O	N/O	N/O	YES
4. Little Oyster Pond	25-09-41 N, 76-12-20 W	N/O	N/O	marine (?)	YES	N/O	N/O	YES	N/O	YES
5. Great Oyster Pond	25-09-39 N, 76-12-17 W	YES	N/O	marine (?)	YES	N/O	YES	YES	red algae	YES
6. Great Fish Pond	25-08-26 N, 76-09-19 W	N/O	N/O	marine (?)	YES	no	no	N/O	red algae	YES
7. *"Peanut" Synaptula*	25-07-35 N, 76-08-44 W	N/O	N/O	marine (?)	YES	no	no	no	YES	YES
8. Great Pond	25-08-04 N, 76-08-05 W	N/O	N/O	marine (?)	YES	no	N/O	?	no	N/O
9. Great Pond (S)	25-08-04 N, 76-08-03 W	N/O	N/O	marine (?)	YES	no	N/O	?	no	N/O
10. (?) *"Big lagoon"*	24-55-11 N, 76-08-55 W	YES	N/O	MARINE	YES	N/O	N/O	N/O	N/O	YES
11. (?) *"Nurse Shark"*	24-54-44 N, 76-08-37 W	YES	N/O	MARINE	YES	N/O	YES	???	N/O	YES
12. Red Pond	24-53-29 N, 76-08-28 W	no	N/O	marine (?)	YES	no	cyanobacteria	YES	no	N/O
13. (?)	24-46-30 N, 76-11-10 W	N/O	N/O	marine (?)	YES	no	YES	no	N/O	no
14. (?) *"hawksbill"*	24-43-46 N, 76-12-42 W	N/O	YES	marine (?)	YES	no	YES	no	no	no
15. (?)	24-43-20 N, 76-12-40 W	N/O	N/O	marine (?)	YES	no	N/O	no	N/O	YES
16. (?) *"blue lagoon"*	24-46-44 N, 76-17-15 W	YES	N/O	MARINE	no	YES	YES	YES	no	no

Note: N/O indicates "*not observed*". Cyanobacteria indicates carbonates presumed to be deposited by biotic processes (cyanobacterial mats or stromatolite).

LITERATURE CITED

Al-Hasan, R. H., Ghannoum, M. A., Sallal, A.K., Abu-Elteen, K. H., and Radwan, S. S. (1987). Correlative changes of growth, pigmentation and lipid composition of *Dunaliella salina* in response to halostress. Microbiology 133(9), 2607-2616.

Aref, M. A., Basyoni, M. H., and Bachmann, G. H. (2014). Microbial and physical sedimentary structures in modern evaporitic coastal environments of Saudi Arabia and Egypt. Facies, 60(2), 371-388.

Aronson, R. B., and Harms, C. A. (1985). Ophiuroids in a Bahamian saltwater lake: The ecology of a Paleozoic□like community. Ecology, 66(5), 1472-1483.

Assereto, R. L., and Kendall, C. G. S. C. (1971). Megapolygons in Ladinian limestones of Triassic of southern Alps; evidence of deformation by penecontemporaneous desiccation and cementation. Journal of Sedimentary Research, 41(3), 715-723.

Assereto, R. L., and Kendall, C. G. (1977). Nature, origin and classification of peritidal tepee structures and related breccias. Sedimentology, 24(2), 153-210.

Baeza, J. A. (2018). "Sexual systems in shrimps (Infraorder Caridea Dana, 1852), with special reference to the historical origin and adaptive value of protandric simultaneous hermaphroditism," in Transitions Between Sexual Systems (Springer, Cham), 269-310.

Bellemain, E., and Ricklefs, R. E. (2008). Are islands the end of the colonization road? Trends in Ecology & Evolution, 23(8), 461-468.

Bishop, R.E., W.F. Humphreys, N.Cukrov, V. Žic, G.A. Boxshall, Marijana Cukrov, Thomas M. Iliffe et al. (2015). 'Anchialine' redefined as a subterranean estuary in a crevicular or cavernous geological setting. Journal of Crustacean Biology, 35(4), 511-514.

Calderón-Gutiérrez, F., Solís-Marín, F. A., Gómez, P., Sánchez, C., Hernández-Alcántara, P., Álvarez-Noguera, F., and Yáñez-Mendoza, G. (2017). Mexican anchialine fauna—With emphasis in the high biodiversity cave El Aerolito. Regional Studies in Marine Science, 9, 43-55.

Carew, J. L. and Mylroie, J. E. (1994). Geology and Karst of San Salvador Island, Bahamas: A Field Trip Guidebook, Bahamian Field Station, San Salvador, Bahamas.

Cole, E. S., Schares, H., Barton, S., Porterfield, J., Morrison, J. and Lor, K. (2016). Evolutionary vs environmental influences on life history traits in the scaly pearl oyster, *Pinctada longisquamosa* on San Salvador Island, Bahamas. The Proceedings of the 1st Joint Natural History & Geology Symposium of the Bahamas.

Cole, E. S., Crumley, A. and Carlson, S. (2010). Patterns of sex determination in the scaly pearl oyster in four anchialine ponds on San Salvador Island, Bahamas. The Proceedings of the 13th Symposium on the Natural History of the Bahamas.

Cole, E. S., Hoft, L., Campion, J. and Cole, B. G. (2006). The effect of hurricane activity on atlantic pearl oysters, *Pinctada longisquamosa*, in two dissimilar inland marine ponds on San Salvador Island, Bahamas. The Proceedings of the 11th Symposium on the Natural History of the Bahamas.

Cutress, C. E. *Bunodeopsis medusoides* Fowler and *Actinodiscus neglectus* Fowler, two Tahitian sea anemones: redescription and biological notes. Bulletin of Marine Science 29, no. 1 (1979): 96-109.

Dalman, M. R. (2009). Paleotempestology and Depositional History of Clear Pond, San Salvador Island, Bahamas (dissertation/ doctoral thesis, University of Akron).

Dawson, M. N., L. E. Martin, L. J. Bell, and Patris, S. (2009). "Marine lakes," in Encyclopedia of Islands, 603-607.

Dawson, M. N., and Hamner, W. M. (2005). Rapid evolutionary radiation of marine zooplankton in peripheral environments. Proceedings of the National Academy of Sciences, 102(26), 9235-9240.

Edwards, D. C., Teeter, J. W., and Hagey, F. M. (1990). Geology and ecology of a complex of inland saline ponds, San Salvador Island, Bahamas. In Field Trip Guidebook-5th Symposium on the Geology of the Bahamas, Bahamian Field Station, San Salvador, Bahamas (pp. 35-45).

Erdman, R. B., Lanterman, L. L. and Button, J. A. (2009). *Aequorea floridana*: An enigmatic hydromedusan from an anchialine lake on San Salvador Island, Bahamas. P.127-130.

Fowler, A. E., Lor, D. J., Farrell, C. E., Bauman, M. A., Peterson, M. N., and Langerhans, R. B. (2018). Predator loss leads to reduced antipredator behaviours in Bahamas mosquitofish. Evolutionary Ecology Research, 19(4), 387-405.

Godfrey, P. J., Edwards, D. C., Davis, R. L., and Smith, R. R. (1993). Natural history of northeastern San Salvador island, a "new world" in the new world. Field guide, Bahamian Field Station, San Salvador, Bahamas, 28.

Goodfriend, G.A., and S. J. Gould. Paleontology and chronology of two evolutionary transitions by hybridization in the Bahamian land snail *Cerion*. Science 274, no. 5294 (1996): 1894-1897

Hagey, F. M., and Mylroie, J. E. (1995). Pleistocene lake and lagoon deposits, San Salvador island, Bahamas. Special Papers-Geological Society of America, 77-90.

Halvorson, H. M., K. Yang, S. Onstad, K. Phillips, Millis, A. and Cole, E.S. (2012). The evolution of life histories: New insights on differential sex determination in the scaly pearl oyster *Pinctada longisquamosa*. The Proceedings of the 14th Symposium on the Natural History of the Bahamas.

Harasewych, M. G., and Manuel J. Tenorio. (2018) The genus *Cerion* (Gastropoda: Pulmonata: Cerionidae) on San Salvador [Watling Island], Bahamas: A geometric morphometric analysis of shell morphology. Nautilus 132, no. 3-4: 71-82.

Holthuis L. B. (1973). Caridean shrimps found in land-locked saltwater pools at four Indo-West Pacific localities (Sinai Peninsula, Funafuti Atoll, Maui and Hawaii Islands), with the description of one new genus and four new species. Zool. Verh. 128:1–48

Kohn, A. J. (1972). January. Conus-milliaris at Easter Island-ecological release of diet and habitat in an isolated population. In American Zoologist (Vol. 12, No. 4, pp. 712-712). 1041 New Hampshire St., Lawrence, KS 66044: Amer Soc Zoologists.

MacArthur. R. H. and Wilson, E. O. (1963). An equilibrium theory of insular zoogeography. Evolution 17:373-87.

MacArthur, R. H. and Wilson. E. O. (1967). The Theory of Island Biogeography. Princeton. NJ: Princeton Univ. Press. 203 pp.

Marshall, H. G. (1982). Phytoplankton composition from two saline lakes in San Salvador, Bahamas. *Bulletin of Marine Science*, *32*(1), 351-353.

Martin, C. H., and Wainwright P. C. (2013). A remarkable species flock of Cyprinodon pupfishes endemic to San Salvador Island, Bahamas. Bulletin of the Peabody Museum of Natural History 54, no. 2: 231-241.

Masonjones, H., Rose, E., Elson, J., Roberts B., and Curtis-Quick, J. (2019). High density, early maturing, and morphometrically unique *Hippocampus erectus* population makes a Bahamian pond a priority site for conservation. Endangered Species Research 39: 35-49.

Mitchell, A. S. (2017). A biotic survey of outcroppings and *Pinctada longisquamosa* in Oyster Pond, San Salvador Island, Bahamas, one year after Hurricane Joaquin. An honors thesis submitted to the faculty of the University of Tennessee at Chattanooga in partial fulfillment of the requirements of the degree of Bachelor of Science.

Mylroie, J. E. (2019). "Chapter 34 - Coastal caves," in Encyclopedia of Caves (Third Edition), ed. William B. White, David C. Culver, Tanja Pipan, Academic Press, 301-307.

Mylroie, J. E., and Carew, J. L. (1995). Karst development on carbonate islands. In Speleogenesis and Evolution of Karst Aquifers. www.speleogenesis.info

Mylroie, J. E. and Mylroie, J. R., (2007). Development of the carbonate island karst model. J. Cave Karst Stud. 69, 59–75.

Novosel, M., Jalžić, B., Novosel, A. E., Pasarić, M., Požar□Domac, A., and Radić, I. (2007). Ecology of an anchialine cave in the Adriatic Sea with special reference to its thermal regime. Marine Ecology, 28, 3-9.

Panikkar, N. K. (1937). The morphology and systematic relationships of a new boloceroidarian from brackish-water near Madras, together with an account of its asexual reproduction. In Proceedings of the Indian Academy of Sciences-Section B, vol. 5, no. 2, pp. 76-90. Springer India.

Park, L. E., Siewers, F. D., Metzger, T., and Sipahioglu, S. (2009). After the hurricane hits: Recovery and response to large storm events in a saline lake, San Salvador Island, Bahamas. Quaternary International, 195(1-2), 98-105.

Park, L. E., Myrbo, A., and Michelson, A. (2014). A qualitative and quantitative model for climate-driven lake formation on carbonate platforms based on examples from the Bahamian Archipelago. Carbonates and Evaporites 29: 409-418.

Park, L. E. (2012). Comparing two long-term hurricane frequency and intensity records from San Salvador Island, Bahamas. Journal of Coastal Research, 28(4), 891-902.

Richardson, K. M., Iverson, J. B., and Kurle, C. M., (2019). Marine subsidies likely cause gigantism of iguanas in the Bahamas. Oecologia 189, no. 4: 1005-1015.

Rose, E., Masonjones, H. D. and Jones, A. G. (2016). A DNA-based assessment of the phylogenetic position of a morphologically distinct, anchialine-lake-restricted seahorse. Journal of Heredity 107, no. 6: 553-558.

Schlesinger, A., Kramarsky-Winter, E., Rosenfeld, H., Armoza-Zvoloni, R., and Loya, Y. (2010). Sexual plasticity and self-fertilization in the sea anemone *Aiptasia* diaphana. PLoS One 5, no. 7: e11874.

Schwartz, A. and Carey, M., (1977). Systematics and evolution in the West Indian iguanid genus *Cyclura*. Studies on the Fauna of Curacao and other Caribbean islands, 53(1), pp.15-97.

Seidel, B., Brasher, A., Auerswald, K., and Geist, J. (2016). Physicochemical characteristics, community assemblages, and food web structure in anchialine pools along the Kona Coast on the Island of Hawaii, USA. Hydrobiologia, 770(1), 225-241.

Stock J. H. T., Iliffe, M., and Williams, D. (1986) The concept "anchialine" reconsidered. Stygologia 2(1/2):90–92.

Teeter, J. W. (1995). Holocene saline lake history, San Salvador Island, Bahamas. Geological Society of America Special Papers, 300, 117-124.

Thomas, M. L., Logan, A., Eakins, K. E., and Mathers, S. M. (1992). Biotic characteristics of the anchialine ponds of Bermuda. Bulletin of Marine Science, 50(1), 133-157.

Turner, B.J., Duvernell, D.D., Bunt, T.M., and Barton, M.G. (2008). Reproductive isolation among endemic pupfishes (Cyprinodon) on San Salvador Island, Bahamas: microsatellite

evidence. Biological Journal of the Linnean Society 95, no. 3: 566-582.

Van Hengstum, P. J., Cresswell, J. N., Milne, G. A., and Iliffe, T. M. (2019). Development of anchialine cave habitats and karst subterranean estuaries since the last ice age. Scientific reports, 9(1), 1-10.

White, D. A., Campion, J. and Cole, E. S. (2007). Characterization of Three Roses Cavern and its accompanying conduit system on San Salvador Island, Bahamas: An inland refuge for coastal fish. The Proceedings of the 12th Symposium on the Natural History of the Bahamas.

Woolbright, S. A., Birchfield, H. A., Ford, D. M., Sheehan, K. L., Ashworth, M. P., Yeager, R. A., Martin, C. H., Manning, S. R., Shroat-Lewis, R. A. and Ruhl, L. S. (2019). Anchialine lakes of the Bahamas support unusually dense populations of *Acetabularia* spp. and other Dasyclad algae. In 2019 ESA Annual Meeting (August 11--16). ESA, 2019.

GEOCHEMISTRY AND MICROBIAL DIVERSITY COMPARISON OF TWO NATURAL HYDROCARBON SEEPS ON THE ISLAND OF BARBADOS

[1]Jeanne Sumrall, [2]Andrea Michele Dearing, [3]Jonathan Sumrall, [4]Hans Machel, [5]Aaron Lynne, [6]Embriette Hyde

[1]Department of Geosciences, Fort Hays State University, 600 Park Street Hays, KS 67601 – corresponding author jlsumrall@fhsu.edu

[2]7026 Plantation Dr. Baytown, Texas 77523

[3]Department of Geosciences, Fort Hays State University, 600 Park Street Hays, KS 67601 – jbsumrall@fhsu.edu

[4]University of Alberta, Canada, Edmonton, Alberta TG2 2E3, Canada- hmachel@telus.net

[5]Department of Biological Sciences, Sam Houston State University, Huntsville, TX 77341
9500 Gilman Dr, MC0763, La Jolla, CA 92093

ABSTRACT

This manuscript characterized the relative abundance and diversity of microorganisms present in two natural crude oil and bitumen seeps on the island of Barbados. The two natural macro-seeps, Turner Hall Woods and Conset Bay, are characterized by different environments: siliciclastic versus carbonate, fresh water versus salt water, and crude oil versus bitumen seepage. Samples were collected for microbial diversity assessment and water geochemistry analysis to determine if the possibility of microbial degradation of hydrocarbons has occurred. It was found that the two locations are similar at the phylum level yet differ greatly at the genus level, with the fresh water location being more diverse than the salt water location. Several hydrocarbon degrading bacteria were identified at both locations, making it possible for some degree of degradation to have occurred. Several unclassified species were also detected, thus opening the door for further research into what role each new species may play in the oil seep environments of Barbados. More research should also be conducted to determine the metabolic activity of the known microbial species found at these oil seeps.

Keywords: geomicrobiology, hydrocarbon microbial communities, microbial diversity, Caribbean

INTRODUCTION

Microbes play a major role in the degradation of petroleum hydrocarbons in marine environments (Rosano-Hernandez et. al., 2011). So-called hydrocarbonoclastic microbes hold the potential to be used for bioremediation, a natural "cleanup" process, in the event of an oil spill or in heavily polluted industrial areas. While 79 hydrocarbon-degrading bacterial species have been identified, 9 cyanophyte, 103 fungal, and 14 algal species are also capable of degrading hydrocarbons (Head *et al.*, 2006). Most hydrocarbon-degrading microbial species are capable of degrading only a limited number of organic compounds, and microbes are known to be active/or most effective in consortia (e.g. Vinas *et al.* 2001; Roling *et al.* 2002).

GEOLOGIC BACKGROUND

Barbados is located approximately 125 km east of the Lesser Antilles volcanic arc. Unlike this chain of islands, Barbados formed as an accretionary prism that was tectonically uplifted (e.g., Speed *et al.*, 2012). The oldest strata of the island are Eocene pelagic clastic sediments that have been tectonically deformed, overlain by Miocene chalks and marls, in turn overlain by Pleistocene carbonate terraces that have experienced extensive karstification (Speed 1990; Taylor & Mann 1991; Jones & Banner 2003a, 2003b; Machel *et al.* 2012; Kambesis and Machel 2013).

The oldest strata of Barbados are Eocene deep sea clastic sediments, referred to as the Scotland Formation. This sequence is composed of turbidites and gravity flows (Speed *et al.* 2012), which are extensively faulted and folded due to tectonic compression and mud diapirism, creating many small-scale structural traps for hydrocarbons (Payne *et al.* 1988). Natural seeps occur on the island ranging from gas to highly viscous bitumen (tar), locally known as manjak (Senn 1946; Schombourgh 1948; Parnell *et al.* 1994). A natural gas seep known as 'Boiling Spring' existed in this formation and was a curiosity for locals for many years prior to its destruction (Schombourgh 1948). Other natural oil seeps have since been discovered in the area as well. A light oil seep is located nearby in Turner Hall Woods, and a bitumen seep is found at Conset Bay (Figure 1). This natural resource supported bitumen mining in the early 20th century, as well as a small local oil industry that continues to thrive today.

The Scotland Formation, where both study locations are located, is overlain by Miocene chalks and marls, known as the Oceanics Group (Senn 1944). This sequence is hardly deformed except for a locally dense fracture network, which allows for the infiltration and/or passage of natural oil and gas through this otherwise impermeable rock sequence. The Oceanics Group is overlain by three major Pleistocene carbonate terraces, known as the Upper Coral Rock Terrace,

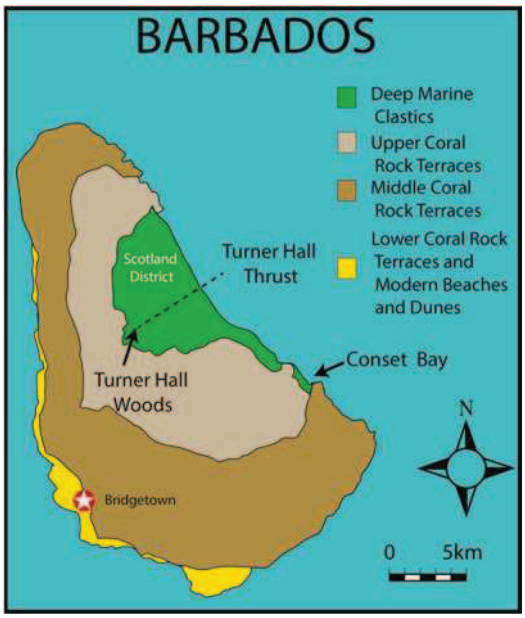

Figure 1 is a simplified geologic map of Barbados with the sampling sites of Turner Hall Woods and Conset Bay. Turner Hall Thrust Fault runs through the Scotland District and terminates at Turner Hall Woods. (Modified from Sumrall et al., 2013)

Middle Coral Rock Terrace, and Lower Coral Rock Terrace (Figure 1), which cover about 70% of the surface of the island today. These terraces formed through tectonic uplift along with sea level rises and falls caused by glacial and interglacial periods (Schellmann and Radtke 2002, 2004). Oil and gas were derived from thermal maturation of organic-rich sediments – chiefly Kerogen III, with minor contributions of Kerogen II – in the accretionary prism (Speed 1987). Based on Sr- and C-isotope data in authigenic carbonates, the hydrocarbons have been seeping from the Eocene source strata into the overlying Oligocene chalks and Pleistocene carbonates since the Late Oligocene, with a spike around 5 m.y. ago (Sumrall *et al.* 2013; Machel *et al.* 2014). Additional information on the geotectonic and sedimentary evolution of the island can be found in Speed (1990, 2012) and Machel (1999, 2011).

The purpose of this study is to identify and compare microbial communities of a natural crude oil and a bitumen seep on Barbados. The oil seep in Turner Hall Woods is associated with a fresh water stream that cuts a deep incised

gully into siliciclastic sediments. The second locality is a bitumen seep in the chalks of Conset Bay located on the Atlantic coast; therefore, this area is influenced by wave action, sea spray, and tidal processes.

SITE DESCRIPTION AND FIELD OBSERVATIONS

There are significant differences in geological setting between the sampling sites of Turner Hall Woods and Conset Bay. The seep in Turner Hall Woods is found within poorly lithified, deep marine clastic sediments (Figure 2A). A fault, Turner Hall Thrust, runs through this area (Figure 1) and may be instrumental in the migration of crude oil to the surface. Several narrow fresh water streams run through this area and many small pools of oil in various consistencies and volatilities (ranging from light crude to cohesive, sticky orange, brown, and black crude oil) (Figure 2B) can be seen floating on top of the water for a considerable length of the streams.

Figure 2. A) Faulted oil stained rocks in Turner Hall Woods. These rocks are poorly lithified sandstones with intermixed clay layers. B) Orange organics growing in small pool of water and oil mixture located along the freshwater stream in Tuner Hall Woods, camera cap for scale.

Conset Bay is located along the Atlantic coast and is influenced by seawater and tidal processes. The rocks that host the seep here are chalks of the Oceanics Group, which are nearly impermeable, although a few beds appear to have sufficient matrix permeability to transmit hydrocarbons. Faulting likely enhanced the infiltration of bitumen (Figure 3A). In stark contrast to the seep at Turner Hall Woods, the hydrocarbons at Conset Bay are a highly viscous, sticky black tar. A shaggy, hunter green, algae-like material covers the bitumen in the intertidal zone (Figure 3B). Deeper into the intertidal zone, the material changes from hunter green to light green and has a rougher, less shaggy texture. At the base of the seep, light brown microbial mats are found.

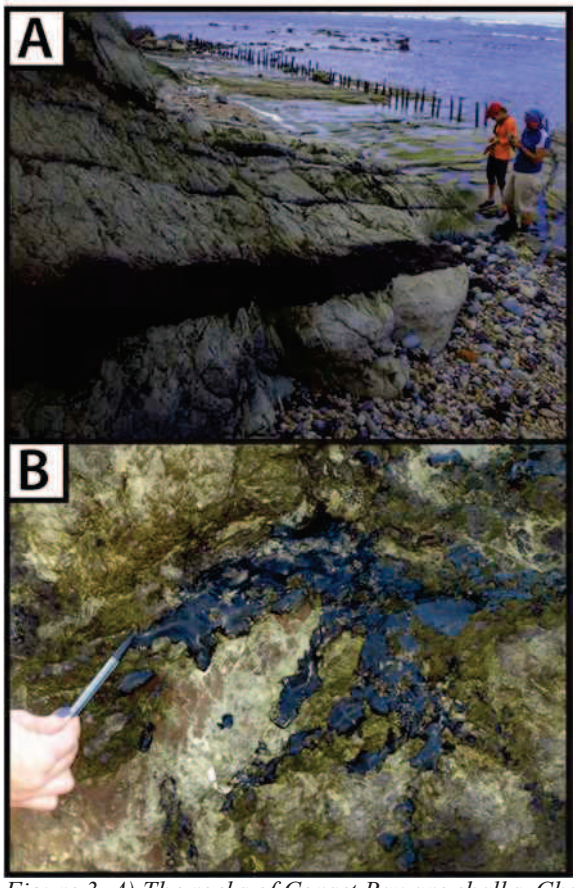

Figure 3. A) The rocks of Conset Bay are chalks. Chalks are typically impermeable and must have been faulted to allow the infiltration of hydrocarbons. B) Crystalline bitumen is pictured with a shaggy, hunter green algae-like growth on and surrounding the bitumen; mechanical pencil for scale.

METHODS

Fieldwork was conducted in late December to early January of 2013-2014. For this pilot study three 50 ml water samples and

five microbial swab samples were collected from separate localities within Turner Hall Woods; the samples were collected from water surrounding small pools of crude oil thought to be affected by microbial communities (Figure 4). Eight microbial swab samples were collected from Conset Bay (Figure 5). These samples were taken where microbes were growing on the bitumen substrate. Water samples were not collected from Conset Bay due to the high energy tidal environment of this area, and because the only water present in and around the outcrop is seawater. Multiple microbial samples were collected from each location to better ensure a successful study, in case of destruction during transport. These locations are difficult to access, and remote. The microbial samples were collected at the same locations as the water samples in progresses pools of water around the oil seep.

Figures 4 and 5 depict the sampling process at Turner Hall Woods and Conset Bay, respectively.

The lower the sample number, the closer it was to the oil seep. All samples were collected at the surface from the aerobic zone.

Water Sampling procedure and analysis

In order to better understand the potential source of the water and salinity, water samples were collected at Turner Hall Woods using unopened, sterilized, Nalgene sampling bottles. The bottles were completely filled with the samples and allowed no head space. They were then capped and wrapped with parafilm to prevent contamination. The bottles were refrigerated at 4° C until analysis. The samples were analyzed within a month of returning from Barbados using Inductively coupled plasma-optical emission spectroscopy (ICP-OES) at the Texas Research Institute of Environmental Studies (TRIES) at Sam Houston State University.

Aliquots (of 25 ml) were acidified for four hours using 0.5 mL concentrated HNO3 and 1.25 ml concentrated HCl. The volume was then diluted to 25 ml using distilled water before analysis. Samples with oil residue were filtered with a 0.45 micron filter prior to analysis.

Microbial sample processing and sequencing:

Sample processing, 16s rRNA gene amplification and sequencing was performed through the Alkek Center for Metagenomics and Microbiome Research and the Human Genome Sequencing Center (Baylor College of Medicine, Houston, TX) following protocols benchmarked as part of the Human Microbiome Project (http://www.hmpdacc.org/doc/HMP_MOP_Version12_0_072910.pdf, PMID 22699609, PMID 22699610). Bacterial genomic DNA was extracted from samples using the PowerSoil DNA Isolation Kit (MoBio, Carlsbad, CA). The V4 region of the bacterial genomic DNA was amplified using barcoded primers 515f (5'-GTGCCAGCMGCCGCGGTAA-3') and 806r (5'-GGACTACHVGGGTWTCTAAT-3'). The PCR reaction contained the following: 2uL 4uM barcoded primer stock, 5uL DNA, 2uL Taq Buffer II (Invitrogen), 0.15uL Taq enzyme (Invitrogen), and 10.85uL PCR-grade water. The reactions were amplified in an Eppendorf mastercycler Thermocycler under the following conditions: initial denaturation step for 2 minutes at 95oC, followed by 30 cycles of 20 second denaturation at 95oC, 45 seconds of annealing at 50oC, and 90 second annealing at

72oC. Barcodes allowed pooling of samples for sequencing. All samples were pooled and sequenced on one lane of an Illumina HiSeq 2000 sequencer (Illumina, San Diego, CA) at the BCM Human Genome Sequencing Center.

16S rRNA gene data analysis:

Using custom perl scripts, Reads 1 and 2 were pre-quality filtered by trimming the sequences at the first ambiguous base and then joining reads 1 and 2 with a minimum required overlap of 12 bases. Two samples (B7 and B9) did not have any reads and were not included in the subsequent analysis. Sequences were then de-multiplexed and quality trimmed using QIIME version 1.8 (PMID 20383131). Sequences with any ambiguous bases, with a phred quality score less than 20, and with more than 1.5 barcode errors were discarded and not used in further analyses. Quality trimming resulted in 310,826 high quality reads. Sequences were binned into OTUs and assigned taxonomy by clustering sequences using UCLUST against a reference database (the Greengenes May 2013 release) at 97% identity. The OTU table was then filtered to remove any OTUs that composed less than 0.0005% of the entire dataset (roughly the equivalent of singleton OTUs) and rarefied to 5651 sequences per sample (the lowest number of reads associated with any one sample). Diversity was assessed by calculating the Shannon diversity metric and the number of observed species for each sample, from 10 to 5,510 reads per sample (steps of 500 reads per sample). Non-parametric t-tests using Monte Carlos permutations (999) to calculate the p-value (Bonferonni corrected) determined significant differences in diversity between groups. Stacked bar charts were also constructed to visualize the taxa present in each sample and across sample groups.

RESULTS

Water Samples

Samples B2-W, B3-W, and B5-W were collected from a freshwater stream that runs through Turner Hall Woods to better understand the chemistry of the water in the pools nearest the oil seep. Three samples were taken in the three surrounding pools of water with sample B2-W being the closed pool to the seep and containing large amounts of oil in the water, B3-W was collected from the next closest pool, and B5-W was the furthest from the seep being approximately 5 feet away. Sample B2-W (filtered) contained petroleum and was filtered prior to analysis. The elements found in highest abundance in the three water samples from Turner Hall Woods are listed in Table 1. High values of calcium (>30 ppm), magnesium (>65 ppm), and sodium (>180ppm) were observed for all three water samples. Sample B2-W possesses significantly higher quantities of magnesium, sodium, and sulfur in relation to the other two samples. Sample B3-W is characterized by a higher abundance of aluminum, iron, and silicon when compared to the other samples. Data for sample B5-W is an even distribution between the three samples.

Microbial Swab Samples

The richness and evenness of the sequenced microbial communities sampled were surveyed using the Shannon diversity index. The sequenced microbial communities at Turner Hall Woods are more diverse than those at Conset Bay (Figure 6). When the data were organized to a phylum level, it is clear the two locations differ (Figure 7). Both locations are dominated by Proteobacteria; however, Turner Hall Woods has a higher relative abundance of this phylum than did Conset Bay. Cyanophytes represent an abundant proportion of the sequenced community at Conset Bay, yet not Turner Hall Woods. At the phylum level, both locations are composed of similar relative abundances of Firmicutes, Bacteroidetes, and Actinobacteria.

The differences in sequenced microbial communities between the two sample locations

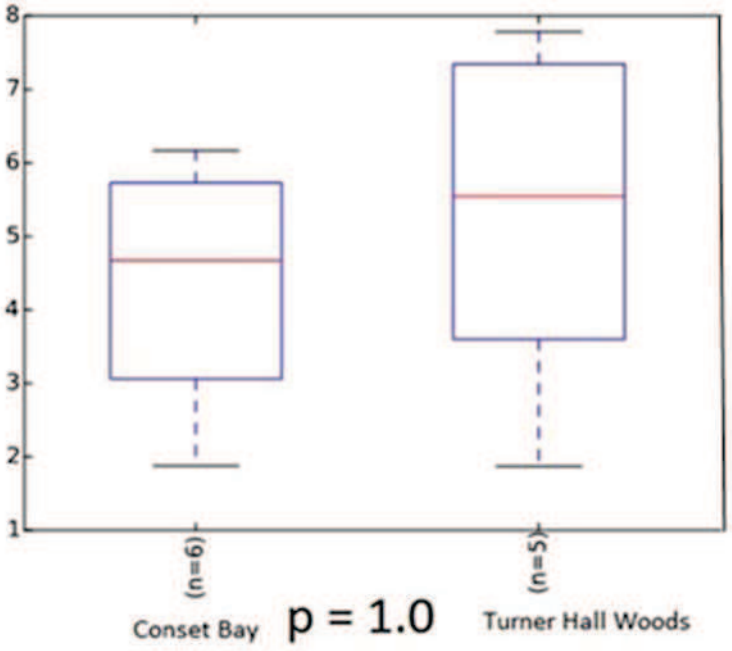

Figure 6- A box plot diagram for the Shannon Diversity Index of Turner Hall Woods and Conset Bay.

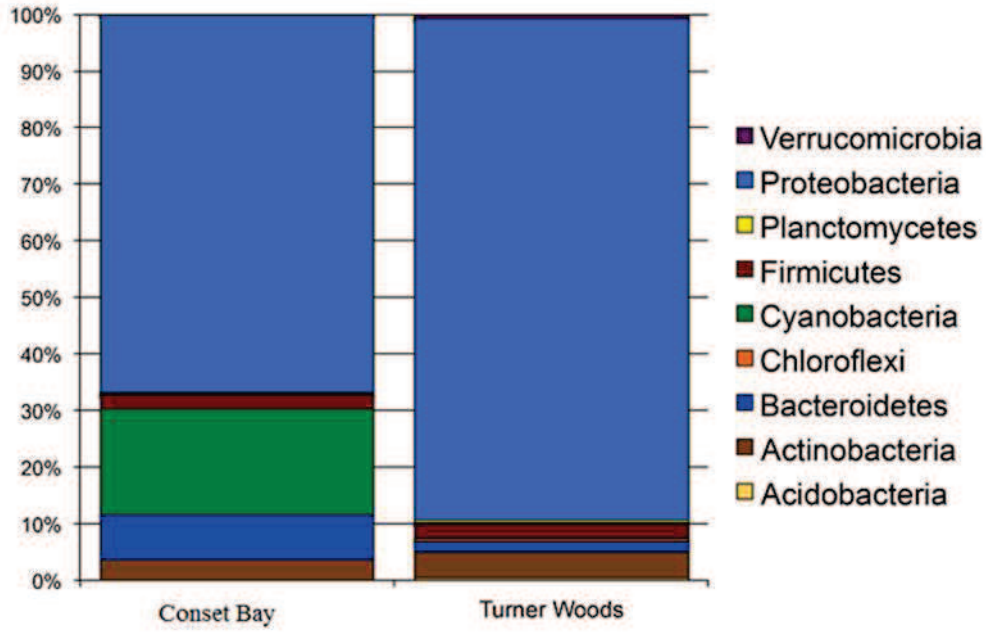

Figure 7. Microbial community data is broken down to the phylum level from Turner Hall Woods and Conset Bay. Both samples are dominated by Proteobacteria. Turner Hall Woods contains roughly 90% Proteobacteria while Conset Bay is characterized by approximately 65%.

becomes more apparent when examined at the genus level (Figure 8). Turner Hall Woods is more diverse at the genus level than Conset Bay, meaning more genera are present at Turner Hall Woods than Conset Bay. The bitumen from Conset Bay harbors several marine genera including *Pseudoalteromonas*, an unclassified genus of the family Rhodobacteraceae, an unclassified genus of the order Stramenopiles, *Vibrio*, *Rivularia*, an unclassified genus of the

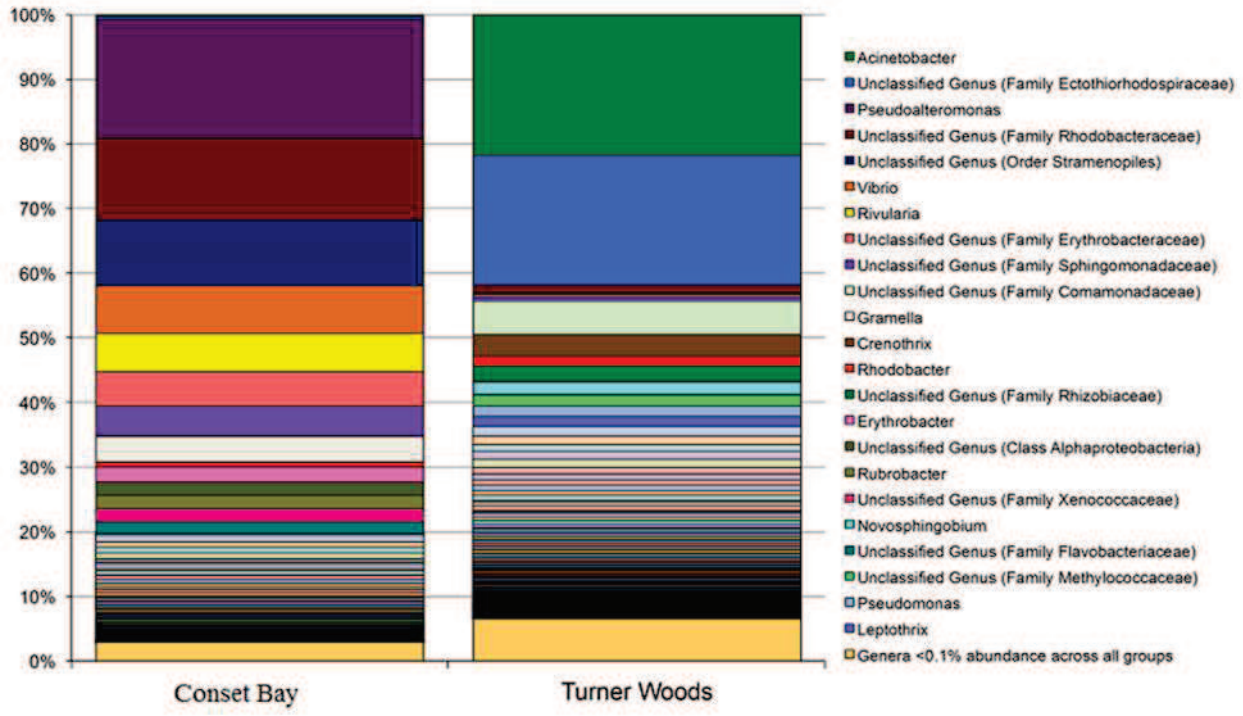

Figure 8. The microbial communities are displayed at the genus level. Turner Hall Woods is mainly dominated by Acinetobacter while Conset Bay is characterized by Pseudoalteromonas. Each genus is represented by a color and its percentage present is read from the left-hand percentage column.

family Eythrobacteraceae, and *Gramella*. Turner Hall Woods is mainly composed of Acinetobacter, an unclassified genus of the family Ectothiorhodospiraceae, an unclassified genus of the family Comamonadaceae, *Crenothrix*, *Rhodobacter*, and an unclassified genus of the family Rhizobiaceae.

These apparent differences are also seen when the data are visualized on a sample-by-sample basis (Figure 9). All microbiome samples from Turner Hall Woods are composed of *Acinetobacter* (4% - 85%), while samples from Conset Bay are composed of only 0% to 3%. All Turner Hall Woods microbiome samples are also dominated by an unclassified genus of the family Ectothiorhodospiraceae (1% - 52%) and an unclassified genus of the family Comamonadaceae (1% to 15%). Conset Bay microbiome samples are dominated by *Pseudoalteromonas* (0% - 86%) and an unclassified genus of the family Rhodobacteraceae (0% to 15%), followed by an unclassified genus of the family Erythrobacteraceae (0% - 22%).

DISCUSSION

Water Samples

The water samples from Turner Hall Woods have elevated concentrations of calcium, magnesium, and sodium compared to standard (normal) seawater (Table 1). Furthermore, the ratios of the three major ion concentrations in the samples from Turner Hall Woods differs from the same ratios in standard (normal) seawater (Table 1). The higher concentrations of calcium, magnesium, and sodium and accompanying elevated ionic ratios are interpreted to result from inorganic salts and brine carried by the hydrocarbons present at Turner Hall Woods. Inorganic salts are known to be suspended in crude oils or dissolved in associated waters (Kraus 2011).

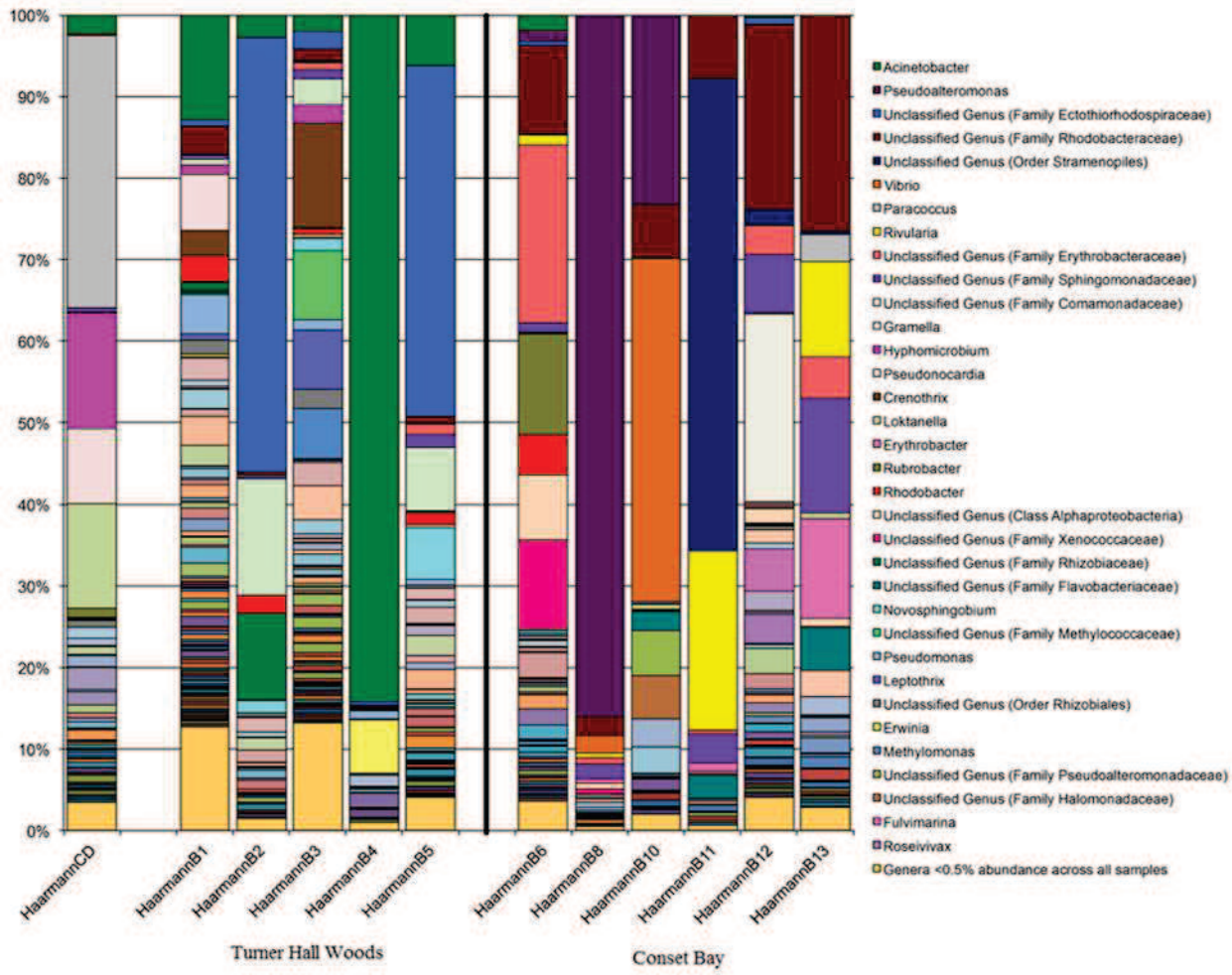

Figure 9. Microbial community data is displayed on a sample-by-sample basis. Each genus is represented by a color and the percentage present is read from the left-hand percentage column. Sample CD data was not included in this study, and Samples B7 and B9 were not analyzed.

	Al (ppm)	Ca (ppm)	Fe (ppm)	K (ppm)	Mg (ppm)	Na (ppm)	S (ppm)	Si (ppm)
B2-W (filtered)	**0.3**	**34.4**	**0.2**	**28.0**	**123.7**	**345.1**	**202.7**	**23.0**
B3-W	**13.7**	**32.3**	**34.7**	**29.0**	**68.0**	**191.5**	**92.8**	**66.5**
B5-W	**0.3**	**32.0**	**0.1**	**25.8**	**69.0**	**187.0**	**99.6**	**20.8**

Table 1. Table of elements found in highest abundance in Barbados water samples. Samples B2-W, B3-W, and B5-W were collected from a freshwater stream that runs through Turner Hall Woods. Elements present are listed as parts per million in columns and sample numbers are listed as rows. Sample B2-W (filtered) contained petroleum and was filtered prior to analysis.

In addition, two water samples from Turner Hall Woods have elevated concentrations of sulfur (B2-W), aluminum (B3-W), and iron (B3-W). Sample B2-W was collected from an oil-filled 'pool' as an oil-water mixture. Thus it is possible, if not likely,

that the higher concentration of sulfur observed in this water sample is derived from the associated oil, either via dissolution of organosulfur compounds in the water, or from microbial sulfate reduction, which can be viewed as a form of anaerobic biodegradation of oil (Machel 2001; Hill and Schenk 2005). The higher concentration of iron in sample B3-W possibly resulted as a by-product of biodegradation of the oil, which may happen aerobically or anaerobically. At Turner Hall Woods, both options are possible, i.e., biodegradadation is likely to happen anaerobically some distance from the surface yet aerobically right at the surface, rendering iron predominantly in the ferrous or ferric state, respectively (e.g., Machel 1995). Sample B3-W was collected from a surface pool of petroliferous water that contained an orange mucilaginous microbial community. Genera of iron-oxidizing bacteria such as *Crenothrix* and *Leptothrix* (Cullimore and McCann 1978) are present in the microbial analysis of the same sampling site. A reason for the elevated aluminum concentration is not evident.

Microbial Swab Samples

Turner Hall Woods and Conset Bay differ at the phylum level. Both locations are dominated by Proteobacteria, but the relative abundances of Proteobacteria are higher in the siliclastic sediment environment of Turner Hall Woods. Many well-known species present in hydrocarbon degrading environments are members of the Proteobacteria phylum. It is possible the Proteobacteria present at these locations are functioning as hydrocarbon degraders considering the environment, but more work needs to be done to determine metabolic activity of the specific species sequenced. A study of petroleum influenced beach sediments from a siliciclastic and carbonated region in Mexico produced similar results (Rosano-Hernandez 2011). In addition, this study found Alphaproteobacteria and Gammaproteobacteria to be the most abundant classes, and the siliciclastic sediments were more diverse than the carbonate sediments (Rosano-Hernandez 2011).

Cyanobacteria are more abundant at Conset Bay than Turner Hall Woods, which is likely due to the presence of microbial mats at Conset Bay. Cyanobacteria are adapted to withstand low nitrogen environments and can fix nitrogen themselves (Sanchez 2005). Cyanobacteria (Cyanophyte) are unlikely to degrade petroleum compounds, but may play an indirect role in mixed populations and support the growth of those microorganisms that degrade petroleum (Sanchez 2005). Both sites had Firmicutes, Bacteroidetes, and Actinobacteria present at the phylum level. Similar microbes were found in Brazilian oil fields (Silva 2012).

The richness of Turner Hall Woods is greater the Conset Bay at the Genus level (Figure 8). The diversity of microbes within each site, sample compared to sample, (Figure 9) is also notable. Greater diversity at the Genus level is present in the samples closest to the oil seeps. More research could help determine metabolic functions that may lead to a better understanding of these locational differences. Both locations are characterized by common microbes found in hydrocarbon degrading environments. Turner Hall Woods is strongly influenced by *Acinetobacter* and an unclassified genus of family Ectothiorhodospiraceae. *Acinetobacter* is typically associated with aerobic hydrocarbon degradation and is found worldwide (Silva 2012). Conset Bay's microbial community consists of several marine genera such as *Pseudoalteromonas*, Vibrio, an unclassified genus of family Rhodobacteraceae, and an unclassified genus of family Eythrobacteraceae. The Erythrobacteraceae are known to metabolize organic substrates, with light enhancing their growth (Roling 2002). This family is also known to play a critical role in the carbon cycle in the ocean (Roling 2002), so its presence at Conset Bay is not surprising. The genera distribution at both locations is somewhat surprising. *Pseudomonas* and *Vibrio* are among the most common hydrocarbon

degraders globally (Rosano-Hernandez 2011), yet *Pseudomonas* are not found in high abundances at either location, and only one sample at Conset Bay contained Vibrio (Figure 9).

In marine settings, a highly specialized genera, *Marinobacter*, was found to dominate in hydrocarbon-rich areas (Rosano-Hernandez 2011). Because of its ability to outcompete other microbial competitors, it was surprising that *Marinobacter* was not found within samples from Conset Bay. Certain strains of *Marinobacter* thrive when degrading hydrocarbons in moderate to hypersaline conditions (Al-Mailem *et al.* 2013). The salinity values may play a role in the lack of *Marinobacter* found in Conset Bay. It is also possible the absence of *Marinobacter* at Conset Bay could be due to nature of the highly viscous hydrocarbons found in Conset Bay.

While many of the genera present at the two hydrocarbon seeps in Barbados are known to be present in hydrocarbon degrading environments, several are known for different applications. Many of the genera present are more commonly associated with the medical field and are human pathogens. While these pathogenic bacteria typically use a human host as a carbon source, they could now be adapting to thrive off hydrocarbons. Higher petroleum concentration often produces lower microbial diversity (Rosano-Hernandez 2011). Our samples from Turner Hall Woods and Conset Bay also contain several unclassified genera. With bacteria known for different functions as well as several unclassified genera, further research into what role each microbe plays in the degradation of hydrocarbons from Barbados is necessary. The role each organism plays in biodegradation and their abundances have the potential to be applied to recreate consortiums aiding in the remediation of oil spills. The two oil seeps from vastly different environments were analyzed, allowing for the availability of a broader spectrum of microbial consortiums. Habitats in need of bioremediation vary geochemically as well as biologically. This study characterizes the microbes of specific marine-influenced bitumen seeps and a lighter oil seep. This could be beneficial when designing future bioremediation communities for similar geochemical or biological settings. Further data collection and analysis efforts in Barbados including in-depth water, oil, and substrate sampling will enable greater understanding of these unclassified genera and their potential usage.

CONCLUSIONS

The two natural hydrocarbon seeps on Barbados offer a unique opportunity to observe and compare contrasting seep environments. Turner Hall Woods and Conset Bay differ in the environments they are characterized by as well as the microbial communities that reside at each location. Turner Hall Woods is more diverse than Conset Bay and both areas are mostly characterized by well-known hydrocarbon degraders. The presence of these hydrocarbonoclastic bacteria indicate the possibility of hydrocarbon biodegradation. Further research focused on the role these microbes play in the degree of biodegradation and metabolic activities should be pursued, as well as their potential use in bioremediation.

LITERATURE CITED

Al-Mailem D.M., Eliyas, M. & Radwan, S.S., (2013). Oil-bioremediation potential of two hydrocarbonoclastic, diastrophic Marinobacter strains from hypersaline areas along the Arabian Gulf coasts. Extremophiles. 17: 463-470.

Cullimore, D.R. & McCann, A.E., (1978). The identification, cultivation and control of iron bacteria in ground water. Aquatic Microbiology, Editors Skinner & Shewan Academic Press.

Head, I.M., Jones, D.M. & Roling, W.F.M., (2006). Marine microorganisms make a meal of oil. Nature Reviews Microbiology. 4, 173-182.

Hill, R.J. & Schenk C.J., (2005). Petroleum geochemistry of oil and gas from Barbados: Implications of distribution of Cretaceous source rocks and regional petroleum prospectivity. Marine and Petroleum Geology. 22, 917-943.

Jones, I.C. & Banner, J.L., (2003)a. Estimating recharge thresholds in tropical karst island aquifers: Barbdos, Puerto Rico and Guam. Journal of Hydrology, 278: 131-143. http://dx.doi.org/10/1016/S0022-1694(03)00138-0

Jones, I.C. & Banner, J.L., (2003)b. Hydrogeologic and climatic influences on spatial and interannual variation of recharge to a tropical karst island aquifer. Water Resources Research, Vol. 39, No. 9, 1253. Doi:10.1029/2002WR001543,2003

Kambesis, P. N., & Machel, H. G. (2013). Caves and Karst of Barbados. In Coastal Karst Landforms (pp. 227-244). Springer Netherlands.

Kraus, R.S., (2011). Exploration, drilling, and production of oil and natural gas. ILO Encyclopedia of Occupational Health & Safety. www.ilo.org/oshenc/part-xi/oil-exploration-drilling-and-production-of-oil-and-natural-gas

Machel, H.G., (1995), Magnetic mineral assemblages and magnetic contrasts in diagenetic environments - with implications for studies of paleomagnetism, hydrocarbon migration and exploration. In: Turner, P. and Turner, A. (eds), Paleomagnetic applications in hydrocarbon exploration and production. Geological Society Spec. Pub., No. 98, p. 9-29.

Machel, H.G., (1999). Geology of Barbados: a brief account of the island's origin and its major geological features. Barbados Museum and Historical Society, The Garrison, St. Michael, Barbados, 52 p.

Machel, H.G., (2001), Bacterial and thermochemical sulfate reduction in diagenetic settings – old and new insights. Sedimentary Geology, 140, 143-175.

Machel, H.G., (2011). Geology of Barbados: a little paradise in its own right. In: Carrington C.M.S. (Ed.), Prserving paradise. Barbados Museum and Historical Society: 13-51.

Machel, H.G., Kambesis, P.N., Lace, M.J., Mylroie, J.R., Mylroie, J.E., & Sumrall J.B., (2012). Overview of Cave Development on Barbados. In: Kindler, P. and Gamble, D.W., eds, Proceedings of the 15th Symposium on the Geology of the Bahamas and Other Carbonate Regions, p. 96-106.

Machel, H.G., Sumrall, J.B. and Kambesis, P.N., (2014). Episodic fluid flow and dolomitization by methane-bearing pore water of marine parentage in an accretionary prism setting, Barbados, West Indies. Journal of Sedimentary Research, 84. 58-71.

Parnell, J., Ansong, G., & Veale, C., (1994). Petrology of the bitumen (manjak) deposits of Barbados: hydrocarbon migration in an accretionary prism. Marine and Petroleum Geology, 11: 743-755. http://dx.doi.org/10.1016/0264-8172(94)90027-2

Payne, P., Sargeant, M., & Jones, K., (1988). An approach to the Evaluation and Exploration of Hydrocarbons from the Barbados Accretionary Prism. Transactions of the 11th Carribean Geological Conference, Barbados, July 20-26, 1986. Government Printing Department, Bridgetown, Barbados, p. 39:1-39:25.

Roling, W.F.M., Milner, M.G., Jones, D.M., Lee, K., Daniel, F., Swannell, R.J.P., & Head, I.M., (2002). Robust Hydrocarbon

Degradation and Dynamics of Bacterial Communities during Nutrient-Enhanced Oil Spill Bioremediation. Applied and Environmental Microbiology. 68, 5537-5548. Doi:10.1128/AEM.68.11.5537-5548.2002.

Rosano-Hernandez, M., Ramirez-Saad, H., Fernandez-Linares, L., (2011). Petroleum-influenced beach sediments of the Campeche Bank, Mexico: Diversity and bacterial community structure assessment. Journal of Environmental Management 95, S325-S331.

Sanchez, O., Diestra, E., Esteve, I., & Mas, J., (2005). Molecular Characterization of an oil-degrading cyanobacterial consortium. Microbial Ecology 50, 580-588. DOI:10.1007/s00248-005-5061.

Schellmann G. & Radtke U., (2002). The coral reef terraces of Barbados – a guide. Barbados 2002 – International Conference on "Quaternary Sea Level Change" with field trips. And: Fourth Annual Meeting of IGCP Project 437 "Coastal Environmental Change During Sea Level Highstands: A global Synthesis with Implications for Management of Future Coastal Change. INQUA Commission on Coastlines, IGU Commission on Coastal Systems. 26 October – 2 November 2002, Barbados (W.I.), 118 pages.

Schellmann G. & Radtke U., (2004), The Marine Quaternary of Barbados. KoelnerGeographische Arbeiten Heft 81, 137 pages.

Schombourgh, R.H., (1848) – The History of Barbados. Longman, Brown, Green, and Longmans, 722p. http://archive.org/details/historybarbados00schogoog

Senn A., (1944). Inventory of The Barbados Rocks and their Possible Utilization. Department of Science and Agriculture Bulletin, 1: 1-40.

Senn A., (1946). Geological investigations of the groundwater resources of Barbados, B.W.I.: Report of the British Union Oil Company LTD., 123 p.

Silva T.R. et al., (2012). Diversity analyses of microbial communities in petroleum samples from Brazilian oil fields. International Biodeterioration & Biodegradation 81 (3013) 57-70.

Speed R.C., (1990) – Volume loss and defluidization history of Barbados. Journal of Geophysical Research, 95: 8983-8996. http://dx.doi.org/10.1029/JB095iB06p08983

Speed, R.C., Speed, C., and Sedlock, R., (2012), Geology and Geomorphology of Barbados: A Companion Text to Maps with Accompanying Cross Sections, scale 1:10,000: Geological Society of America, Special Publication 485, 63p.

Sumrall J.B., Mylroie J.E. and Machel H.G., (2013). Unusual polygenetic void and cave development in dolomitized Miocene chalks on Barbados, West Indies. International Journal of Speleology, 42 (3) 247-255. Tampa, FL (USA) ISSN 0392-6672 http://dx.doi.org/10.5038/1827-806X.42.3.8

Taylor F.W. & Mann P., (1991) – Late Quaternary folding of coral reef terraces, Barbados. Geology, 19: 103-106. http://dx.doi.org/10.1130/00917613(1991)019<0103:LQFOCR>2.3.CO:2

Vinas M., Grifoll M., Sabate j., and Solanas A.M., (2002). Biodegradation of a crude oil by three microbial consortia of different origins and metabolic capabilities. Journal of Industrial Microbiology & Biotechnology.

SIZE DISTRIBUTION AND POPULATION FLUX OF THE FLAT TREE OYSTER, *ISOGNOMON ALATUS,* IN TWO INLAND LAKES ON SAN SALVADOR ISLAND, THE BAHAMAS

Katlyn Beebout[1], Lexy Teerink[1], and Alyssa M. Anderson[2*]

[1]Department of Biology, Northern State University, Aberdeen, SD 57401
[2]Department of Biology, Southwest Minnesota State University, Marshall, MN 56258
*Corresponding author: alyssa.anderson@smsu.edu

ABSTRACT

The flat tree oyster (*Isognomon alatus*) is often found in mangrove marshes growing on or around the intricate aerial root network of red mangrove trees. Work with *I. alatus* is limited and literature provides little information about their response to different environmental conditions. The purpose of this study was to examine the size distribution of *I. alatus* in two inland waterbodies, Oyster Pond and Osprey Lake on San Salvador Island, Bahamas. While these systems are spatially close and similar in size, they vary in terms of ocean connectivity, salinity, and dominant vegetation. During March of 2015 and 2018, samples of at least 100 oysters were collected randomly from each body of water. The hinge lengths of individuals were recorded in the field and size distribution was compared between years. Surprisingly, no live oysters were found in Osprey Lake in 2018; however, the lake bottom was covered in *I. alatus* shell remains, which were used to assess population size in 2018. Both Oyster Pond and Osprey Lake had a significant change in average hinge length from 2015 to 2018; Oyster Pond had a significantly smaller-sized population in 2018, while collections from Osprey Lake suggested a larger-sized population. We believe that a combination of hurricane activity and differential conduit connectivity to the ocean account for the differences seen between the ponds. Specifically, we think that hurricane activity damaged the red mangroves in Osprey Lake that provide habitat for *I. alatus*, thereby impacting *I. alatus* recruitment; additionally, lack of connectivity to the ocean and associated tidal activity may have resulted in a rapid and longer-term, detrimental drop in salinity. A shorter-term salinity drop in conduit-regulated Oyster Pond, on the other hand, may have triggered a mass spawning event resulting in high recruitment. Additional ecological information for *I. altatus* is necessary in order to draw further conclusions on the population fluctuations found in San Salvador's inland lakes.

INTRODUCTION

The flat tree oyster (*Isognomon alatus* Gmelin 1791) is widely distributed throughout the Caribbean region and is often found in mangrove marshes, growing on or around the intricate aerial root network of mangrove trees. *I. alatus* can spawn throughout the year, and mass spawning events are particularly common following significant rain fall, which cause water salinity to decrease. Prodissoconch larva are then released into the water column, where they grow and eventually attach to red mangrove roots via byssus threads. The oysters become reproductively mature after approximately one year; however, the general lifespan is unknown (Siung 1980).

On San Salvador, *I. alatus* can be found in several interior lakes and ponds. These inland waterbodies are unique, anchialine habitats as their salinity levels vary from brackish to hypersaline, depending on the level of subterranean connectivity to the ocean and impact of recent rainfall events (Edwards 2001). Those ponds that exhibit predictably marine conditions

are often heavily influenced by conduits and associated tidal influence, while hypersaline ponds have more limited connectivity and are influenced by evaporative processes (Mylroie and Carew 1995). *Isognomon alatus* is known for its ability to tolerate a range of salinities (Siung 1980), more so than many of its invertebrate counterparts (Goodbody 1961); this is confirmed by the species' presence in a range of anchialine habitats on San Salvador Island.

The aerial root system of red mangroves (*Rhizomorpha mangle*) provides excellent habitat for *I. alatus* as well as a host of other invertebrate species (sponges, cnidarians, bivalves, gastropods, annelids, ascidians, etc.). Their root system dips into the water looking for substrate, allowing for further stabilization of the main stem. This rhizomatous tree can tolerate salinity levels up to 60 ppt; however, once this salinity level is surpassed, the trees experience stress (Liang *et al.* 2008). Red mangroves also tend to be intolerant to heavy wind and wave action caused by hurricanes, particularly as compared to the black mangrove (*Avicennia germinans*); furthermore, mangrove forests as a whole are less resistant to hurricanes as compared to semi-deciduous dry forests and rainforests (Imbert 2018). Considering the high dependency other marine organisms have on red mangroves, tropical storms can be detrimental to multiple populations including *I. alatus,* which depends on the roots system for support (Siung 1980).

Here, we examine and compare the size distribution of *I. alatus* in two of San Salvador's anchialine ponds that differ in terms of ocean connectivity and thus also salinity, Oyster Pond and Osprey Lake. We also compare oyster populations from these water bodies collected in March 2015 to those in March 2018. Notably, these sampling events were separated by Hurricane Juaquin, a category 4 hurricane that made landfall on San Salvador Island on October 2, 2015.

FIELD-SITE DESCRIPTION

Oyster Pond and Osprey Lake are both located less than 1 km south of the Gerace Research Centre (Figure 1). These water bodies are similar in location and size; however, they differ chemically and physically. Oyster Pond is a dissolution, marine water body that is influenced by a connection to the ocean that causes a tidal flux in water depth and stabilizes salinity. Rothfus (2012) reported an average salinity of 37.1 ppt from monthly data collected over a 22-month period in Oyster Pond; salinity does, however, decrease temporarily with precipitation. The shoreline is dominated by red mangroves, which protect the pond from strong winds and erosion. In 2015 and 2018, the red mangrove population surrounding Oyster Pond appeared to be in good health with a dense canopy cover, thick aerial root system, and evidence of reproduction (visual observations). The sediment of Oyster Pond is a mix of flocculants and shell hash.

Osprey Lake, a dissolution lake classified as a hypersaline water body, is found just northwest of Oyster Pond; the ponds are separated by only ~50 m in some areas (Figure 1). This water body is influenced by conduits, although not as heavily as Oyster Pond (Edwards 2001, McGee *et al.* 2010). Osprey Lake's hypersaline state (52.1 ppt on average, as documented by Rothfus 2012) is strongly regulated by evaporation as well as seepage from a nearby hypersaline water body, Blue Pond, found at its southwestern edge (McGee *et al.* 2010); Edwards (2001) reported a salinity range of 38.0-61.0 ppt for Osprey Lake, with rainy years accounting for reduced salinity. The dominant shoreline vegetation is the black mangrove with several off-shore patches of red mangroves. In 2015, the red mangrove patches were visually healthy and supported invertebrate life, such as *I. alatus*. In 2018, the patches were visually suffering; bark was discolored, aerial roots were fragile and broke easily, and the canopy cover was sparse (Figure 2); similar observations were made in June, 2019 (Beebout and Anderson, personal observation). The main organism living on the red mangroves was fuzzy finger algae (*Batophora oerstedii*). The sediment of Osprey Lake is a mix of flocculants and shell hash.

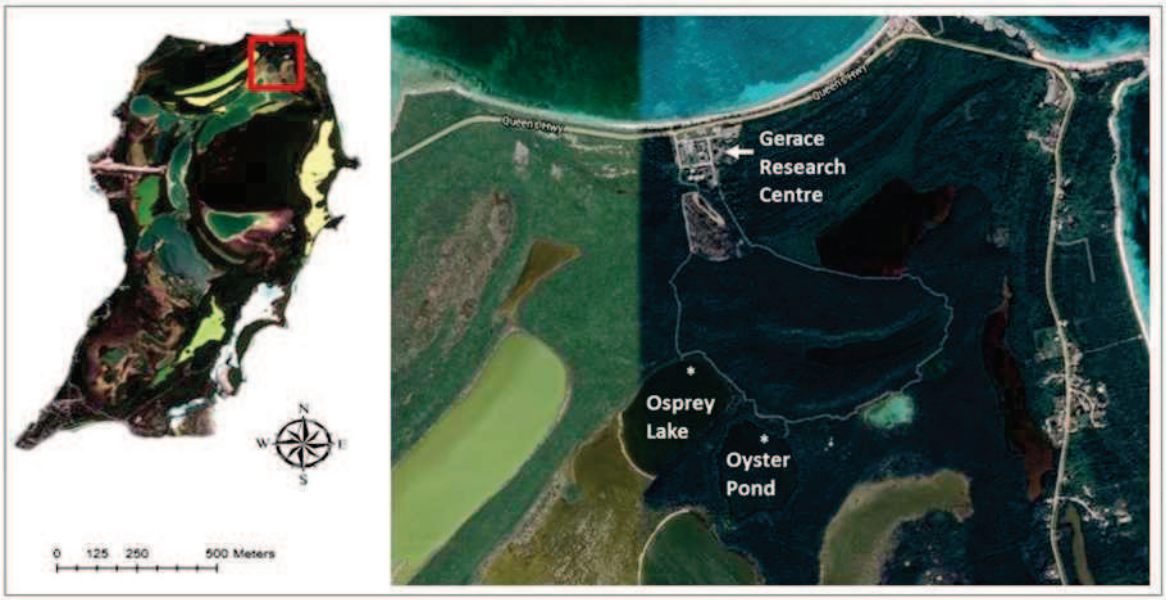

Figure 1: Location of Oyster Pond and Osprey Lake with respect to the Gerace Research Centre. Island map inset courtesy of the U.S. Geological Survey, Accessed 10-January 2019. Close-up image of ponds and Gerace Research Centre modified from Google Earth. Accessed 13-May 2020.

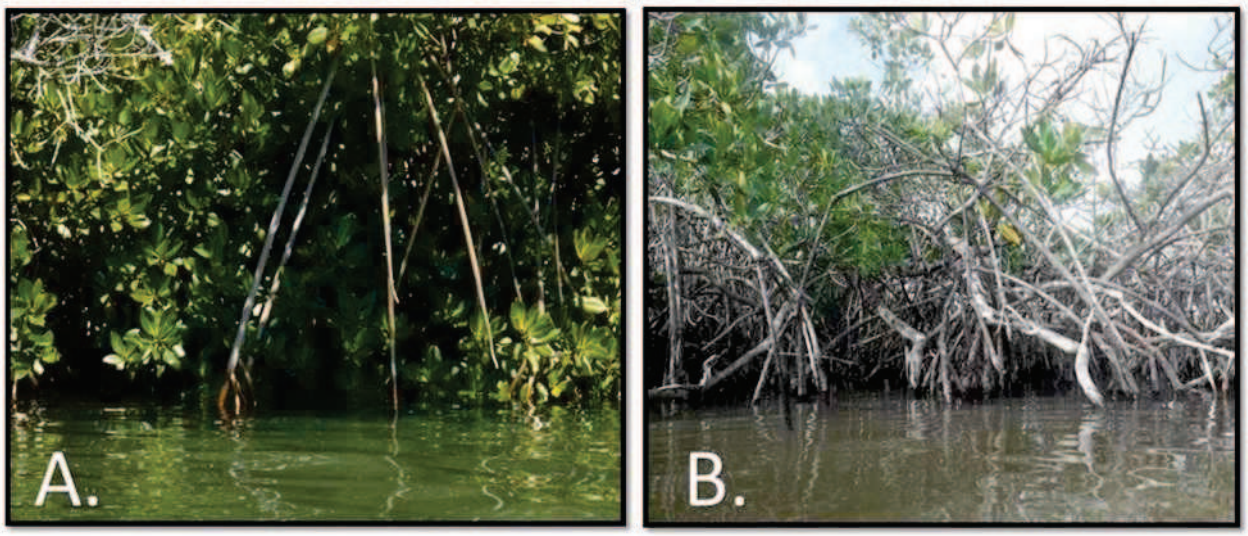

Figure 2. View of red mangroves in Osprey Lake in 2015 (A) and 2018 (B).

METHODS

At Oyster Pond and Osprey Lake, patches of *I. alatus* were identified and qualitatively assessed in March of 2015 and 2018. At both sites, collections of at least 100 individual oysters were taken and hinge length was measured with a hand-held caliper. All measurements occurred in the field and oysters were returned to their habitat following measurement. Considering the unique metazoan communities known to each pond, samples were collected from each system on different days so as not to introduce novel organisms. In Oyster Pond, *I. alatus* were collected from red mangrove prop roots along a ~100 m perimeter along the northern shoreline; up to five oysters were collected from each root. In 2015, Osprey Lake oysters were collected from prop roots of red mangrove stands located within 100 m of the lake's northern shoreline (Figure 1). In 2018, these mangroves were devoid of live oysters; however, the shell hash on the lake floor surrounding red mangrove stands included

numerous flat tree oyster shells. We took measurements of shells found within this hash. Two-way analysis of variance (ANOVA) and Tukey Pairwise Comparisons were conducted to examine the effect of pond and year on hinge length.

RESULTS

Two-way ANOVA found significant interaction between the effects of pond and year on hinge length ($F_{1,506}$ = 232.9, p < 0.001). Significant main effects were also found for both pond and year (p < 0.001 for each factor). In Oyster Pond, we found a comparatively smaller-sized population in 2018, with an average hinge length of 17.0 mm in 2015 (n = 123) and 14.6 mm in 2018 (n = 103).

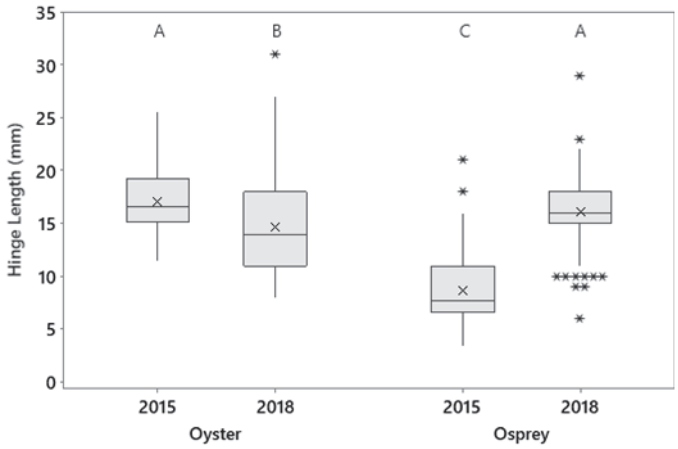

Figure 3. Box-plot of the hinge length distribution in I. alatus in Oyster Pond and Osprey Lake from samples collected in 2015 and 2018. Lower and upper box boundaries at 25th and 75th percentiles, respectively and whiskers extend to data points within 1.5 times box heights. Medians are represented by the horizontal line within the box, means are represented by an 'x' and outliers are shown with an "". Different letters indicate significant differences between groups, as indicated by Tukey Pairwise Comparison.*

In 2015, Osprey Lake had an abundance of living oysters growing on the red mangrove roots; however, live oysters were absent during the 2018 sampling event and also in June of 2019 (Beebout and Anderson, personal observation). The red mangrove patches within the lake also appeared stressed as compared to 2015 (Figure 2). Data from oyster shell hash suggested significantly larger hinge length in 2018 as compared to 2015; mean hinge lengths were 16.0 mm (n = 129) and 8.7 mm (n = 155) respectively (Figure 3).

Flat tree oysters also differed in size when comparing between ponds in a given year, with Oyster Pond having significantly larger oysters in 2015 as compared to Osprey Lake. The reverse was found in 2018 (Figure 3).

DISCUSSION

Our data led to two key findings: First, population size structure of *I. alatus,* as gauged by hinge length, differed between ponds and across years. Second, while Oyster Pond exhibited a thriving oyster population in both years, no live oysters were found in Osprey Lake in 2018. Considering that Oyster Pond's size distribution was lower in 2018 compared to 2015, we hypothesize that a younger population of *I. alatus* was present in 2018; this is likely because spawning does not occur at regular intervals but instead typically follows significant storm events, which are unpredictable. This would lead to different annual cohort size structure. Osprey Lake, however, had no live oysters in 2018. After measuring shells collected from the substrate, we found the reverse trend as compared to Oyster Pond; on average, the hinge length of flat tree oysters was 8.3 mm greater in 2018 as compared to 2015. This led us to believe that a younger population of *I. alatus* was originally sampled in 2015 and mass mortality followed hurricane activity, resulting in limited reproduction, recruitment, and establishment.

We recognize that comparing hinge lengths from samples of live oysters to those in the shell hash introduces confounding variables. Specifically, shells within the hash could have accumulated over a significant period of time, including the time-frame prior to this study; we attempted to account for this by randomly collecting shells and discarding shells that were not whole or were significantly degraded. There is also potential for smaller shells to break down faster or be overlooked more easily as compared

to larger shells. We do not know the breakdown rate of *I. alatus,* nor did we assess whether smaller shells were comparatively more degraded than larger. These factors could have biased our results, and it is possible that the mean hinge length value for Osprey Lake reported in 2018 is artificially elevated. However, considering that no live specimens were present, there was little alternative. Additionally, the result of finding no live oysters in Osprey Lake in 2018 is certainly notable in itself.

Factors that may help explain our findings include variations in water chemistry, physical parameters, dominant vegetation, and significant storm events, such as Hurricane Joaquin. Oyster Pond and Osprey Lake are similar in size and location; however, the dominant vegetation and salinity influence varies greatly between these systems. The vegetation around the two water bodies demonstrates the effects of differential salinity. Red mangroves have limited tolerance of hypersaline conditions (Imbert 2018, Liang et al. 2008). In Oyster Pond, the tidal flux keeps salinity levels at near-marine conditions, making this system an ideal location for red mangroves to govern the shoreline. In Osprey Lake, black mangroves, which are more salt tolerant (Imbert 2018, Liang et al. 2008), dominate the shoreline with some patches of red mangroves just offshore; these patches are likely more prone to influence from environmental change and disturbance events.

Hurricane-caused disturbances are common throughout the Bahamas. After the initial sampling period in spring of 2015, Hurricane Joaquin hit San Salvador head on in October 2015. This hurricane caused major infrastructural damage throughout the island, with winds up to 110 knots (204 kph); while no official rainfall observations are available, estimates indicate the storm produced 12-25 cm of rain (Berg 2016). In 2018, when oyster sampling was repeated, damage to the red mangroves was apparent in Osprey Lake (Figure 2). Imbert (2018) describes the limited resistance that mangroves, especially red mangroves, have against hurricanes. Red mangroves depend on their aerial prop roots and rhizomous, underground root structure for support and stability. The strong winds brought with a hurricane can dislodge and destroy prop roots and whole trees, therefore damaging optimal habitat that *I. alatus* depends on for survival. The red mangroves that border the shoreline of Oyster Pond are more protected than the clustered populations found in Osprey Lake that are much more exposed to the elements. Damage to red mangroves can lead to cascading effects of less optimal habitats for mangrove-reliant invertebrates such as *I. alatus,* potentially contributing to mortality of the population that existed in 2015.

Along with damaging winds, hurricanes also bring in great amounts of precipitation. *I. alatus,* like many other marine bivalves, depends on these rain events to reduce the salinity levels of a water body and trigger mass spawning events (Siung 1980). However, Goodbody (1961) noted that too much rain in a limited time frame may cause mass mortality of sessile mangrove invertebrates. Considering the tidal activity in marine ponds such as Oyster Pond, it appears that storm events cause only a short-term drop in salinity that, in turn, could trigger mass spawning events for *I. alatus.* Conversely, Osprey Lake has little tidal influence, is hypersaline, and is influenced by evapotranspiration and seepage from Blue Pond (McGee *et al.* 2010). Precipitation events can cause rapid salinity drops in hypersaline ponds due to limited conduit regulation, and return to pre-storm salinity levels takes longer because of the evaporative-controlled conditions (Rothfus 2012). A prolonged drop in salinity also could have negatively impacted *I. alatus* populations in Osprey Lake.

Interestingly, Carlson *et al.* (2011) found similar, hurricane-driven results when examining populations of scaly pearl oysters (*Pinctada longisquamosa*) in ponds with varying salinity levels on San Salvador Island. Specifically, scaly pearl oysters in Oyster Pond exhibited a high level of resilience to hurricane events while adult oysters in Six Pack Pond, a hypersaline pond with limited conduit exchange that is much more susceptible to hurricanes, were nearly decimated following hurricane activity. Notably, the Six Pack Pond population rebounded within months,

indicating that impending mortality of the adult population triggered a "suicide spawning" event. Further work on this system by Cole *et al.* (2016) concluded that storm-driven salinity and temperature drops induce mass spawning prior to adult decimation in ponds that are not buffered by conduit action.

The rainy season on San Salvador results in a salinity drop, thereby promoting spawning in *I. alatus* (Siung 1980). This stimulates the growth of new generations, and this appears to have been the case in Oyster Pond; however, in the case of hypersaline ponds, how much rain is too much? When there is a significant salinity drop, for example after a hurricane, and return to pre-storm salinity levels in hypersaline ponds is delayed because of the limitations imposed by the evaporative process, *I. alatus* is predicted to go into mass reproduction, similar to that seen by Carlson *et al.* (2011) in the scaly pearl oyster. However, unlike Carlson *et al.* (2011), we did not observe a rebound in *I. alatus;* if *I. alatus* populations in Osprey Lake followed a similar trajectory as scaly pearl oysters in Six Pack Pond, there should have been an ample number of adults by 2018. If the observed mortality was associated with Hurricane Joaquin, it is plausible that there *was* an associated mass spawning event, followed by adult mortality. However, perhaps juveniles were unable to re-establish due either to suboptimal salinity levels, limited available colonization habitat due to stress on the red mangrove patches, or a combination of these factors.

To summarize, we propose here that rainfall from hurricane activity in conduit-driven Oyster Pond lowered the salinity enough to trigger a successful spawning event; conversely, in hypersaline Osprey Lake, the lack of conduit-driven tidal regulation resulted in a more dramatic and extended salinity drop. This, paired with damage to red mangrove patches, created the 'perfect storm' that resulted in the demise of flat tree oysters in Osprey Lake.

While rainfall events that lower water salinity levels are necessary to trigger reproductive activity, our results reinforce the need to maintain a delicate balance. Too much fluctuation without the regulative activity driven by conduits may be detrimental, and past work has shown that major salinity drops can decrease *I. alatus* in the plankton (Siung 1980). None-the-less, there are still many unanswered questions related to the life history of *I. alatus,* thus drawing strong conclusions is difficult. The growth rate and age/size at maturity is still unexplored, and could vary depending on unique evolutionary trajectories within a certain habitat. There is also possibility that size differences seen here could be associated with differential growth rate in different years as opposed to differential age; changes in water quality parameters could lead to differential growth. Optimal water quality parameters are unknown as well. We know salinity is a factor in triggering spawning events, but what is the optimal threshold range? Longer-term water quality data for these inland waterbodies would also be beneficial. Also, it would be valuable to compare other sedentary invertebrates in Oyster Pond and Osprey Lake, especially after storm events, to further our understanding of the recovery time of each system. Finally, we recognize that the exact timing of mortality in Osprey Lake is unknown, so while we hypothesize that Hurricane Joaquin may have played a significant role, we recognize that we cannot draw firm conclusions.

While it is evident that flat tree oysters can tolerate a range of salinities, climate change may impact their survival either by enhancing evaporation rates, which will elevate already hypersaline conditions or by increasing frequency of severe storm events, which may result in rapid, dramatic drops in salinity. Either of these scenarios could exceed *I. alatus* tolerance limits, or impact the mangrove communities which they depend upon, thus hindering growth and reproduction. A continual study of these oysters, along with other members of the invertebrate community, is needed to further understand the stability of the unique inland ponds on San Salvador Island, the Bahamas.

ACKNOWLEDGEMENTS

We thank Northern State University (NSU) for providing equipment to conduct this work and the NSU Marine and Island Ecology classes of 2015 and 2018 for assistance with data collection and processing. Special thanks also to Dr. Troy Dexter (Executive Director of the Gerace Research Centre) and Dr. Tom Rothfus (former Executive Director of the Gerace Research Centre), as well as all of the staff members of the Gerace Research Centre.

LITERATURE CITED

Berg, Robbie. National Hurricane Center. National Hurricane Center tropical cyclone report Hurricane Joaquin (Al112015) 28 September – 7 October 2015. National Oceanic and Atmospheric Administration and the National Weather Service. (2016). Available at: https://www.nhc.noaa.gov/data/tcr/AL112015_Joaquin.pdf

Carlson, S., Bieraugel, K, Carlson, R., Cada, R., Crumley, A., Haimes, B, Hultgren, K., Marty, M., Stachowski, M., Swanson, K., Tolen, N., William, A., Roback, P., Rothfus, E., Schade, J. and E.S. Cole. (2011). "The demographic history of the scaly pearl oyster in four anchialine ponds on San Salvador Island, Bahamas" in The Proceedings of the 13th Symposium on the Natural History of the Bahamas, eds. J. E. Baxter and E. S. Cole (Gerace Research Centre, San Salvador Island, Bahamas), 140-150.

Cole, E. S., Urnes, C., Hinrichs, A., Roback, P., Rothfus, E. and Anderson, A. (2016). "Rainfall drives synchronous spawning in the Scaly Pearl Oyster, *Pinctada longisquamosa* on San Salvador Island, Bahamas" in The Proceedings of the 15th Symposium of the Natural History of the Bahamas, eds. R. Erdman and R. Morrison (Gerace Research Centre, San Salvador Island, Bahamas), 45-52.

Edwards, D.C. (2001). "Effects of salinity on the ecology of molluscs in the inland saline waters of San Salvador Island: A natural experiment in progress" in The Proceedings of the 8th Symposium of the Natural History of the Bahamas, eds. C. A. Clark-Simpson and G. W. Smith. (Gerace Research Centre, San Salvador, Bahamas), 15-26.

Goodbody, I. (1961). Mass mortality of marine fauna following tropical rains. Ecology 42, 150-155.

Imbert, D. (2018). Hurricane disturbance and forest dynamics in east Caribbean mangroves. Ecosphere 9, e02231. doi: 10.1002/ecs2.2231

Liang, S., Zhou, R. C., Dong, S. S., and Shi, S. H. (2008). Adaptation to salinity in mangroves: Implication on the evolution of salt-tolerance. Chinese Science Bulletin 53, 1708–1715.

McGee, D. K., Wynn, J. G., Onac, B. P., Harries, P. J., and Rothfus, E. A. (2010). Tracing groundwater geochemistry using d13C on San Salvador Island (southeastern Bahamas): implications for carbonate island hydrogeology and dissolution. Carbonates and Evaporites 25, 91-105

Mylroie, J. E., and Carew, J. L. (1995). Geology and karst geomorphology of San Salvador Island, Bahamas. Carbonates and Evaporites 10, 193–206.

Rothfus, E. A. (2012). "Water-quality monitoring of San Salvadorian Inland Lakes" in The Proceedings of the 15th Symposium of the Natural History of the Bahamas, eds. R. Erdman and R. Morrison (Gerace Research Centre, San Salvador Island, Bahamas), 129-138.

Siung, A. M. (1980). Studies on the biology of *Isognomon alatus* Gmelin (Bivalvia: Isognomonidae) with notes on its potential as a commercial species. Bulletin of Marine Science 30, 90–101.

NEW ADVANCES IN LONG-TERM MONITORING OF STORM-DEPOSITED BOULDER RIDGES ALONG ROCKY SHORELINES OF SAN SALVADOR ISLAND, BAHAMAS

Bosiljka Glumac*, Ursula Miguel, and H. Allen Curran

*Corresponding author; e-mail: bglumac@smith.edu; phone: 413-531-6801

Department of Geosciences, Smith College, Northampton, MA 01063 USA

ABSTRACT

Beginning in January 2012, we have monitored two boulder ridges on San Salvador: Singer Bar Point (SBP, length ~790 m) along the reef- and lagoon-protected northern coast and The Gulf (TG, length ~460 m) on the island's high-energy southern coast. This long-term monitoring aims at documenting changes in ridge morphology and distribution, and the direction and amount of movement of individual boulders to gain insights into the intensity and effects of storms on these coastal areas.

In the initial stage of our investigations, the largest boulders from each site were photographed, GPS-located, measured, and characterized by composition and morphology. Boulders at SBP are generally smaller (15 total; ~150-4000 kg; with most <1500 kg) than those at TG (12 original; ~700-6500 kg; most >1000 kg). Our monitoring surveys from January 2013, 2016, and 2017, after Hurricanes Sandy (October 2012), Joaquin (October 2015), and Matthew (October 2016), respectively, indicated only modest modifications at SBP, and major changes to TG, where we were unable to relocate 2 boulders post-Sandy, and 5 of the 10 remaining original boulders after Joaquin. Two TG boulders, weighing ~1 and 3 tons, were transported inland to the NNW by 20 and 26 meters, respectively during Hurricane Joaquin, and there was significant movement inland of the entire boulder ridge.

Even though documentation of boulder movement allows calculation of minimum flow velocity needed to initiate transport, our experience indicated that lack of adequate tagging made it challenging or impossible to relocate individual boulders after major storms. This problem was addressed by the application of RFID (radio frequency identification) tagging in June 2019. With a larger cohort of boulders now tagged, our monitoring program is well established to continue into the future, as passive tags are inductively charged by the reader and can remain operational for decades. Drilling to insert small tags (23 and 32 mm long, and <4 mm in diameter) is minimally destructive and also allows tagging of pebbles and cobbles. This is especially important for monitoring at SBP where large boulders are not moved often or much by waves, but smaller-sized sediment movement is significant during storms.

INTRODUCTION TO STUDY AREA AND METHODS

Coastal ridges made primarily of limestone boulders (clasts >25 cm in diameter) are common but little studied features along rocky shorelines on many islands of the Bahama Archipelago. Origin and transport of large individual boulders in the Bahamas, especially the scattered "megaboulders" on North Eleuthera, however, has been hotly debated during the past two decades (Hearty 1997; Panuska *et al.* 2002; Kelletat *et al.* 2004; Mylroie 2008, 2018; Kindler *et al.* 2010; Hearty and Tormey 2017; Rovere *et*

al. 2017, 2018). Even though the debate over transport mechanisms for these large boulders is ongoing, the results of recent studies from the northern Atlantic of western Ireland unequivocally proved that storm waves can move limestone megaboulders on cliffs located 10 meters or higher above high-water level (Cox *et al.* 2012, 2018). Similarly, observations from San Salvador Island in the aftermath of 1999 Hurricane Floyd (Curran *et al.* 2001; Walker *et al.* 2001) and 2004 Hurricane Frances (Niemi *et al.* 2008; Niemi 2017) documented formation and transport of rock boulders by high energy storm waves.

Our long-term monitoring of the impact of storms on the rocky coastline of San Salvador since January 2012 has focused on two prominent boulder ridges, one along the reef- and lagoon-protected northern coast west of and around Singer Bar Point (SBP), and the other on the high-energy southern coast of the island west of The Gulf (TG; Figure 1). Singer Bar point is located about 1 km (0.6 miles) west of the Gerace Research Centre (GRC) campus. The total length of this boulder ridge is ~790 m, and this study focused on an area ~450 m long, located to the east of the boat ramp, which is about 1.5 km (0.9 miles) west along the Queen's Highway from GRC (Figure 1B). Similarly, even though the boulder ridge at TG is ~460 m, we focused primarily on the ~200 m section located on the coastal cliff between The Cut and The Gulf embayments (Figure 1B).

Both boulder ridges were deposited by storm waves, and comparison of these two coastlines of very different energy-level characteristics provides insight into the relationship between wave intensity and boulder formation, morphology, and transport. The main objectives of this study are to gather information about the distribution and morphology of these boulder ridges, and on the movement of individual boulders to better understand the influence of storms on geomorphology of the coastal landscape. The results of such long-term monitoring efforts should be informative to decision making regarding future coastal development on this and similar coastal areas on other Bahamian islands. Cumulative data also will provide information for continuing documentation of boulder transport by storm waves, and development of criteria for analyzing coastal boulder deposits in general (e.g., Cox *et al.* 2018).

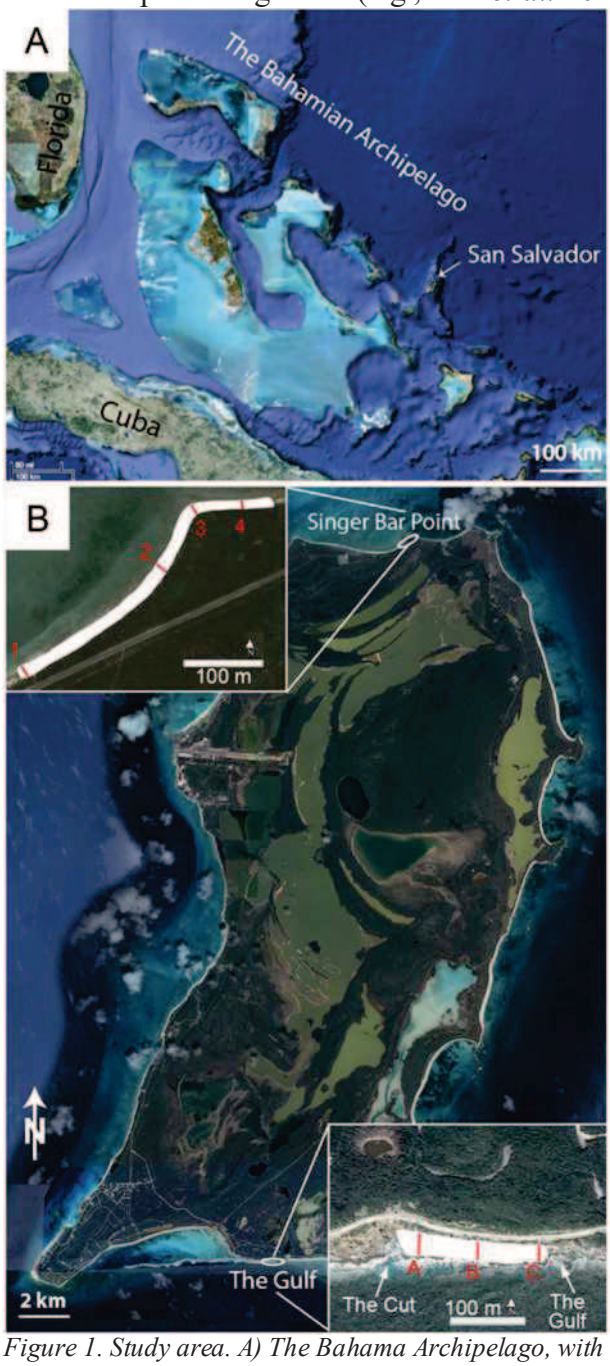

Figure 1. Study area. A) The Bahama Archipelago, with Florida and Cuba for context, and San Salvador Island. B) Map of San Salvador with the two study sites labeled: Singer Bar Point (SBP) along the relatively low-energy north coast, and The Gulf (TG) on the high-energy south coast. Insets show the study sites outlined in white, with red lines and labels marking the location of profiles shown in Figure 2 (source: Google Earth).

Initial fieldwork for this study was conducted on San Salvador in January 2012 after Hurricane Irene passed as a Category 2 storm about 80 km (50 miles) to the SW of the island in August 2011 (National Hurricane Center). This initial work included GPS data-point recording and measurements of coast-normal transects (4 for SBP and 3 for TG) over the boulder ridges (Figure 1B). The largest boulders from each site (15 SBP and 12 TG boulders) were photographed and located with GPS coordinates for future reference. Boulders were measured (length, width, thickness), characterized by composition (subtidal calcarenite, coral rubblestone, eolianite, paleosol), shape (tabular or irregular), and degree of roundness. Approximate boulder weight was determined using average limestone density of 2.4 g/cm^3 and by subtracting 20% from calculated values to account for irregular boulder size and porosity distribution.

Additional field observations were made in early 2013 to assess the impact of October 2012 Hurricane Sandy, in January 2016 to document modifications by Hurricane Joaquin that passed directly over San Salvador in October 2015, and in January 2017 after October 2016 Hurricane Matthew. While Hurricane Matthew passed too far west of San Salvador to have any major impact on the island, this research documented significant modifications by Hurricane Sandy and especially by Joaquin, which are detailed here. Documentation of boulder movement also allowed calculation of minimum flow velocity required to initiate their transport using equations from Nandasena *et al.* (2011), which are dependent on boulder size, density of boulders and water, coefficients of lift, drag, gravity, and slope angle.

In January 2016, we also initiated use of drone technology for high-resolution imaging of the study areas (Perlmutter *et al.* 2016). Subsequent drone imaging was conducted in January 2017 and 2020, and in June 2019 we also implemented RFID (radio frequency identification) technology to tag boulders at each study site to aid in their relocation after major storm events. This proved necessary because we learned from experience that when boulders move, even very large ones, they can be difficult to relocate.

RFID technology uses small (23 and 32 mm long and <4 mm in diameter) PIT (passive integrated transponder) tags. These passive tags have unique identifying numbers that are recorded by an RFID reader at a short distance, depending on tag size and antenna design. The tags are inductively charged by the reader, and because they do not have a battery, they can theoretically remain operational indefinitely. Their small size and relatively low cost allows tagging of a large number of clasts, which in addition to boulders can also include smaller cobbles and pebbles. Moreover, tagging of particles is minimally invasive. Small holes (only about 5 mm in diameter and up to 40 mm deep) are drilled into boulder surfaces using a hand-held, battery-operated hammer drill with a carbide drill bit. Holes are lined with silicone adhesive and then patched with water-resistant epoxy putty whose color closely matches that of the rock surface.

These advances in our long-term monitoring of storm-deposited boulder ridges significantly increased our database and are expected to add significantly to our efforts to communicate information about vulnerability to hurricanes with stakeholders on San Salvador and elsewhere in The Bahamas. Such efforts are becoming increasingly important as the consequences of changing climate and rising sea levels are amplified by powerful storms, exemplified by the devastating impact of Hurricane Dorian on Grand Bahama and Abaco Islands in September 2019.

RESULTS

Initial Survey (January 2012)

Our initial work in January 2012 described the Singer Bar Point (SBP) boulder ridge on the low energy north coast as wide (up to 14 m) and with a low crest (~1.5 m above mean sea level), whereas The Gulf (TG) ridge on the high energy south coast was generally narrower, with a sharp crest located on a cliff-bench 3-5 m above mean sea level (Figure 2; Table 1). Profiles through the boulder ridges were constructed from the measured transects (Figures 1B and 2), the largest

boulders along the transects were documented (Table 2), and 15 additional large boulders from SBP and 12 from TG were photographed and located with GPS coordinates (Table 3).

The largest boulders at SBP are generally smaller (~150-4000 kg; with most <1500 kg) and more rounded than those at TG (~700-4500 kg; with all but one >1000 kg; Tables 1-3).

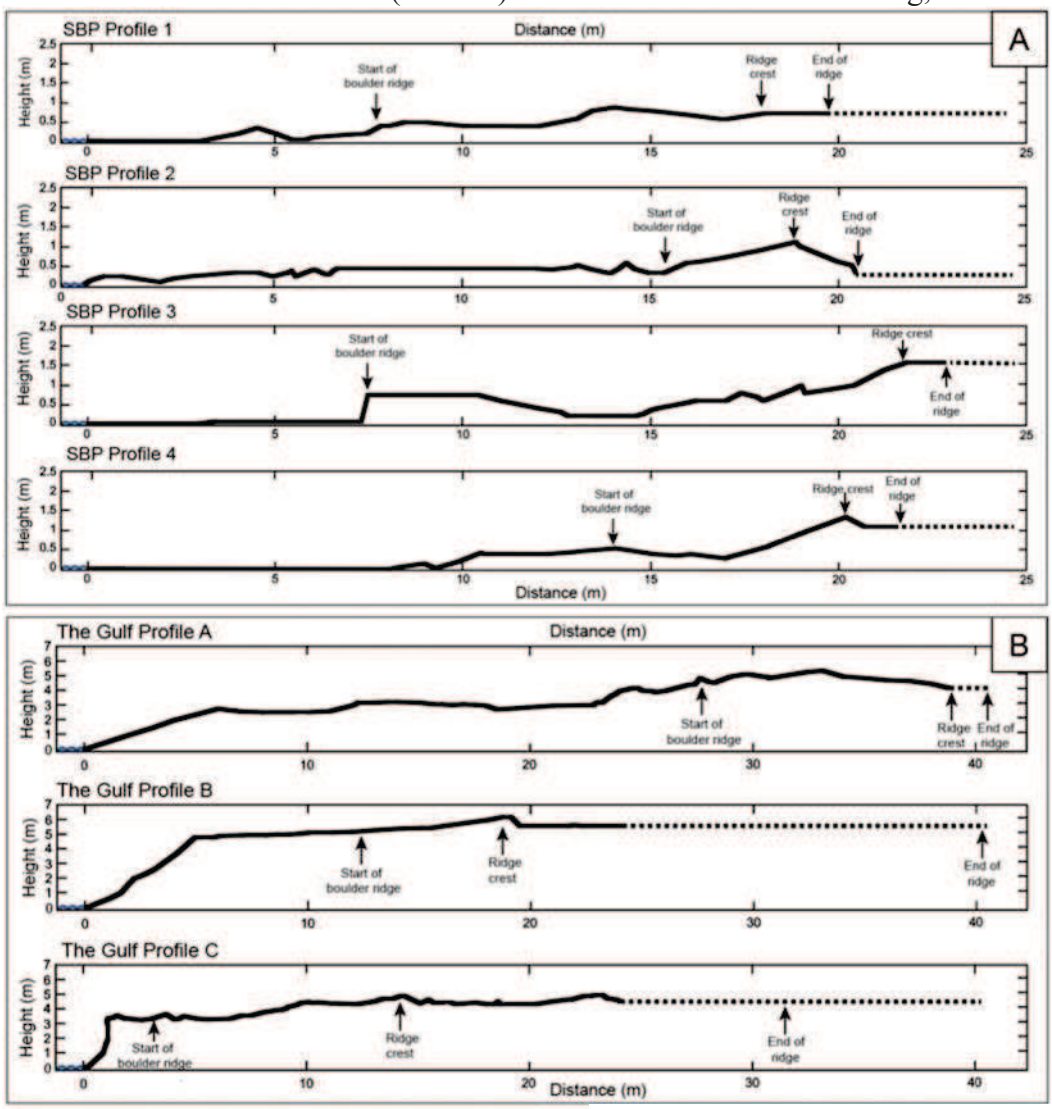

Figure 2. Profiles through the boulder ridges measured in January 2012 at SBP (A) and TG (B). Location of four SBP profiles was measured in relation to SBP boat landing: Profile 1 at 147 m, Profile 2 at 436 m, Profile 3 at 568 m, and Profile 4 at 630 m east of the boat landing. Location of three TG profiles was measured in relation to a benchmark at TG: Profile A at 181 m, Profile B at 98 m (midpoint between A and C), and Profile C at 15 m west of the benchmark (see Figure 1B). Note that SBP profiles start at sea level and then the rocky beach and boulder ridge emerge, followed by maritime forest. SBP boulder ridge is up to 14 m wide and has a low crest (~1.5 m above mean sea level). TG profiles start at sea level, followed by steep cliffs, a barren rocky area and boulder ridge, and end in dense shrub vegetation. TG boulder ridge has a sharp crest, and is on a cliff bench 3-5 m above mean sea level. C) Pleistocene carbonate succession exposed in TG cliffs (from Carew and Mylroie 1985). Note the top of coral reef exposed at modern-day sea level, and the three identified source rocks for boulders deposited by storms on top of TG cliffs.

Table 1. Comparison summary between characteristic features of Singer Bar Point (SBP) vs The Gulf (TG) sites.

Features:	SBP	TG
Boulders	Generally smaller and well rounded	Large, irregular, angular
Boulder ridge	Crest broad, slopes gentle	Crest sharp, well defined
Offshore shelf	Wide, protected	Narrow, open
Wave energy	Gentle, but constant fair-weather waves action	Powerful, even in fair-weather conditions

Table 2. Data on boulders along transects at SBP (A) and TG (B) shown in Figure 2.

A)

Site	Place on Profile (m)	Boulder No.	X Axis (cm)	Y axis (cm)	Z Axis (cm)	Volume (cm^3)	Mass (kg)	Probable Comp.	Shape
1	13.4	1	130	138	23	412620	792	Eolianite	Irregular
1	14.6	2	66	73	25	120450	231	Eolianite	Irregular
1	18.1	3	32	37	5	5920	11	Paleosol	Tabular
1	19.1	4	49	29	20	28420	55	Paleosol	Irregular
2	16.0	1	57	36	14	28728	55	Paleosol	Tabular
2	16.3	2	22	32	9	6336	12	Eolianite with Paleosol	Irregular
2	19.9	3	45	30	4	5400	10	Beach Rock	Irregular
3	17.8	1	107	62	15	99510	191	Paleosol	Irregular
3	18.7	2	76	85	5	32300	62	Eolianite with Paleosol	Tabular
3	20.2	3	54	38	6	12312	24	Paleosol	Irregular
3	21.2	4	45	71	6	19170	37	Paleosol	Irregular
3	21.9	5	87	36	10	31320	60	Paleosol	Irregular
4	12.8	1	160	184	16	471040	904	Paleosol	Irregular
4	14.3	2	42	85	22	78540	151	Subtidal	Irregular
4	14.4	3	55	33	14	25410	49	Paleosol	Tabular
4	14.7	4	45	60	12	32400	62	Subtidal	Irregular
4	15.2	5	21	37	7	5439	10	Paleosol	Irregular
4	15.6	6	47	28	4	5264	10	Shelly Calcaranite	Tabular
4	17.2	7	37	27	7	6993	13	Subtidal	Irregular
4	18.6	8	24	30	8	5760	11	Eolianite	Irregular

B)

Site	Place on Profile (m)	Boulder No.	X Axis (cm)	Y axis (cm)	Z Axis (cm)	Volume (cm^3)	Mass (kg)	Probable Comp.	Shape
A	23.0	1	32	32	12	12288	24	Paleosol	Irregular
A	24.1	2	85	73	42	260610	500	Paleosol	Irregular
A	25.0	3	57	27	35	53865	103	Coral Rubblestone	Irregular
A	26.8	4	33	38	13	16302	31	Eolianite	Rectangle
A	30.0	5	51	102	40	208080	400	Paleosol	Irregular
A	30.7	6	57	39	10	22230	43	Eolianite	Irregular
B	13.5	1	140	106	17	252280	484	Paleosol	Tabular
B	14.1	2	120	43	15	77400	149	Paleosol	Tabular
B	14.9	3	70	64	15	67200	129	Paleosol	Irregular
B	16.4	4	118	69	17	138414	266	Subtidal	Irregular
B	17.1	5	33	32	9	9504	18	Subtidal	Tabular
B	18.0	6	41	53	12	26076	50	Paleosol	Tabular
B	18.7	7	90	37	21	69930	134	Subtidal	Irregular
C	9.00	1	43	22	17	16082	31	Coral Rubblestone	Tabular
C	9.75	2	21	35	20	14700	28	Paleosol	Irregular
C	10.40	3	150	88	29	382800	735	Paleosol	Irregular
C	11.80	4	62	45	17	47430	91	Paleosol	Irregular
C	12.80	5	52	43	13	29068	56	Coral Rubblestone	Tabular
C	14.20	6	101	92	17	157964	303	Paleosol	Tabular
C	15.75	7	57	47	18	48222	93	Paleosol	Irregular
C	16.30	8	45	44	34	67320	129	Paleosol with Coral Encrusters*	Irregular
C	18.90	9	48	36	8	13824	27	Paleosol (Flipped)	Tabular

Table 3. Data on 15 largest boulders at SBP (A) and 12 largest boulders at TG (B) documented in January 2012.

A)

Boulder No.	X Axis (cm)	Y Axis (cm)	Z Axis (cm)	Volume (cm^3)	Mass (kg)
1	130	130	25	422500	811
2	120	70	50	420000	806
3	85	70	15	89250	171
4	200	105	15	315000	605
5	240	120	40	1152000	2212
6	140	100	14	196000	376
7	130	105	14	191100	367
8	170	125	15	318750	612
9	125	120	50	750000	1440
10	190	150	25	712500	1368
11	185	130	20	481000	924
12	310	225	30	2092500	4018
13	205	140	20	574000	1102
14	145	100	20	290000	557
15	205	185	30	1137750	2184

B)

Boulder No.	X Axis (cm)	Y Axis (cm)	Z Axis (cm)	Volume (cm^3)	Mass (kg)
1	185	75	65	901875	1732
2	215	110	15	354750	681
3	200	155	25	775000	1488
4	155	125	55	1065625	2046
5	215	130	20	559000	1073
6	205	160	30	984000	1889
7	260	210	20	1092000	2097
8	190	170	25	807500	1550
9	140	120	40	672000	1290
10	210	145	55	1674750	3216
11	215	160	25	860000	1651
12	300	265	30	2385000	4579

All boulders were eroded from the seaward rocky coast, transported and deposited by high-energy storm waves. Clasts of smaller size and better rounding are more common at SBP than TG, indicating multiple events of movement and milling in the surf and/or along the rocky shore prior to deposition along this low-profile coast, as compared to the high cliff-profile TG coast (Figure 2C). The presence of larger boulders and fossil coral rubblestone boulders at TG indicates that much stronger storm waves were

required to form and move them in this setting (Dwyer *et al.* 2013).

Impact of Hurricanes Sandy (October 2012) and Joaquin (October 2015)

Similar to Hurricane Irene (August 2011), Hurricane Sandy passed about 80 km (50 miles) to the west of San Salvador Island as a Category 1 to 2 storm on October 25, 2012 (Figure 3A). According to personal communication with Dr. Tom Rothfus (Director of the Gerace Research Centre at that time), minimal island infrastructure damage resulted, and there were no major coastal effects. October 26 was relatively quiet on San Salvador, but on the following day, a strong wave surge began to affect the coast. The largest waves pounded the west and south coasts for 2 days and only diminished on October 29. Considerable coastal erosion resulted, particularly along Fernandez Bay (west coast) and on the south coast between The Gulf and The Cut (our TG study area).

In early February 2013, we resurveyed the largest SBP and TG boulders, which were originally located, measured, and photographed in January 2012 (Table 3). All 15 SBP boulders were easily relocated, indicating that Hurricane Sandy generated only minor coastal effects here. Although a few boulders experienced some movement (e.g., boulder 7 moved inland about 2.5 m; Figure 4), the background of smaller boulders and clasts changed significantly around many of the boulders (Figures 4 and 5). Boulders located to the east of Singer Bar Point did not exhibit position change and showed less background changes than those to the west of the point, confirming local observations that the wave surge effects from Hurricane Sandy were greatest along San Salvador's west and south coasts.

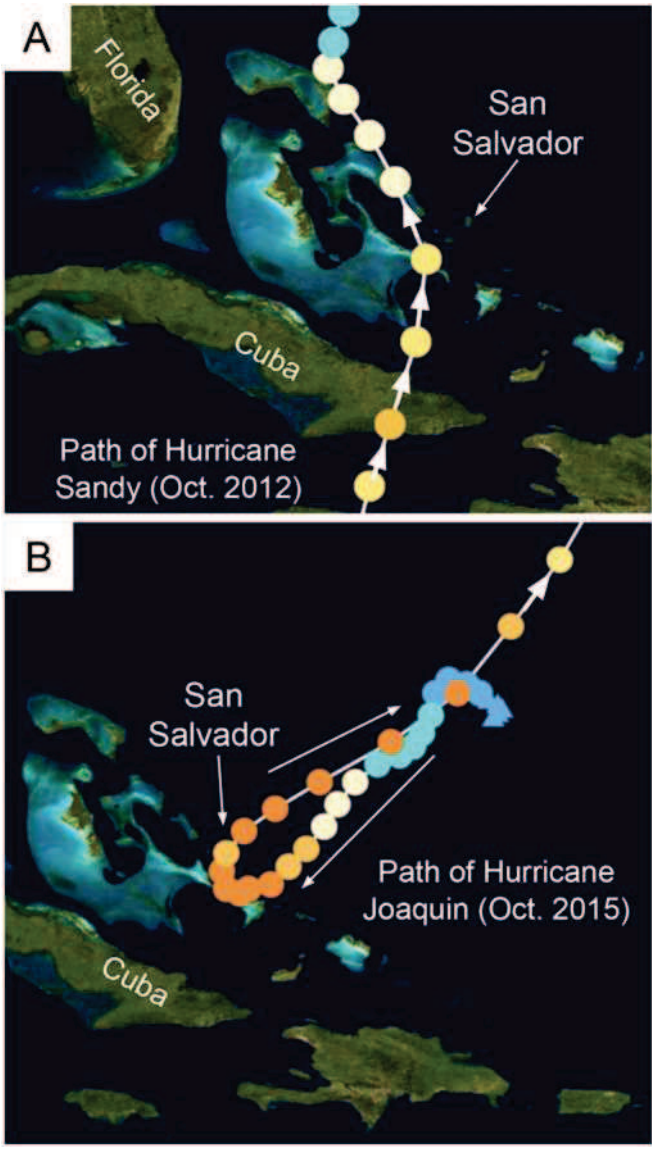

Figure 3. Hurricane pathways. A) Sandy (October 2012) passed about 80 km (50 miles) west of San Salvador and weakened as it moved north from Category 2 (dark yellow circle) to Category 1 (light yellow) and tropical storm (teal circle). B) Joaquin started as a tropical depression (light blue symbols) in the Atlantic to the NE of The Bahamas in late September 2015. It strengthened to Category 4 (dark orange circle) as it moved SW towards The Bahamas, before it made a sharp turn back to the NE and its eye passed directly over San Salvador as a strong Category 3 (light orange circle) hurricane in early October 2015 (source: National Hurricane Center).

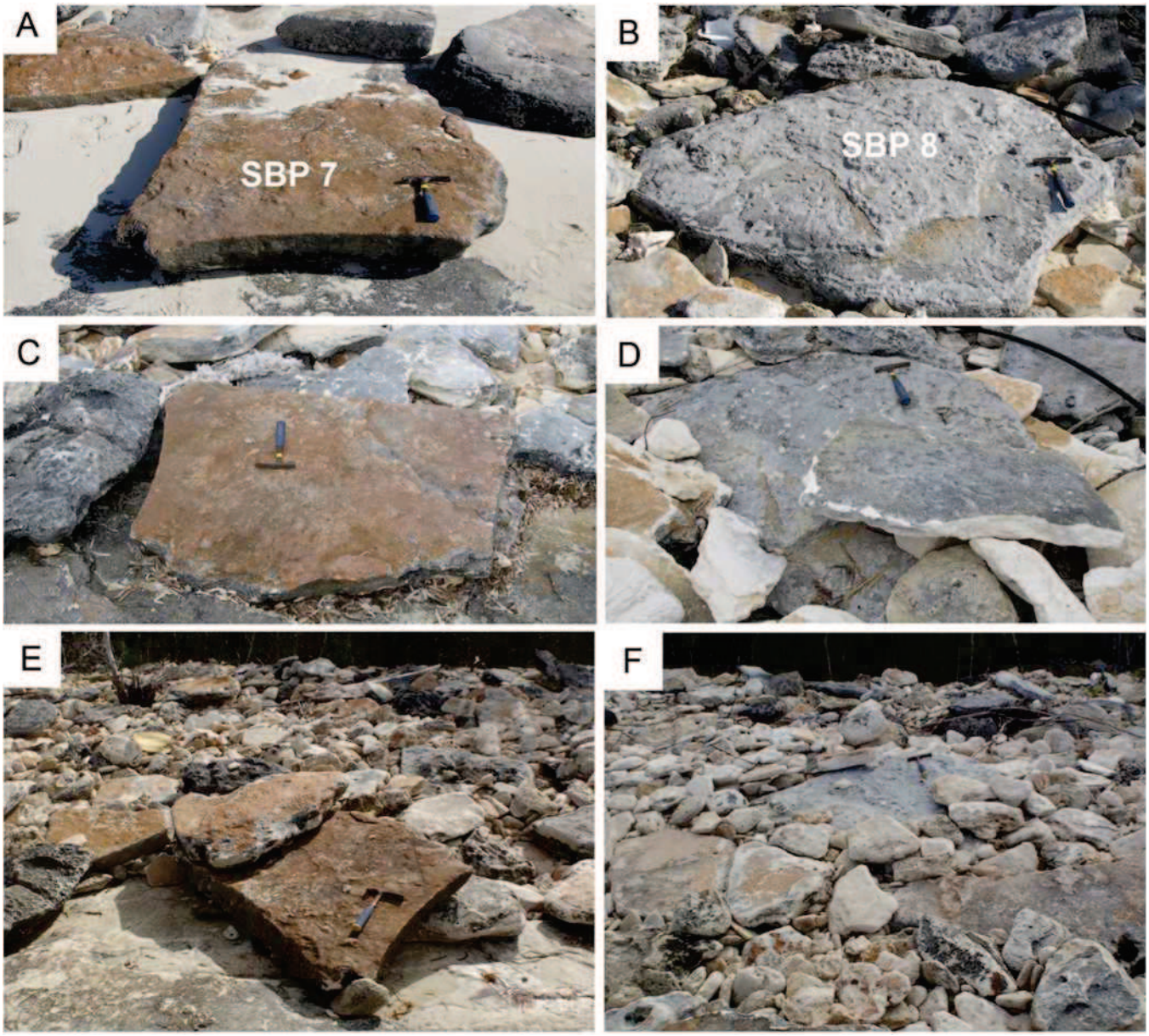

Figure 4. Examples of modifications to boulders at SBP through time. Left column: Boulder 7 (~350 kg); Right column: Boulder 8 (~600 kg). A & B) before Hurricane Sandy (January 2012); C & D) after Hurricane Sandy (February 2013); E & F) after Hurricane Joaquin (January 2016). Hammer for scale and to mark the location of boulders. Boulder 7 was moved about 2.5 m inland (to the south) by Hurricane Sandy (4C), and was transported an additional 3 m to the west and rotated ~180° by Hurricane Joaquin, which also deposited large clasts on top of it and made some new dents in its surface (4E). No major change in the location of boulder 8 was noted since January 2012, but after Sandy and Joaquin this boulder was partially buried in a new arrangement of clasts (4D & F).

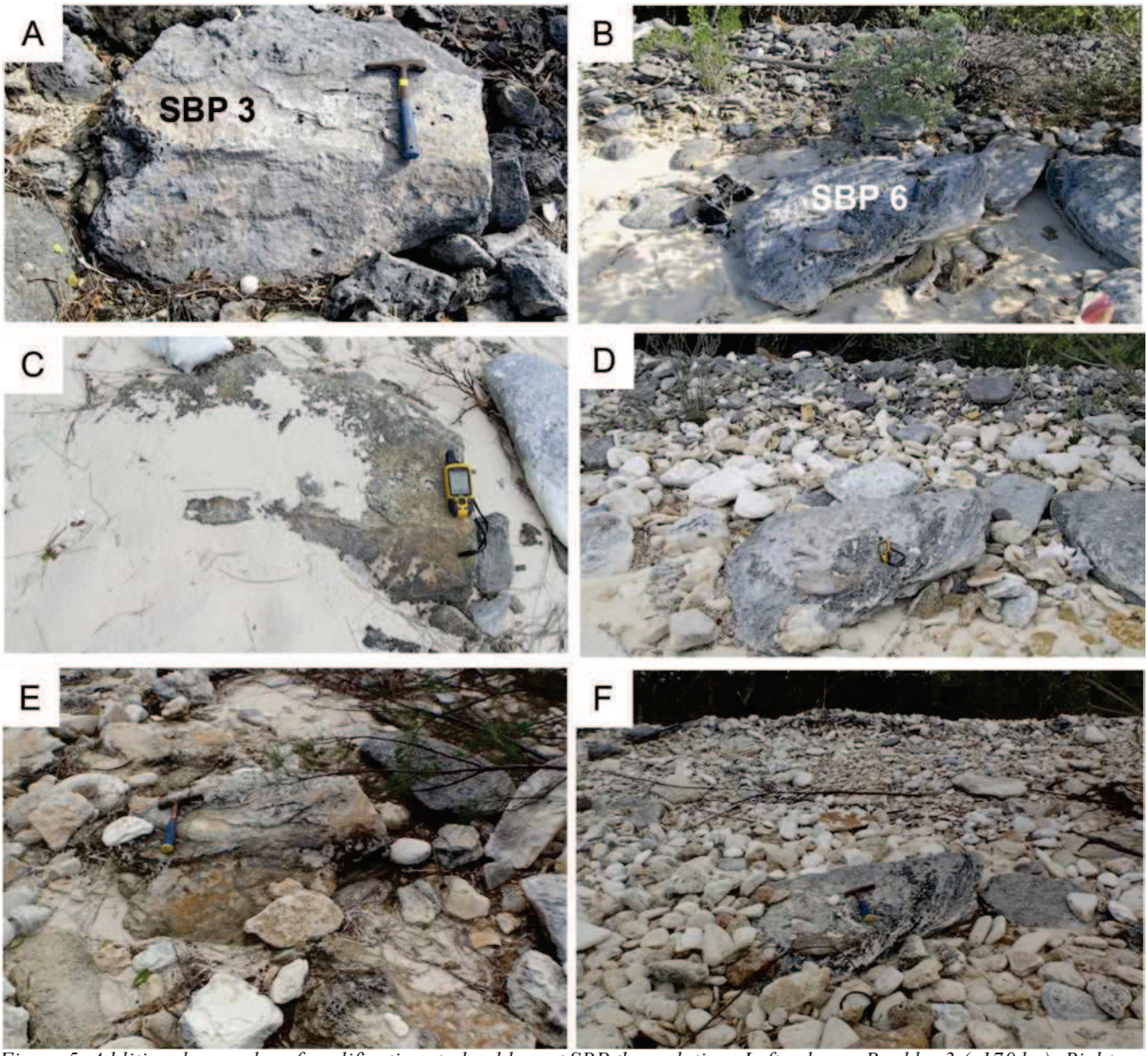

Figure 5. Additional examples of modifications to boulders at SBP through time. Left column: Boulder 3 (~170 kg); Right column: Boulder 6 (~375 kg). A & B) before Hurricane Sandy (January 2012); C & D) after Hurricane Sandy (February 2013); E & F) after Hurricane Joaquin (January 2016). Hammer and GPS unit for scale and to mark the location of boulders. Even though these boulders have not moved since January 2012, the surrounding sediment (sand and smaller clasts) experienced significant changes through time.

This was further supported by our survey of The Gulf area where the effects of Hurricane Sandy were profound (Figures 6 and 7). Two of 12 original boulders (numbers 1 and 3) could not be relocated in the 2013 survey, and there were scour zones at their former locations (Table 4). Other examples of boulder modifications include 90° rotation of boulder 2, and breakage of its upper quarter (the broken segments could not be located). Boulder 4 was moved inland about 3 m, and boulder 5 moved about 9.5 m to the west (Figure 6C). The largest boulder (#12, ~4.5 tons) did not move, but it exhibited the scar of a fresh break on its forward edge. The boulder leaning up against its right side in 2012 was gone, and new clasts surrounded the boulder in the aftermath of Hurricane Sandy (Figure 7D). None of the boulder movement and breakage would have been obvious without knowledge from the pre-storm survey.

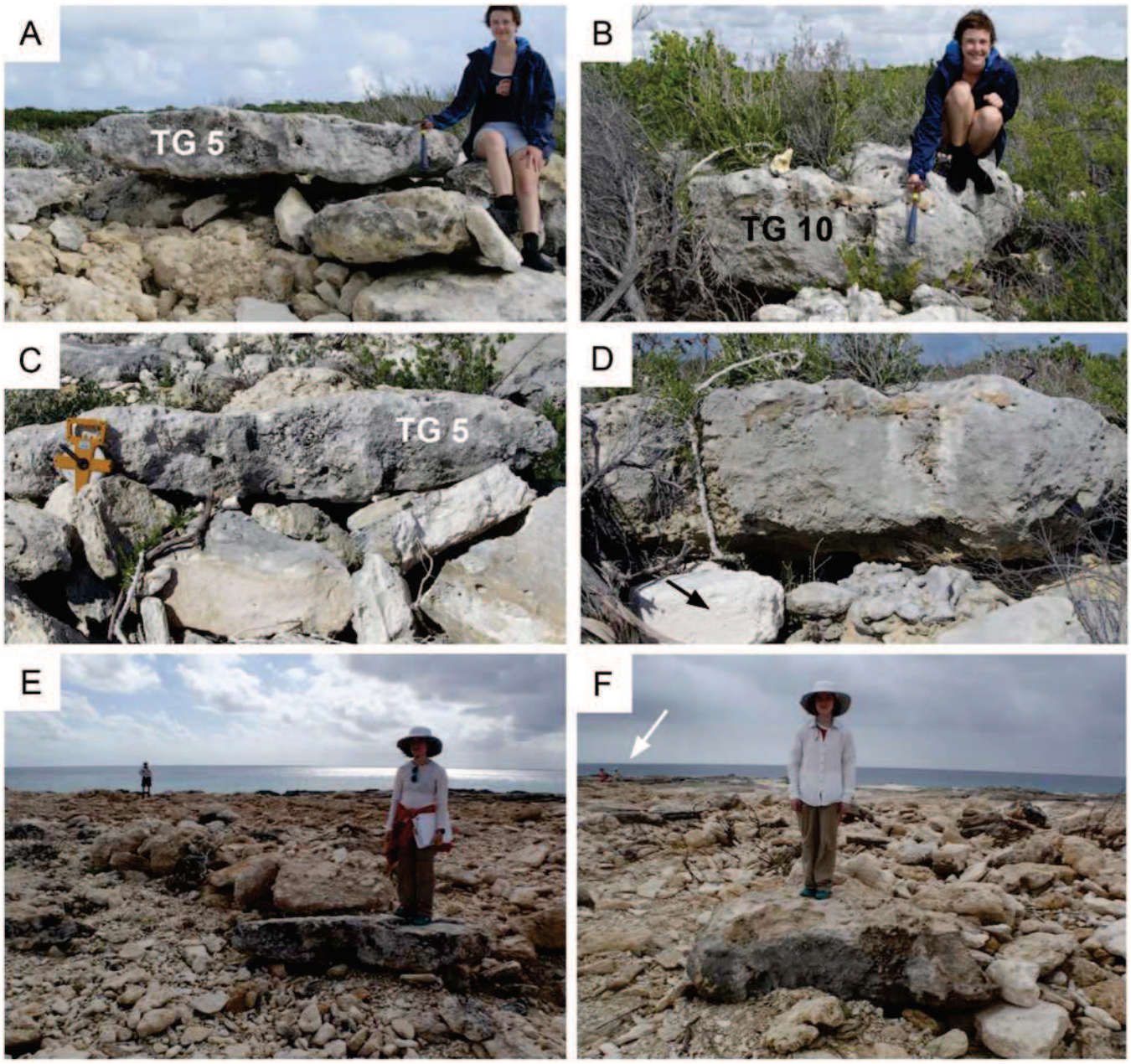

Figure 6. Examples of modifications to boulders at TG through time. Left column: Boulder 5 (~1 ton); Right column: Boulder 10 (~3 tons). A & B) before Hurricane Sandy (January 2012); C & D) after Hurricane Sandy (February 2013); E & F) after Hurricane Joaquin (January 2016). Hurricane Sandy waves moved boulder 5 about 9.5 m to the west (6C), but boulder 10 remained in its original place despite some changes in the surrounding vegetation and deposition of a new large clast (arrow) in front of it (6D). Hurricane Joaquin waves moved boulders 5 and 10 about 20 and 26 m inland to the NNW, respectively (6E and F; person in front is standing on transported boulders and people in distance (arrow in 6F) are at their former location).

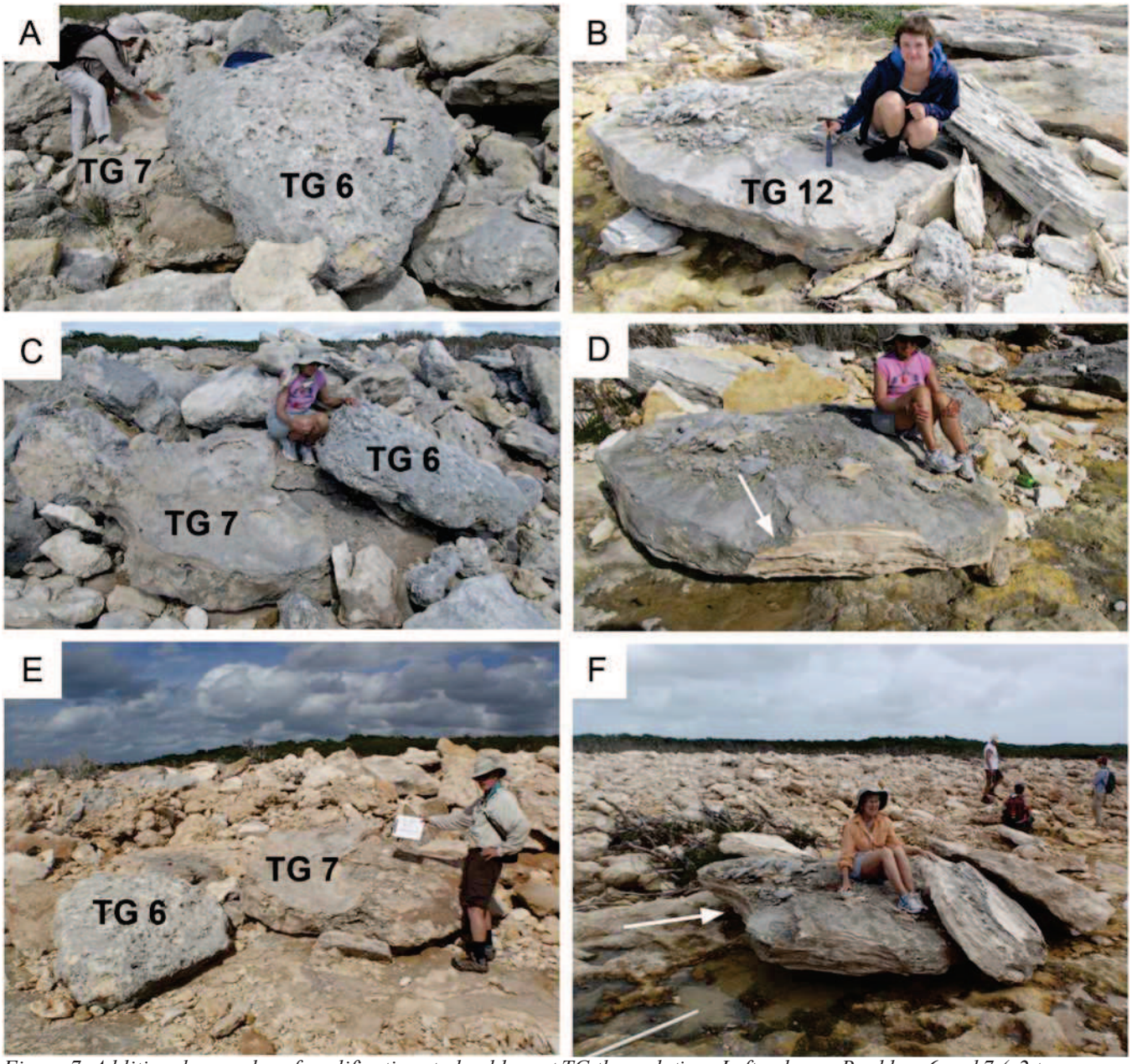

Figure 7. Additional examples of modifications to boulders at TG through time. Left column: Boulders 6 and 7 (~2 tons each); Right column: Boulder 12 (~4.5 tons). A & B) before Hurricane Sandy (January 2012); C & D) after Hurricane Sandy (February 2013); E & F) after Hurricane Joaquin (January 2016). Hurricane Sandy did not move these large boulders, but there are noticeable changes in the surrounding sediment, and boulder 12 also lost one corner (arrow in 7D). Hurricane Joaquin waves moved boulder 6 about 4 m W over boulder 7, which maintained about the same location, while smaller surrounding clasts were stripped away (7E). Boulder 12 has not moved since the start of our monitoring, but in Joaquin it lost another edge (arrow) and new smaller boulders were deposited and now lean on it (7F).

Table 4. Status of TG boulders 2012-2016 and calculation of minimum velocity needed to initiate boulder transport.

TG Boulder	Size (m)	*Mass (kg)	Composition	†Status	✦flow velocity (m/s) - sliding	✦flow velocity (m/s) - rolling
1	1.85 x 0.75 x 0.65	1732	coral rubblestone	missing (Sandy)	2.6	3.2
2	2.15 x 1.1 x 0.15	681	eolianite with caliche	missing	2.7	4.3
3	2 x 1.55 x 0.25	1488	eolianite with caliche	missing (Sandy)	3.3	5.4
4	1.55 x 1.25 x 0.55	2046	coral rubblestone	missing	3.2	5.1
5	2.15 x 1.3 x 0.2	1073	coral rubblestone	moved 20 m NNW	3.0	4.9
6	2.05 x 1.6 x 0.3	1889	coral rubblestone	moved 4 m W	3.4	5.7
7	2.6 x 2.1 x 0.2	2097	eolianite with thick paleosol	slight movement/ rotation	3.5	5.2
8	1.9 x 1.7 x 0.25	1550	eolianite with thick paleosol	moved 8 m (?) NNW	3.4	5.5
9	1.4 x 1.2 x 0.4	1290	soil breccia	missing	3.1	5.2
10	2.1 x 1.45 x 0.55	3216	coral rubblestone	moved 26 m NNW	3.4	5.6
11	2.15 x 1.6 x 0.25	1651	eolianite with caliche	missing	3.3	5.4

* calculated using 2.4 g/cm^3 for limestone density and by subtracting 20% to account for porosity and irregular size
† October 2012 Hurricane Sandy; all other boulders moved during October 2015 Hurricane Joaquin
✦ calculated using hydrodynamic equations by Nandasena et al. (2011); dependent on boulder size, density of boulders and water, coefficients of lift, drag, gravity, and slope angle (here kept at zero)

Hurricane Joaquin made landfall on islands of the central Bahamas in October 2015, with significant coastal effects (Berg, 2016). The storm was Category 4 at its strongest, but Category 3 with sustained winds of 120-130 mph when its eye passed directly over San Salvador on October 1-3, 2015, impacting the island from multiple directions over several days (Figure 3B). This storm caused major infrastructure damage to about 80% of the buildings, roads, utilities, and the airport on San Salvador (Savarese *et al.* 2016, 2017).

Observations at or study sites in January 2016 revealed only modest modifications at SBP (Glumac *et al.* 2016; Jahan *et al.* 2016). We documented the movement of only one of 15 boulders: boulder 7, ~350 kg in weight, was rotated ~180°, transported about 3 m to the west, had another large clast on top of it, and new dents on its surface (Figure 4E). We also observed changes to the clasts and sediment in the vicinity of the remaining boulders: some were no longer buried in sand, and many had new clasts, as large as 40 cm in diameter, surrounding them (Figures 4 and 5).

In contrast, we documented major changes to TG, where we were unable to relocate 5 of the remaining 10 original boulders (Table 4). At TG, storm waves overtopped the coastal cliffs, causing erosion at the leading edge and extensive landward movement of boulders (Glumac and Curran 2018). New boulders, as large as 3 m in diameter and weighing ~4.5 tons, were generated, and blocks from prior storms, estimated to weigh 1-3 tons,
moved up to 26 m inland (Figures 6 and 7; Table 4). Our calculations indicate that minimum wave-generated flow velocities needed to initiate transport of these boulders ranged between 2.6 and 5.7 m/s (Table 4; equations from Nandasena *et al.* 2011). The formerly sharp-crested, narrow boulder ridge was modified into a larger and much broader boulder field, ~6.3 ha in area, stripped of vegetation (Figure 8). The principal coastal road was damaged and inundated by rock debris and sand (Figure 8B). The southern edge of the boulder ridge moved landward by 4-5 m exposing an underlying Pleistocene/Holocene boundary *terra rossa* paleosol (Figure 8D), which stands out in aerial images and marks the extent of storm erosion (Figure 8E). Storm erosion also exhumed an older portion of the boulder ridge, characterized by a variety of clasts partially lithified within an iron-oxide rich matrix.

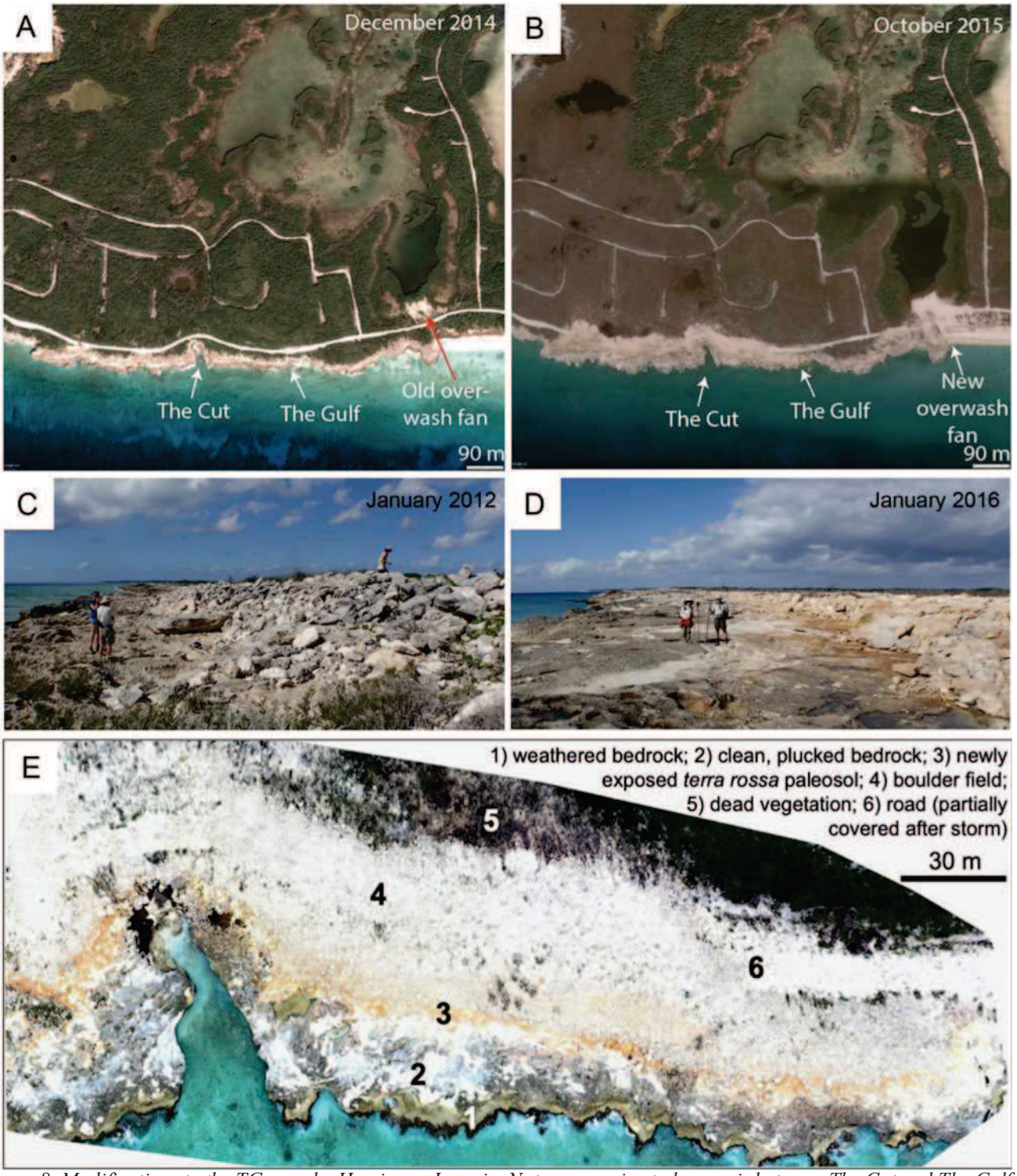

Figure 8. Modifications to the TG area by Hurricane Joaquin. Note: our main study area is between The Cut and The Gulf embayments. A & B) Google Earth images before (December 2014) and after (October 2015) Hurricane Joaquin. Note major vegetation damage (brown areas) generated by Hurricane Joaquin, the coastal road inundated by storm debris, including large boulders, and a new fan deposited by overwash east of The Gulf (8B). C & D) Photographs of the boulder ridge before (January 2012) and after (January 2016) Hurricane Joaquin. The formerly sharp-crested, narrow TG boulder ridge (8C) was modified into a larger, broad boulder field (8D), stripped of vegetation, and partially covering the road (8B). The southern edge of the boulder ridge moved landward by 4-5 m exposing an underlying Pleistocene/Holocene boundary terra rossa paleosol (dark brown areas in 8D), which stands out in aerial images (8E, January 2016) and marks the extent of storm erosion.

Our future research efforts will include study of the origin and lithification of this welded ridge.

Implementation of Drone (2016-Present) and RFID (June 2019-Present) Technologies

Post-hurricane Joaquin, in January 2016, we started to use drones for high-resolution imaging of our study area to document storm impact (Figure 9) and to form a baseline for future comparisons (Perlmutter *et al.* 2016; Glumac and Curran 2017). In January 2017, post-Hurricane Matthew (October 2016), which passed too far west from San Salvador to have any major impact, we added 12 new boulders (boulders 13-24) and additional drone imagery to our monitoring program at the TG site (Figure 9C and D).

Relocation of boulders after major storms by using only their photos, descriptions and former GPS locations proved to be rather difficult and also kept our boulder database relatively small (Figure 9). We addressed these problems by application of RFID technology in June 2019 when >50 boulders were tagged at each study site (Figure 10). Their locations were checked in January 2020, after the 2019 hurricane season, and will continue to be monitored into the future. Since there were no major hurricanes that impacted San Salvador in 2019 (Hurricane Dorian passed too far north to have any impact), we observed no movement of tagged boulders at TG, but our January 2020.

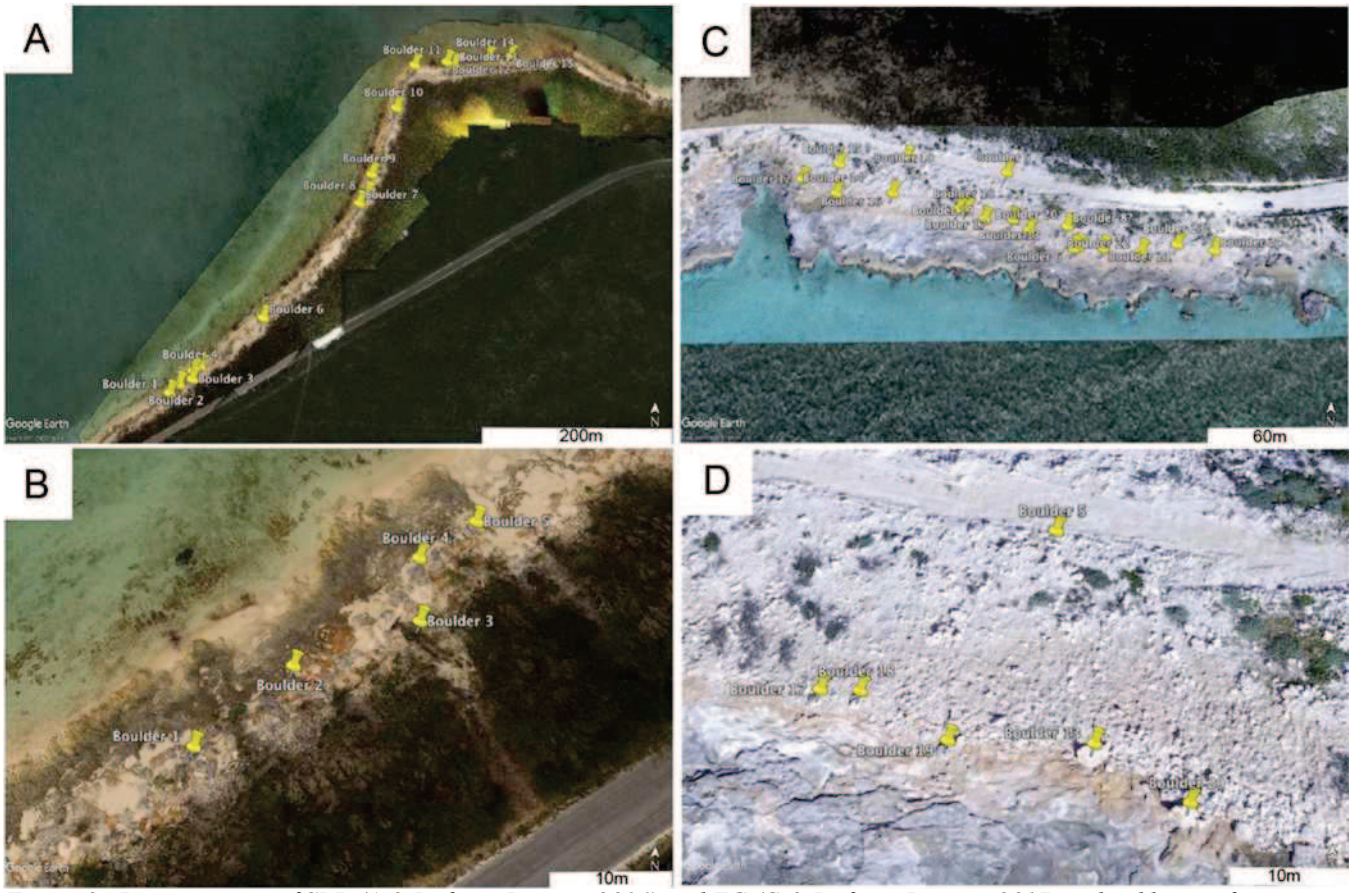

Figure 9. Drone images of SBP (A & B, from January 2016) and TG (C & D, from January 2017, with addition of new boulders). A & C) Entire sites with all boulders (pined) superimposed on Google Earth background to show the difference in resolution between these two sets of images. GPS location of SBP boulders: from N24°07.055' W74°28.640' (Boulder 1) to N24°07.237' W74°28.432' (Boulder 15); TG boulders: from N23°56.813' W74°30.759' (Boulder 1 original location) to N23°56.824' W74°30.805' (Boulder 12); B & D) Close-ups highlighting high-resolution of drone images. Dark brown Pleistocene/Holocene boundary terra rossa paleosol and partially cleared coastal road can be seen in 9D. Scale: A) 200 m; B & D) 10 m; C) 60 m.

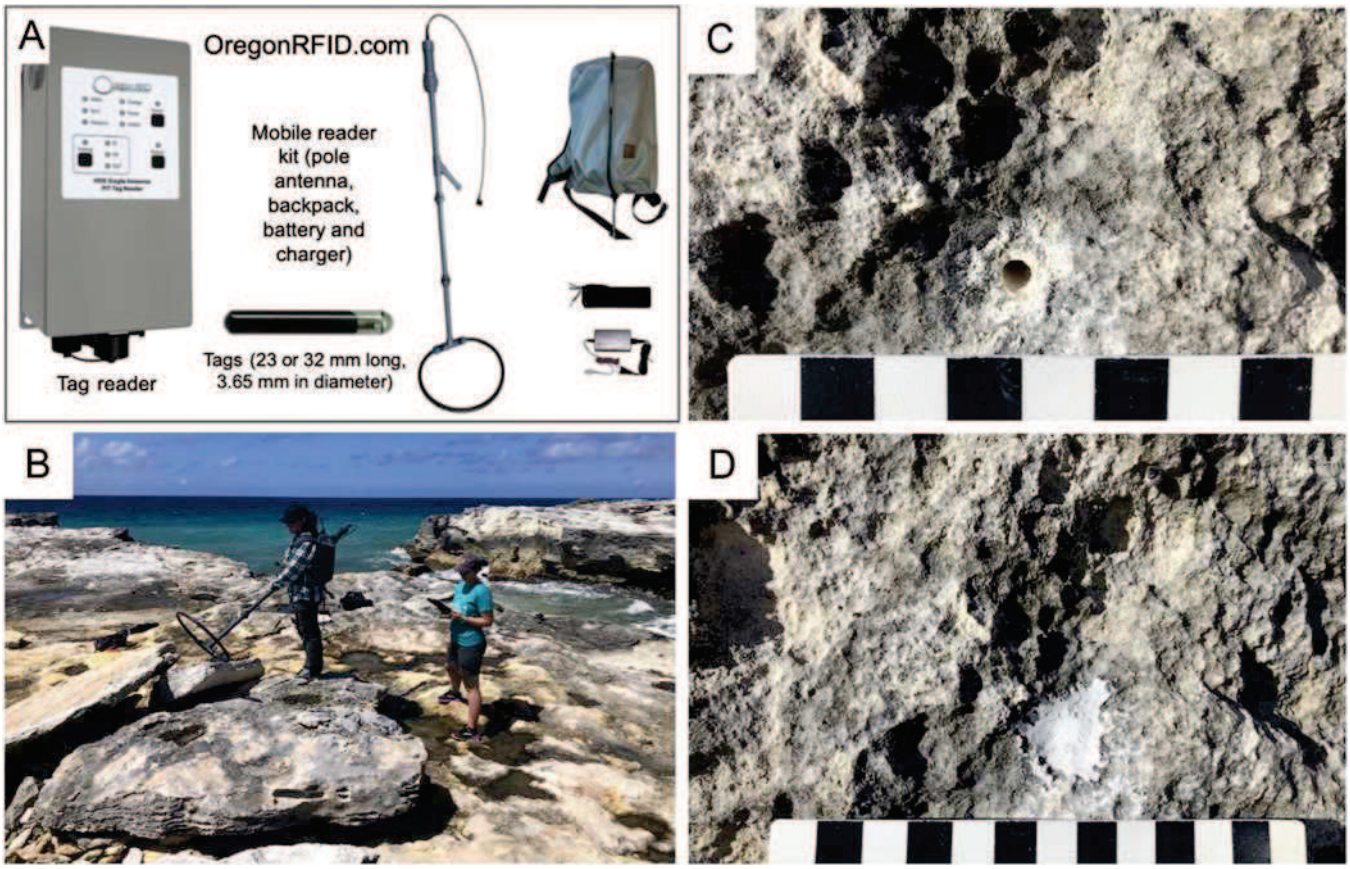

Figure 10. RFID (radio frequency identification) technology. A) System components (from: www.OregonRFID.com). B) Application of RFID at TG. C) Drilled hole for tag inserting. Scale in cms. D) Patched hole with inserted tag. Note its very small size and inconspicuous appearance.

observations documented significant movement of cobbles and smaller boulders by winter storms (i.e. from cold fronts) at SBP

This documentation was possible because RFID technology allowed us to tag and relocate such smaller clasts, thus substantially improving our monitoring efforts. The results of this continuing monitoring will be in the focus of our future presentations and publications.

CONCLUSIONS

1) Our long-term monitoring of storm-deposited boulder ridges along rocky shorelines of San Salvador Island, Bahamas, aims at documenting changes in ridge morphology and distribution, and the direction and amount of movement of individual boulders to gain insights into intensity and effects of storms impacting this small, low relief, tropical carbonate island.

2) Monitoring of storm impact at our two study sites in January 2013, 2016, and 2017, after Hurricanes Sandy (October 2012), Joaquin (October 2015), and Matthew (October 2016), respectively, indicated only modest modifications to Singer Bar Point along the reef- and lagoon-protected gently seaward-sloping northern coast, and major changes to The Gulf on a cliff bench, 3-5 m above mean sea level, along the high-energy southern coast, where we were unable to relocate 2 boulders post-Sandy, and 5 of the remaining 10 original boulders after Joaquin.

3) Even though documentation of boulder movement allows calculation of minimum flow velocity required to initiate their transport, the lack of adequate tagging made it challenging or impossible to relocate many individual boulders after major storms. This problem was addressed by application of RFID (radio frequency identification) tagging in June 2019 when >50 boulders and cobbles were tagged at each study

site using PIT (passive integrated transponder) tags, which are inductively charged by the reader and can remain operational for decades.

4) In conjunction with continuing high-resolution drone imaging, use of tagging that can uniquely identify an object within a large population allows significant increase in our database and improvement of these long-term monitoring efforts.

ACKNOWLEDGMENTS

We are grateful to: The Bahamas Environment, Science & Technology (BEST) Commission of The Ministry of the Environment for permits to conduct scientific research; The Department of Air Transport Licensing of The Bahamas Ministry of Transportation & Aviation for drone operation permits; Smith College Department of Geosciences, CFCD, and CEEDS for funding; Tony Caldanaro and Abigail Beckham (Smith College), Warren Leach (Oregon RFID, Inc.), and Wayne Stephenson (Univ. of Otago, New Zealand) for help with RFID; numerous Smith College students (2012 to present), Michael Savarese, Allison Rolfe and Samantha Gibson (Florida Gulf Coast University), Matt Wright (Eckerd College), Lisa Park Boush (University of Connecticut), Ilya Buynevich and Karen Kopcznski (Temple University), and Blanka Cvetko Tešović (Univ. of Zagreb, Croatia) for help with field work; Jon Caris, Tracy Tien, Emma Harnisch, and other members of the Spatial Analysis Lab at Smith College (2016 to present) for drone imaging; Gerace Research Centre (San Salvador, Bahamas) for logistical support; Ronadh Cox (Williams College) for general research advice and encouragement; Deedie Steele and Jane Curran for photo support and field assistance; and David Griffing and Mark Kuhlmann (Hartwick College) for organizing The Third Joint Symposium of the Natural History and Geology of The Bahamas in June 2019 and for editing this proceedings volume.

LITERATURE CITED

Berg, R. (2016). Hurricane Joaquin. National Hurricane Center Tropical Cyclone Report, 36 p.

Carew, J.L., and Mylroie, J.E. (1985). Pleistocene and Holocene stratigraphy of San Salvador Island, Bahamas, with reference to marine and terrestrial lithofacies at French Bay. *In* Curran, H.A., ed., Guidebook for Geological Society of America, Orlando Annual Meeting Field Trip #2, Fort Lauderdale, Florida. CCFL Bahamian Field Station, p. 11-61.

Cox, R., Jahn, K.L., Watkins, O.G., and Cox, P. (2018). Extraordinary boulder transport by storm waves (west of Ireland, winter 2013–2014), and criteria for analysing coastal boulder deposits. Earth-Science Reviews, v. 177, p. 623-636.

Cox, R., Zentner, D.B., Kirchner, B.J., and Cook, M.S. (2012). Boulder ridges on the Aran Islands (Ireland): Recent movements caused by storm waves, not tsunami. The Journal of Geology, v. 120, p. 249-272.

Curran, H.A., Delano, P., White, B., and Barrett, M. (2001). Coastal effects of Hurricane Floyd on San Salvador Island, Bahamas. *In* Greenstein B., and Carney C., eds., Proceedings of the 10th Symposium on the Geology of the Bahamas and Other Carbonate Regions. Gerace Research Center, San Salvador, Bahamas, p. 1-12.

Dwyer, C., Glumac, B., and Curran, H.A. (2013). Storm-deposited boulder ridges on San Salvador Island, Bahamas: characteristics and implications for coastal development. Southeastern Section, Geological Society of America Meeting Abstracts with Programs, v. 45(2), p. 14.

Glumac, B., and Curran, H.A. (2017). Storm-deposited boulder ridges along rocky

shorelines of San Salvador Island, Bahamas: Long-term monitoring and significance. The 2nd Joint Symposium on the Natural History and Geology of the Bahamas. Gerace Research Centre, San Salvador, Bahamas, p. 7-8.

Glumac, B., and Curran, H.A. (2018). Documenting the generation and transport of large rock boulders by storm waves along the high-energy southern coast of San Salvador Island, Bahamas. American Geophysical Union Annual Fall Meeting, Washington, D.C., Abstract #EP23C-2296.

Glumac, B., Jahan, N. and Curran, H.A. (2016). Monitoring changes in boulder ridges along rocky shorelines of San Salvador Island, Bahamas, as indicators of storm activity. Geological Society of America Abstracts with Programs, Annual Meeting, Denver, Colorado, v. 48(7). doi: 10.1130/abs/2016AM-282135

Hearty, P.J. (1997). Boulder deposits from large waves during the last interglaciation on North Eleuthera, Bahamas. Quaternary Research, v. 48, p. 326-338.

Hearty, P.J., and Tormey, B.R. (2017). Sea-level change and superstorms; geologic evidence from the last interglacial (MIS 5e) in the Bahamas and Bermuda offers ominous prospects for a warming Earth. Marine Geology, v. 390, p. 347–365.

Jahan, N., Glumac, B., and Curran, H.A. (2016). Storm-deposited coastal boulder ridges on San Salvador Island, Bahamas in the aftermath of Hurricane Joaquin. Geological Society of America Abstracts with Programs, Annual Meeting, Denver, Colorado, v. 48(7). doi: 10.1130/abs/2016AM-282132

Kelletat, D., Scheffers, A., and Scheffers, S. (2004). Holocene tsunami deposits on the Bahaman Islands of Long Island and Eleuthera. Zeitschrift für Geomorphologie, v. 48, p. 519-540.

Kindler, P., Mylroie, J.E., Curran, H.A., Carew, J.L., Gamble, D.W., Rothfus, T.A., Savarese, M., and Sealey, N.E. (2010). Geology of Central Eleuthera, Bahamas: A Field Trip Guide for The 15th Symposium on the Geology of the Bahamas and Other Carbonate Regions. Gerace Research Centre, San Salvador, Bahamas, 75 p.

Mylroie, J.E. (2008). Late Quaternary sea-level position: evidence from Bahamian carbonate deposition and dissolution cycles. Quaternary International, v. 183, p. 61-75.

Mylroie, J.E. (2018). Superstorms: Comments on Bahamian fenestrae and boulder evidence from the Last Interglacial. Journal of Coastal Research, v. 34, p. 1471–1483.

Niemi, T.M. (2017). Large boulders on Green Cay, San Salvador Island, The Bahamas. *In* Landry, C.L., and Kjar, D.S., eds., Proceedings of the 1st Joint Symposium on the Natural History and Geology of The Bahamas, June 2015. Gerace Research Center, San Salvador, Bahamas, p. 121-129.

Niemi, T.M., Thomason, J.C., McCabe, J.M., and Daehne, A. (2008). Impact of the September 2, 2004 Hurricane Frances on the coastal environment of San Salvador Island, the Bahamas. *In* Park, L.E., and Freile, D., eds., Proceedings of the 13th Symposium on the Geology of the Bahamas and Other Carbonate Regions. Gerace Research Center, San Salvador, Bahamas, p. 43-64.

Panuska, B.C., Boardman, M.R., Carew, J.L., Mylroie, J.E., Sealey, N.E., and Voegeli, V. (2002). Eleuthera Island Field Trip Guide for The 11th Symposium on the Geology of the Bahamas and Other

Carbonate Regions. Gerace Research Center, San Salvador, Bahamas, 20 p.

Perlmutter, E., Caris, J., Widstrand, A., Curran, H.A., and Glumac, B. (2016). Drone use in rapid assessment of Hurricane Joaquin coastal impact on San Salvador Island, Bahamas. Geological Society of America Abstracts with Programs, Annual Meeting, Denver, Colorado, v. 48(7). doi: 10.1130/abs/2016AM-282290

Rovere, A., Casella, E., Harris, D.L., Lorscheid, T., Nandasena, N.A.K., Dyer, B., Sandstrom, M.R., Stocchi, P., D'Andrea, W.J., and Raymo, M.E. (2017). Giant boulders and Last Interglacial storm intensity in the North Atlantic. Proceedings of the National Academy of Sciences of the United States of America, v. 114, p. 12144-12149.

Rovere, A., Casella, E., Harris, D.L., Lorscheid, T., Nandasena, N.A.K., Dyer, B., Sandstrom, M.R., Stocchi, P., D'Andrea, W.J., and Raymo, M.E. (2018). Reply to Hearty and Tormey: Use the scientific method to test geologic hypotheses, because rocks do not whisper. Proceedings of the National Academy of Sciences of the United States of America, v. 115, E2904–E2905.

Savarese, M., Buynevich, I.V., Caris, J., Curran, H.A., Glumac, B., Park Boush, L., and Kopcznski, K. (2016). Heterogeneous vulnerability to Hurricane Joaquin's influence along the perimeter of San Salvador Island, Bahamas. Geological Society of America Abstracts with Programs, Annual Meeting, Denver, Colorado, v. 48(7). doi: 10.1130/abs/2016AM-282743

Savarese, M., Buynevich, I., Caris, J., Curran, H.A., Glumac, B., Park Boush, L., and Kopcznski, K. (2017). A vulnerability analysis of Hurricane Joaquin's effects along the perimeter of San Salvador Island, Bahamas. Abstracts and Program, The 2nd Joint Conference on the Natural History and Geology of the Bahamas, Gerace Research Centre, San Salvador, Bahamas.

Nandasena, N.A.K., Paris, R., and Tanaka, N. (2011). Reassessment of hydrodynamic equations: Minimum flow velocity to initiate boulder transport by high energy events (storms, tsunamis). Marine Geology, v. 281, p. 70-84.

Walker, S.E., Holland, S.M., and Gardiner, L. (2001). Cockburn Town Fossil Reef: A summary of effects from Hurricane Floyd. *In* Greenstein, B., and Carney, C., eds., Proceedings of the 10th Symposium on the Geology of the Bahamas and Other Carbonate Regions. Gerace Research Center, San Salvador, Bahamas, p. 13-19.
.

INVESTIGATION OF FLORAL DIVERSITY AND SPATIAL DISTRIBUTION OF SPECIES IN COASTAL PLANT COMMUNITIES

Johnny Green and Carol L. Landry [1]

Department of Evolution, Ecology, and Organismal Biology, The Ohio State University,
1760 University Dr. Mansfield, OH 44906
[1] Corresponding author

ABSTRACT

There are six coastal plant communities in The Bahamas, determined by their distance from the ocean, substrate composition, and relative degree of disturbance. These communities are dynamic, ever subject to wind and water, including significant disturbances due to tropical storms and hurricanes. Coastal plant communities are important ecologically and economically; they reduce erosion by stabilizing sediments and protect inland communities by absorbing the energy of storm surge. To better understand interactions between plants from different communities that share pollinators, we investigated the species composition, relative species abundance, and spatial distribution in four of the six community types. In this preliminary study, we surveyed seven 100-m^2 plots on San Salvador, two each in the *Coccothrinax*-shrub, beach-foredune, and rock terrace communities, and one in the shrub-thicket community. All plant species were identified, their canopies mapped, and the total canopy coverage for each species was estimated for each plot. To compare the relative floral diversity, as perceived by insect pollinators, the relative canopy coverage of each species was used to calculate species evenness and the Shannon diversity index for each community. Our preliminary results demonstrate that the *Coccothrinax*-shrub and shrub-thicket communities have the greatest canopy coverage and floral diversity. Ultimately, these data will be compared to insect visitation records to determine whether pollinator diversity is correlated with floral diversity, or if the presence of communities with greater floral diversity influences pollinator diversity in adjacent communities with less floral diversity.

INTRODUCTION

The purpose of this long-term study is to understand interactions between plants from different communities that share pollinators. There are six coastal plant communities on San Salvador (Smith 1993); these communities are dynamic, ever subject to wind and water, including significant disturbances caused by tropical storms and hurricanes. Coastal plant communities are important ecologically and economically, in part because they reduce erosion by stabilizing sediments and protect inland communities by absorbing the energy of storm surge (Miller *et al.* 2010). The formation and persistence of each community type is determined by several factors, including the distance from the ocean, substrate composition, and relative degree of disturbance.

In this preliminary investigation, we determined species composition, estimated relative species abundance, and described the spatial distribution of plants in four of the six community types: shrub-thicket, *Coccothrinax*-shrub, beach-foredune, and rock terrace. To estimate the relative floral diversity as perceived by insect pollinators, we used the relative canopy coverage as a proxy to calculate a Shannon diversity index for each community. Ultimately these data will be compared with insect visitation records to determine if pollinator diversity and abundance is correlated with floral diversity, and to determine whether the diversity and abundance of pollinators observed in one community type is influenced by the floral diversity of adjacent plant communities.

FIELD SITE DESCRIPTION

This work was performed at two general locations in the coastal ecosystem on San Salvador Island: along Snow Bay (aka Sandy Hook) on the southeastern end of the island, and at the northern end of East Beach near the United Estates Settlement. Snow Bay is a biologically diverse area that includes all six coastal plant communities. It is bordered by the ocean to the south and east and the Pigeon Creek lagoon system to the north. The north end of East Beach includes beach-foredune and coppice thicket communities.

METHODS

A total of seven 100-m^2 plots were established in June 2017 at two locations on San Salvador Island. Along Snow Bay, two plots were established in *Coccothrinax*-shrub and rock terrace communities, and one plot was established in a shrub thicket community; two plots were also established in a beach foredune community at East Beach. GPS coordinates were recorded for each plot, and the directional orientation of each plot was determined using a compass.

All animal-pollinated plants within the plots were identified and mapped. The canopy area of each individual (or group of individuals, when their canopies were continuous) was estimated using measuring tapes, and the areas were summed to estimate the total canopy area of each species in the plot. Canopy area estimates for were then used to calculate the Shannon diversity index (H) and the species evenness (E_H) within each plot, using the following equations:

$H = (-1)\Sigma p_i * \ln p_i$, where $i = 1, 2, \ldots N$ species, and p_i = the proportion of the ith species in the plot; and

$E_H = H/\ln(S)$, where S = # species in the plot.

Vines were treated differently because the plants climb over and through the branches of other plants, making it difficult to determine the actual "canopy" size. For these species, the overall area where the vines were located was measured to estimate the relative area they occupied. Vining species were excluded from Shannon diversity index and species evenness calculations.

RESULTS

A total of 38 species and 12 morphospecies of animal-pollinated plants were identified during the study, but only a subset were found in each community type (Table 1). The most speciose communities were shrub thicket (24 species, 7 morphospecies) and *Coccothrinax*-shrub (19 species, 5 morphospecies); in contrast, the beach-foredune and rock terrace communities had far fewer species (7 and 4 species, respectively). The relative contribution of floral resources made by each species was relatively even in shrub thicket (E_H = 0.77) and *Coccothrinax*-shrub (E_H = 0.80 – 0.83) communities (Figure 1), contributing to the highest diversity indices (H = 2.50 and 2.22 – 2.43, respectively; Figure 1). The plots in rock terrace communities were variable in terms of species evenness (E_H = 0.28 – 0.67; Figure 1) and diversity indices (H = 0.31 – 0.73; Figure 1), while these metrics were more consistent in beach-foredune plots (E_H = 0.53 – 0.72; H = 1.03 – 1.40; Figure 1). In addition, the canopies of plants in the shrub-thicket community provided near-complete coverage of the total plot area (81%), and plants in the *Coccothrinax*-shrub community plots provided considerable coverage (54 – 59%). In contrast, the total canopy coverage was quite limited in beach-foredune (14 – 21%) and rock terrace (12 – 13%) communities.

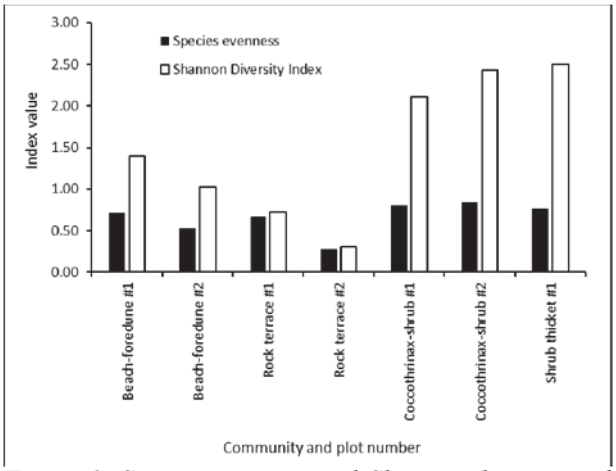

Figure 1. Species evenness and Shannon diversity indices for each plot

Table 1: List of plant species identified in each community type, with number of plots in each community that included the species indicated. Morphospecies were excluded from this list.

Family	Species	Community type			
		Beach-foredune	Rock terrace	*Coccothrinax*-shrub	Shrub thicket
Aizoaceae	*Sesuvium portulacastrum* (L.) L.	1			
Apocynaceae	*Metastelma bahamense* Griseb.			2	1
Apocynaceae	*Pentalinon luteum* (L.) B.F. Hansen & Wunderlin				1
Arecaceae	*Coccothrinax argentata* (Jacq.) L.H. Bailey			1	
Arecaceae	*Leucothrinax morrisii* (H. Wendl.) C. Lewis & Zona			1	1
Arecaceae	*Sabal palmetto* Thunb.			2	1
Asteraceae	*Borrichia arborescens* (L.) DC.		1		
Asteraceae	*Gundlachia corymbosa* (Urb.) Britt.			1	1
Asteraceae	*Iva imbricata* Walt.	2			
Boraginaceae	*Bourreria baccata* Raf.				1
Boraginaceae	*Tournefortia gnaphalodes* L.	2			
Boraginaceae	*Varronia bahamensis* Urb.			1	1
Brassicaceae	*Cakile lanceolata* (Willd.) O.E. Schutz	2			
Combretaceae	*Conocarpus erectus* L.		2		
Convolvulaceae	*Jacquemontia cayensis* Britt.			2	1
Euphorbiaceae	*Croton discolor* Willd.				1
Euphorbiaceae	*Euphorbia lecheoides* Millsp.			2	1
Euphorbiaceae	*Euphorbia mesembryanthemifolia* Jacq.	2			
Fabaceae	*Chamaecrista lineata* (Sw.) Green			2	1
Fabaceae	*Pithecellobium keyense* Britt. Ex Britt. & Rose			2	1
Goodeneaceae	*Scaevola plumieri* (L.) Vahl	1			
Lauraceae	*Cassytha filiformis* L.				1
Tiliaceae	*Corchorus hirsutus* L.			1	
Myrtaceae	*Mosiera longipes* (Berg) McVaugh				1
Passifloraceae	*Passiflora cuprea* L.			1	1
Passifloraceae	*Passiflora pectinata* Griseb.				1
Polygonaceae	*Coccoloba uvifera* (L.) L.			2	1
Rhamnaceae	Reynosia septentrionalis Urb.			2	1
Rubiaceae	*Antirhea myrtifolia* (Griseb.) Urb.			2	
Rubiaceae	*Erithalis diffusa* Correll			2	1
Rubiaceae	*Erithalis fruticosa* L.				1
Rubiaceae	*Ernodea littoralis* Sw.			2	1
Rubiaceae	*Rachicallis americana* (Jacq.) O. Ktze.		2		
Rubiaceae	*Strumpfia maritima* Jacq.		1		
Sterculiaceae	*Waltheria bahamensis* Britt.				1
Surianaceae	*Suriana maritima* L.	2			

DISCUSSION

Our preliminary findings demonstrate that shrub-thicket and *Coccothrinax*-shrub communities have the greatest canopy coverage and floral diversity. This is somewhat expected because these communities are further from the shoreline, so the severity of disturbance events like hurricanes is tempered – particularly with respect to the surge typically associated with these storms. Plants in these communities frequently grow in mixed stands, with smaller individuals growing below taller plants, and with vines growing over and among the branches of shrubs and trees. Greater complexity in the vertical structure of the community can contribute to greater diversity in the animals that utilize these plants, including birds (e.g. Suarez-Rubio and Thomlinson 2009) and arthropods (e.g. Gardner *et al.* 1995).

In contrast, plants in beach-foredune and rock terrace communities have sparse canopy coverage and lower floral diversity due to lower species richness and greater unevenness of floral resource contributions made by each species. In combination, these characteristics may help explain the reduced pollinator abundance and diversity previously observed in the beach-foredune communities along East Beach (Landry *et al.* 2013), where pollinator activity was confined to a few plant species that provided a large fraction of the floral resources available (data not published).

More surveys need to be performed to better estimate the floral diversity present in these plant communities, and in the other coastal communities found on San Salvador that are not represented in this study. Ultimately these data will be compared with insect visitation records to determine if pollinator diversity and abundance is generally correlated with floral diversity or if the presence and abundance of a subset of plant species is more informative. In addition, we will determine whether the diversity and abundance of pollinators observed in one community type is influenced by the floral diversity of adjacent plant communities, or if other factors, such as the availability of nesting sites, are more important.

ACKNOWLEDGEMENTS

This research was supported by travel and research grants from the Ohio State University at Mansfield, and performed with permission of the Bahamas Environment, Science, and Technology (BEST) Commission, Ministry of the Environment and Housing. We thank the Gerace Research Centre for its continued support of our research activities on San Salvador; we also give special thanks to Dr. Agustin Munoz-Garcia for assistance with data analysis.

LITERATURE CITED

Gardner, S.M., Cabido, M.R., Valladares, G.R., and Diaz, S. (1995) The influence of habitat structure on arthropod diversity in Argentine semi-arid Chaco forest. Journal of Vegetation Science 6, 349-356.

Landry, C.L., Elliott, N.B., Finkle, A., and Kass, L.B. (2013) "Pollination networks- what's the buzz? A preliminary study of coastal community pollination dynamics on San Salvador Island, The Bahamas," in The Proceedings of the 14th Symposium on the Natural History of The Bahamas, eds. C. Tepper and R. Shaklee (San Salvador Island, Bahamas: Gerace Research Centre), 95-112.

Miller, T.E., Gornish, E.S., and Buckley, H.L. (2010) Climate and coastal dune vegetation: disturbance, recovery, and succession. Plant Ecology 206, 97-104.

Smith, R.R. (1993) Field guide to vegetation of San Salvador Island, the Bahamas, 2nd Edition. San Salvador Island, Bahamas: Bahamian Field Station.

Suarez-Rubio, M., and Thomlinson, J.R. (2009) Landscape and patch-level factors influence bird communities in an urbanized tropical island. Biological Conservation 142, 1311-1321.

BOULDER MOVEMENT FROM HURRICANES ALONG THE ROCKY SOUTHERN COAST OF SAN SALVADOR ISLAND, THE BAHAMAS

Tina M. Niemi, Joseph A. Nolan, Stephanie M. Caples, Anna Murray, Tori Rose, Linda Rucker, Jennica Grady, Sara Lamprise, Jessy Zapata, and John D. Rucker

Earth and Environmental Sciences, Division of the Natural and Built Environment
School of Science and Engineering, University of Missouri-Kansas City
Kansas City, MO 64110 U.S.A.

ABSTRACT

Located along the northeastern edge of the Bahamian archipelago, San Salvador Island sees a high frequency of Atlantic hurricanes that track through the Caribbean. This makes the island an excellent location for studying geomorphological processes and changes to the coastal environment due to high-energy waves. The focus of this study is to report on monitoring of coastal erosion and boulder movement along the southern rocky coast at the location called the Gulf on San Salvador Island caused by hurricanes that passed within 60 nautical miles of the island during 2011-2019, including Hurricane Irene (2011), Hurricane Joaquin (2015), and Hurricane Matthew (2016). To map the hurricane-related changes in the coastal environment, two aerial imaging techniques were utilized to photograph the boulder field at the Gulf. Aerial imagery was collected using a kite-mounted camera in June 2015 and March 2016, and using an uncrewed aerial vehicle in March 2016-2018 and June 2016, 2017, and 2019. All data were processed using Agisoft Metashape to render both a high-resolution digital orthophoto mosaic image and a georeferenced digital elevation model. Additionally, ground-based photographic and orientation data for boulder location, imbrication, and beach conditions were collected. The high-resolution, low-altitude imagery allowed us to map the boulder field and calculate boulder movement by matching erosion scars to boulder position, and boulder size to position. Boulders of the Pleistocene fossil reef that are exposed along the wave-cut platform at low tide have been transported up the cliff and inland in storm events based on boulder identification. Coastal reentrants along a rocky island cliff face are the location of coves where wave action is focused, and thus increase the potential to lift boulders. Coastline retreats where cliffs collapse downward are located along these coves and provide large boulders which are available for transport upward. These coves become the staging ground for boulders to be elevated in extreme storm events. Our data show that the coves have a greater storm surge height and transport boulders farther landward. The pronounced landward movement of the entire boulder field during Joaquin is likely due to wave heights as big as 14 m that were caused by the unique intensity, storm track direction from the south with the eyewall passing directly over the island, and long duration of the storm surge.

INTRODUCTION

As the number of annual extreme weather events increases and triggers natural disasters, there is growing data to indicate that the increase in global temperature plays a significant role (UNDRR, 2020). Over the past 150 years, North Atlantic hurricanes may not be getting more frequent (Vecchi *et al.* 2021), but major tropical cyclones since 1980 are getting stronger, intensify faster, and cause more precipitation on landfall as they decay slower (e.g., Bhatia *et al.* 2019; Kossin *et al.* 2020; Li and Chakraborty, 2020). This is of particular consideration to small island nations in the tropics that reside at low elevations and are vulnerable to hurricane storm surge and

inundation (Oppenheimer *et al.* 2019). One country that is notably at risk for hurricane damage is The Bahamas. The Bahamas is a country in the Caribbean that includes over 3000 low-lying islands and cays north and northwest of Cuba and Hispaniola, respectively, and southeast of Florida. It lies along the path of most North Atlantic hurricane storm trajectories. Assessing the effects of past hurricanes in The Bahamas can help inform strategies for mitigation and resilience for all small island nations.

In this study, we report on monitoring the effects of hurricanes on San Salvador Island in The Bahamas over the period between 2012 and 2018. San Salvador is an isolated, small carbonate island located on the eastern or windward side of the Bahamian archipelago (Figure 1). It is surrounded by deep Atlantic Ocean waters, which may play a role in the pattern of hurricane damage on the island. Because the Gerace Research Centre (now the Gerace Research Institute and formerly called the Bahamian Field Station) has been operational on the island since the 1970s, there has been an extensive amount of focused research on San Salvador Island. Attention to documenting the damage and coastal changes caused by tropical storms on the island started with a study posted online by Garver (1996) detailing effects from the category 3 Hurricane Lili (1996), the eyewall of which directly passed over San Salvador. Hurricane Lili traveled from the southwest toward the northeast and had major impacts on the western and southern sides of the island (Garver, 1996).

Statistics of hurricane activity compiled by the Caribbean Hurricane Network (stormcarib.com) indicate that the most active 5-year-perod of storm activity to affect San Salvador during the historical record dating back to 1850 was 1930-1934 when seven tropical storms passed near San Salvador, of which three were major (greater than category 3) hurricanes (Figure 2). However, these same data show that the interval

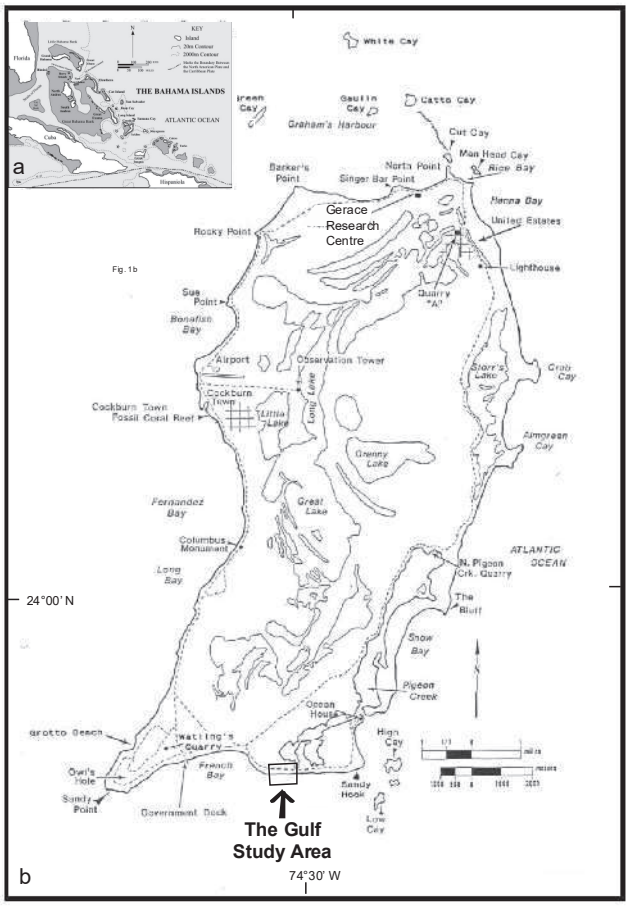

Figure 1. a) San Salvador is a small, isolated carbonate island with deep Atlantic Ocean waters surrounding it located on the eastern, windward side of the Bahamian archipelago. b) The study site called "The Gulf" is located on the southern rocky shore of San Salvador Island. Map after Mylroie and Carew (2010).

1995-1999 was the most active hurricane period with five storms passing within 60 nautical miles (69 mi; 111 km) of the island. These hurricanes included Erin (1995), Bertha (1996), Lili (1996), Dennis (1999), and Floyd (1999). In 1999, the eyewall of the powerful category 4 Hurricane Floyd passed 20-30 nautical miles north of San Salvador. Structural damage from the storm was reported by Gamble *et al.* (2000) and coastal damage was documented by Curran *et al.* (2001). Winds from Hurricane Floyd were most intense from the NW-W thus causing significant coastal erosion on the northern and western sides of the island including erosion of beach sand, formation of beach scarps along the coastal backshore dunes, and rock rubble along beachrock or bedrock strandlines (Curran *et al.* 2001).

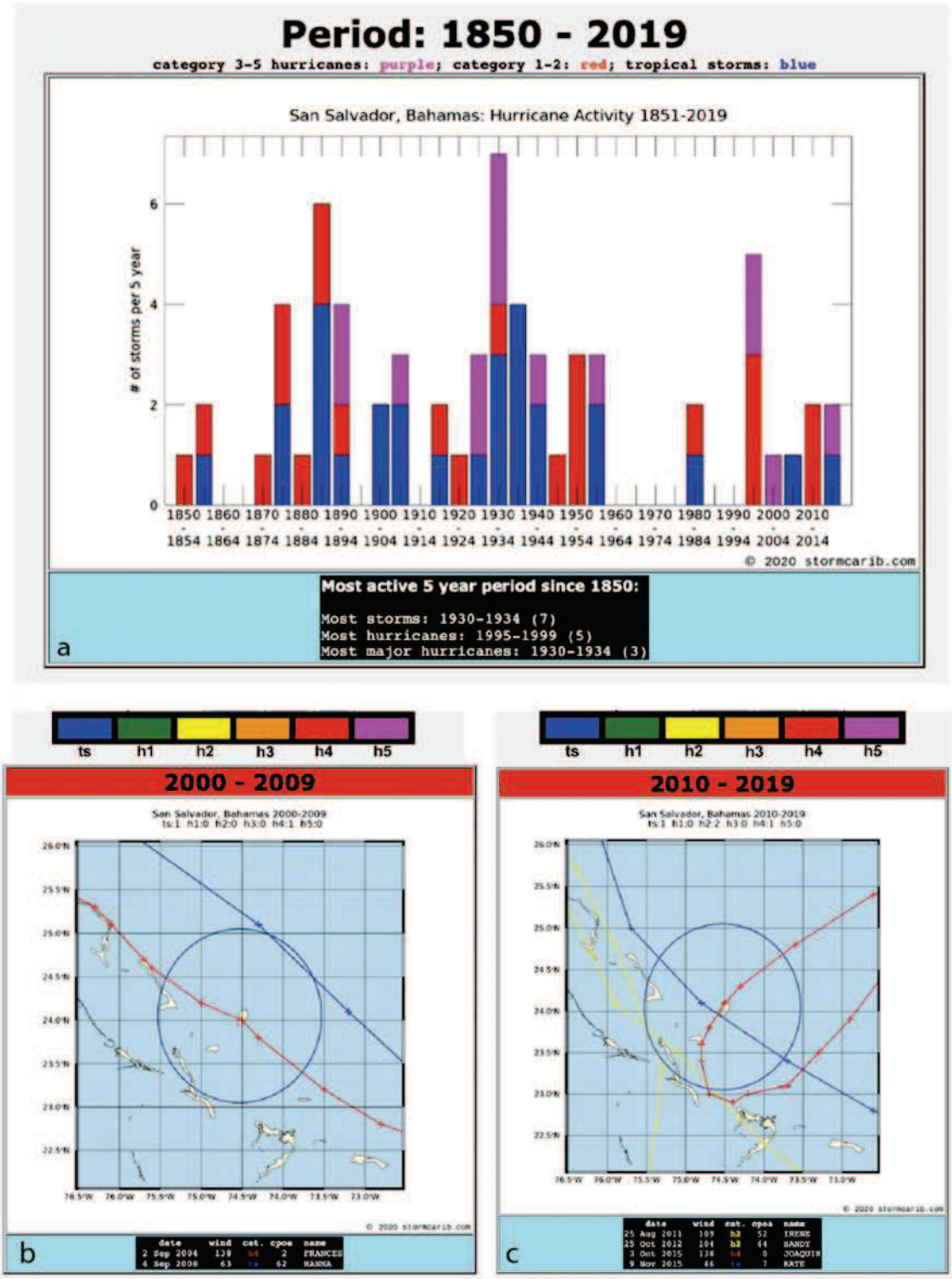

Figure 2. a) Histogram of tropical storms, category 1-2 hurricanes, and major category 3-5 hurricanes in the Bahamas for the time period 1850-2019. The stormiest 5-year period and one with the most major hurricanes was 1930-1934. The most hurricanes of all categories occurred in 1995-1999. b) During the decade 2000-2009, Hurricane Frances (2004) made a direct pass over San Salvador. The only other storm within 60 nautical miles was Tropical Storm Hanna (2008) that passed NW of the island. c) Four tropical cyclones passed close to San Salvador during the interval 2010-2019. The eyewall of category 4 Hurricane Joaquin (2015) tracked directly over the island, followed in the same year one month later by a close pass by Tropical Storm Kate. Hurricane Irene (2011) and Hurricane Sandy (2012) followed a NW track across the Bahamas to the W-SW of San Salvador. (Data source: stormcarib.com).

During the decade between 2000-2009 only two storms passed close to San Salvador, including the direct hit by category 4 Hurricane Frances on September 2, 2004, and Tropical Storm Hanna on September 4, 2008 (Figure 2b). The eyewall of Hurricane Frances passed directly over San Salvador Island from the southeast with a maximum wind speed of 138 mph (Beven 2005) (Figures 2 and 3). Because Gerace Research Centre located on the island provided logistical support for researchers, there are a number of studies that have documented the damage and geological effects from this hurricane (Parnell *et al.* 2004; Niemi *et al.* 2008; McCabe and Niemi 2008; Daehne and Niemi 2010; Dick and Cartright 2011; Curran *et al.* 2012). A storm surge height of greater than 5 m was documented by determining the elevation of the wrack line along the eastern rocky shoreline of the island (Niemi *et al.* 2008; Dick and Cartright 2011). Together these data provide a baseline for continued research on potential hurricane impacts on a small island like San Salvador in The Bahamas.

During the decade between 2010-2019, four tropical storms passed within 60 nautical miles of San Salvador. These included category 2 Hurricane Irene on August 15, 2011, category 2 Hurricane Sandy on October 25, 2012, category 4 Hurricane Joaquin on October 2, 2015, and Tropical Storm Kate on November 9, 2015 (Figure 2c). In this study, we focus on coastal geomorphic changes during the time period of 2012-2018 on San Salvador Island based on our aerial imaging and ground survey data. The goal of our research is to document changes along a rocky shore of the south side of San Salvador Island at a place called the Gulf (Figure 1). High-resolution imagery from kite-mounted and drone cameras over the past decade, along with field observations and data on the direction of boulder imbrication help to illuminate the processes of cliff retreat, boulder formation, and boulder transport along a rocky cliff shoreline during hurricanes. Preliminary results of this study were published in Rose *et al.* (2017) and presented at professional meetings by Preisberga *et al.* (2016), Niemi *et al.* (2017), Caples and Niemi (2018), and Caples *et al.* (2019). Below we outline the parameters for the hurricanes during the period of 2011-2021 that have impacted San Salvador and our data documenting the changes in the coastal environment along the rocky southern coast of the island. These data can help model the potential hazards of cliff retreat, boulder ridge formation and movement, and inundation levels for future hurricanes in The Bahamas and on other small island nations.

Hurricanes Impacting San Salvador Island (2011-2021)

The most significant hurricanes to have impacted San Salvador over the past decade that we have been collecting data at the Gulf site include Hurricane Irene (2011), Hurricane Joaquin (2015), and Hurricane Matthew (2016). Below we summarize the meteorological history and storm tracks of these hurricanes. We also describe subsequent powerful and destructive hurricanes that impacted The Bahamas during the time period 2017-2020.

In 2011, Hurricane Irene (August 21-29) brought strong winds and a storm surge to San Salvador Island. The storm traveled north of Hispaniola on a northwest trajectory and intensified into a category 3 cyclone as the eyewall passed between Mayaguana and Grand Inagua in The Bahamas (Avila and Cangialosi 2011). The hurricane shifted toward the N-NW south of San Salvador as the eye passed over Eleuthera and the winds weakened to category 2 on August 25 as it passed Abaco Island. The diameter of Hurricane Irene was larger than normal size (Avila and Cangialosi 2011).

Hurricane Joaquin was the "strongest October hurricane known to have affected The Bahamas since 1866" (Berg 2016, p. 3), but that record was superseded by subsequent cyclones (see below). The hurricane was unusual as it did not originate in the tropics, but at 27°N or about 360 nautical miles northeast of San Salvador and traveled an atypical path southwest toward the central Bahamas (Berg 2016) and was poorly forecast (Miller and Zhang 2019; Nystrom *et al.* 2018). On October 1, 2015, the storm intensified to a category 4 hurricane, then slowed, and abruptly made a clockwise hairpin turn and

traveled northeast. The unusual looping track caused intense winds for 2 days to be focused on the central southeast Bahamas (Berg 2016). The container ship, *SS El Faro*, sank, killing all 33 members of the crew when it lost power north of The Bahamas and east of San Salvador as it traveled into the eye of the hurricane on October 1, 2015. Hurricane Joaquin passed directly over San Salvador Island on October 2, 2015, with wind speeds of 125 mph (~200 kph) approaching the island from the south. Re-analysis of wind, wave, and ocean current data for the location of the *El Faro* conclude that individual wave heights were >10 m (Bell and Kirtman 2021). Wave simulations and hindcasting of sea state models find wave crests that exceeded 14 m (Fedele *et al.* 2017). Sahoo *et al.* (2019) modeled the hydrodynamic response for the Bahamian archipelago and calculated a maximum significant wave height of 15 m and coast currents of 4 m/s. Together these data indicate Hurricane Joaquin created rogue waves and extreme high-energy wave conditions from October 1-2, 2015. Fuhrmann *et al.* (2019) assessed the storm surge and structural damage of Hurricane Joaquin and found that the average storm surge height was 2.6-3.4 m on San Salvador, with the highest wrack line for storm surge measured on the north side of the island at 5.7 m. However, it must be noted that wrackline elevation for storm surge are only accurate when sufficient unimpeded topographic elevation exists along a coast to record the wave run-up height. The paper by Fuhrmann *et al.* (2019) also does not directly address the boulder field movement at the Gulf location on the island.

Although not within 60 nautical miles of San Salvador Island, Hurricane Matthew was a category 5 hurricane that passed north between Hispaniola and Cuba and then traveled northwest along the southern Bahamian archipelago. It crossed over western New Providence Island on October 6, 2016, as a category 4 hurricane (Stewart 2017). Hurricane-force winds, heavy wave action in the storm surge, and intense rainfall caused damage in Nassau and other northern islands in The Bahamas. Most of the central and south Bahamas including San Salvador Island experienced tropical-storm-force winds (Stewart 2017).

Between 2017-2021, no major hurricanes passed close to San Salvador Island in the central-east Bahamas, but the island likely experienced tropical storm conditions due to several major hurricanes that affected the Caribbean. In 2017, two major hurricanes passed near The Bahamas. The catastrophic Hurricane Irma made four category 5 intensity landfalls as it passed the southeastern Bahamas, paralleled the north coast of Cuba and turned northwest to make landfall in the Florida Keys (Cangialosi *et al.* 2021). Hurricane Maria caused major damage as it passed directly over Puerto Rico and then headed north. In 2018, Hurricane Florence was a major hurricane that passed well north of The Bahamas, making landfall in North Carolina (Stewart and Berg, 2019). In 2019, Hurricane Dorian passed north of San Salvador Island. Hurricane Dorian was the strongest hurricane to make landfall in The Bahamas in modern history, leaving over 200 people dead and massive destruction (Avila *et al.* 2020). It made landfall on Great Abaco and Grand Bahama Islands on September 1-2, 2019, as a category 5 hurricane with minimum low pressure of 910 millibars, an estimated wind of 184 mph (296 kph), and an associated storm surge of >6 m which caused catastrophic flooding (Avila *et al.* 2020). The slow movement of Hurricane Dorian over the northwest Bahamas led to high levels of rainfall exacerbating the coastal inundation. Hurricane Isaias (2020) passed southwest of San Salvador with recorded wind speeds of 54 mph (87 kph) (Latto *et al.* 2021). No hurricanes passed through or near The Bahamas in 2021.

STUDY SITE AND METHODS

Our study focuses on the Gulf site located along the southern coast of San Salvador Island where the deep water of the Atlantic Ocean is closest to the island (Figure 1). The wall of the fringe reefs is as close as 25 m offshore. At the Gulf boulder field site, the shallow carbonate platform extends ~50 m offshore and begins a steep drop to the 2000 m isobath at 130 m from the shoreline. The east-west-oriented rocky coastline at the Gulf site extends for about 1.5 km

and forms the boundary of French Bay to the west. To the east lies the accretionary sand ridge complex that forms the southeastern tip of the island known as Sandy Hook (Figure 1).

The shoreline at the Gulf is marked by a cliff that is approximately 3-4 m in height. The late Pleistocene bedrock at the study site that outcrops along the roadcut and along the shoreline cliff face was described as Fieldtrip Stop 14 by Mylroie and Carew (2010). The rocks belong to the Cockburn Town Member of the Grotto Beach Formation (Figure 3). The uppermost exposed bedrock at the Gulf location is a cross-bedded, oolitic calcarenite deposited in a paleo-sand dune (eolianite). It has a thin paleosol at the top and in the roadcut, the bedrock is topographically higher than the surrounding area because the original sand dune morphology is preserved. In places the exposure of the eolianite along the sea cliff has a much thicker upper paleosol that includes brecciated calcarenite and a penetrative mass of rhizoliths that extend to a depth of 3 m in friable calcarenite (Mylroie and Carew 2010). At low tide, the rock unit below the eolianite that is exposed along the modern wave-cut platform belongs to the lower Cockburn Town Member. It is a calcrudite containing cemented fossil coral reef rubble. We made field observations of coastal erosion of the bedrock exposure and boulder movement and deposition along the eroded cliff face, along a ~600-m-long section of the Gulf outcrop from an access point to the intertidal zone that we call "east cove" to the western edge of the boulder field that was mobilized in 2015 (Figures 3-5). Our field

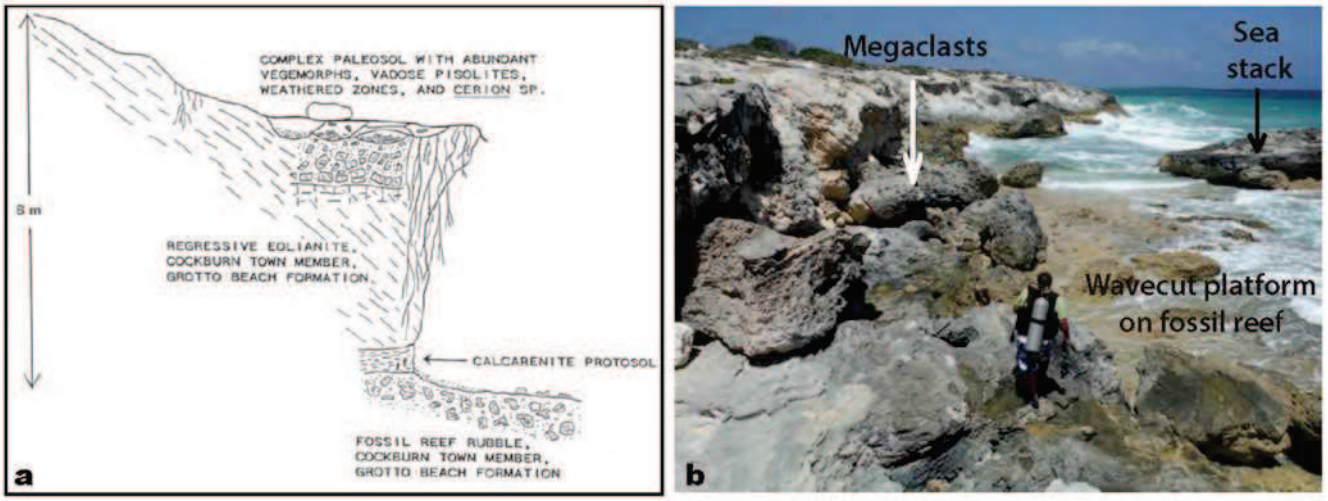

Figure 3. Diagram of the stratigraphy exposed in the cliff and roadcut at the Gulf site showing late Pleistocene fossil coral reef overlain by cross-bedded calcarenite of a fossil sand dune (eolianite). The paleosol on the upper portion of eolianite bedrock contains abundant rhizoliths (vegemorph), is brecciated, and contain red calcrete or terra rosa (from Mylroie and Carew, 2010). b) Photograph from June 2017 of the cliff face at the Gulf looking toward the east showing a sea stack, a wavecut platform developed on the fossil coral reef rumble and the cliff composed of the eolianite. Megaclasts are derived from the collapse of the cliff. Note that the bedrock in the intertidal zone is yellowish in color, the megaclasts have a gray weathered pattern, and the cliff face in the distance is whitish denoting recent erosion.

descriptions began in 2012 (Figure 4) after Hurricane Irene (2011) at east cove and continued each year between 2015-2018. During that time, we also made multiple aerial orthophoto mosaic images of the Gulf cliff edge and boulder field. Below we describe the data collection methods.

In June 2015 before Hurricane Joaquin, aerial photographs were acquired by a camera mounted on a kite that was flown above the Gulf site. Overlapping images were taken using a Canon PowerShot S95 camera with integrated GPS mounted on a Brooxes KAP Delux gondola, carried on an Into-the-Wind Parafoil 10 kite. The gondola uses a servo to trigger the camera mechanically, controlled by an operator using a four channel Futaba 4YF RC transmitter and receiver, operating in the 2.4 GHz range. The camera was stabilized by a three-axis gimbal and

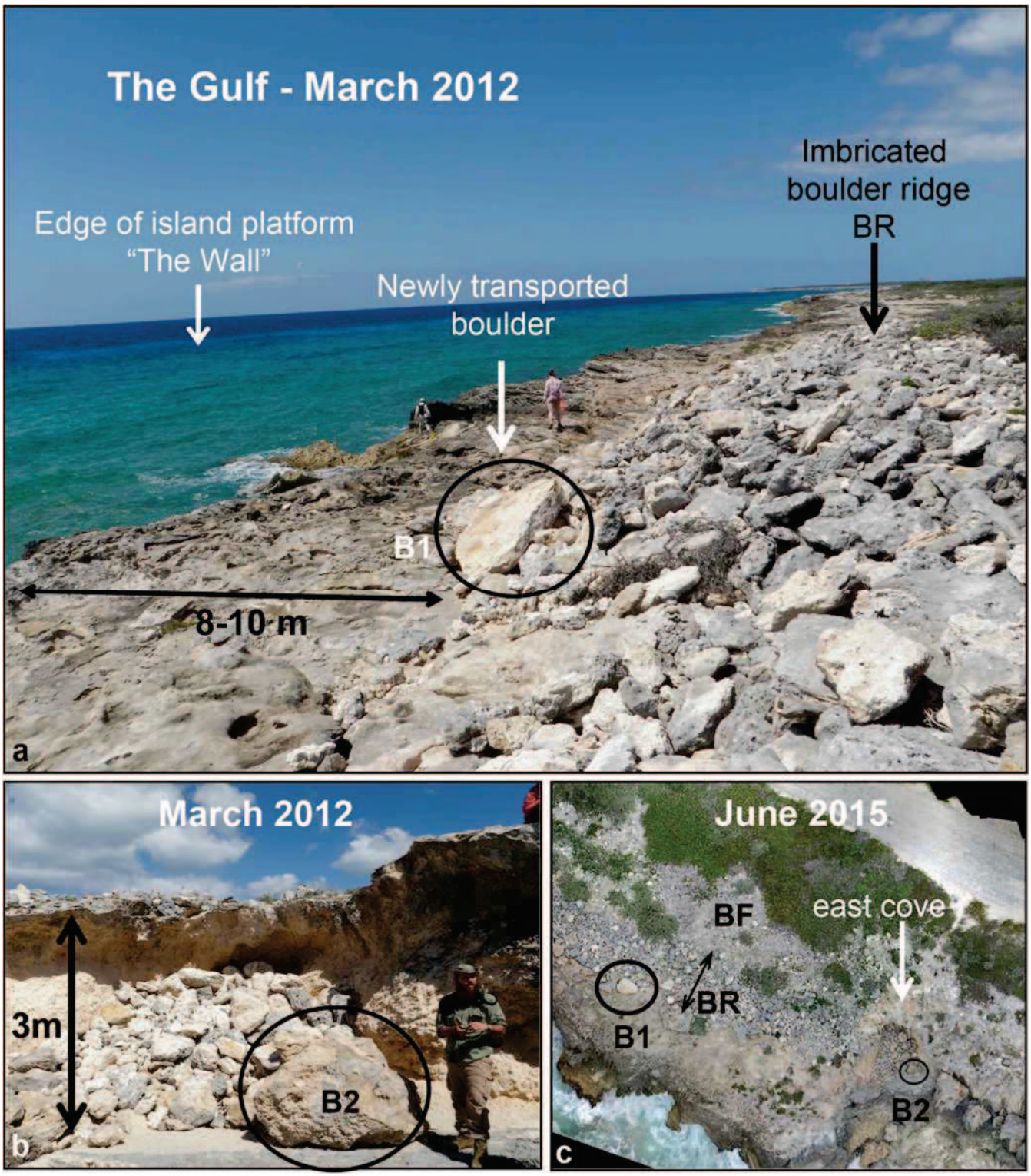

Figure 4. Photographs of the Gulf site prior to Hurricane Joaquin. a) View west along the boulder ridge showing imbricated boulders and freshly transported boulders with light color. Large Boulder B1 can be identified in aerial image shown in Fig. 4c. b) View north of the east cove showing accumulation of boulders at the base of the cliff. Note location of Boulder B2. c) Kite camera aerial photograph of the east cove showing the boulder ridge complex with the ridge (BR) and an inland boulder field (BF). Boulders B1 and B2 from the ground photos are highlighted.

was set to a 3648 x 2736 resolution with ISO 80, shutter speed 1/1000, and a focal ratio of *f*/6.3. Post-Joaquin aerial imagery was collected in 3/2016, 6/2016, 3/2017, 6/2017, 3/2018, and 6/2019. High-resolution aerial orthophotos were collected using a DJI Phantom 3 Advanced uncrewed aerial vehicle (UAV) mounted with a 12 Megapixel, 4K video camera. We preprogrammed flight paths designed to acquire 70% image overlap using a smartphone app designed by Pix4D. In 2018, ground control points (GPC) were placed at strategic locations along the drone flight path and RTK GNSS points were established at each of the GPC using Emlid RS2 antennae receivers. All kite camera and UAV photographic data were processed using Agisoft Metashape to render a high-resolution, digital orthophoto mosaic image. Georeferenced digital elevation models (DEM) were also created by identifying coordinates of stationary points, such as the corner of megaclasts within the imagery field and with GPCs.

Boulder composition, dimensions, and orientation as well as identification of individual boulders at the Gulf boulder field were vital in assessing the wave action and directionality of pre- and post-hurricane boulder movement along the bedrock platform and at the cliff face and base. Prior to Hurricane Joaquin, field data were documented with a tape measure, Brunton compass, and camera. Subsequently, data were collected using a smart phone application, Fieldmove Clino, designed for rapid geologic georeferenced data acquisition. Using the internal compass, GPS, and built-in sensors of the smart phone, the orientation of over 150 individual boulders was acquired, paying special attention to flow directions in the coves and cliff reentrants. This application also allowed the capture of geotagged scaled images of over 30 individual boulders used to verify both size measurements of these boulders, and can potentially serve as good boulder identification markers for any future boulder transport monitoring.

And finally in June 2017, we conducted an underwater scuba dive survey of the subtidal zone at the Gulf site. The purpose of the dive was to inventory the seafloor conditions adjacent to the boulder ridge complex. Two divers entered the ocean at the east cove location and photographed the smooth bedrock, boulders, reef rubble, and patch reefs on the seafloor at various depths along a 30 m transect to water depth of about 20 m.

RESULTS

Coastal Boulder Complex Before Hurricane Joaquin

In March 2012, our ground survey documented the presence of a ridge of imbricated boulders parallel to the rocky southern coast of San Salvador Island at the Gulf site. The boulder ridge is located on top of a bedrock platform that lies above a ~3-m-high sea cliff (Figure 4). Prior to Hurricane Joaquin, the boulder ridge deposit was about 2 m in height and approximately 10 m in width. The seaward edge of the boulder ridge was located 8-10 m landward of the bedrock platform cliff edge and is marked by a few coastal scrub plants. Landward of the boulder ridge was a boulder field that extended about 10-20 m inland (BF in Figure 4). The boulder field was only sparsely vegetated, and the inland limit is shown in Figure 5. The combined boulder ridge and boulder field are defined by Morton *et al.* (2008) as a boulder ridge complex.

The composition of the boulder ridge and boulder field is of locally directed slabs of bedrock and cliff-derived boulders along with smaller offshore cobbles and pebbles. The fresh, unweathered surfaces, i.e., lacking a gray weathering veneer, on several boulders within and at the front of the imbricated boulder ridge in March 2012 (Figure 4), indicated that they had been recently transported by storm waves. One boulder that we measured in 2012 with a long dimension of 2.5 m slid about 50 cm landward in Hurricane Irene exposing unweathered bedrock beneath (Rose *et al.* 2017). Rose *et al.* (2017) report a boulder with a long dimension of 30 cm residing directly on vegetation located 18 m inland along an azimuth of 300°. Multiple white unweathered surfaces on clasts in the boulder ridge and boulder field indicate that individual cobbles and boulders are actively transported across the boulder ridge complex.

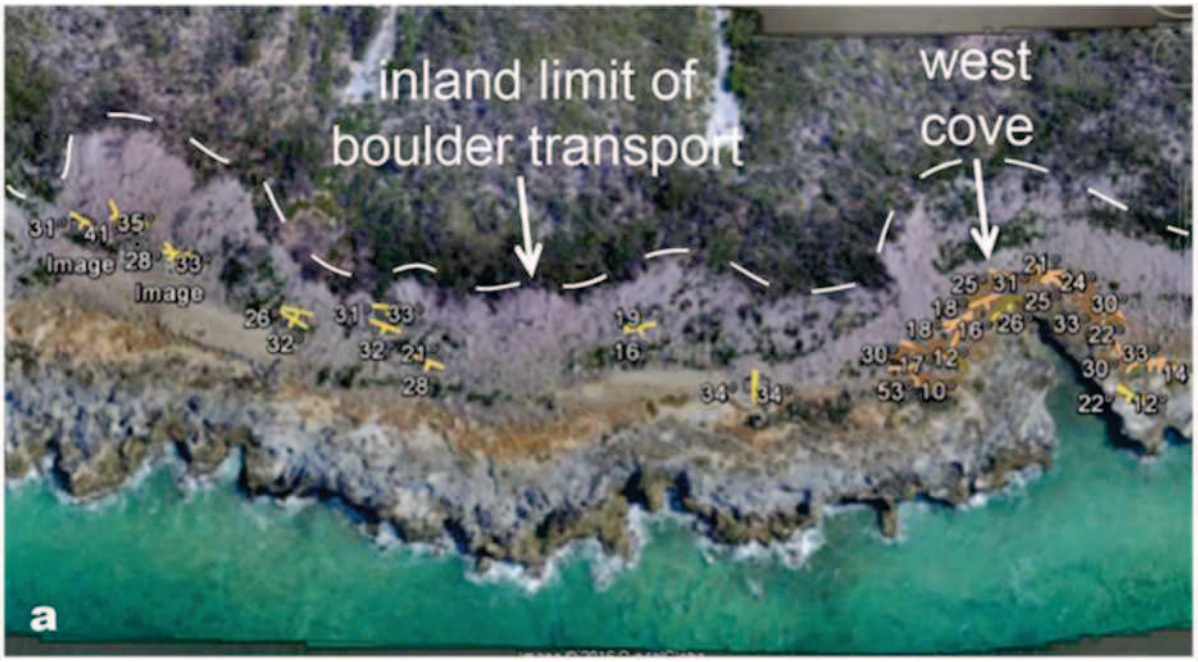

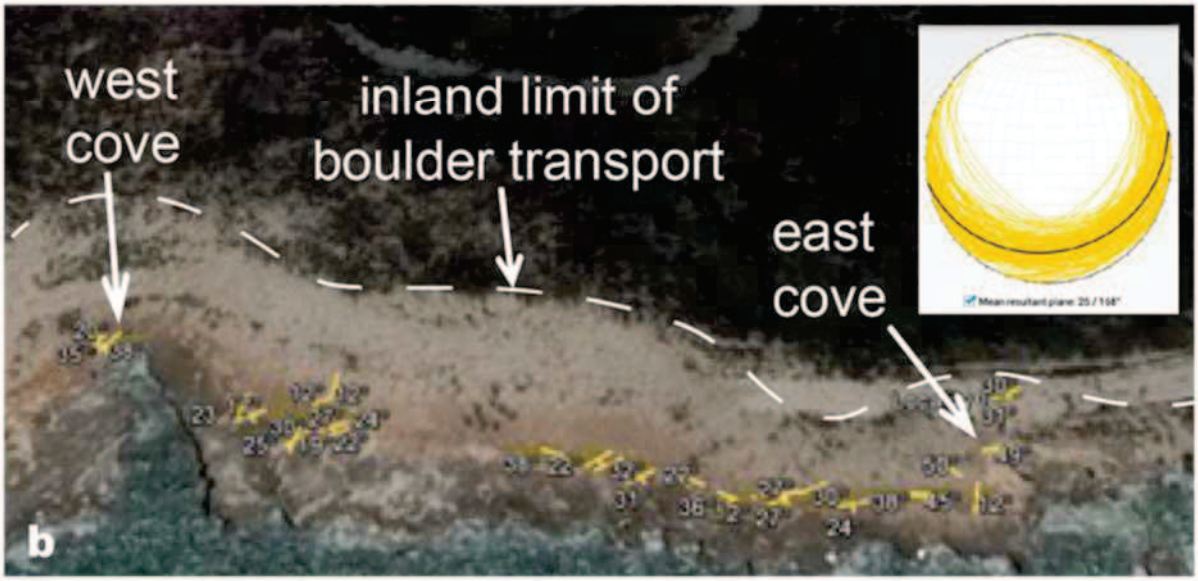

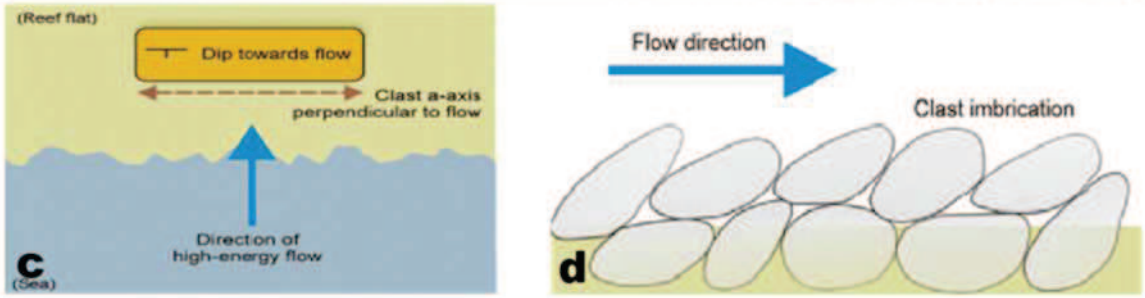

Figure 5. Aerial images marking the inland extent of boulder field transport at the Gulf after Hurricane Joaquin (2015) and shown on the west (a) and east (b) side, respectively, with the west cove in each image. The strike and dip of >100 imbricated boulders is shown along with a stereonet plot of the data collected in March 2018. c) Sketch map shows the long axis of a boulder will align perpendicular to the flow direction and will dip toward the seaward. d) Boulders imbrication in cross section showing clasts stacked and dipping toward the flow direction (Figures 5c and 5d from Terry et al., 2013).

Transport and Deposition of the Boulder Field in Hurricane Joaquin

In the 2015 Hurricane Joaquin, the boulder ridge moved inland, blocked access to the coastal road, and created a larger boulder field that extended ~ 50 m north of the cliff edge. The road running parallel to the shoreline was heavily damaged during Hurricane Joaquin. The boulder field was so thick and wide that the road had to be detoured around it. Coastal shrubs which grew along the backstop of the boulder ridge were uprooted, stripped of foliage, and entrained in the sandy cobbly boulder mobilization. The seaward edge of the boulder field has the largest imbricated clasts and landward edge is a 1.4 m-thick-deposit of poorly sorted cobble breccia. The boulder field can be separated into three lobes or washover fans. Two of these debris lobes are located landward of reentrants or coves that are developed at a high angle to the shoreline cliff face. Because of the poor sorting of most of the boulder deposits in the debris field, imbrication is not pervasive. Although some weathered clasts are present (ones with weathered gray surfaces or reddish with paleosol material), there appear to be an abundance of clasts that have new exposure surfaces without significant evidence of surface weathering. This suggests that the clasts were newly formed from erosional processes. Additionally, erosion of a partially cemented, buried boulder breccia likely provided clasts that moved as debris in the washover fans.

At the seaward edge of the boulder field is a new imbricated boulder ridge composed of large bedrock slabs. The long axis of elongated boulders tends to orient perpendicular to the flow direction and the intermediate axis dips toward the flow direction (e.g. Terry *et al.* 2013). Therefore, measurement of the boulder orientation and imbrication direction can be used to infer the flow direction. Imbricated clasts have a mean dip direction toward an azimuth of 168° (Figure 5). It is clear from our high-resolution imagery time series that high-energy waves routinely sweep above the cliff and have moved cobbles and boulders, but Hurricane Joaquin waves approached from the south-southeast.

Composition and Origin of Clasts

The types of clasts within the boulder field and former imbricated boulder ridge are derived from five main sources and have different transport trajectories. These include: 1) intertidal and subtidal bioclastic material, 2) newly detached and transported boulders from the clifftop, 3) cliff-derived rockfall that is remobilized, 4) boulder ridge breccia, and 5) anthropogenic debris from flotsam and jetsam and local road construction material.

Bioclastic sand, pebbles, and cobbles that are rounded and include coral fragments and shells were deposited around the boulders in the accumulated boulder field. This sediment was also deposited in the hollows or depressions of newly detached slabs (Figure 6). This subtidal sand and gravel are mostly well rounded and sometimes polished showing evidence of prolonged transport within the high-energy surf zone. The beach at the base of the bedrock coastal cliff is a very narrow beach and widens into reentrants or coves along the cliff face. From our observations, sediment of grain sizes smaller than boulders (<25 cm) is not abundant at these beach settings. Our scuba survey conducted in June 2017 in the shallow subtidal zone at the Gulf revealed locations of offshore sediment production and storage. In <10 m water depth, there are subrounded cobbles and boulder and coral fragments in low-lying areas of the wave-cut platform, which may preserve the spur and groove morphology of the underlying fossil reef (Figure 7). In other places, there is a smooth, nearly sediment-free seafloor that appears like an egg carton, with multiple pothole-like depressions scattered across the sea floor. There are a few subrounded boulders in the pothole-like lows (Figure 7). In water depths >12 m, there are active patch reefs that are surrounded by coral rubble and sand. Clasts on the seafloor appear to have a sparse amount of green algae growing on them.

New boulder slabs were clearly dislodged from the top of the bedrock cliff in the storm (Figure 6). The slab thickness of these boulders is controlled by bedding planes of the cross laminated eolianites bedrock. The thickness of the detached slabs is generally 10-30 cm (c-axis). The

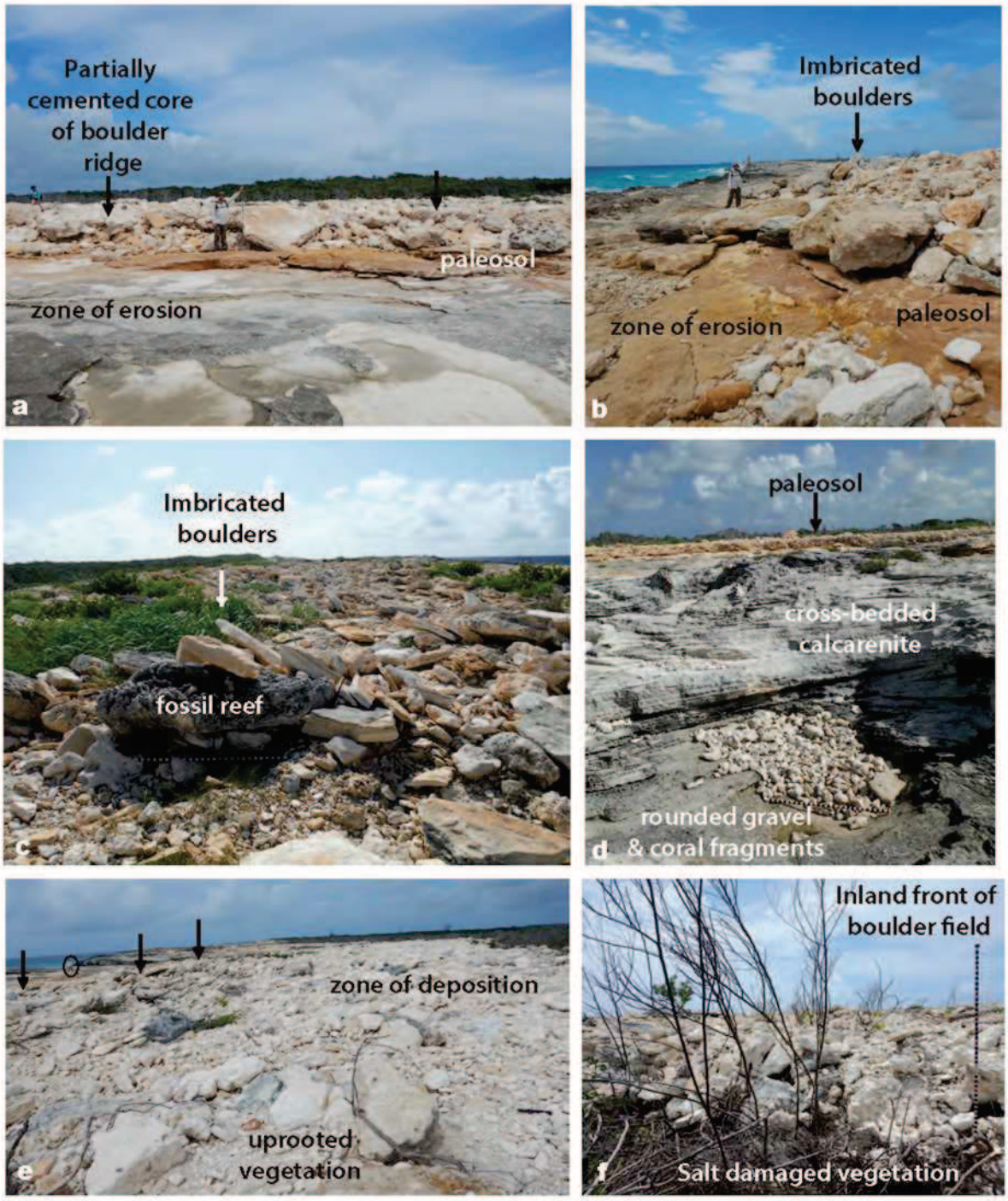

Figure 6. Erosion and deposition of clasts by Hurricane Joaquin at the Gulf site. a) The zone of erosion is characterized by large boulder slabs that have been plucked from the bedrock platform and moved inland to a new ridge. Erosion also exposed the core of the former boulder ridge and the terra rosa paleosol. b) Boulders, some with a long axis >2m, form the edge of a new imbricated boulder ridge inland of the former location. c) A few boulders are of the fossil coral reef and originated at sea level. Newly-formed boulders from the eolianite are imbricated and blade shaped. d) Photograph showing an eroded section through the cross-bedded calcarenite and newly-exposed paleosol and breccia. Rounded clasts and coral fragments have collected in a small cliff reentrant about 1.5 m below the top of the platform. e) Photographic view to the west of the boulder field showing an unsorted sandy gravel deposit that is 40-50 m wide. Arrows point to the shoreward edge of a new imbricated boulder ridge. f) The inland front of the boulder field is about 1.5 thick and terminated in coastal vegetation. Photographs in Fig. 6a, 6b, 6e, 6f are from March 2016, and Fig. 6c and 6d are from June 2016. Pole in photos has markers every 2 cm.

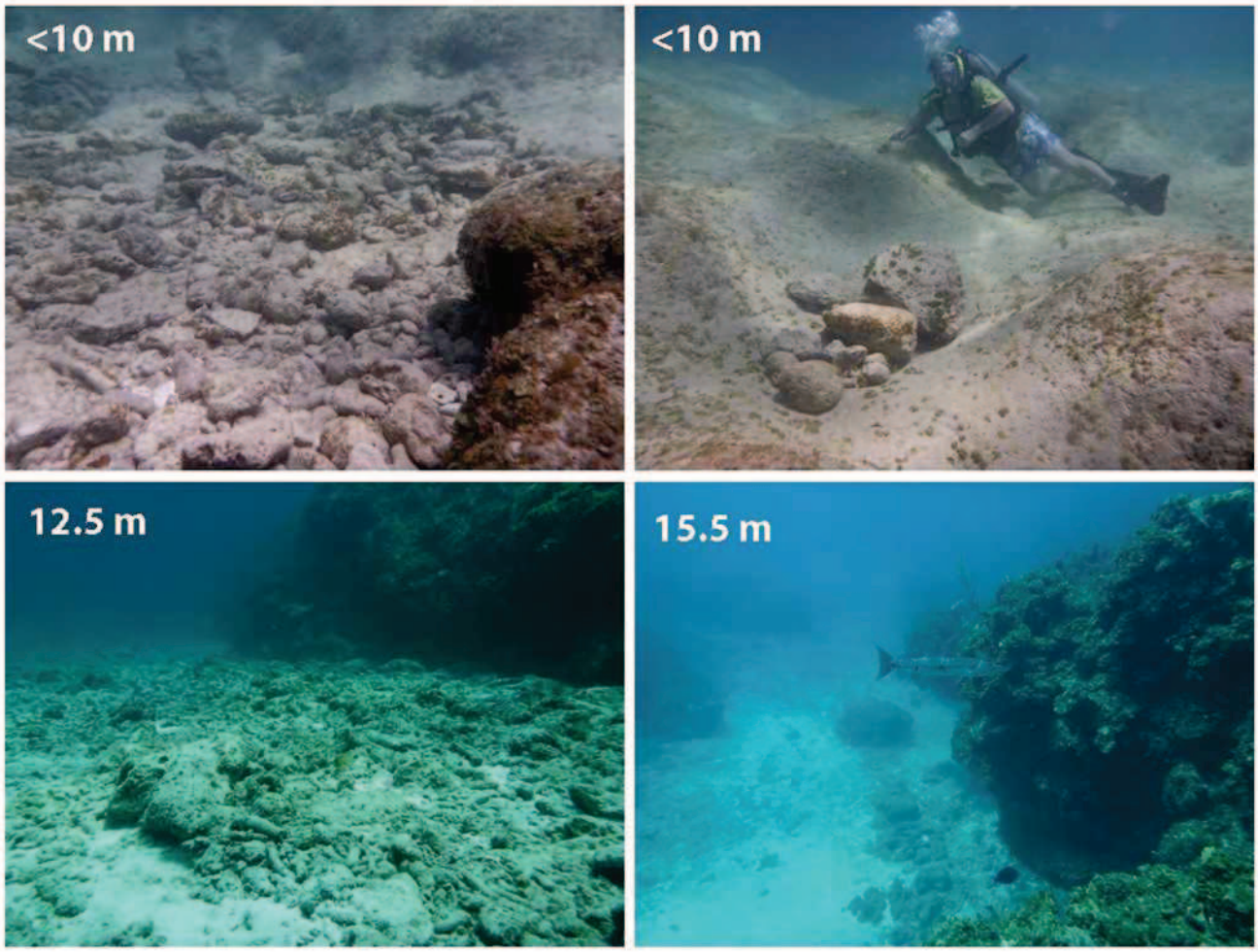

Figure 7. Underwater photographs from June 2017 of the subtidal zone at the east cove of the Gulf site. In <10 m water depth, there are subrounded boulder and coral fragments in low-lying areas of the wavecut platform. Spur and groove topography on the seafloor may be remnants of the underlying fossil reef bedrock. Some areas are completely swept clean of sediment except a few subrounded boulders in pothole-like lows. In water depths >12 m and ~40 m from the intertidal zone, patch reefs are surrounded by sand and coral rubble. Underwater photographs by Jamie R. Stevens, University of Exeter, United Kingdom.

long dimension (a-axis) of these new slabs is on average <1 m and rarely exceeds 2 m. Detachment of new boulders requires more wave energy than in boulder transport (e.g., Terry *et al.* 2013).

Other boulders are derived from cliff erosion and rockfall. Sections of the cliff have collapsed downward to the intertidal zone and have created megaclasts which are boulders with an intermediate b-axis greater than 4.1 m in the modified Udden-Wentworth classification system of Terry and Goff (2014). Cliff-derived Pleistocene calcarenite boulders that are extensively bioturbated with root casts are derived from the uppermost part of the paleodune and are mostly blocky and equant and range from cobbles to boulders with maximum length <2 m in size. Boulders of Pleistocene fossil coral reef from the modern wave-cut platform at sea level are also found, albeit rarely, as clasts with long axes of >1 m.

Erosion of the boulder field in Hurricane Joaquin reveals that the active boulder ridge and boulder field lies above a partially cemented approximately 1.5 m-thick boulder breccia (Figure 6). The boulder breccia deposits were exposed (Figure 6) and provided a large number of clasts for mobilization in the boulder field movement in Hurricane Joaquin.

The Gulf boulder field lies between two topographical highs that mark late Pleistocene

sand dune ridges. When the road was constructed, the bedrock of these high topographic positions was excavated. The road outcrops display excellent crossbedding of sand dunes. It is possible and even probable that part of the clastic accumulation at this site is anthropogenic material deposited during road construction. The deposit is mostly devoid of cultural debris, flotsam and jetsam, that have been prevalent in other hurricane deposits on the island. The storm surge likely elevated the wrack line with the inland run-up and inundation elevation much farther inland than surveyed in this study.

Zone of Erosion

When the boulder ridge was moved inland, it left an exposure of the top of the carbonate bedrock platform showing three zones. This includes an area where new clasts were plucked from the outcrop, exposures of the reddish-colored paleosol, and a cross-section of a partially cemented breccia. New boulder slabs were clearly dislodged from the top of the bedrock cliff in the storm. The slab thickness of these boulders is controlled by bedding planes of the cross laminated eolianites bedrock and is generally 20-30 cm (c-axis). The dimensions of these new slabs are on average 1-2 m and are likely controlled by an orthogonal joint pattern. The long dimension (a-axis) in most cases does not exceed 2 m. In the Zingg particle shape diagram (Zingg 1935), these would be classified as blades or discs. The largest detached boulder slabs appear to have slid. If detachment of new boulders requires more wave energy than in boulder transport (e.g., Terry *et al.* 2013), then this observation is therefore quite significant. The second exposed zone is the base of a reddish-colored paleosol that appears on the top of the bedrock. Mylroie and Carew (2010) call this the terra rossa surface. This is exposed at other locations on the island and is used to identify Pleistocene from Holocene rocks. The new emergence of this 3-4-m-wide paleosol surface suggests that this bedrock area has not been recently or even previously exposed, indicating the uniqueness of Hurricane Joaquin. Some of the cobbles and boulders that have been transported are coated in reddish-colored paleosol suggesting these clasts have not moved for a long time. Finally, the hurricane exposed a stratigraphic section of the boulder ridge and boulder field interior (Figure 6a) that shows the recent cobble and boulders overlie a weakly cemented cobbly boulder breccia. Boulders of breccia are also found in the boulder field.

Monitoring of the cliff face shows that two separate reentrants or coves have formed that we call east cove and west cove (Figure 5). The eastern cove is growing along an azimuth of 325°. East cove was highly eroded during the 2015 Hurricane Joaquin from a perimeter of 31 m and an area of 45 m^2 in 2015, to a perimeter of 46 m and an area of 103 m^2 as observed in March 2016. This erosion occurred through the fracturing of the bedrock cliff surrounding the cove forming into boulders at the cliff base and transported inland (Figure 8). The east cove has continued to grow through jointing and cliff wall collapse as well as wave action. In 2018, the east cove had a 48 m perimeter and was 112 m^2 in area.

Similarly to east cove, west cove is growing along a strike of 325°. Figure 9 shows that there is a conjugate fracture with a strike of 35°. Cliff collapse follows the dominant joint directions and occurred mostly with wave action in Hurricane Matthew (2016). The perimeter and area of the west cove were 152 m and 842 m^2, respectively, in 2014 as observed through satellite imagery. UAV data of the west cove was collected in 2018 and compared to satellite imagery which shows an increase of perimeter to 169 m and the area to 942 m^2. The increase in size is the result of wave activity eroding underlying material creating undercut bedrock beyond the material's angle of repose. Additionally, a significant amount of overhanging bedrock was observed in 2018, which will quickly lengthen and widen the western cove in the near future or during the next hurricane event.

DISCUSSION

The large tsunamis generated in the subduction zone earthquakes in Indonesia in 2004 and Japan in 2011 stimulated an increase in coastal hazards studies from extreme marine

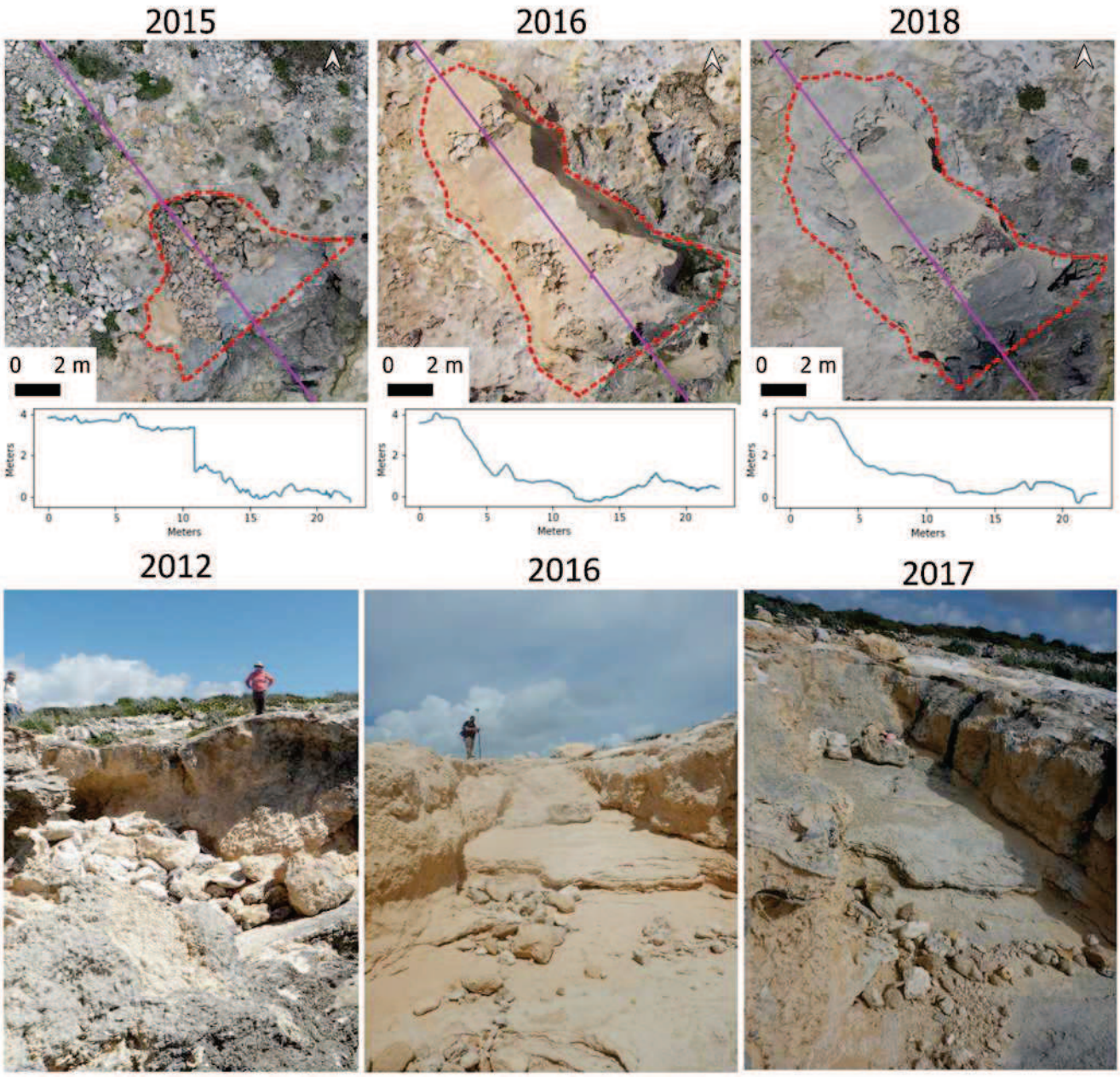

Figure 8. High-resolution kite camera (6/2015) and UAV (2016, 2018) images of the east cove showing the erosion and lengthening of the reentrant (top) and changes to the topographic profiles (middle) before and after Hurricane Joaquin (10/2015). The lower photographs show the boulders accumulated at the cliff base in 2012 (left) and the transport of the boulders up to the platform and erosional elongation of the cove in 2016 (middle). The 2017 photo shows that gray weathering on the bedrock occurs within 2 years. Hurricane Mathew (2016) deposited a buoy and moved boulders. The large boulder at the top of the cliff and the one at the base did not move.

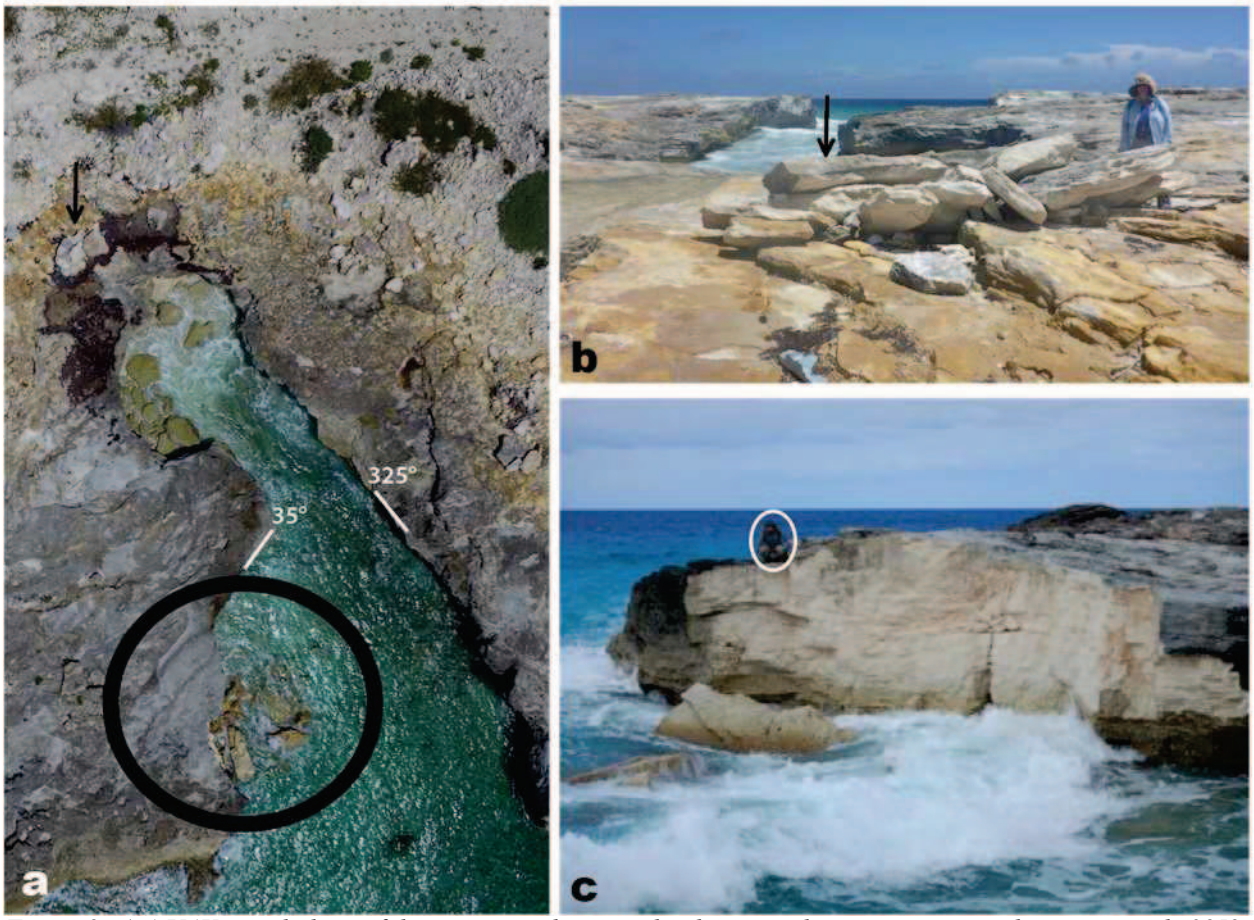

Figure 9. a) A UAV aerial photo of the west cove shows its development along a joint oriented approximately 325°. A second conjugate joint direction is 35°. The arrow points to imbricated boulders deposited in Hurricane Joaquin (2015) and the circle highlights the location of cliff collapse. B) Imbricated boulders deposited at the landward edge of the cove. c) Image of the west side of the cove showing a fresh face of exposed strata and megaclasts in the intertidal zone. The cliff collapsed sometime between June 2017 and March 2018. Oval around a person squatting.

inundation events and has spawned debate as to whether coastal boulder deposits are the result of storm or tsunami waves. Numerous coastal studies around the world published between 2004-2020 interpreted megaboulders to have been transported by tsunamis based on the hydrodynamic equations presented by Nott (2003a, b). The equations use measured boulder dimensions to determine wave height and discern between tsunami and storm waves.

It has become increasingly clear that there are flaws in using the Nott equations as a determination for tsunamic wave transport (Cox *et al.* 2020). Photographic analyses of coastal boulders before and after North Atlantic winter storms along the Irish coast show that boulders as large as 620 tonnes were transported inland over 200 m and to elevations of 29 m above high water (Cox *et al.* 2018). Boulders are larger than ones that are inferred to only have been transported by tsunami waves elsewhere in the world. Furthermore, Cox *et al.* (2019) use scaled wave-tank experiments to model imbricated coastal boulder deposits and showed that storm waves can move megaclasts. Based on linear wave theory and stability analysis, Weiss (2012) concluded that because of the shorter period and longer duration of storm waves that storms have a greater total energy compared to long-period tsunami waves. He further argued that tsunamis should produce unorganized scattered boulder deposits in a dispersed boulder field as was documented in the 2004 Indian Ocean tsunami (Paris *et al.* 2009), the 2009 South Pacific tsunami (Goff and Dominey-Howes 2011), and the 2011 Tohoku tsunami (Goto *et al.* 2012), and that storms would

produce boulder ridges and boulder clusters. Numerical modeling (Weiss and Diplas 2015; Zainali and Weiss 2015; Weiss and Sheremet, 2017) showed that the initiation of large boulder movement is a function of the surface roughness and slope angle. A summary of the debate as to whether storm-transported coastal boulder deposits can be differentiated from tsunami deposits can be found in Dewey *et al.* (2021). In most cases and unlike tsunami waves, high-energy storm waves are unlikely to carry high suspended load (Dewey *et al.* 2021).

On San Salvador, Niemi (2012) and Niemi *et al.* (2015) originally presented the hypothesis that a boulder with a long axis of 4 m and an estimated weight of 14 metric tons on the small island of Green Cay located along the northwestern edge of Graham's Harbour (Figure 1) was transported in a tsunami. However, analyses of aerial imagery before and after Hurricane Frances show that the boulder was transported by wave action in the 2004 storm, and subsequent analyses of our high-resolution aerial imagery helped show how coastal reentrants focus wave action, stage cliff collapse boulders, and result in landward movement of boulders (Niemi 2017; Nolan and Niemi 2020). Boulder movement from the storm surge of Hurricane Frances (2004) was documented at the Gulf site on the south side of San Salvador Island by Niemi *et al.* (2008), and the sliding of bedrock boulder slabs were documented after Hurricane Irene in 2011 (Rose *et al.* 2017).

Our aerial imagery and ground survey data from 2012 and 2015 prior to Hurricane Joaquin revealed the presence of a boulder ridge parallel to the Gulf shoreline on top of a bedrock platform. This site is exposed to high wave energy during most of the year because of the proximity of deep water offshore and the exposed south-southeast windward location. Based on other sites in the Caribbean, linear boulder ridges on top of coastal cliffs and parallel to the shore with imbricated clasts are interpreted to form by transport from high energy waves in successive storms over an extended period of time (Morton *et al.* 2006, 2008; Etienne and Paris 2010). Morton and others (2008) suggested that a coastal boulder ridge is periodically overtopped and makes a boulder field. Together the deposits were defined as a boulder ridge complex (Morton *et al.* 2008). The imbrication of boulders begins because of an obstacle or backstop which can be a steeper slope as demonstrated in wave-tank experiments (Cox *et al.*
2020). Our data show that coastal vegetation may provide the backstop for the development of the boulder ridge. In fact, coastal vegetation may be the predominant factor in the development of boulder ridges. Even a relatively small amount of vegetation can serve as the anchor for a large boulder ridge that builds up after the first layer is caught by the vegetation.

Boulder ridge-complex morphologies and crest elevations are largely controlled by the availability of sediments, clast sizes, and the heights of wave run-ups (Morton *et al.* 2008). Boulders move by sliding, rolling, and saltation, respectively, as the velocity of the water flow increases (e.g. Terry *et al.* 2013). The shape of boulder, whether equidimensional, slabs, or rod-shaped, is an important factor in boulder transport and helps predict whether the boulder will slide and imbricate or roll. The removal of bedrock and formation of boulders through the process of plucking requires higher wave energy than boulder transport (Dewey and Ryan 2017). Hydraulic fracturing plays a dominant role in boulder quarrying from coastal bedrock (Herterich *et al.* 2018).

Structure-from-motion photogrammetry has been used to successfully monitor change in coastal boulder fields, such as along the Irish coast (Nagle-McNaughton and Cox 2020) and in the Philippines (Boesl *et al.* 2019). Sherwood *et al.* (2018) used before and after imagery from the 2016 Hurricane Matthew of a coastal site in Florida and compared it to LIDAR data to determine coastal erosion. Similar to our study, Glumac and Curran (2018, 2019) and Glumac *et al.* (2019) have been monitoring the movement of boulders at various sites including the southern rocky high-energy coastline at the Gulf. They photographed and GPS-located boulders before and after hurricane Joaquin and found that 1-3 ton boulders moved up to 26 m inland. This research

team added UAV aerial imagery in January 2016 (Perlmutter *et al.* 2016) and radio frequency identifiers in 2020 (Lu *et al.* 2020). For our study, we have high-resolution aerial imagery from 2012 and 2015-2018 thus allowing us to also monitor the erosional and depositional processes at the Gulf site.

In general parameters that drive the height of storm surge and wave run-up include the conditions of the storm including atmospheric pressure, wind field size, and wind speed, and other factors include storm trajectory, coastline shape, and offshore bathymetry. On San Salvador the storms that caused the most coastal damage were those that passed directly over the island. Hurricane Frances (2004) moved directly over San Salvador from the southeast to the northwest and Hurricane Irene (2011) passed to the south of island. Hurricane Joaquin (2015) passed over the island from the south, but the clockwise turn in the storm path, two-day duration of intense winds, and rogue waves made the storm unique. The extreme wave energy from Joaquin caused the coastal erosion and boulder transport at the Gulf site. Fuhrmann *et al.* (2019) suggest that the storm surge from Hurricane Joaquin was less than that of Hurricane Frances. Our data show that extraordinary wave heights must have been present locally at the Gulf site.

The coastal configuration of the Gulf site also helps to heighten and focus wave energy as shown in Herterich *et al.* (2018). The shelf is very narrow at the Gulf site and deep water is near to the shore which increases the high wave energy, wave height, and wave run-up. A groove and spur seafloor morphology on the shelf at the Gulf documented in our scuba survey likely further focuses flow and amplifies hydrodynamic forces as has been shown, for example, in an elevated Holocene reef platform in Taiwan (Terry *et al.* 2021). Along the coastal cliff, reentrants and coves also focus wave energy as we documented on Green Cay (Niemi 2017; Nolan and Niemi 2020) and on New Providence Island after Hurricane Matthew in 2016 (Rucker *et al.* 2020). Herterich *et al.* (2018) show bathymetric and topographic lows help focus wave energy and help to hydraulically produce boulders.

Our data from the Gulf show that coves form at locations where the bedrock is weakly cemented with extensive rhizolith formation and along coastal extensional fractures. Cliff retreat processes are controlled by a conjugate joint pattern that trend approximately 35° and 325°. Focused wave energy within the coastal reentrants causes a cove to elongate and widen. The development of a wave-cut notch along the intertidal zone undercuts the cliff. Storm wave action within the cove causes the sidewalls of the cove to collapse. The rockfall at the base of the cliff from the collapse produces megaclasts and boulders. Wave action then reduces the size of the boulders and transports them toward the coves where they collect. Boulders act as an abrasive agent to further grind and erode the end and sides of the cove. Boulders in the cove provide a staging ground for clasts that are then transported to the top of the cliff and inland to the boulder ridge by storm surge and wave run-up bores. Some smaller clasts fill gaps in the boulder ridge and others move farther inland to the boulder field. Within two years newly exposed bedrock in the cove that was enlarged in the Joaquin storm surge has a surface veneer of gray weathering. New boulders identified by the freshly eroded white surface are continuously being added to the coastal boulder deposits at the top of the cliff platform.

CONCLUSIONS

There has been heightened research on investigating coastal boulders and applications for quantification of coastal hazards. Mapping the zone of coast boulder ridges and boulder fields can help to determine the inland extent of inundation and the maximum run-up height. Washover fans, debris aprons, and imbricated boulders are used to determine the direction of transport and the angle of approach of storms. New methods to track boulders and image before and after storm boulder fields help to determine the mechanism for the generation and movement of boulders into staging areas, boulder ridges, and boulder fields and limitations to these movements. One of the major challenges that small, low-lying

island nations face is the determination of the likelihood of a potential extreme marine inundation event and whether existing coastal deposits can be used to back-calculate storm wave energy and run-up parameters.

Coastal boulder deposits accumulate on rocky coastlines with high amounts of wave energy. This is most common when there is a combination of open-ocean exposure and steep topography combining to create boulder supply and high wave heights and storm surge. Waves are amplified by these conditions and can create and transport large clasts as the bedrock of the coastline is broken up. Our aerial imagery shows in 2012 that the boulder ridge and boulder field are actively moving boulders based on the clear white, unweathered appearance of the boulders. Waves from the storm surge of the category 3 Hurricane Joaquin (2015) at the Gulf site transported the previously well-defined, shore-parallel boulder ridge landward, exposed the terra rossa paleosol and the internal structure of a partially cemented boulder breccia, eroded boulder slabs from the coastal bedrock platform, and deposited a new boulder field ~50 m inland of the cliff edge. As confirmed from sea-state modeling of Hurricane Joaquin (Fedele *et al.* 2017; Bell and Kirtman 2021), wave heights may have been in excess of 14 m along at the Gulf site on the southern rocky shore of San Salvador.

ACKNOWLEDGEMENTS

This research was performed under a permit issued by The Bahamas Environment, Science, and Technology Commission to Niemi. We would like to thank Dr. Troy Dexter, director of the Gerace Research Center, and all of the GRC staff for their logistical support. We would also like to acknowledge the help of Jamie R. Stevens in leading the scuba dive survey at the Gulf site in 2017 and for underwater photography. Caples and Zapata were funded through University of Missouri-Kansas City's SEARCH and SUROP undergraduate research grants.

LITERATURE CITED

Avila, L., and Cangialosi, J., 2011, Hurricane Irene, 21–28 August 2011: *NOAA National Hurricane Center Tropical Cyclone Report*, AL092011, 36 p.

Avila, L., Stewart, S.R., Berg, R., and Hagen, A.B., 2020, Hurricane Dorian, 24 August-September 2019: *NOAA National Hurricane Center Tropical Cyclone Report*, AL052019, 74 p.

Bell, R., and Kirtman, B., 2021, Extreme environmental forcing on the container ship SS El Faro: *Journal of Operational Oceanography*, v. 14, no. 2, p. 98-113.

Berg, R., 2016, Hurricane Joaquin - 28 September - 7 October 2015: *NOAA National Hurricane Center Tropical Cyclone Report*, AL112015, 25 p.

Beven II, J.L., 2005, Hurricane Frances 25 August – 8 September 2004: *NOAA National Hurricane Center Tropical Cyclone Report*, AL062004, 30 p.

Bhatia, K.T., Vecchi, G., Knutson, T.R., Murakami, H., Kossin, J., Dixon, K.W., and Whitlock, C.E., 2019, Recent increases in tropical cyclone intensification rates. *Nature Communications*, 10, Article number: 3942.

Boesl, F., Engel, M., Eco, R.C., Galang, J.B., Gonzalo, L.A., Llanes, F., Quiz, Ev., and Brückner, H., 2019, Digital mapping of coastal boulders—high resolution data acquisition to infer past and recent transport dynamics: *Sedimentology*, doi: 10.1111/sed.12578.

Cangialosi, J.P., Latto, A.S., and Berg, R., 2021, Hurricane Irma – 30 August - 12 September 2017: *NOAA National Hurricane Center Tropical Cyclone Report*, AL112017, 111 p.

Caples, S.M. and Niemi, T.M., 2018, Comparing Hurricane Matthew (2016) and Hurricane Joaquin (2015) boulder transport on San Salvador Island, The Bahamas: *Geological Society of America Abstracts with Programs*. Vol. 50, No. 4, doi: 10.1130/abs/2018NC-313107

Caples, S.M., Niemi, T.M., Nolan, J., Rucker, J., Moore, L., and Grady, J., 2019, High-resolution imagery of boulder field movement in Hurricanes Irene (2011), Joaquin (2015), and Matthew (2016) on San Salvador, The Bahamas: *3rd Joint Symposium on the Natural History and Geology of The Bahamas,* Gerace Research Centre, San Salvador, The Bahamas, June 8-12, 2019.

Cox, R., Ardhuin, F., Dias, F., Autret, R., Beisiegel, N., Earlie, C.S., Herterich, J.G., Kennedy, A., Paris, R., Raby, A., Schmitt, P., and Weiss, R., 2020, Systematic review shows that work done by storm waves can be misinterpreted as tsunami-related because commonly used hydrodynamic equations are flawed: *Frontiers in Marine Science*, doi: 10.2289/fmars.2020.00004.

Cox, R., O'Boyle, L., and Cytrynbaum, J., 2019, Imbricated coastal boulder deposits are formed by storm waves, and can preserve a long-term storminess record: *Scientific Reports*, doi.org/10.1038/s41598-019-47254-w.

Cox, R., Jahn, K.L., Watkins, O.G., and Cox, P., 2018, Extraordinary boulder transport by storm waves (west of Ireland, winter 2013-2014), and criteria for analysing coastal boulder deposits: *Earth-Science Reviews*, v. 177, p. 623-636.

Curran, H.A., Schultz-Baer, M., Durkin, K., and Glumac, B., 2012, Recovery of carbonate sand beaches on San Salvador island, Bahamas from damage by Hurricane Frances (2004), *in* Gamble, D.W., and Kindler, P., eds., *Proceedings of the 15th Conference on the Geology of the Bahamas and Other Carbonate Islands*: San Salvador, Bahamas, Gerace Research Centre, p. 1-14.

Curran, H.A., Delano, P., White, B., and Barret, M., 2001, Coastal effects of Hurricane Floyd on San Salvador Island, Bahamas, *in* Greenstein, B.J., and Carney, C.K., eds., *Proceedings of the 10th Conference on the Geology of the Bahamas and Other Carbonate Islands*: San Salvador, Bahamas, Gerace Research Centre, p. 1-12.

Daehne, A., and Niemi, T.M., 2010, Changes in vegetation and coastal morphology on San Salvador, Bahamas following Hurricane Frances in 2004, *in* Siewers F., and Martin, J.B., eds., *Proceedings of the 14th Conference on the Geology of the Bahamas and Other Carbonate Islands*: San Salvador, Bahamas, Gerace Research Centre, p. 42-52.

Dewey, J.F., Goff, J., and Ryan, P.D., 2021, The origins of marine and non-marine boulder deposits: a brief review: *Natural Hazards*, v. 109, p. 1981-2002.

Dewey, J.F., and Ryan, P.D., 2017, Storm, rogue wave, or tsunami origin for megaclast deposits in western Ireland and North Island, New Zealand?: *Proceedings of the National Academy of Sciences*, www.pnas.org/cgi/doi/10.1073/pnas.1713233114.

Dick, J.C., and Cartright, G.R., 2011, Assessment of the Hurricane Frances storm surge on San Salvador, *in* Baxter, J.A., and Cole, E.S., eds., *Proceedings of the 13th Conference on the Natural History of the Bahamas and Other Carbonate Islands*: San Salvador, Bahamas, Gerace Research Centre, p. 59-63.

Etienne, S., and Paris, 2010, Boulder accumulations related to storms on the south coast of the Reykjanes Peninsula (Iceland): *Geomorphology,* v. 114, p. 55-70.

Fedele, F., Lugni, C., and Chawla, A., 2017, The sinking of the El Faro: Predicting real world rogue waves during Hurricane Joaquin: *Scientific Reports*, v. 7, no. 1, doi:10.1038/s41598-017-11505-5.

Fuhrmann, C.M., Wood, K.M., and Rodgers, J.C., Assessment of storm surge and structural damage on San Salvador Island, Bahamas, associated with Hurricane Joaquin (2015): *Natural Hazards,* v. 99, p. 913-930.

Gamble, D. W., Brown, M. E., Parnell, D., Brommer, D., and Dixon, P. G., 2000, Lessons learned from Hurricane Floyd damage on San Salvador: *Bahamas Journal of Science*, v. 8, p. 25-31.

Garver, J., 1996, Some effects of Hurricane Lili (Oct 1996) on San Salvador Island, Bahamas. Retrieved 13 April 2022 from https://idol.union.edu/garverj/Geo35/hurricane/Damage.htm.

Glumac, B., Miguel, U., and Curran, A.H., 2019a, New advances in long-term monitoring of storm-deposited boulder ridges along rocky shorelines of San Salvador Island, Bahamas: *3rd Joint Symposium on the Natural History and Geology of The Bahamas*, Gerace Research Centre, San Salvador, The Bahamas, June 8-12, 2019.

Glumac, B., and Curran, A.H., 2019b, Generation and transport of large rock boulders by storm wavs along the high-energy southern coast of San Salvador Island, Bahamas: *3rd Joint Symposium on the Natural History and Geology of The Bahamas*, Gerace Research Centre, San Salvador, The Bahamas, June 8-12, 2019.

Glumac, B., and Curran, A., 2018, Documenting the generation and transport of large rock boulders by storm waves along the high-energy southern coast of San Salvador Island, Bahamas: American Geophysical Union, Fall Meeting 2018, abstract #EP23C-2296.

Goff, J., and Dominey-Howes, D., The 2009 South Pacific Tsunami: Earth-Science Revies, v. 107, doi:10.1016/j.earscirev.2011.03.006.

Goto, K., Sugawara, D., Ikerma, S., Miyagi, T., 2012, Sedimentary processes associated with sand and boulder deposits formed by the 2011 Tohoku-oki tsunami at Sabusawa Island, Japan: *Sedimentary Geology*, v. 282, p. 188-198.

Herterich, J.G., Cox, R., and Dais, F., 2018, How does wave impact generate large boulders? Modeling hydraulic fracture of cliffs and shore platforms: *Marine Geology,* doi: 10.1016/j.margeo.2018.01.00.

Kossin, J.P., Knapp, K.R., Olander, T.L., Velden, C.S., 2020, Global increase in major tropical cyclone exceedance probability over the past four decades: *Proceedings of the National Academy of Sciences*, v. 117, no. 22, p. 11,975-11,980.

Latto, A., Hagen, A., and Berg, R., 2021, Hurricane Isaias – 20 July - 4 August 2010: *NOAA National Hurricane Center Tropical Cyclone Report*, AL092020, 84 p.

Li, L., and Chakraborty, P., 2020, Slower decay of landfalling hurricanes in a warming world: *Nature*, v. 587, p. 230-234.

Lu, K., Mugabekazi, V.R., Pharris, G., Atkinson, E., Fischer, N., Gahwagy, R., Holt, C., Harnishch, E., Glumac, B., and Curran, H.A., 2020, Application of drones in monitoring limestone boulder generation and transport by storm waves along rocky shorelines of San Salvador Island, Bahamas: *Geological Society of America Abstracts with Programs*, v. 52, no. 6, doi: 10.1130/abs/2020AM-353424.

McCabe, J.M. and Niemi, T.M., 2008, The 2004 Hurricane Frances overwash deposition in Salt Pond, San Salvador, The Bahamas, *in* Park, L.E., and Freile, F., eds., *Proceedings*

of the 13th Conference on the Geology of the Bahamas and Other Carbonate Islands: San Salvador, Bahamas, Gerace Research Centre, p. 25-41.

Miller, W., and Zhang, D.-L., 2019, Understanding the unusual looping track of Hurricane Joaquin (2015) and its forecast errors: *Monthly Weather Review,* doi:10.1175/MWR-D-18-0331.1.

Morton, R.A., Richmond, B.M., Jaffe, B.E., and Gelfenbaum, G., 2006, Reconnaissance investigation of Caribbean extreme wave deposits—Preliminary observations, interpretations, and research directions: U.S. Geological Survey, Open-File Report 2006-1293, 41 p.

Morton, R.A., Richmond, B.M., Jaffe, B.E., and Gelfenbaum, G., 2008, Coarse-clast ridge complexes of the Caribbean: A preliminary basis for distinguishing tsunami and storm-wave origins: *Journal of Sedimentary Research*, v. 78, p. 624-637.

Mylorie, J.D., and Carew, J.L, 2010, Field guide to the geology and karst geomorphology of San Salvador island. [Publisher unknown], USA.

Nagle-McNaughton, T., and Cox, R., 2020, Measuring change using quantitative differencing of repeat structure-from-motion photogrammetry: The effect of storms on coastal boulder deposits: *Remote Sensing*, v. 12, no. 42; doi:10.3390/rs12010042.

Niemi, T.M., 2012, Tsunami boulders, storm deposits, and sea level variation on San Salvador in the Bahamas: *16th Conference on the Geology of The Bahamas and Other Carbonate Islands*, Gerace Research Centre, San Salvador, The Bahamas, June 14-18, 2012.

Niemi, T.M., Grady, J., and Billingsley, A., 2015, Evidence of a possible tsunami on San Salvador Island, The Bahamas: *1st Joint Symposium on the Natural History and Geology of The Bahamas*, Gerace Research Centre, San Salvador, The Bahamas, June 12-17, 2015.

Niemi, T.M., 2017, Large boulders on Green Cay, San Salvador Island, The Bahamas, in *Proceedings of the 1st Joint Symposium on the Natural History and Geology of The Bahamas,* Landry, C., and Florea, L., (eds.), Gerace Research Centre, San Salvador, The Bahamas, p. 121-129.

Niemi, T.M., Preisberga, A., Rucker, J.D., Nolan, J., and Rose, T.L., 2017, Mapping coastal boulders with an unmanned aerial vehicle (UAV): *Proceedings of the 2nd Joint Symposium on the Natural History and Geology of The Bahamas*, Gerace Research Centre, San Salvador, The Bahamas, June 8-12, 2017.

Niemi, T.M., Thomason, J.C., McCabe, J.M., and Daehne, A., 2008, Impact of the September 2, 2004 Hurricane Frances on the coastal environment of San Salvador island, The Bahamas, *in* Park, L.E., and Freile, D., eds., *Proceedings of the 13th Conference on the Geology of the Bahamas and Other Carbonate Islands*: San Salvador, Bahamas, Gerace Research Centre, p. 42-62.

Nolan, J., and Niemi, T.M., 2020, Detection of boulder transport via storm surge using drone imagery on Green Cay, San Salvador, The Bahamas: *Proceedings of the 2nd Joint Symposium on the Natural History and Geology of The Bahamas,* Niemi, T.M. and Sullivan Sealey, K., (eds.), Gerace Research Centre, San Salvador, The Bahamas, p. 94-102.

Nott, J., 2003a, Waves, coastal boulder deposits and the importance of the pre-transport setting: *Earth and Planetary Science Letters*, v. 210, p. 269-276.

Nott, J., 2003b, Tsunami or storm waves?—Determining the origin of a spectacular field of wave emplaced boulders using numerical storm surge and wave models and hydrodynamic transport equations: *Journal of Coastal Research,* v. 19, p. 348-356.

Nystrom, R.G., Zhang, F., Munsell, E.B., Braun, S.A., Sippel, J.A., Weng, Y., and Emanuel, K., 2018, Predictability and dynamics of Hurricane Joaquin (2015) explored through convection-permitting ensemble sensitivity experiments: *Journal of the Atmospheric Sciences*, v. 75, no. 2, p. 401-424.

Oppenheimer, M., B.C. Glavovic , J. Hinkel, R. van de Wal, A.K. Magnan, A. Abd-Elgawad, R. Cai, M. Cifuentes-Jara, R.M. DeConto, T. Ghosh, J. Hay, F. Isla, B. Marzeion, B. Meyssignac, and Z. Sebesvari, 2019, Sea level rise and implications for low-lying islands, coasts and communities. In: *IPCC Special Report on the Ocean and Cryosphere in a Changing Climate* [H.-O. Pörtner, D.C. Roberts, V. Masson-Delmotte, P. Zhai, M. Tignor, E. Poloczanska, K. Mintenbeck, A. Alegría, M. Nicolai, A. Okem, J. Petzold, B. Rama, N.M. Weyer (eds.)]. Cambridge University Press, Cambridge, UK and New York, NY, USA, pp. 321–445. doi.org/10.1017/9781009157964.006.

Paris, R., Wassmer, P., Sartohadi, J., Lavigne, F., Barthomeuf, B., Desgages, E., et al., 2009, Tsunamis as geomorphic crises: lessons from the December 26, 2004 tsunami in Lhok Nga, West Banda Aceh (Sumatra, Indonesia): *Geomorphology*, v. 104, p. 59–72.

Parnell, D.B., Brommer, D., Dixon, P.G., Brown, M.E., and Gamble, D.W., 2004, A survey of Hurricane Frances damage on San Salvador: *Bahamas Journal of Science*, v. 12, p. 2-6.

Perlmutter, E., Caris, J., Widstrand, A., Curran, H.A., and Glumac, B., 2016, Drone use in rapid assessment of Hurricane Joaquin coastal impact on San Salvador Island, Bahamas: *Geological Society of America Abstracts with Programs.* v. 48, no. 7, doi: 10.1130/abs/2016AM-282290

Preisberga, A., Niemi, T.M., Rucker, J., Nolan, J., Grady, J., and Lamprise, S., 2016, High-resolution UAV imaging and mapping of coastal erosion and boulder movement produced by the 2015 Hurricane Joaquin on San Salvador, The Bahamas: *Geological Society of America Abstracts with Programs.* v. 48, no. 7, doi: 10.1130/abs/2016AM-287520.

Rose, T.L., Moore, L., Preisberga, A., and Niemi, T.M., 2017, Monitoring changes in the coastal environment on San Salvador Island using beach profiling, real-time kinematic GPS surveys, and kite imagery, in *Proceedings of the 1st Joint Symposium on the Natural History and Geology of The Bahamas,* Landry, C., and Florea, L. (eds.), Gerace Research Centre, San Salvador, The Bahamas, p. 131-141.

Rucker, J.D., Niemi, T.M., Nolan, J., and Rose, T., 2020, Aerial photography of coastal erosion and large boulder transport from Hurricane Matthew along Clifton Beach, New Providence Island, The Bahamas, in *Proceedings of the 2nd Joint Symposium on the Natural History and Geology of The Bahamas,* Niemi, T.M. and Sullivan Sealey, K., and (eds.), Gerace Research Centre, San Salvador, The Bahamas, p. 83-93.

Sahoo, S., Jose, F., and Bhaskaran, P.K., 2019, Hydrodynamic response of Bahamas archipelago to storm surge and hurricane generated waves—A case study for Hurricane Joaquin: *Ocean Engineering,* v. 184, p. 227-238.

Sherwood, C.R., Warrick, J.A., Hill, A.D., Ritchie, A.C., Andrews, B.D., and Plant, N.G., 2018, Rapid, remote assessment of Hurricane Matthew impacts using four-dimensional structure-from-motion

photogrammetry: *Journal of Coastal Research*, v. 34, no. 6, p. 1303-1316.

Stewart, S.R., 2017, Hurricane Matthew – 28 September – 9 October 2016: *NOAA National Hurricane Center Tropical Cyclone Report,* AL142016, 82 p.

Stewart, S.R., and Berg, R., 2019, Hurricane Florence – 31 August – 17 September 2018: *NOAA National Hurricane Center Tropical Cyclone Report,* AL062018, 98 p.

Terry, J.P., Lau, A.Y.A., and Etienne, S., 2013, *Reef-Platform Coral Boulders: Evidence for High-Energy Marine Inundation Events on Tropical Coastlines*: Springer Briefs in Earth Sciences, Heidelberg, Germany, 105 p.

Terry, J.P., and Goff, J., 2014, Megaclasts: proposed revised nomenclature at the coarse end of the Udden-Wentworth grain-size scale for sedimentary particles: *Journal of Sedimentary Research*, v. 84, p. 192-197.

Terry, J.P., Lau, A.Y.A, Nguyen, K.A., Liou, Y.-A., and Switzer, A.D., 2021, Clustered, stacked and imbricated large coastal rock clasts on Ludao Island, Southeast Taiwan, and their application to palaeotyphoon intensity assessment: *Frontiers in Earth Science*, doi:10.3389/feart.2021.792369.

UNDRR, 2020, *Human Cost of Disasters: An Overview of the Last 20 Years (2000-2019)*: United Nations Office of Disaster Risk Reduction, 30 p.

Vecchi, G.A., Landsea, Zhang, W., Villarini, G., and Knutson, T., 2021, Changes in Atlantic major hurricane frequency since the late-19th century: *Nature Communications*, v. 12, Article number: 4054.

Weiss, R., 2012, The mystery of boulders moved by tsunamis and storms: *Marine Geology*, v. 295-298, p. 28-33.

Weiss, R., and Diplas, P., 2015, Untangling boulder dislodgement in storms and tsunamis: Is it possible with simple theories?: *Geochemistry, Geophysics, Geosystems,* v. 16, p. 890–898. doi: 10.1002/2014GC005682.

Weiss, R., and Sheremet, A., 2017, Toward a new paradigm for boulder dislodgement during storms: *Geochemistry, Geophysics, Geosystems,* v. 18, p. 2717–2726. doi: 10.1002/2017GC006926

Zainali, A., and Weiss, R., 2015, Boulder dislodgement and transport by solitary waves: insights from three-dimensional numerical simulations: *Geophysical Research Letters*, v. 42, p. 4490–4497, doi: 10.1002/2015GL063712.

Zingg, T., 1935, Beitrag zur Schotteranalyse: *Schweizeriscke Mineralogische und Petrologische Mitteilungen*, v. 15, p. 39–140.

CORAL REEF RESTORATION TECHNIQUES FOR REMOTE AND ISOLATED COMMUNITIES: PART I - LOGISTICS AND PLANNING

John Rollino

Natural Resources and Environmental Permitting, AECOM, New York, NY USA

ABSTRACT

In recent years, there have been notable advances in coral reef restoration demonstrated throughout the world; however, reef restoration can be an expensive endeavor. For countries with substantial financial resources (e.g., United States, Australia, etc.), large-scale restoration efforts can be readily funded; however, for smaller nations, or especially isolated island communities with limited tourism, restoration investment by government or well-funded NGOs is minimal. In response to the observed coral reef decline on San Salvador over the last 25 years, and around the world, a group of scientists and I are attempting to develop low-cost coral reef restoration techniques, targeted for remote and isolate communities. The research is being conducted on the shallow water patch reefs of San Salvador. The research is envisioned to occur in three parts. This paper (Part I) reports on the initial trial runs of underwater construction, overall logistics, planning, and manpower estimates. Parts II and III of this project, which would include rigorous scientific testing, are scheduled to continue over the next four to six years.

INTRODUCTION

In 1992, a long-term coral ecology and bleaching response study was initiated on San Salvador Island (McGrath *et al.* 2007). Based on the reductions in coral coverage observed both on the island and sites worldwide, I, circa 2010, initiated planning for experiments to identify and develop low-cost coral restoration techniques.

The restoration efforts seek to accelerate recovery of coral reef ecological functions and values, lost through mortality and erosion, by increasing the following: species diversity, reef rugosity, and hard substrate surface areas for Scleractinia coral colonization. The research is designed specifically to develop low-cost restoration efforts that could be implemented by indigenous personnel using locally available and/or recycled items.

Coral restoration costs can vary substantially depending on scale, techniques, and regional labor costs. For example, one hectare of restoration in the United States could easily exceed $150,000 USD (Bayraktarov *et al.* 2016). I hope to identify methods and materials to provide similar restoration to a similar area for under $1,000 per hectare (costs assume indigenous personnel volunteering time). A key component of the reef restoration is the transplant of live corals, either harvested (fragmented using a mallet and sanitized chisel) or "rescued" (corals collected after being recently dislodged from the reef to sandy locations). Coral mortality is certain if a dislodged coral is deposited on a sand substrate (Jaap 2000). Using these corals' living tissue as transplant material reduces the reliance on fragmenting healthy corals.

For this study, fragmented donor corals for transplant came from Gaulin Reef, a large reef tract about one mile from the Gerace Research Centre (GRC) and dislodged corals originated from Gaulin Reef, French Bay, Lindsay's Reef, Rice Bay, and Dump Reef (Figure 1).

FIELD SITE DESCRIPTION

Initial logistics and planning experiments were carried out on Rocky Point Reef, with Dump Reef used as a training ground. Rocky Point Reef is located 70-100 meters from shore. Water depths at high tide over the reef measure from 1 – 4 meters. At low tide, the tops of sea fans are often exposed, and water depths are less than 1.5 meters over large portions of the reef. Dump Reef is located approximately 10 meters from shore and

500 meters west of the GRC. Much of the water column above Dump Reef is very shallow (less than 1 meter) and makes an ideal training ground.

The reef restoration experiments were carried out in very shallow-water patch reefs for the following reasons: 1) shallow reefs and wave surge provide challenging logistics; thus, if restoration techniques can be shown as effective, it would suggest that restoration would work in deeper areas; and 2) as shallow water patch reefs are most often encountered by people, mastering reef restoration techniques on these reefs are imperative.

METHODS

Three major components of reef restoration were studied for incorporation into further studies: 1) underwater drilling, 2) construction of rugosity enhancing devices (REDs), and 3) coral transplant techniques.

Underwater Drilling

In order to place REDs, plugs with coral transplants, or other structures on the reef, holes must be drilled into the reef to hold rebar or other supporting elements of the structures. We experimented with different drilling techniques to create holes that varied in width from 0.4 to 1.5 cm in diameter, and from 0.7 to 20 cm in depth.

The first technique used a pneumatic air drill attached to a 15 m length of hose connected to a small air compressor located in a boat. Drilling into the reef surface was attempted using several drill bits, including small masonry bits up to a 1.25 cm diameter, 0.33 m long diamond-tip rock coring bit.

The second method used the same pneumatic drill attached to a pressurized SCUBA tank. The connections between the drill and tank were accomplished using an altered first stage SCUBA air octopus (Figure 2). The regulator was removed and connections were added to accommodate an air drill. The air tank pressure valve was opened in a similar manner to using a SCUBA tank, which powered the drill (using the same bits as previous).

A Nemo V2 Diver's submersible 1.75 cm electric drill was also evaluated. The drill, powered by a 6-volt battery, was used with various drill bits to make an array of holes.

Construction of Rugosity Enhancing Devices

REDs are solid structures designed to increase reef rugosity, provide structures to accept coral transplants, and/or allow for the fixation of tile collection plates. It was envisioned that because of the level of decline of coral reefs and prolific increase in macroalgae, simple transplantation would need to be augmented with the placement of REDs on the reef surface.

REDs were placed by drilling a hole into the reef surface. A piece of rebar was then inserted into the hole packed with marine epoxy. The RED (which contains a similar-diameter hole in the base) was then placed on to the rebar, and the hole filled with marine epoxy or underwater concrete. Within 48 hours, the RED is permanently affixed to the reef.

The RED construction experiments occurred in two phases. The first phase constructed several initial structures to be placed on the reef for a two-year period to determine initial material stability and potential for colonization. The initial structure was a 40 cm by 40 cm square that rested on a base 15 cm in dimeter by 20 cm in height, (Figure 3) all constructed from underwater cement.

After the initial RED was constructed, I experimented with other RED designs using a similar volume of material (Figure 4). The goal was to determine the largest durable branching structure that could be created that would provide adequate surface areas for colonization, areas to attach collection plates, and serve as a platform for the placement of coral transplants.

The preferred prototype structure was a winged or X-shaped structure that was supported above the reef surface by a 9 cm-diameter stalk, 30-40 cm in length. Each wing of the X measured approximately 30 cm in length, with the base of each wing 10 cm in width, tapering to 6 cm in width at the end (Figure 5). Larger variations of this structure were tested; however, the size and weight of larger structures resulted in difficulty maneuvering underwater by hand.

Photo Credit: Google Earth Imagery, 2020

Figure 1, Project research sites.

Figure 2 – SCUBA regulator and hoses modified to power air drill with an air tank.

Figure 3. Initial RED Structure placed on the reef

The structures were constructed using underwater concrete or marine grout. A mold for the structure was dug into the beach sand. Sand within 1 meter of the high-tide line provides enough saturation to retain the mold shape when dug (Figure 6).

Prior to pouring the concrete into the mold, a PVC rod (1.25 cm in diameter) was placed vertically in the middle of the mold. The PVC pipe was covered in clean plastic film (food wrap). After the PVC was placed, the concrete was then mixed and poured into the mold from the bottom up. As the concrete was being poured into the central stalk of the mold, a cylinder of 1.25 cm metal construction mesh, measuring 5 cm in diameter and the length of the stalk, was then inserted into the mold over the PVC pole, leaving at least 1.5

cm of concrete between the PVC and mesh and at least 1 cm of concrete on the outside of the mesh. In addition, metal construction mesh wings cut to approximately 75 percent width of each wing were inserted into the middle of the wing for additional support. The structures were then allowed to dry in the sand for approximately 48 hours, after which the hardened structures were removed by hand. The PVC was then removed, leaving a void in the central portion of the mold to allow for placement on the rebar. The clean film around the pipe allowed the PVC to be easily removed from the mold.

Coral Transplants

I tested a variety of techniques to affix transplanted or rescued corals back on the reef, including tying with cable ties or steel wire, attaching with epoxy, or fastening to ceramic plugs (Figure 7). Coral transplants have been studied, to date, for up to one year after transplant.

Figure 4. Experimental RED designs.

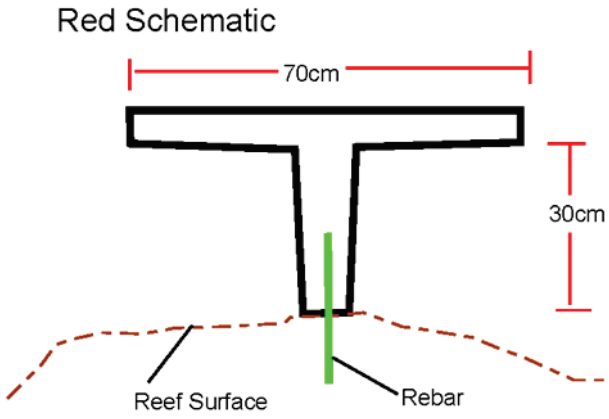

Figure 5. Profile view of RED.

Figure 6. Mold for REDs hand dug in beach sand.

Figure 7. Plug affixed to a piece of rock with a coral.

Coral fragments varying in size from 10 to 40 cm in length were attached to the reef surface and REDs by cable ties. For this method, the fragment was placed parallel to a flat surface and then a cable tie (at least 6 mm in width) was placed to secure the coral fragment to the reef. The use of steel wire was also tested in a similar manner. Steel wire varying in width from 0.5 mm to 2 mm was wrapped around the coral and the reef a number of times until the coral was secure to the reef surface; the wire was then cut and the cut end secured.

The epoxy tested was quick setting, commercially available marine epoxy. Epoxy was first applied to the side of a coral with dead tissue, the coral (with epoxy side facing the reef) was then pressed and held into place for several minutes.

Ceramic plugs (Figure 7) of 1.25 cm length were tested. Ceramic plugs serve as an excellent vehicle to transplant a hard coral to the reef's surface. For each plug, a coral fragment (or rock with attached coral) was set firm on the top ceramic plug with marine epoxy. The plug was placed in a submerged holding platform about 1.5 m below the water surface and 2 m above the bottom in Grahams Harbour in front of the GRC. After being allowed to cure for 24 – 48 hours, the plug was brought to the receiving reef. The coral with plug was then transported out to the reefs and the bottom of the plug was inserted into a pre-drilled hole with marine epoxy

RESULTS

All three drilling techniques proved effective, although, due to wave action in shallow areas, using a boat-mounted small air compressor should only be considered for locations with at least 3 meters of water above the reef surface. Working with a boat over a reef in waters less than 3 meters is not recommended. Wave surge and currents result in difficulty keeping the boat positioned whilst not having the hoses foul on the reef and/or having a vessel avoid isolated rock columns that rise vertically from the reef's surface.

The use of an air tank to drill into the reef worked well. Holes were drilled up to 1.5 cm in diameter and to depth of 20 cm. Use of an air drill did cause some vision obscuration due to bubbles, and the drilling was most efficient when two persons were employed – one person to drill and the other person to hold the tank and watch the air gauge.

For time and manpower estimates, a 1.5 by 15 cm hole can be drilled into the reef in approximately 15 – 30 minutes using 2 – 7 air tanks pressurized to 3,000 PSI. Smaller holes to accommodate coral plugs can be drilled much more quickly. Drilling up to 40 small holes per tank was achieved in testing. The efficiency of the drilling can be increased by obtaining proper fittings with less air leakage.

The electric drill was the most versatile as one person could easily manipulate the drill. The lack of wires, hoses, or additional weight made for the best versatility. With the electric drill, holes large enough to accommodate a coral plug were drilled at the rate of 1 hole per 1 – 3 minutes.

The Nemo electric drill retails for approximately $1,200 USD and may be outside of the price range of many communities; however, as many coastal communities have some association with SCUBA diving operators, the conversion of old SCUBA equipment to accommodate the drill plus the cost of the air drill and drill bits could be as little as $125 USD.

There were large variations in the rate of holes drilled, attributed mainly to working in the shallows where personnel were often hindered by wave surge, currents, drill bits, and air loss from poor connection fittings between the drill and air hose and performing much of the activities using snorkel gear. The use of SCUBA in deeper water produces more drilling efficacy, as wave surge is considerably lessened and divers can exert better physical pressure on the drill.

An initial RED structure did recruit coral colonization within one year of placement on the reef. The other X-shaped structures were placed on Rocky Point reef in an area that appears to be affected by wave action (as there are markedly fewer corals than other portions of the reef) and left for six years. After six years in place, the

structures remained intact, except for two structures that appeared to have suffered a failure of the rebar. During the six-year period, the structures were afflicted by many storms, including Hurricane Joacain which hit San Salvador on September 30 and October 1, 2015 (Rothfus 2016). The hurricane battered the islands with winds of 178.6-207.6 kph (Curran 2016).

The different attachment techniques yielded interesting results. Metal wire, regardless of size or composition was, ineffective. The wire would often rust and break, allowing the coral fragment to become dislodged, sometimes in as little as 10 days. Similar results were documented with thin cable ties as well. The use of epoxy proved to be reliable means of attaching coral, especially when combined with a cable tie. In fact, we documented an instance of the coral growing over the cable tie. Ceramic plugs have worked very well in securing coral fragments to the reef.

Coral transplants have shown good initial success. *Acropora* sp. fragment plugs placed upon old *Acropora* sp. skeletons using either ceramic plugs or marine epoxy and cable ties had a 90 percent survival and averaged 8 percent new tissue growth from summer 2018 to winter 2019. *Acropora sp.* placed on REDs had poor survival (approximately 5 percent). It is unclear at this time if the poor survival was attributed to the REDs themselves or that the REDs are located in an area of poor conditions (high sedimentation and scour).

DISCUSSION

Based on the results to date, I have determined feasible low-cost methods to restore shallow water patch reefs using materials readily available in isolated coastal communities These materials include SCUBA tanks, air drill, drill bits, marine cement or Quickrete, aquarium epoxy, plastic plugs, hand saws, and chisels. Based on our initial results, two persons could drill enough holes to cover a 20 m x 20 m area of reef with coral transplants spaced every 0.5 meter in one day's time. Using efficiencies learned from the efforts documented in this paper, a work party of local persons could rehabilitate a small patch reef in several days. Thus, I have concluded that I will initiate Part II of the research, scheduled for 2021-2022.

In Part II, I will establish test plots for statistical analyses to better quantify and compare reef restoration results, refine manpower estimates, and test the scale of rehabilitation. We will collect a number of coral fragments from the inner reefs and recent storm damaged corals from Gualin Reef and transport them to the shallow waters adjacent the GRC. There I will erect a temporary coral processing station where we will fragment the rescued corals and affix them to small plugs. The small plugs will be affixed to the reef surface or REDs. We will construct REDs and will affix either plugs or place tiles on the facias for spawning coral collection. The tiles will be placed on the REDs in the later summer, prior to coral spawning on San Salvador, to increase potential colonization success. Through the placement of transplanted corals in close proximity to collection devices, we will determine approximate rates of colonization through the proposed restoration techniques.

In addition, the recent findings of coral microfragmentation (Page *et al.* 2018), will be considered and incorporated into the restoration efforts. Coral microfragmentation is a recent discovery by which the small fragments (less than 1 sq cm) of an intentionally fragmented coral will grow at an accelerated growth rate than normal coral growth rates, making it possible to rapidly increase the amount of coral biomass on the reef. I envision that a coral nursery/repository will also be established in front of the GRC. Future restoration efforts in Part II will incorporate additional measurements of labor efforts, survival rates and growth rates resulting from coral transplants and microfragmentation efforts, and coral recruitment.

ACKNOWLEDGEMENTS

I would like to thank the Bahamas Environment, Science & Technology (BEST) Commission for issuance of permits to conduct this research.

This research would not have been possible without the assistance of the following scientists who have donated many weeks of their time: Andy Martin (AECOM), Ted Yoder (St. Stephen's & St. Agnes School), Anne Paul (AEML, Inc.), Colin Nugent (Northern Ireland Dept. of Agriculture, Envr, & Rural Affairs), Petra Fagerholm (European Environment Agency), Kristina Willmarth (Eau Claire, WI - School District), Rei-hua Wang (Jacobs Engineering), and Lisa Montana (National Grid). In addition, a special thanks goes to Robert "Bob" Cassidy – Chief Petty Officer, United States Navy "Seabees" (retired) whose unparallel knowledge of marine construction was invaluable.

LITERATURE CITED

Bayraktarov, E., Saunders, M., Abdullah, S., Mills, M., Beher, J., Possingham, H., Mumby, P., and Lovelock, C. (2016). The cost and feasibility of marine coastal restoration. Ecological Applications, 26(4), 1055–1074

Curran, A. (2016). Overview of Hurricane Joaquin effects in The Bahamas (29 September-3 October 2015). GSA Annual Meeting. Denver, CO, USA.

Jaap, W.C. (2000). Coral reef restoration. Ecological Engineering 15 (3-4), 345-364.

McGrath, T., Smith, G., And Rollino, J. (2007). A decade-long evaluation of three coral patch reefs off San Salvador, Bahamas. Naturalist & Journal of Science 2, 4-13.

Page, C., Muller, E., and M.,Vaughn, (2018). Microfragmenting for the successful restoration of slow growing massive corals. Ecological Engineering. 123, 86-94.

Rothfus, T.A. (2016). Hurricane Joaquin and the Gerace Research Centre, San Salvador, The Bahamas: Preparations and recovery. Conference: GSA Annual Meeting. Denver, CO, USA.

THE 3RD JOINT SYMPOSIUM ON THE NATURAL HISTORY AND GEOLOGY OF THE BAHAMAS

June 8th to June 12th, 2019

GERACE RESEARCH CENTRE
UNIVERSITY OF THE BAHAMAS
SAN SALVADOR, THE BAHAMAS

PROGRAM CO-CHAIRPERSONS:

Mark Kuhlmann
Hartwick College
Department of Biology
Oneonta, NY 13820

David Griffing
Hartwick College
Department of Geology
& Environmental Science
Oneonta, NY 13820

KEYNOTE SPEAKER:

John E. Mylroie

Department of Geosciences
Mississippi State University
Mississippi State, MS 39762

ORGANIZER:

Troy A. Dexter

Executive Director
Gerace Research Centre
University of The Bahamas
San Salvador, The Bahamas

UNUSUAL KARST PHENOMENA FROM CAT ISLAND, BAHAMAS

Albury, Nancy A. Bahamas National Museum, Abaco, Bahamas; **Lace, Michael J.** Coastal Cave Survey, West Branch, IA 52358; **Mylroie, Joan R.** Mississippi State University, Mississippi State, MS 39762; **Mylroie, John, E.** Mississippi State University, Mississippi State, MS 39762.

Cat Island, Bahamas, contains some unusual island karst features. Cat's Cradle, a blue hole in east-central Cat Island, is a progradational collapse structure that breached a large eolian calcarenite dune. The subaerial walls of the collapse are stepped at 3 m elevation, with the upper wall wider than the lower wall. This upper wall contains a complete ring of flank margin caves that open inward to the blue hole. If the mixing model for flank margin speleogenesis is correct, then the blue hole was marine during the 6 m high MIS 5e sea-level highstand. A 2 km long section of the east coast of Cat Island is a late Pleistocene back-beach breccia facies, indicating strand plain progradation, followed by wave erosion of that plain to create back-beach breccia, and subsequent continuing progradation of the strand plain. The fresh-water lens followed that progradation and created flank margin caves within the breccia facies, indicating the rapidity with which flank margin cave speleogenesis operates, as the entire sequence of rock deposition and dissolution had to be accomplished within the ~ 9 ka long MIS 5e event. Big Cave, in central Cat Island, is found at 55 m elevation on a shoulder of Mount Alvernia, the highest point in The Bahamas at 62 m elevation. The cave has all the small and large scale bedrock morphologies found in flank margin caves, but cannot be a flank margin cave in the traditional sense given its elevation above any possible Quaternary sea-level highstand. Cave genesis within freshwater lens perched on a terra rossa paleosol has been offered as a possible explanation.

DISTRIBUTION, COMPOSITION AND SIGNIFICANCE OF ENCRUSTERS ON CORALS FROM PLEISTOCENE REEFS IN THE BAHAMAS: EXAMPLES FROM SAN SALVADOR AND GREAT INAGUA ISLANDS

Beckham, Abigail Department of Geosciences, Smith College, Northampton, MA; **Mannucci, Agnese.** Department of Earth Science, University of Florence, Florence, Italy; **Glumac, Bosiljka,** Department of Geosciences, Smith College, Northampton, MA ; **Curran, H. Allen,** Department of Geosciences, Smith College, Northampton, MA ; **Griffing, David,** Department of Geology and Environmental Sciences, Hartwick College, Oneonta, NY.

The Pleistocene coral reef exposed at the Cockburn Town Fossil Reef site (west coast of San Salvador Island, Bahamas) lies ~3 m above present sea-level, and the succession is separated by the Devil's Point erosional discontinuity into Reef I and II. These deposits from the Cockburn Town Member of the Grotto Beach Formation (Eemian; MIS 5e) are an important source of information about paleoenvironmental conditions and sea-level fluctuations during the last interglacial highstand. Our field and petrographic work analyzed the abundance, distribution, and succession of various types of encrusters on corals from Cockburn Town Fossil Reef. Stable isotope analysis was conducted to provide insights into the depositional and diagenetic history of these deposits. The transition from clean fragments of branching acroporid corals to the occurrence of coral fragments with thick (up to 8-9 cm) encrustations made by red crustose coralline algae, foraminifera, serpulids, stromatolites and clotted microbialites has been interpreted as a change in Reef I development from bank barrier to restricted backreef and lagoonal environments in response to sea-level changes. Reef II corals are dominated by domal forms and lack thick encrustations. A comparison is made with The Gulf site (south coast of San Salvador) where similar succession of encrusters is observed in storm generated and transported boulders of Pleistocene coral material. The top of the reef here

is exposed at sea-level and outcrops are not available. Another comparison is made with a reef exposure at Devil's Point (west coast of Great Inagua Island, Bahamas), which is also separated into Reef I and II, but corals in these outcrops have only typical taphonomic modifications with very thin algal encrustations. A Reef II exposure of *Acropora palmata*, however, has a crust up to 2 cm thick made of red algae, serpulids, and foraminifera, but lacking microbialites. Displaced boulders from Matthew Town Marina excavation (west coast of Great Inagua), revealed *Orbicella annularis* with microbial and algal encrustations similar to those on San Salvador. Our ongoing research aims at better understanding such important differences and similarities among Pleistocene coral reefs and at evaluating Holocene stromatolites and coralline algal facies from elsewhere in the Bahamas as potential encruster analogs.

SIZE DISTRIBUTION AND POPULATION FLUX OF *ISOGNOMON ALATUS* FROM 2015 AND 2018 IN TWO INLAND LAKES OF SAN SALVADOR ISLAND, BAHAMAS

Beebout, Katlyn, E. Northern State University, Aberdeen, South Dakota; **Anderson, Alyssa M.** Southwest Minnesota State University, Marshall, Minnesota.

The Flat Mangrove Oyster (*Isognomen alatus*) is often found in mangrove marshes growing on or around the intricate aerial root network of red mangrove trees. Work with *I. alatus* is limited and literature provides little when assessing their response to fluctuation in the environment. The purpose of this study was to examine the size distribution of *I. alatus* in Oyster Pond and Osprey Lake on San Salvador Island, Bahamas. While these water bodies are spatially close and similar in size, they vary in terms of salinity and dominate vegetation. At each water body, samples of at least 100 oysters were collected randomly. The hinge length of individuals was recorded and compared to 2015 sample results. Both Oyster Pond and Osprey Lake had a significant change in hinge length from 2015 to 2018. We believe that hurricane action during the three-year time span damaged the Red Mangroves, thereby impacting *I. alatus* populations. In Oyster Pond, the damaged habitat caused older individuals to die, which lead to high recruitment and populations of smaller individuals. Surprisingly, no live oysters were found in Osprey Lake; however, the lake bottom was covered in shell remains from *I. alatus*. We hypothesized that the population measured in 2015 had low recruitment and weak establishment. However, additional ecological information for *I. altatus* is necessary in order to draw further conclusions on the population fluctuations found in San Salvador's inland lakes.

CHARACTERIZATION OF POLAR ORGANIC CONTAMINANTS IN WATER BODIES OF SAN SALVADOR ISLAND

Brado, Mark Elmira College, Elmira, NY; **Downs, Garrett** Elmira College, Elmira, NY; **Harrison, Tre'Mesha** Elmira College, Elmira, NY**; Salvatierra, Yhon,** Elmira College, Elmira, NY; **Barzen-Hanson, Krista, A.** Elmira College, Elmira, NY

Synthetic organic compounds are omnipresent and are found in many household and personal products. These compounds enter aquatic systems through discharge and disposal and are classified as environmental contaminants. Diffusive gradients in thin films for organics (o-DGT) passive samplers capture aqueous contaminants. Two types of agarose gels are used as the thin films, a diffusive gel (all agarose), and a binding gel (agarose with HLB). The housing for a binding/diffusive gel set was designed and 3D printed using ABS. Four housing units serve as a single sampler. The center of the sampler contains sensors to monitor environmental conditions in collaboration with Dr. Corey Stilts. The samplers will be deployed for 14 days in the ocean and fresh and saline lakes on San Salvador Island, The Bahamas. Following deployment, binding gels will be brought back to Elmira College and analyzed by methanol extraction followed by gas chromatography-mass spectrometry.

HIGH-RESOLUTION IMAGERY OF BOULDER FIELD MOVEMENT IN HURRICANES IRENE (2011), JOAQUIN (2015), AND MATTHEW (2016) ON SAN SALVADOR, THE BAHAMAS

Caples, Stephanie, University of Missouri-Kansas City, Kansas City MO; **Niemi, Tina,** University of Missouri-Kansas City, Kansas City MO; **Rucker, Linda,** University of Missouri-Kansas City, Kansas City MO; **Rucker, John ,** University of Missouri-Kansas City, Kansas City MO; **Nolan, Joseph,** University of Missouri-Kansas City, Kansas City MO.

Located along the northeast edge of the Bahamian archipelago, San Salvador Island (SSI) sees a high frequency of Atlantic hurricanes that track through the Caribbean. This makes the island an excellent location for studying geomorphological processes and changes to the coastal environment. In this study, we report on our monitoring of the coastal erosion and boulder movement along the southern rocky coast at the location called the Gulf on SSI after Hurricanes Irene, Joaquin, and Matthew. Hurricane Irene tracked north of Hispaniola and traveled NW through the Bahamas as a Category 3 hurricane on August 24, 2011 passing SW of SSI. SSI was directly affected by Hurricane Joaquin over a two-day period on Oct. 1-2, 2015 when the storm travelled SW from Bermuda, passed SE of the island then turned, intensified to a Category 4 hurricane, and then passed across the island from the SSW. The Category 4 Hurricane Matthew traveled north between Cuba and Hispaniola and then passed NW through the Bahamas as a Category 4 on October 6, 2016 similar to Hurricane Irene. To map the hurricane-related changes in the coastal environment, we utilized two different aerial imaging techniques to photograph the boulder field at the Gulf. In June 2015 and March 2016, we utilized a kite-mounted camera, and in June 2016 and 2017, we utilized a DJI Quadcopter 3 mounted with 12 Megapixel, 4K video camera to collect aerial data. We preprogrammed flight paths designed to acquire 70% image overlap using a smartphone app designed by Pix4D. All data were processed using Agisoft PhotoScan to render both a high-resolution, digital orthomosaic, as well as a georeferenced digital elevation model (DEM). These datasets were compared to satellite imagery from Google Earth. Our time series data from June 2015 before Joaquin to March 2017 after Matthew allow us to determine how the coastline changed. Our field research provide ground-based photographic and orientation data on boulder location, imbrication, and beach conditions. The high-resolution, low-altitude imagery allowed us to map the boulder field, measure the evidence of storm surge height by flotsam lines surrounding the boulder field, and calculate boulder movement by matching erosion scars to boulder position, and boulder size to position. We also noted where road construction debris provided boulders that had moved. It is clear that boulders that are exposed along the wave-cut platform at low tide of the Pleistocene Cockburn Town Reef have been transported up the cliff and inland in storm event based on boulder identification. We have previously noted that coastal reentrants are the location of coves where wave action is focused and thus increase lift. Coastline retreat where cliffs collapse downward are located along these coves and provide large boulders which are available for transport upward. These coves become the staging ground for boulders to be elevated in extreme storm events. Our data show that the coves have a greater storm surge height and transport boulders farther landward. The pronounced landward movement of the entire boulder field during Joaquin is likely due to the unique intensity, storm track direction, and duration of the hurricane.

NORTH POINT SAN SALVADOR ISLAND REINTERPRETED: EVOLUTION AND INTERNAL ARCHITECTURE OF EOLIAN DOME DUNES

Caputo, Mario, V. San Diego State University, San Diego, CA.

Earlier studies of calcarenite features in the Holocene North Point Member, Rice Bay Formation at North Point, San Salvador Island, Bahamas indicated unequivocal sedimentation by wind. Further evidence based on sedimentary architecture from this study supports a new interpretation of eolian dunes that deposited the North Point Member. Primary architectural elements are wind-ripple strata in sets bounded by discordant erosional surfaces. They comprise >90% of stratification, forming topset, brinkset, and especially foreset strata herein termed wind-ripple crossbeds. Secondary elements are bedsets of mainly sandflow strata mixed with wind-ripple and grainfall strata. Such bedsets are scarce, ~1 m thick, and herein termed slipface crossbeds. Dip azimuths span nearly 360 degrees for bedset bounding and reactivation surfaces, wind-ripple and slipface crossbeds, and dune flanks. Furthermore, dominance of wind-ripple crossbeds, scarcity of slipface crossbeds, and overall mound-swale landscape of the present-day North Point peninsula that mimics Holocene dune landscape suggest the build-up of eolian dome dunes, a rarely developed dune type in sand-sized siliciclastic and carbonate sediment and sedimentary rocks. Deeply eroded exposures show cores of juvenile dome and lobate dunes buried by overlapping mature domes and interdome swales. In the path of unobstructed Northeast Trade Wind, low mounds of rippled sand enabled growth of small dome and lobate dunes. On this foundation, mature dome dunes merged laterally to build the peninsular ridge at North Point. Evidence for periodic rainfall and elevated water table during build-up of the Holocene dome dunes at North Point is recorded by climbing adhesion ripples preserved in interdome swales. They definitively indicate moist, wind-transported ripple sand. First discovered by this study on San Salvador, they are preserved in the North Point Member and in the Pleistocene Grotto Beach Formation. Crest orientation, northeastward climb of adhesion ripples, crest orientation and southwest climb of wind ripples, and strata of juvenile lobate dunes convex to the southwest show a wind flow to the southwest, consistent with Northeast Trade Winds prevailing during Holocene time. Rainfall and coastal moisture rendered the dune sand cohesive so that avalanches or grainflows on dome flanks rarely happened.

ANCHIALINE PONDS, A REFUGE FOR MARINE DIVERSITY: A QUICK BIOTIC SURVEY OF 10 ANCHIALINE PONDS ON THE ISLAND OF ELEUTHERA

Cole, Eric, S. St. Olaf College, Northfield, MN; **Robinson, Nathan, J.** Cape Eleuthera Institute, Rock Sound, Eleuthera; **Campion, John** Kirckof & Associates, Northfield, MN.

In the Bahamas, the inland ponds serve as refuges for unique species that are often uncommon in the open coastal environments. These salt-water habitats are sheltered, and protected by natural barriers from all manner of environmental threats. While many of these habitats are species-poor, some have undergone a remarkable process of spot-colonization and population explosion where one or two species dominate, creating incredibly simplified, but productive marine communities. Each pond also represents a laboratory of adaptive change as organisms respond to the unique characteristics of their particular pond-habitat through natural selection. On a recent trip to Eleuthera, my team made a rapid survey covering ten anchialine ponds in ten days. The goal of this preliminary, non-invasive survey, was to evaluate how rich the various ponds were in species diversity, and to begin investigating the unique adaptations of some of their resident invertebrates. The species richness in several of these ponds was beyond anything we have seen before, and argues both for more investigation and documentation, and for advocacy for their preservation or conservation as the island develops.

DEVELOPMENT OF BOTH WATER-BASED AND LAND-BASED

ENVIRONMENTAL SENSORS USING ARDUINO MICROPROCESSORS

Decker, Destiny Elmira College, Elmira, NY; **Holden, Tyra** Elmira College, Elmira, NY; **Stilts, Corey E.** Elmira College, Elmira, NY.

This project involved the development, coding, and construction of low-cost environmental sensors for use on land and water habitats. The sensors are built using the Arduino mini pro architecture. These low-energy small devices allow for the creation of small sensors capable of lasting days in the field. They are powered by a 9V battery. The land-based sensor is housed in a 3D printed case and is capable of monitoring and recording time-stamped data to a microSD card. The water-based unit is encased a waterproof 3D printed case and will measure water temperature, conductivity, and turbidity. This data will be recorded as a time-stamped data recording to a microSD card in the sensor.

A NOVEL TOOL FOR SCIENCE EDUCATION: THE STUDENT PRODUCED AUDIO NARRATIVE (SPAN)

Fioravanti, Geremea, HACC, Lancaster, PA; **Kraal, Erin** Kutztown University Kutztown, PA.

This poster will detail the process of participating in a NSF Improving Undergraduate STEM Education grant, including collaborations with Kutztown Univ., Penn State Univ., MIT, Albright Coll. and various community colleges (E.g., HACC). Students were encouraged to use their smartphones to record stories involving the geosciences. Assignments included audio collages, workforce explorations, public service announcements, documentaries, science "minutes", or place-based explorations. These projects were called Student Produced Audio Narratives (SPAN)s. Instruction involved teaching students how to record, produce sound-logs, outline their projects, and prepare the final script. Then the narratives, interviews, sound effects, music, and natural sound recordings were combined using Audacity™ software to form final projects. To date, the narratives have generally been well received. However, limitations such as student individual needs and tensions between completing learning objectives and creating free-form narratives are potential pitfalls. The novelty, varied opportunities and low barrier to entry may make SPAN projects ideal for application in remote field environments like that on San Salvador, Bahamas.

RECENT UPDATES TO THE LUCAYAN TRAIL FIELD GUIDE

Ford, Dawn, M. UTC, Chattanooga, Tennessee; **Jobe, Laurel M.** UTC, Chattanooga, Tennessee.

The Lucayan Trail located off the site of the Gerace Research Center on San Salvador Island has served as a key place for research in the last several decades. In 1994, a field guide entitled *The Natural History of Northeastern San Salvador Island: A New World Where the New World Began* (Godfrey et al., 1994) was published and has since been utilized by researchers working on the Lucayan Trail. Four working groups in a 2018 UTC Faculty-led trip conducted a biological survey examining similarities and differences in the environment created over the past 24 years due to hurricane damage and general evolutionary changes, particularly in plant life, animal life, and water quality. The primary strategy involved taking samples and photographs of unfamiliar vegetation and identifying them using resources such as books and digital publications. Some bodies of water were more accessible than others for snorkeling, though all sites were at least sampled for water quality and data were compared to previous studies. The four working groups each had their own hypotheses in regards to their specific part of the trail; however, it was commonly assumed that there would be a shift in species richness/biodiversity over the last 24 years, especially following Hurricane Joaquin in 2015. Notable findings from the working groups include: an increased presence of ammonia (0.5ppm) in Osprey Lake, an additional conduit

formation at Purslane Pit, the absence of flamingos, the addition of a smaller trail, a decrease in sponge spicule and hydroid presence in Pain Pond, limited cave access, misidentification of three epiphyte species noted in the original guide, and the presence of several previously undocumented plant species. All research groups contributed their suggestions and edits to the original trail guide which will be discussed more extensively in the following presentation.

MINECRAFT AS A TEACHING TOOL FOR CAVE CARTOGRAPHY

Francis, David Fort Hays State University, Hays, KS; **Andersen, Zachary** Fort Hays State University, Hays, KS; **Sumrall, Jeanne L.** Fort Hays State University, Hays, KS; **Kambesis, Patricia** Wester Kentucky University, Bowling Green, KY.

In the field of Geology, specifically the field of karst landscape studies, cave investigation and analysis is a critical component to the understanding of the landscape. The current process to train new speleologists to conduct fieldwork is not practical in many geographic locations. It can be difficult to train a multitude of individuals to cave map due to constraints caused by the scarcity of caves in certain regions, the cost of the necessary equipment, and the physical constraints posed by the cave. We proposed that by using the current advancements in gaming technology we can mitigate and remove a few of the obstacles. For the purpose of this study we chose to use the computer game Minecraft because it can simulate a variety of cave environments in an online setting, it is widespread with over one hundred million users, and it requires only a computer or mobile phone to operate. Minecraft could be implemented as an educational tool to introduce and practice cave cartography outside of a cave setting and expose younger generations to mapping caves in an enjoyable and interactive way. This is important as one of the most difficult tasks in training students and geologists in cave cartography is practice. By using Minecraft to practice the math and process of mapping we avoid the need to travel or prepare the necessary tools. Students and scientists alike can be better prepared for field experiences which may reduce error and the expense of time lost in the field due to training activities.

GENERATION AND TRANSPORT OF LARGE ROCK BOULDERS BY STORM WAVES ALONG THE HIGH-ENERGY SOUTHERN COAST OF SAN SALVADOR ISLAND, BAHAMAS

Glumac, Bosiljka Department of Geosciences, Smith College, Northampton, MA ; **Curran, H. Allen** Department of Geosciences, Smith College, Northampton, MA.

Documenting changes in morphology and distribution of coastal boulder ridges and the direction and amount of transport of individual large boulders provide useful information about the intensity and effects of storms in The Bahamas. We have been monitoring a boulder ridge on a cliff-bench, 3-5 m above mean sea level, between The Gulf and The Cut along the high-energy southern coast of San Salvador Island since January 2012. Twelve large boulders (~700-4500 kg; with all but one >1000 kg) were initially photographed, located with GPS coordinates, measured, and characterized by composition (subtidal calcarenite, coral rubblestone, eolianite, lithified paleosol), shape, and degree of roundness. The boulders were eroded from the seaward rocky coast, transported and deposited by high-energy storm waves. Our continuing monitoring in January 2013, 2016, and 2017, after Hurricanes Sandy (October 2012), Joaquin (October 2015), and Matthew (October 2016), documented drastic modifications to the boulder ridge. We were not able to relocate 2 boulders post-Sandy, and only 5 of the remaining boulders were relocated with certainty after Joaquin, which passed directly over the island as a high category 3 hurricane with 120-130 mph sustained winds. Storm waves overtopped the coastal cliffs, causing erosion at the leading edge and extensive

landward movement of boulders. This modified the formerly sharp-crested, narrow boulder ridge into a larger, broad boulder field, ~6.3 ha in area and stripped of vegetation. New boulders, as large as 3 m in diameter, were generated, and blocks from prior storms, estimated to weigh 1-3 tons, moved up to 26 m inland. The principal coastal road was damaged and inundated by debris. The southern edge of the boulder ridge moved landward by 4-5 m exposing an underlying Pleistocene/Holocene boundary terra rossa paleosol, which stands out in aerial images and marks the extent of storm erosion. Post-Hurricane Matthew, which passed too far from the island to have a major impact, 11 new boulders and high-resolution drone aerial imagery were added to our monitoring program to expand our database and allow continuing documentation and communication of information on vulnerability to hurricanes with stakeholders on San Salvador and elsewhere in the Bahamas. A January 2019 survey of the key boulders revealed only minor changes in positions of smaller boulder-cobble debris since 2017.

NEW ADVANCES IN LONG-TERM MONITORING OF STORM-DEPOSITED BOULDER RIDGES ALONG ROCKY SHORELINES OF SAN SALVADOR ISLAND, BAHAMAS

Glumac, Bosiljka, Department of Geosciences, Smith College, Northampton, MA; **Miguel, Ursula** Department of Geosciences, Smith College, Northampton, MA; **Curran, H. Allen** Department of Geosciences, Smith College, Northampton, MA.

Since January 2012 we have been monitoring two boulder ridges on San Salvador: 1) Singer Bar Point (SBP, length ~790 m) along the reef- and lagoon-protected northern coast; and 2) The Gulf (TG, length ~460 m) on the high-energy southern coast. This long-term monitoring aims at documenting changes in ridge morphology and distribution, and the direction and amount of movement of individual boulders to gain insights into the intensity and effects of storms. The largest boulders from each site were photographed, GPS-located, measured, and characterized by composition and morphology. Boulders at SBP are generally smaller (15 total; ~150-4000 kg; with most <1500 kg) than those at TG (12 original; 12 added by 2017; ~700-6500 kg; most >1000 kg). Our monitoring from January 2013, 2016, and 2017, after Hurricanes Sandy (October 2012), Joaquin (October 2015), and Matthew (October 2016), respectively, indicated only modest modifications at SBP, and major changes to TG: we were unable to relocate 2 boulders post-Sandy, and only 5 of the 12 original boulders were relocated after Joaquin. Two of those, ~2 tons each, were transported NNW by 20 and 26 meters. Even though documentation of boulder movement allows calculation of minimum flow velocity needed to initiate their transport, the lack of adequate tagging made it challenging or impossible to relocate individual boulders after major storms. This problem will be addressed by application of RFID (radio frequency identification) tagging in June 2019 and January 2020, before and after the 2019 hurricane season, respectively, and far into the future, as passive tags are inductively charged by the reader and can remain operational for decades. Drilling to insert small tags (23 and 32 mm long, and <4 mm in diameter) is minimally invasive and will also allow tagging of pebbles and cobbles. This is especially important for monitoring at SBP where large boulders have not been moved much by waves in the recent past, but smaller clasts do move actively. In conjunction with continuing high-resolution drone imaging, the use of tagging that can uniquely identify an object within a large population will significantly increase our database and improve our long-term monitoring efforts.

BIOTURBATED AND SUBAERIALLY ALTERED SUBTIDAL PLEISTOCENE LIMESTONE IN THE BAHAMAS: PETROGRAPHIC AND STABLE ISOTOPE ANALYSIS

Graveline, Alyssa, Department of Geosciences, Smith College, Northampton, MA; **Beckham, Abigail** Department

of Geosciences, Smith College, Northampton, MA; **Glumac, Bosiljka** Department of Geosciences, Smith College, Northampton, MA; **Curran, H. Allen** Department of Geosciences, Smith College, Northampton, MA.

Pleistocene subtidal ooid-skeletal-peloidal grainstone of the Cockburn Town Member, Grotto Beach Formation, at Harry Cay on Little Exuma Island contains well-developed *Ophiomorpha*, *Conichnus*, *Planolites* and *Skolithos*. Samples of these trace fossils were analyzed petrographically and for stable isotopes to determine extent of modification of matrix sediment, which was initially lithified in the marine realm, but later experienced meteoric diagenesis and formation of a caliche cap. *Ophiomorpha* from Harry Cay was compared with Pleistocene samples from San Salvador, Rum Cay, Great Inagua, Great Exuma and Grand Cayman Islands, as well as Holocene examples from San Salvador and Lee Stocking Islands. Pleistocene *Ophiomorpha* wall pellets have more micrite than host rock, indicating that callianassid shrimp tracemakers concentrated mud during burrow construction. Stable isotope values of *Ophiomorpha* range -1.5 to -4 ‰ VPDB $\delta^{18}O$ and 0 to 3.5 ‰ VPDB $\delta^{13}C$, with complete overlap among multiple sites and substantial overlap with calcarenite host rock and burrow fills. Holocene *Ophiomorpha* has higher values, typical of unaltered marine carbonate, clustering ~0 ‰ $\delta^{18}O$ and 4.5 ‰ $\delta^{13}C$. Some *Ophiomorpha* tubes are filled with caliche similar to the cap at Harry Cay. $\delta^{18}O$ values of these caliche fills overlap with *Ophiomorpha* walls, but their low $\delta^{13}C$ values (-8 to -9 ‰) reflect soil-derived ^{12}C. $\delta^{13}C$ values of some calcarenite fills are between those of burrow walls and caliche, forming an inverted J trend indicative of meteoric diagenesis, with burrows providing fluid pathways. This resulted from preferential meteoric diagenesis of micrite in burrow walls as supported by their $\delta^{18}O$ values being lower than associated matrix, and their calcitic composition compared to mixed aragonite-calcite host rock. *Planolites* traces appear finer-grained than the host rock, suggesting that ballanoglossid worms, the probable tracemakers, can sort sediment while ingesting it. *Conichnus* contains sand grains that appear more loosely packed than host sediment, indicating that burrowing activity, possibly by sea anemones, created a porous fabric. *Skolithos* tubes were too thin to examine petrographically, but isotopic composition of calcarenite within these three trace fossils is not systematically different from the host rock, reflecting similarity in their composition and diagenesis despite textural and fabric modifications by burrowing organisms.

INTERNAL DISCONTINUITIES AND THE DEPOSITIONAL HISTORY OF EEMIAN REEF DEPOSITS (COCKBURN TOWN MEMBER, GROTTO BEACH FORMATION) ON SAN SALVADOR ISLAND, BAHAMAS

Griffing, David, H. Hartwick College, Oneonta, NY, USA; **Glumac, Bosiljka,** Smith College, Northampton, MA, USA; **Curran, H. Allen** Smith college, Northampton, MA, USA.

In addition to coral geochronology and the mid-reef Devil's Point erosional discontinuity, depositional features within the Eemian Cockburn Town Member fossil reef deposits yield insights into paleoenvironmental changes potentially associated with sea-level fluctuations during the last interglacial. On San Salvador, lower reef (Reef I) exposures in Cockburn Town exhibit a facies transition from coral floatstone/bafflestone/framestone to coral-microbial bindstone, whereas the upper reef (Reef II) is dominated by coral-mollusc-corallinacean rudstone (with essentially no microbialite). Although minor sub-horizontal discontinuities pervade Reef I deposits, a quarry exposure displays at least 17 inclined, progressively shallowing, grainstone-draped discontinuities that define decimeter-scale lateral accretion surfaces. Each accretion deposit contains branching coral fragments coated by laminated micritic microbialite and poorly-laminated/clotted sandy microbialite, and suggests episodic introduction of coral clasts. Microbialite-coated corals are separated by discontinuous, mm- to cm-scale drapes of ooid-peloid-skeletal grainstone similar

to foreshore deposits. Reef I features suggest the following history of reef development: 1) establishment of branching coral stands in a bank-barrier setting; 2) development of backreef and lagoonal subenvironments; 3) subsequent restriction, likely from a minor sea-level drop or a stillstand; 4) coating of coral clasts by microbial communities thriving in the backreef; 5) repeated introduction of new coral clasts via storms from reef-front settings followed by microbial coating; and 6) gradual migration of foreshore sand draping the shallow backreef. Repeated episodes of Reef I microbialite development, microbialite abundance and thickness, and the truncation of Reef I by the Devil's Point discontinuity (>60 cm of relief), indicate a significant period of backreef restriction followed by erosional truncation (sea-level drop). In contrast, Reef II deposits contain extensively bored and coral-encrusted discontinuities overlain by rudstone beds of coarse, pristine coral and mollusk rubble that suggest episodic but rapid accumulation of reef debris in an unrestricted, energetic nearshore setting. Reef II is capped by a sharp, low-relief erosional discontinuity (wave-cut bench?) overlain by foreshore sands bearing traces that reflect the hardground nature of this discontinuity. Recognizing a similar facies distribution within the Eemian reefs elsewhere, in order to confirm a eustatic sea-level origin for the Devil's Point discontinuity, is complicated by the extent of backreef exposures and different tectonic histories. Yet similar coral-hosted microbialites have been observed in the Sue Point outcrops and in storm-transported boulders at The Gulf (both San Salvador), and in blocks quarried during marina enlargement on Great Inagua.

MAPPING CULTURAL GEOGRAPHY OF SAN SALVADOR ISLAND, THE BAHAMAS, CIRCA 1800 TO 2010

Jackson, Christopher C. Athens, GA.

The rich and unique cultural heritage of The Bahamas is experienced through both tangible and intangible resources, such as buildings, landscapes, archaeological remains, and social events and expressions. Cultural geographers and archaeologists have studied cultural heritage resources of The Bahamas for at least the past three decades; however, little has been said regarding their preservation, promotion, and interpretation. An important first step in the process of safeguarding and promoting such resources is identification and inventory. The inventory can then be evaluated in terms of what heritage resources are significant and why their preservation and interpretation matters to Bahamians. Cultural mapping is an important tool in the process of evaluation. This project serves a glance into how heritage resource managers can use Geographic Information Systems (GIS) to enhance the process of identification, evaluation, and interpretation of cultural heritage resources in The Bahamas. The mapping and findings presented are based on a 2017 case study of the Bahamian island of San Salvador. As an active cultural landscape, the island's heritage resources include historic plantations, archaeological sites, historic buildings, active cemeteries, and public parks/green spaces. These resources are evaluated, through mapping, in terms of an established framework of historic periods, patterns, and themes in Bahamian history and cultural development.

AN INDEX FOR DESCRIBING ANT COMMUNITY DIFFERENCES USING SPECIES' ARRIVAL AND RECRUITMENT AT BAITS

Kjar, Daniel, Elmira College, Elmira, NY; **Park, Zachory** Georgetown University, Washington, DC.

Monitoring changes in ant communities can be difficult in habitats where using common trapping methods is not possible. To address this problem, we developed an index based on an ant species' presence at baits as well as their time of arrival and recruitment to baits. In this study, we compared the index across three distinct habitats on San Salvador Island, The Bahamas. We found that a species' index value changed depending on

habitat and the changes appear to reflect actual differences in the ant community among sites. We also discuss the importance of not including bait dominance in the index.

TESTING THE TATOR INDEX: A NEW 3D PRINTED PITFALL TRAP

Kjar, Daniel Elmira College, Elmira, New York; **Franklin, Lauren** Elmira College, Elmira, New York; **Breheny, Emily,** Elmira College, Elmira, New York.

Over the last 6 years the Kjar lab has used behavioral observations of ant species at baits to describe differences among sites on San Salvador Island, The Bahamas. The island is entirely composed of calcium carbonate rock and this makes trapping ants by common methods very difficult. In order to test the TATOR (Time of Arrival and Time of Recruitment) index's ability to describe an ant community we will be using a new pitfall trap designed by the Kjar lab and produced here at Elmira College. The pitfall trap is modular in design with a funnel and lid. The traps will be placed in the Palmetto habitat in multiple locations on San Salvador Island. We will leave the traps for 48 hours and then compare ant incidence and richness to the results of the behavioral observations underlying the TATOR index.

GENOTYPING PARATRECHINA LONGICORNIS USING GENERAL PURPOSE AGAROSE AND MICROSATELLITE MARKERS

Krohn, Alexandra Elmira College, Elmira, NY; **Haywood, Alyna** Elmira College, Elmira, NY; **Smugereski, Catherine** Elmira College, Elmira, NY; **Kjar, Daniel** Elmira College, Elmira, NY.

Identifying colony level genetic differences requires rapidly evolving sequences of DNA (Microsatellite Markers). These regions of DNA range from 50 to 400 base pairs and consist of repeated AT sequences. Polymerase frequently makes mistakes when copying these repeated sequences. Normally, we would amplify the sequences using PCR (Polymerase Chain Reaction), tag the product with a fluorescent probe using an additional PCR step, and finally visualize the products on a large, long-run Polyacrylamide gel. This is expensive, time consuming, and Polyacrylamide is carcinogenic. Here we attempt to genotype Paratrechina longicornis using general purpose agarose and avoid the second PCR and Polyacrylamide gel steps, reducing the time, cost, and danger associated with this technique.

DO CONCH FISHERY DISCARDS FACILITATE OCTOPUS POPULATIONS?

Kuhlmann, Mark, L. Hartwick College, Oneonta, NY.

Common octopuses (*Octopus vulgaris*) shelter in crevice dens during the day. In a previous study of *O. vulgaris* diet at San Salvador, we found significant variation in octopus den type among locations that corresponded to differences in apparent octopus abundance (Kuhlmann and McCabe 2014): at most locations, octopuses denned primarily in solution holes or other natural crevices but were widely dispersed, but at one location where the benthos is dominated by seagrass and lacks exposed rock, octopuses denned almost exclusively in conch shells discarded by the fishery and seemed more abundant than at other locations. I hypothesize that, in the seagrass habitat, food is abundant but shelter, in the absence of human-provided conch shells, is limiting for the octopus population; in other habitat types, shelter is abundant but another factor, possibly food, is limiting. Thus, shells discarded by the conch fishery may be allowing octopuses to exploit a food-rich habitat that would otherwise be unavailable because of the lack of crevice shelters. I conducted a year-long shell addition experiment to test this hypothesis. I predicted that adding empty conch shells in seagrass habitat (lower shelter) would increase octopus abundance; adding shells in mixed hard-bottom habitat (higher shelter) would not increase octopus abundance. One year after adding shells, octopus abundance had increased on sites with added shells in seagrass but not on hard-bottom

addition or any control sites, supporting the hypothesis. Statistical support of this conclusion was hampered by very low numbers of octopus overall, so I plan to test this hypothesis again with a more robust experimental design.

INVESTIGATION OF FLORAL DIVERSITY AND THE SPATIAL DISTRIBUTION OF PLANTS IN COASTAL ECOSYSTEMS, AND THEIR EFFECTS ON PLANT-POLLINATOR DYNAMICS AT COMMUNITY AND METACOMMUNITY SCALES

Landry, Carol, L. Ohio State University, Columbus OH; **Green, Johnny, C.** Ohio State University, Columbus OH; **Elliott, Nancy, B.** Siena College, Greenlawn NY.

There are six coastal plant communities in The Bahamas, determined by their distance from the ocean, substrate composition, and relative degree of disturbance. These communities are dynamic, ever subject to wind and water, including significant disturbances due to tropical storms and hurricanes. Coastal plant communities are important ecologically and economically; they reduce erosion by stabilizing sediments, and protect inland communities by absorbing the energy of storm surge. To better understand interactions between plants from different communities that share pollinators, we investigated the species composition, relative species abundance, and spatial distribution in four of the six community types. In this preliminary study, we surveyed seven 100 m^2 plots on San Salvador, two each in the *Coccothrinax*-shrub, beach-foredune, and rock terrace communities, and one in the shrub-thicket community. All plants were identified, their canopies mapped, and the total canopy coverage for each species was estimated for each plot. To compare the relative floral diversity, as perceived by insect pollinators, the relative canopy coverage of each species was used to calculate a Shannon Diversity Index for each community. Our preliminary results demonstrate that the *Coccothrinax*-shrub and shrub-thicket communities have the greatest canopy coverage and floral diversity. These data will be compared to insect visitation records to determine whether pollinator diversity is correlated with floral diversity, or if the presence of communities with greater floral diversity influences pollinator diversity in adjacent communities with less floral diversity.

FEASIBILITY OF BIODIESEL USE AT THE GERACE RESEARCH STATION, SAN SALVADOR, BAHAMAS: HEALTH AND ENVIRONMENTAL PERSPECTIVES

Lashley, Victoria Fort Hays State University, Hays, KS; **Straley, Charlotte** Fort Hays State University, Hays, KS; **Sumrall, Jeanne L.** Fort Hays State University, Hays, KS; **Kambesis, Patricia** Wester Kentucky University, Bowling Green, KY.

This academic study analyses the environmental and human health implications of adding a biodiesel facility to the Gerace Research Centre (GRC), San Salvador, Bahamas. The study examines implications from start to finish including constructing the facility and ending with replacing diesel with biodiesel. Conclusions were made by conducting personal interviews and critically analyzing other materials on biodiesel. The biodiesel will be produced on the GRC campus. It will require developing a new building from a previous concrete foundation and additional storage sheds. The new building will store the various chemicals and the biodiesel maker, the Freedom Fueler Deluxe. The biodiesel will be cooking oil based which is different from typical algae biofuel which is more widespread and commonly used. Biodiesel will be made with used cooking oil donated by various businesses around the island. A certain part of the vehicle?s engines will also need to be replaced if the car model is before 1993. The study found replacing diesel with biodiesel would be excellent for the environment and not cause human harm. Initially, biodiesel emits 20-60 percent fewer greenhouse gasses than fossil fuels and 70-90 percent fewer long-term (New Delhi, 2009). This is significant and will drastically reduce the carbon footprint of

the GRC and eventually the island of San Salvador. This will also reduce the current environmental impacts of traditionally transporting diesel to the island.

ENCRUSTING FORAMINIFERA FROM PLEISTOCENE CORAL REEFS ON SAN SALVADOR AND GREAT INAGUA ISLANDS IN THE BAHAMAS

Mannucci, Agnese Department of Earth Science, University of Florence, Florence, Italy; **Beckham, Abigail** Department of Geosciences, Smith College, Northampton, MA ; **Glumac, Bosiljka** Department of Geosciences, Smith College, Northampton, MA; **Curran, H. Allen** Department of Geosciences, Smith College, Northampton, MA; **Griffing, David** Dept. of Geology and Environmental Sciences, Hartwick College, Oneonta, NY.

Pleistocene coral reefs (Grotto Beach Formation, Cockburn Town Member) from San Salvador and Great Inagua Islands, Bahamas, offer important insights into paleoenvironmental and sea level changes during the last interglacial highstand (Eemian; MIS 5e). Field and petrographic observations provide information on distribution and abundance of encrusting organisms, their role in taphonomic modifications of corals, and the environmental transition from healthy to microbially encrusted reefs. Stromatolites, clotted microbialites, red crustose coralline (RCC) algae, serpulids, and foraminifera form several cm thick encrustations on *Acropora, Pocillopora,* and *Orbicella* corals. Identification of encrusting foraminifera is commonly based on surficial morphology, but many examples are embedded within other encrusters and had to be studied in thin sections. The result is a set of criteria for the recognition of the following four foraminiferan species present at all study sites: 1) *Homotrema rubra* is the most common type, characterized by red tests of variable morphology (globose, hemispherical, flat, branching, spiny), up to 8 mm in diameter (d), and made of multiple layers of chambers (d=40-200 μm) with continuous or perforated walls 20-60 μm thick; 2) *Gypsina plana* comprises ~5% of the total specimen count; its discoidal tests are up to 3 mm wide and consist of few layers of elliptical chambers (d up to 1.4 mm) with convex upper surface and perforated septae 60-200 μm thick; 3) *Carpenteria utricularis* has plano-convex, trochospiral tests (d ~2 mm) of conical or globose morphology and a highly convex umbilical side; its chambers are up to 1 mm in diameter and have 50-400 μm thick septae; and 4) *Planogypsina acervalis* is the rarest species; it has thin discoidal tests and elliptical chambers (d up to 300 μm), with thin septae (20 μm) organized in a single layer. Corals are almost exclusively directly encrusted by RCC algae, which in turn are encrusted by foraminifera and serpulids, and commonly covered by more algae. *Homotrema* and *Carpenteria* are also embedded within thicker microbialites, and their abundance decreases away from the coral surface. The prevalence of *Homotrema* and the paucity of *Gypsina* suggest that the encrustation took place in a near-shore, high energy, well-lit marine environment.

EVALUATING THE USEFULNESS OF GOOGLE EARTH HISTORICAL IMAGES TO ASSESS IMPACT OF HURRICANES IN THE BAHAMAS

Miguel , Ursula, Department of Geosciences, Smith College, Northampton, MA; **Glumac, Bosiljka** Department of Geosciences, Smith College, Northampton, MA; **Curran, H. Allen** Department of Geosciences, Smith College, Northampton, MA

This exploratory study relates historical satellite imagery to information about intensity and pathways of hurricanes in the Bahamas to assess amount and style of modifications by major storms during the present times of globally rising sea level. Examples include severe beach erosion, damage to roads, washovers of beach sand and rock boulders into interior settings, and conversion of coastal lakes to lagoons with creation of new inlets. Specifically, this research evaluated the usefulness of Google Earth historical imagery for documenting hurricane impact. Google Earth historical imagery has been available since about 2001, with variable coverage

throughout the Bahamas. Seven major hurricanes (i.e., sustained winds >111 mph or Category 3 and higher on the Saffir-Simpson scale) impacted the Bahamas during this time: Frances (2004), Ike (2008), Irene (2011), Sandy (2012), Joaquin (2015), Matthew (2016), and Irma (2017). Google Earth imagery of all islands impacted by these hurricanes was examined, and some of the most impressive examples from hurricanes Ike, Joaquin, Matthew, and Irma on San Salvador and Great Inagua islands are documented and supplemented by field photos and high-resolution drone images. Google Earth proved to be a useful tool for such documentation, but the variable timing of image acquisition is not ideal for recording hurricane impact before natural and human-assisted recovery processes begin. Google Earth images also have limited resolution compared to high-resolution drone images, which are particularly useful, but can be difficult and expensive to acquire. Generating drone images also is dependent upon the ability to travel to impacted areas in a timely manner after major storms. Google Earth was especially useful for historical documentation of examples of storm impact that were previously identified in the field, but it was generally challenging to locate new examples, which could potentially be examined on site in the future. Overall, our methodology and results represent a useful means for documenting and communicating information about vulnerability to hurricanes with local residents, developers, and other decision- and policy-makers in the Bahamas.

THE ROCK ISLANDS OF BELAU (PALAU), WESTERN PACIFIC: AN EXAMPLE OF DROWNED POLYGONAL KARST

Mylroie, Joan, R , Mississippi State University, Mississippi State, MS 39762; **Mylroie, John E.** Mississippi State University, Mississippi State, MS 39762.

The Belau (Palau) Islands are located in the western Pacific (midway between Guam and New Guinea), an independent country in the former western Caroline Islands. The archipelago extends for 160 km in a north-south arc, with 414 km2 of land area. The northern islands are mostly volcanic, but the southern islands are Miocene to Pleistocene limestones which are heavily karstified. The signature feature of the southern archipelago are the Rock Islands, which rise from lagoons as steep-sided towers, some free-standing, others grouped so as to create internal depressions, many which have become inland water bodies. The overall appearance is of a cockpit or polygonal karst that has been drowned as a result of Holocene sea-level rise. Given that for over 90% of the Quaternary, sea level has been lower than the lagoon, these karst features evolved primarily in a subaerial condition. In their current environment, bioerosional notching over a 3 meter tidal range has over-steepened the hills, initiating collapse that has amplified the hills? verticality. Flank margin caves in various stages of erosional removal are found at 1 to 6 m above sea level, consistent with the last interglacial sea-level highstand (MIS 5e), and minimal tectonics or subsidence since. In this case, karst features have helped resolve a debate regarding tectonic motion in the last 100 ka. Some towers contain progradational collapse caves, formed by collapse of deeper caves to elevations above modern sea level. Those deeper caves formed when lower glacioeustatic sea levels exposed the entire carbonate platform, such that conduit flow developed to form large epigenic cave systems. The island caves display significant archeological and historical features, especially from WWII.

DENUDATION IN QUATERNARY EOLIANITES AND THE FORMATION OF PINNACLE TOPOGRAPHY

Mylroie, John, E, Mississippi State University, Mississippi State, MS 39762; **Mylroie, Joan, R.,** Mississippi State University, Mississippi State, MS 39762.

Eogenetic Quaternary eolianites may contain a denudational topography of upstanding rock pinnacles and columns. Examples are shown from Australia, The Bahamas, Bermuda, and

Rodrigues Island. These features have irregular spacing, are decimeters to meters in relief, and usually have a footprint dimension smaller than their height. Many are capped with a red, resistant micritic deposit interpreted to be a remnant terra rossa paleosol. These pinnacles are the product of an inversion of topography, initiating as small dissolutional pits in the eolianite, which collect soil and other surface debris, utilized by the rooting of plants that subsequently become rhizomorphs and microbiolites. The soil infill results in the micritization of the pit walls and bottom, creating a resistant lining. As overall denudation proceeds, the pit infills and the micritic lining projects above the lowering land surface as round, columnar features. Continued denudation results in the exposure of the pit bottom, where the terra rossa paleosol is the thickest, the most strongly cemented, and hence the most resistant part of the local landscape. The pit bottom now completes the inversion of the topography by becoming a pinnacle top. Eventually, the terra rossa cap is removed (some times by simply sliding off), and a sharp, pointed pinnacle forms,which continues to degrade, as does the surrounding landscape. The inherited inverted topography thus persists long after evidence of the causation by pit formation has disappeared. The scale of the pinnacles indicates five or more meters of denudation, consistent with denudation rates calculated from first principles and from field examples. Deposition of new eolianites can result in overprinting, creating columns and pinnacles from several denudation cycles, commonly tied to glacioeustasy.

FLANK MARGIN CAVES OF THE TURKS AND CAICOS ISLANDS: IMPLICATIONS FOR PLATFORM GEOLOGY

Mylroie, John E. Mississippi State University, Mississippi State, MS 39762; **Mylroie, Joan R.** Mississippi State University, Mississippi State, MS 39762; **Lace, Michael, J.** Coastal Cave Survey, West Branch, IA 52358; **Albury, Nancy, A.** Bahamas National Museum, Abaco, Bahamas.

The Turks and Caicos Islands (TCI) are the southeastern extension of the Bahamian Archipelago with important subtle tectonic distinctions revealed by their flank margin caves. Many TCI caves have pronounced joint control, which is not observed in the simple carbonate islands to the northwest. Dissolutional passages were observed at elevations up to 12 m, twice as high as expected for MIS 5e, ~120 ka; other workers report dissolutional passage elevations to 17 m and stalagmite U/Th dates >195 ka. These data contradict prior interpretations from this archipelago that only cave passages from MIS 5e exist. The TCI platforms lie ~100 km from the North American/Caribbean plate boundary and seismic and bathymetric data suggest minor tectonic uplift may have occurred; isostatic rebound as a result of karst denudation may also play a role. The common occurrence of joint-oriented passages coupled with the age and elevation of some caves support a tectonic component. Recent work on West Caicos has shown that pre-MIS 5e subtidal deposits older than MIS 5e exist in the TCI. While West Caicos fossil coral data for that highstand is problematic, no pre-MIS 5e subtidal deposits are known in the archipelago north of Mayaguana Island. As elsewhere in the archipelago, karst denudation, at greater values than previously reported, has stripped most pre-MIS 5e deposits from the platform surface; the West Caicos example was protected by pre-MIS 5e eolian deposition. That denudation may have resulted in isostatic rebound, as has been reported for Florida and The Bahamas. One cave on Providenciales intersects a complex deposit displaying back beach breccia facies and a tempestite deposit consisting primarily of the shells of the conch, Strombus gigas, sandwiched between two eolian units.

FLANK MARGIN CAVES IN COASTAL CARBONATES, CAPE RANGE, AUSTRALIA: INTERPRETING TECTONIC AND GLACIOEUSTASY OVERPRINTS

Mylroie, John, E, Mississippi State University, Mississippi State, MS 39762; **Mylroie, Joan, R ,** Mississippi State

University, Mississippi State, MS 39762; **William, Humphreys,** Western Australia Museum, Perth, Australia; **Brooks, Darren,** Western Australia Speleo Group, Exmouth, Australia; **Middleton, Gregory,** Sydney Speleological Society, Sandy Bay, Tasmania

Flank margin caves are common at Cape Range, Australia (northwest coast of the continent), a north-northeast-striking anticlinal ridge 315 m high, 130 km long, and 32 km wide that extends into the sea, consisting of Miocene carbonate rocks with a series of coastal terraces of Pliocene and Quaternary carbonates. Inland coast-parallel escarpments, representing former sea cliffs, and deep valleys cutting the limbs of the anticlinal ridge host many cave entrances at a variety of elevations. Caves initiated with the first tectonic-driven subaerial exposure in the Miocene and continued through to the last Pleistocene interglacial. The lowest and oldest unit, the Mandu Formation, a chalky and marly limestone, contains many tafoni (pseudokarst) caves with simple, single chamber plans and widths up to 15 m and heights up to 10 m. The higher, purer Miocene limestones and the younger Pliocene and Pleistocene coastal terrace limestones host numerous flank margin caves from 300 m elevation in the Miocene rocks to sea level in the Quaternary rocks. These caves have entrances up to 30 m wide and heights of 6 m, with single-chamber caves being common, but complex caves entered by small entrances lead to large phreatic chambers, eliminating both sea cave and tafoni as speleogenetic mechanisms. The close association of these caves with sea cliffs and incised valleys argues against a deep hypogene origin, which would leave a cave pattern unrelated to the surface configuration. Miocene uplift tapered off into the Pliocene. The flank margin caves in the paleo sea cliffs represent the outcome of the interplay of tectonic activity and glacioeustasy over a 300 m vertical range, with lowstands causing valley incision, while highstands raised the fresh-water lens and allowed cave development in the valley walls.

DEPOSITIONAL HISTORY OF TRIANGLE, FRENCH, AND CLEAR PONDS ON SAN SALVADOR, THE BAHAMAS

Niemi, Tina, University of Missouri-Kansas City, Kansas City MO; **Wilson, Darin**, University of Missouri-Kansas City, Kansas City MO; **Grady, Jennika,** University of Missouri-Kansas City, Kansas City MO; **Billingsley, Anne,** University of Missouri-Kansas City, Kansas City MO.

Three lakes located along the perimeter of San Salvador Island and isolated from the ocean by a dune and beackrock barrier were investigated through sediment coring campaigns. We collected ten cores and seven C-14 dates from Triangle Pond (TP), nine cores and five C-14 dates from French Pond (FP), and three cores and four C-14 dates from Clear Pond (CP). The TP stratigraphic record shows that the lake basin was created by a physical barrier between the Pleistocene dune ridge and the sea before 3500 yr BP. This event likely corresponds to the lithification of paleointertidal zone beachrock. Interbedded carbonate mud and sand deposited in an restricted tidal lagoon mark a period of hurricane activity that ends with a large coarse to fine grained, peloidal, bioclastic carbonate sand. At about 2000 yr BP, a 10-50 cm-thick peat was deposited during rising sea level likely within a mangrove swamp. The lack of sandy interbeds in the peat suggests a reduction in storminess or isolation of the basin during lowstand conditions did not permit deposition of tempestites. The peat deposition ends abruptly at 500 yr BP with a packstone sand layer and is capped by algal mat deposition. A similar sedimentary sequence is recorded in the upper part of FP pond deposition with a bioclastic sand overlain by a peat that is capped by algal mats that begin to be deposited ca. 500 yr BP. The phase of hypersaline conditions and algal mat growth in TP and FP marks the complete isolation of these lakes from the sea. The base of the longest CP core contains a peat dated to 5000 yr BP. This is overlain by a meter of carbonate wackestone likely deposited within a restricted lagoon that ended ca. 2800 yr BP with the deposition of a 20-cm-thick, coarse sand. Deposition shifted to a more sand-

dominated environment with a distinct sand bed dated to 1500 yr BP that marks the beginning of a mud and sand lamination interval until ca. 1000 yr BP. The upper bioturbated 40 cm of the core contains a sandy lower section and an upper fossil hash with abundant gastropods and mollusks representing the current brackish conditions.

REEF RESTORATION EXPERIMENTS FOR ISOLATED AND REMOTE ISLANDS AND COMMUNITIES: PART I

Rollino, John A. AECOM, New York, NY.

In response to more than 20 years of observed decline in the health of coral patch reefs around San Salvador Island, Bahamas, we have initiated experiments in reef restoration. Reef restoration is a growing industry in the United States, Australia, and other nations with substantial economic resources; however, many nations and communities that are home to coral reefs are isolated, economically stressed, and/or are located in a geo-politically unstable locations. In order to evaluate reef restoration efforts that could be undertaken in remote locations by a local population, we have embarked on a series of experiments to both increase coral populations, including endangered species, and reef rugosity (three dimensionality). Our experiments, to date, have been based on large-scale commercial reef restoration practices - but have been adapted for isolated and remote communities. The experiments were further adapted to be low cost and use materials and equipment regularly available to isolated communities. The experiments included: construction and placement of concrete rugosity enhancing devices, coral transplants, and rescuing of corals that have become dislodged due to storm events or other activities. To date, we have realized some encouraging results regarding the structural integrity of the rugosity enhancing devices, transplant of endangered species, and improvements in planning and logistics. In this paper we document the following: need for lower-cost reef restoration experiments; our methods and results to date; and identify future experiments. This paper is intended to be an ongoing series that identifies the progress of reef restoration techniques.

GEOCHEMISTRY AND MICROBIAL DIVERSITY COMPARISON OF TWO NATURAL HYDROCARBON SEEPS ON THE ISLAND OF BARBADOS

Sumrall, Jeanne L. Fort Hays State University, Hays, KS; **Elenz, Andrea, M.** TX; **Sumrall, Jonathan B.** Fort Hays State University, Hays, KS; **Machel, Hans** University of Alberta, Alberta, Canada.

In an effort to characterize the diversity of microorganisms that feed on petroleum hydrocarbons, microbial communities of two natural crude oil and bitumen seeps that occur on the island of Barbados were compared. The two natural macro-seeps are characterized by different environments: siliciclastic versus carbonate, fresh water versus salt water, and crude oil versus bitumen seepage. Samples were analyzed for microbial diversity and water geochemistry to determine if the possibility of microbial degradation of hydrocarbons has occurred. It was found that the two locations are similar at the phylum level yet differ greatly at the genus level, with the fresh water location being more diverse than the salt water location. Several hydrocarbon degrading bacteria were identified at both locations, implying at least some degree of degradation has occurred. Several unclassified species were also detected, thus opening the door for further research into what role each new species may play in the seep environments of Barbados.

ADDITIONAL TRIAL FARM RUINS AND OTHERS OF INTEREST

Winter, John Molloy College, NY; **Bernier, Don**; **Brown, Wesley** St. Olaf College, Northfield, MN; **Copich, John**; **Starynchak, Steve**

In January and April 2019, seven days were spent cutting trails and exploring the ruins around the Trial Farm complex, located in the S.E. Corner of San Salvador, near Breezy Hill.

The main set of ruins were explored and written up by Kathy Grace and Ron Shaklee in 1993. Our survey found additional buildings along the ridge top: six dwellings and three kitchen areas. The architecture and debris fields around the buildings reveal twentieth century materials. Aerial photographs from 1942 reveal that the buildings and surrounding area were cleared out and occupied, however 1968 aerial photographs do not reveal any cleared out areas. This perhaps indicates that the buildings were not occupied in 1968. Two additional and separate areas along the ridge line revealed plantation era construction and debris fields near the buildings. One area revealed a dome-shaped masonry oven. Neither of these areas show up in the 1942 and 1968 aerial photographs as being in use. In addition, an unreported outhouse was found at the Trial Farm complex that was written up by Grace and Shaklee. A similar style outhouse was found near a building of the Montreal settlement, which appears to have been occupied in 1942, based upon aerial photographs. Both of these outhouses were built using the slip form masonry technique.